AD- 267 350

U. S. ARMY
TRANSPORTATION RESEARCH COMMAND
FORT EUSTIS, VIRGINIA

TCREC TECHNICAL REPORT 61-106

WIND TUNNEL TESTS AND FURTHER ANALYSIS OF THE FLOATING WING FUEL TANKS FOR HELICOPTER RANGE EXTENSION

VOLUME 5

ANALYSIS OF STABILITY, CONTROL AND PERFORMANCE CHARACTERISTICS

Project 9X38-09-006

Contract DA 44-177-TC-550

August 1961

PROPE[illegible]Y OF U. S. ARMY
TRANSPORTA[illegible] RESEARCH COMMAND
RESEARCH RE[illegible]ENCE CENTER

prepared by :

VERTOL DIVISION
THE BOEING COMPANY
Morton, Pennsylvania

DEC 12 1961

2494-60

DISCLAIMER NOTICE

When Government drawings, specifications, or other data are used for any purpose other than in connection with a definitely related Government procurement operation, the United States Government thereby incurs no responsibility nor any obligation whatsoever; and the fact that the Government may have formulated, furnished, or in any way supplied the said drawings, specifications, or other data is not to be regarded by implication or otherwise as in any manner licensing the holder or any other person or corporation, or conveying any rights or permission, to manufacture, use, or sell any patented invention that may in any way be related thereto.

* * * * *

ASTIA AVAILABILITY NOTICE

Qualified requestors may obtain copies of this report from

Armed Services Technical Information Agency
Arlington Hall Station
Arlington 12, Virginia

* * * * *

This report has been released to the Office of Technical Service, U. S. Department of Commerce, Washington 25, D.C., for sale to general public.

* * * * *

The publication of this report does not constitute approval by USATRECOM of the findings and conclusions contained herein. It is published only for the exchange and stimulation of ideas.

ABSTRACT

TREC 61-106

Vertol Division, The Boeing Company, Morton, Pa., WIND TUNNEL TESTS AND FURTHER ANALYSIS OF THE FLOATING WING FUEL TANKS FOR HELICOPTER RANGE EXTENSION, VOL. 5 - Analysis of Stability, Control and Performance Characteristics by H. Neeb, D. Lawrence, and R. Johnstone, August 1961. 186 pp, incl. illus., tables. Contract (DA44-177-TC-550) USA TRECOM Proj. (9X38-09-006)

Unclassified Report

This report describes an analytical investigation of the stability and performance of a Boeing-Vertol H-21 tandem rotor helicopter equipped with floating wing fuel cells as a means of ferry range extension. The stability of the total system was studied with the wing located forward and directly under the helicopter center-of-gravity (cg). Two methods of stabilizing the wing oscillations about the hinge were studied: (a) A skewed hinge line, introducing a change in angle of attack as a function of the flapping disturbance, and (b) a geared trailing edge flap, mechanically linked to deflect when the wing flaps. Satisfactory stability was obtained with the wing positioned directly beneath the helicopter cg, using an unskewed hinge line, and geared flaps. The forward wing location was found to be unsatisfactory from the standpoint of longitudinal stability for the light wing case. Flight simulator studies emphasize the need for additional lateral control to supplement that produced by the basic aircraft. It was found that full span, differential ailerons with deflections of 2½ degrees per inch of stick, provide satisfactory roll control and wing flapping angles. At a take-off weight of 25,900 lbs and with the wing in the aft position the ferry range is 1975 nautical miles.

Project 9X38-09-006
Contract DA44-177-TC-550
August 1961

WIND TUNNEL TESTS AND FURTHER ANALYSIS OF THE FLOATING WING FUEL TANKS FOR HELICOPTER RANGE EXTENSION

Volume 5

ANALYSIS OF STABILITY, CONTROL AND PERFORMANCE CHARACTERISTICS

R-255

Prepared by:
Vertol Division, Boeing
Morton, Pennsylvania

for
U.S.ARMY TRANSPORTATION RESEARCH COMMAND
FORT EUSTIS, VIRGINIA

ACKNOWLEDGEMENTS

This study was accomplished by the Aerodynamic Department of the Vertol Division of The Boeing Company. Notable contributions were made by the following personnel:

E. Diamond	-	Systems Analyst
R. Johnstone	-	Aerodynamicist
D. Lawrence	-	Aerodynamicist
H. Neeb	-	Aerodynamicist

HEADQUARTERS
U. S. ARMY TRANSPORTATION RESEARCH COMMAND
Fort Eustis, Virginia

FOREWORD

The U. S Army, through the facilities of the U. S. Army Transportation Research Command, Fort Eustis, Virginia, has conducted a research program to determine a method for increasing the range of helicopters of the light-cargo type to 2,000 miles or more. The system that held the most promise was one wherein floating-wing fuel tanks were attached to the helicopter's fuselage.

The report presented in the following pages is the fifth and last volume of the final report. This report contains the results of the analytical investigation of the stability, control, and performance characteristics of the floating wing fuel tank system. The conclusions presented in the report are concurred in by this Command.

A design and fabrication program is now under way as a follow-up to this research program.

FOR THE COMMANDER:

APPROVED BY:

Robert D. Powell, Jr.
ROBERT D. POWELL, JR.
USATRECOM PROJECT ENGINEER

Raphael F. Garofalo
RAPHAEL F. GAROFALO
CWO-4 USA
Assistant Adjutant

CONTENTS

LIST OF FIGURES AND TABLES

LIST OF FIGURES AND TABLES (Continued)

LIST OF FIGURES AND TABLES (Continued)

LIST OF SYMBOLS

α_0	Section Zero Lift Angle
β_H	True Angular Wing Displacement
δ_{F_1}	Inboard Flap Deflection Angle
δ_{F_2}	Outboard Flap Deflection Angle
δ_3	Included Angle between Chord Line and Hinge Line
θ	Helicopter Pitch Angle Referenced to Horizontal X Axis
μ_1	Ratio of Pitching Moment Coefficient to Lift Coefficient Generated by Flap Deflection
ρ	Mass Density of Air
σ_1	Spanwise Static Weight Moment about the Chord Line Intersecting the Hinge Line at the Quarter Chord
σ_2	Chordwise Static Weight Moment about the Quarter Chord Line
ϕ	Helicopter Roll Angle
ψ	Helicopter Yaw Angle
a	Wing Lift Curve Slope
a.c.	Wing Aerodynamic Center
AR	Wing Aspect Ratio
$\bar{c}$	Geometric Mean Chord
c_1	Increment in Profile Drag due to Geared Inboard Flap
c_2	Increment in Profile Drag due to Geared Outboard Flap
C_{D_0}	Total Profile Drag Coefficient
$\bar{C}_D$	Section Steady State Drag Coefficient

C_{D_β}	Rate of Change Section Drag due to Geared Flap
c_f	Flap Chord
$c/4$	Wing Quarter Chord
$\bar{C}_L$	Section Steady State Lift Coefficient
C_{M_α}	Rate of Change of Pitching Moment Coefficient with Angle of Attack
$C_{M_{a.c.}}$	Coefficient of Pitching Moment about the Wing Aerodynamic Center
D	Total Drag of One Wing
D_i	Section Drag
e	Wing Hinge Offset Measured at Section Center-of-Gravity
i_w	Wing Incidence Angle Measured at Intersection of Chord Line and Fuselage Water Line
I_1	Mass Moment of Inertia about the Wing Chord Line which Intersects the Hinge Line
I_2	Mass Moment of Inertia Taken about the Wing Line of Aerodynamic Centers
I_3	Mass Product of Inertia Taken about the Same Axes as I_1 and I_2 were taken
I_β	Mass Moment of Inertia about the Wing Hinge
I_w	Moment of Inertia about Unskewed Hinge + (First Moment about Same Axis)
I_x	Total Roll Moment of Inertia of Rigid System
I_{Y_H}	Helicopter Pitch Moment of Inertia
I_z	Total Yaw Moment of Inertia of Rigid System

K	Induced Drag Factor
K_1	Increment in Lift Due to Geared Inboard Flap
K_2	Increment in Lift Due to Geared Outboard Flap
ℓ_1	Longitudinal Displacement of Wing Quarter Chord with Reference to Helicopter Center-of-Gravity
ℓ_2	Vertical Displacement of Wing Quarter Chord Beneath Helicopter Center-of-Gravity
L	Total Lift of One Wing
L_β	Rolling Moment Derivative with Respect to Wing Flapping Angle
$L_{\dot\beta}$	Rolling Moment Derivative with Respect to Wing Flapping Velocity
$L_{\dot\phi}$	Rolling Moment Derivative with Respect to Roll Rate
$L_{\dot\psi}$	Rolling Moment Derivative with Respect to Yaw Rate
$L_{\dot y}$	Rolling Moment Derivative with Respect to Lateral Velocity
L_i	Wing Section Lift
M_β	Hinge Moment Derivative with Respect to Wing Flapping Angle
$M_{\dot\beta}$	Hinge Moment Derivative with Respect to Wing Flapping Velocity
$M_{\dot\phi}$	Hinge Moment Derivative with Respect to Roll Rate
$M_{\dot\psi}$	Hinge Moment Derivative with Respect to Yaw Rate
M_{θ_H}	Pitching Moment Derivative with Respect to Pitch Angle (Fuselage Rotor Contribution)
$M_{\dot\theta_H}$	Pitching Moment Derivative with Respect to Pitch Rate (Fuselage Rotor Contribution)

$M_{\dot{z}_H}$	Pitching Moment Derivative with Respect to Vertical Velocity (Fuselage Rotor Contribution)
$M_{\dot{x}_H}$	Pitching Moment Derivative with Respect to Longitudinal Velocity (Fuselage Rotor Contribution)
M_H	Mass of Helicopter Only
M_i	Wing Section Pitching Moment
M_W	Mass of One Wing
N_β	Yawing Moment Derivative with Respect to Wing Flapping Angle
$N_{\dot{\beta}}$	Yawing Moment Derivative with Respect to Wing Flapping Velocity
$N_{\dot{\phi}}$	Yawing Moment Derivative with Respect to Roll Rate
$N_{\dot{\psi}}$	Yawing Moment Derivative with Respect to Yaw Rate
$N_{\dot{y}}$	Yawing Moment Derivative with Respect to Lateral Velocity
q	Generalized Coordinate
Q_q	Virtual Work Terms Corresponding to the Generalized Coordinates
S_1	Wing Area of Inboard Section
S_2	Wing Area of Outboard Section
T	Total Kinetic Energy of System
V	Total Potential Energy of System
V_0	Trim Forward Velocity
$X_{\theta H}$	Longitudinal Displacement Derivative with Respect to Pitch Angle (Fuselage-Rotor Contribution)

$X_{\dot{\theta}_H}$	Longitudinal Displacement Derivative with Respect to Pitch Rate (Fuselage-Rotor Contribution)
$X_{\dot{x}_H}$	Longitudinal Displacement Derivative with Respect to Longitudinal Velocity (Fuselage-Rotor Contribution)
$X_{\dot{z}_H}$	Longitudinal Displacement Derivative with Respect to Vertical Velocity (Fuselage-Rotor Contribution)
X_1	Displacement of Center of Lift of Inboard Section from Intersection of Line of Aerodynamic Centers and Hinge Line
X_2	Displacement of Center of Lift of Outboard Section from Intersection of Line of Aerodynamic Centers and Hinge Line
Y_y	Lateral Displacement Derivative with Respect to Lateral Velocity
Y_1	Chordwise Displacement of the Center of Lift of the Inboard Section from the Line of Aerodynamic Centers
Y_2	Chordwise Displacement of the Center of Lift of the Outboard Section from the Line of Aerodynamic Centers
Z_{θ_H}	Vertical Displacement Derivative with Respect to Pitch Angle (Fuselage Rotor Contribution)
$Z_{\dot{\theta}_H}$	Vertical Displacement Derivative with Respect to Pitch Rate (Fuselage Rotor Contribution)
$Z_{\dot{x}_H}$	Vertical Displacement Derivative with Respect to Pitch Longitudinal Velocity (Fuselage Rotor Contribution)
$Z_{\dot{z}_H}$	Vertical Displacement Derivative with Respect to Vertical Velocity (Fuselage Rotor Contribution)

SUMMARY

This report describes an analytical investigation of the stability and performance of a Boeing-Vertol H-21 tandem rotor helicopter equipped with floating wing fuel cells as a means of ferry range extension. The wings are hinged close to the root, and are in equilibrium under the steady-state aerodynamic and gravity forces, minimizing the root shear force and bending moments taken out at the attachment points.

The stability of the total system was studied with the wing located forward and directly under the helicopter center-of-gravity (cg). Two methods of stabilizing the wing oscillations about the hinge were studied: (a) a skewed hinge line, introducing a change in angle of attack as a function of the flapping disturbance, and (b) a geared trailing edge flap, mechanically linked to deflect when the wing flaps.

Satisfactory stability was obtained with the wing positioned directly beneath the helicopter cg, using an unskewed hinge line, and geared flaps. The forward wing location was found to be unsatisfactory from the standpoint of longitudinal stability for the light wing case.

Performance studies indicate that the aft wing position, as determined by stability criteria, is detrimental to the range. In order to insure a 2000 mile ferry range with the wing in a position to satisfy the stability requirements, the wing incidence relative to the helicopter was allowed to vary throughout the flight. Further studies will be conducted to determine the best compromise from both stability and overall performance considerations.

Flight simulator studies emphasize the need for additional lateral control to supplement that produced by the basic aircraft. It was found that full span, differential ailerons with deflections of 2-1/2 degrees per inch of stick provide satisfactory roll control and wing flapping angles.

The present floating wing has an aspect ratio of 8 and a span of 72 feet. The constant chord wing uses an NACA 4418 section. The maximum take-off weight of the system is 25,900 pounds, of which 14,800 pounds is fuel carried in the wings. At this weight and with the wing in the aft position the ferry range is 1975 nautical miles (n.mi.).

A forward wing position would increase the air miles per gallon and permit an increase in the take-off weight to 27,100 pounds, with a resulting range of 2400 n. mi.

CONCLUSIONS AND RECOMMENDATIONS

The results of the present analysis indicate that the ferry range of a tandem rotor helicopter can be extended by the use of floating wing fuel cells. A configuration can be derived that has acceptable stability in cruising flight, at all weights.

Further work is necessary to refine the lateral-directional analysis to include the non-linear dihedral effect, and the work on both the lateral-directional and longitudinal stability should be extended to cover flight speeds below the cruise, down to minimum flying speed.

A conflict exists between wing position requirements for best stability on one hand, and optimum performance on the other. Longitudinal stability requires that the wing be situated near the cg and for maximum range it should be as far forward as possible to avoid rotor downwash. The existing analysis considers two wing positions - one in which the aerodynamic center is 14 feet ahead of the basic helicopter cg, the other in which the aerodynamic center is directly below the cg. It should be noted that the criterion of 2000 miles range was satisfied with the wing in the aft position only by allowing the wing incidence to vary throughout the flight. Further work will be done to optimize wing position, such that satisfactory longitudinal stability characteristics combined with minimum performance penalties may be achieved.

Flight simulator studies indicate that lateral control must be supplemented with full span differential ailerons having a gearing of 2-1/2 degrees per inch of lateral stick movement.

Performance calculations show that ferry range capabilities diminish as the wing is moved to the aft position. Maximum take-off weight, based on available take-off power, is decreased from 27,100 pounds to 25,900 pounds, and the range is reduced from 2400 n. mi. to 1975 n. mi.

INTRODUCTION

The normal mission range of the modern helicopter is 400 n.mi., or less, while ideally, to achieve full global mobility, ferry ranges of 2000n. mi. or more are desired. In providing this range, the basic problem is to increase the lift-drag ratio and/or the fuel weight: empty weight ratio, without resorting to extensive structural modifications to the basic helicopter. While many research programs are today exploring high performance rotor systems, which show promise of yielding high lift-drag ratios, present-day helicopters exhibit values on the order of 4:1.

The Army's ferry range problem is concerned with present-day helicopters, in which no large improvements in lift drag ratio may be expected, so the alternative is to consider means of increasing the effective fuel-weight ratio. This must be achieved without drastic modification to the structure, or undue increase in the drag. Supplementary internal fuel tanks do not increase the range sufficiently; there is a prohibitive performance penalty resulting from the much increased rotor disc loading, and considerable internal modification is necessary to install them.

To be acceptable, any range extension system must meet the following basic criteria:

1. To be usable as a retro-fit item on existing helicopters, with a minimum increase in basic helicopter empty weight, it must entail the minimum of structural modification.

2. There must be no adverse effect on the stability of the aircraft at any weight.

3. Adequate control must be available at all flight speeds and weights.

4. To justify the development of the system, it must yield ultimate ferry ranges of 2000 n. mi. or better.

The floating wing fuel cell has been proposed as the most promising method of carrying the additional fuel without incurring severe drag and weight penalties. The supplementary tankage is fitted to the helicopter in the form of a pair of floating wings that are free to move vertically about hinges placed close inboard. The equilibrium

condition for the wing in steady flight occurs when the static moments of lift and weight about the hinge are equal and opposite. In such a condition, the resultant vertical shear force at the hinge is very small, and the additional power required is a minimum, being just that necessary to overcome the wing drag and the wing-rotor interference drag. Thus the disc loading is not greatly increased, even though the weight of the system may be more than double that of a standard helicopter.

The problems to be dealt with in the design of the proposed range extension system can conveniently be discussed under the following four headings:

1. Overall system stability
2. Wing stability
3. Control
4. Performance

OVERALL SYSTEM STABILITY:

The overall stability must be at least as good as that of the basic aircraft at all weights and speeds. There is a large separation between the maximum and minimum flying weights, and most of the fuel is to be carried in the wings, in the interests of achieving the best lift/drag ratio. Consequently, the moments of inertia, both of the systems as a whole and of the wing about it's hinge, change markedly during the mission. Because of this wide variation in important system parameters it is difficult to achieve satisfactory stability in all flight regimes. The longitudinal stability is more sensitive to changes in weight, and to fore and aft location of the wing, and the final configuration will be a compromise between the requirements of range and longitudinal stability.

WING STABILITY:

The empty wing moment of inertia is approximately one seventh of the fully loaded value. The aerodynamic forces are thus much greater in relation to the inertia forces when the system is at the

minimum flying weight. The problem is to select suitable wing damping and aerodynamic stiffness so that wing deflections do not at any time exceed 15 degrees. Upward deflections are critical, from considerations of rotor clearance, but aside from this, the problems of designing the hinge and the associated connections increase as increasingly larger deflections are permitted. Two simple methods of stabilizing and controlling the floating wing are available:

1. Skewed Hinge

   The hinge lies along some line skewed relative to the chord, in such a manner that as the wing floats up, the angle of attack is reduced, thus providing restoring moments. The disadvantave of this method is that the aerodynamic damping about the hinge is reduced as the stiffness increases, as shown below:

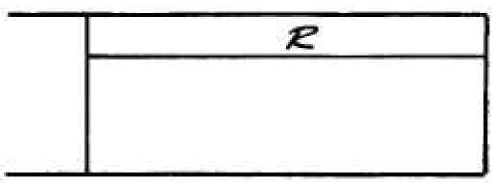

Effective flapping radius = R

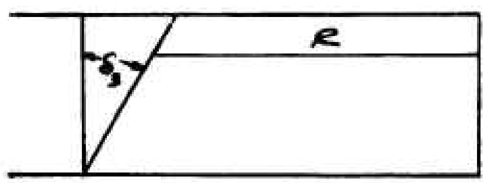

Effective flapping radius = $R \cos \delta_s$

2. Geared Trailing Edge Flaps

   The flaps are mechanically linked to the wing to move as a function of wing flapping angle. By the use of differentially geared flaps (i.e. outboard flaps moving up, inboard down, as the wing flaps up) and the judicious selection of gear ratio, a wide range of aerodynamic

stiffness can be obtained, together with some degree of control over the resultant shear loads at the hinge. Further, there is no loss of damping about the wing hinge by this method.

CONTROL:

The rolling moment of inertia of a helicopter is usually low, but with the addition of large span wings, each holding 7000 pounds of fuel, it becomes large, and the roll control power suffers accordingly. To supplement it, it is proposed to use the flap panels as ailerons, in addition to their function of stabilizing the wing. By the use of differential collective pitch, the tandem rotor helicopter has more than adequate pitch control, and it is not anticipated that control of this mode will present any serious problems as a helicopter. The H-21 is deficient in yaw control sensitivity. Addition of the floating fuel wing will reduce control sensitivity by a factor of five. However, this is not expected to be a problem, as the floating wing system is not capable of hovering and very low speed flight, which is the regime where the H-21 yaw control deficiency is experienced.

PERFORMANCE:

The location of the wing is a compromise between the conflicting requirements of performance and stability. To obtain optimum range, the wing should be located as far forward as possible, to minimize interference drag and the rearward inclination of the lift vector produced by the rotor downwash field. For the same reason, to obtain shortest take-off distances, the wing should be located forward. Because of the much increased maximum weight, take-off will be power limited, and range suffers on two counts if the wing is not located at the optimum forward position. On the other hand, longitudinal stability requires that the wing be located at or near the basic helicopter cg.

LONGITUDINAL ANALYSIS

DERIVATION OF EQUATIONS:

The system being analyzed is one of a very complex nature. The maximum mass ratio of the flapping fuel wing to that of the helicopter is 1.44 to 1. This will give rise to important inertial coupling terms. The Lagrange Equation of Motion for generalized coordinates is a completely rigorous analysis which is well suited to the solution of this type of problem.

The Lagrange Equation yields all the mass and inertial terms (Ref. App. (A)) which must be equated to the external forces acting on the system. The forces include aerodynamic forces acting on the rotors, fuselage and the flapping wings. Those forces acting on the rotor and fuselage were obtained from existing helicopter stability analyses. The aerodynamic forces exerted on the wing were derived by the principal of virtual work (Ref. App. (A)).

Two different types of wing stabilization systems were investigated (i.e. δ_3 hinge and differentially geared trailing edge flaps). Each wing was considered to be composed of two separate spanwise sections, the section span corresponding to the differential flap span. The lift and drag were computed for each section so that changes in aerodynamic forces on the wing could be readily calculated for differential flap deflection. The lift distribution for the inboard section was assumed to be rectangular while that for the outboard section was assumed to be elliptic. The final equations shown in Appendix (A) are completely general and apply to both stability systems.

Assumptions:

1. Since the mass properties and aerodynamic characteristics of each wing are similar, then the flapping motions will be identical and one equation will describe the motion.

2. Small angle assumptions and linearization are applied only to the final set of equations.

3. Initial pitch angle (θ_{H_0}) and wing flap angle (β_{H_0}) are assumed to be small and are excluded from the analysis.

ANALYTIC SOLUTION OF EQUATIONS:

A very effective engineering tool is the root solution of the characteristic equation. The roots not only yield periods and time to double or half amplitudes but serve as a cross check for analog time histories.

Given a set of four linear simultaneous differential equations in four unknowns, the solution thereof is accomplished by arranging the coefficients of the variables into a fourth order determinant having quadratic elements. Expansion of the determinant yields a sixth order polynomial which is then solved for the roots.

In order to determine trends for several configurations, the roots of the corresponding characteristic equations can be presented on root locus plots (Ref. Appendix (B)), where horizontal lines indicate constant frequency and vertical lines indicate time to half or double amplitude. The roots may indicate four types of response:

1. Complex roots where the sign of the real part is positive indicate a divergent oscillation ($A \pm Bi$).

2. Complex roots where the sign of the real part is negative indicate a damped oscillation ($-A \pm Bi$).

3. A positive real root indicates a non-oscillatory divergence.

4. A negative real root indicates a non-oscillatory convergence.

RESULTS OF LONGITUDINAL ANALYSIS:

Throughout the longitudinal investigation, all cases were judged on the basis of the system response to a 30 ft/sec (fps) vertical gust, and the stability characteristics compared with those of the basic helicopter.

The results of the analysis indicate that to satisfy stability criteria, a zero δ_3 hinged wing stabilized with differential trailing edge flaps set at a ± 2 deg/deg gearing ratio, must be

located directly beneath the basic helicopter cg. Cases 21 and 26 are the light and heavy wing cases corresponding to the above description.

With the wing located in this position, flap gearing ratios of ± 3 and ± 1 (Cases 25 and 27 - heavy wing, Cases 20 and 22 - light wing) were also investigated. Examination of the three light wing configurations shows all cases exhibit highly damped oscillations. The roots of the characteristic equations as well as analog time histories indicate minor variations in both period and damping. Similar responses exhibited are high frequency wing modes (avg. period = 1.5 sec) damped to half amplitude in .39 seconds, superimposed on a long period (23 sec) mode. This long period is common to both wing and pitch responses. Both angles are comparatively small.

In order to avoid wing-rotor interference, wing flap angles must be .25 radian or less; therefore, this criterion becomes critical with the light wing configuration. Intuitive reasoning suggests that in response to a 30 ft/sec vertical gust, the empty fuel wings will immediately flap up. This is found to be true by the following analytical study.

If the system is disturbed by a 30 ft/sec vertical gust, the vertical accelerations of the helicopter and the wing viewed separately may be calculated as follows:

$$(\Delta\alpha) = .222 \text{ rad}$$

$$(Z_\alpha)_{hel} = -33000 \text{ lb/rad}$$

$$(Z_\alpha)_{wing} = -46000 \text{ lb/rad}$$

Therefore, the resulting forces will be:

$$Z_{hel} = -7300 \text{ pounds}$$

$$Z_{wing} = -10200 \text{ pounds}$$

$$Mass_{hel} = 344.7 \text{ slugs}$$

$$\text{Mass}_{\text{wings}} = 497 \text{ slugs (heavy) and } 62 \text{ slugs (light)}$$

$$\text{Hel.Acc.} = \frac{7300}{344.7} = 2.12 \text{ ft/sec}^2$$

$$\text{Wing Acc. (heavy)} = \frac{10200}{497} = 20.5 \text{ ft/sec}^2$$

Since both initial accelerations of the wing and helicopter are nearly equal, initial down wing flap angles should be small. However:

$$\text{Wing Acc. (light)} = \frac{10200}{62} = 165 \text{ ft/sec}^2$$

With the high accelerations of the empty wing compared to those of the helicopter, it is probable that large initial wing flap angles will result.

Based on this wing-rotor interference criterion, the minimum gearing ratio is ± 2 deg/deg which shows an initial flapping excursion of .25 radians.

Examination of Cases 25, 26 and 27 shows, again, very little change in either period or damping between all three cases. Wing flap angles are small (less than .1 rad) and mildly divergent. Pitch angles are fairly large with 12 second periods and double amplitude in 6.4 seconds. Maximum amplitude after four seconds is .5 radian. However, sufficient control power is available to make the system flyable.

Both the δ_3 hinged wing and the differential trailing edge geared flap wing located in the forward position (wing a.c. 14 ft fwd of hel. cg.) were analyzed and found to be not feasible. Looking at the two configurations individually, the δ_3 hinged system exhibited static lateral instability. The longitudinal response of the hinge indicated dynamic instability with a 16.6 second period and doubled amplitude in 2.5 seconds.

The effect of increasing the spring stiffness (zero $\delta_3 \rightarrow 45^\circ$ δ_3) resulted in increasing the period and decreasing the time to double amplitude. Thus the configuration approaches that of a fixed wing aircraft with the wing located far forward of the cg. The disadvantage of the skewed hinge lies in the adverse effects on the wing root shear loads. For example, as the helicopter pitches nose

up in response to a vertical gust, the heavy wing initially flaps downward, thus increasing the angle of attack. This results in a net up shear load at the hinge which increases the nose up pitching moments and tends to pitch the aircraft more nose up.

The alternative wing stabilization system (differentially geared flaps) was investigated with the wing located in the same forward position.

The system response to a 30 fps gust indicates that a gearing ratio of 1 deg/deg yields an aerodynamic spring with sufficient stiffness to keep wing flapping excursions acceptably small. However, large pitching motions are also recorded. (See Figure 7)

With fully loaded fuel tanks, the system appeared to be acceptable both longitudinally and from a lateral-directional standpoint. For this configuration, the empty tanks case exhibited longitudinal static instability with .75 second to double amplitude.

Comparison of the incremental lift acting on the fuel wing with full and empty tanks shows that in response to a 30 fps gust, the increment in lift is 70% of the steady lift for the fully loaded wing and 500% of the steady lift for the empty wing. Therefore, initial wing flap angles and accelerations are quite large for the empty wing case. This effect, coupled with the fact that the pitch inertia of the system is reduced by a factor of 2, induces high pitch accelerations which destabilize the system.

In summary, longitudinal stability characteristics dictate that the fuel wing be hinged with zero δ_3 , directly beneath the helicopter cg using a flap gearing ratio of ± 2 deg/deg.

LATERAL-DIRECTIONAL ANALYSIS

DERIVATION OF EQUATIONS:

The application of Lagrange's Equations to the lateral-directional mode is prohibitively long and laborious, approximately four times as much work being required as compared with the longitudinal case. Consequently, a simpler and less time-consuming method, yielding acceptable accuracy, was used. The method is based on an initial assumption of small perturbations and the existence of the following four modes:

1. Roll of the system treated as a rigid body about the compound center-of-gravity.

2. Rigid yaw of the system about the compound center-of-gravity.

3. Rigid lateral translation of the system.

4. Flapping of the wing about the hinge.

Linearized expressions, in terms of small disturbances in the roll, yaw, sideslip and flapping modes, which were derived, enabled the calculation of lift, drag and pitching moment to be made at a general spanwise wing station. The forces and moments, when integrated over the span, yield the conventional fixed wing lateral and directional aerodynamic stability derivatives, and, in addition, include the effect of the flapping freedom on the aircraft motion.

Assumptions:

To keep the equations of motion and the calculation of the stability derivatives from becoming too lengthy, the following assumptions were considered justified:

1. The motion is anti-symmetric about the aircraft plane of symmetry.

2. The initial flapping angle is zero.

3. The angle between the aircraft principal axis and the flight path is small.

The first two assumptions exclude the possibility of investigating the non-linear dihedral effect that occurs in a sideslip when the initial flapping angle is not zero. It is considered that this is potentially the most restrictive assumption in this analysis, and that in any refinement of the method, it should be eliminated.

The inertial terms, forming the left hand side of the final equations of motion form a symmetric matrix, from which the product of inertia terms are excluded by Assumption 3.

Fuselage, Tail and Rotor Contributions to Stability:

The basic helicopter contributions to the stability derivatives were obtained from:

1. Flight test and wind tunnel (for the fuselage and tail).

2. Rigid rotor stability analysis.

Representation of Geared Flap:

The assumption was made that the geared flap contributes only to the aerodynamic spring stiffness and makes no contribution to aerodynamic damping. The effect of the flap can, therefore, be represented by:

1. A change in the effective lift curve slope.

2. An increment in the section drag coefficient, varying linearly with the wing flapping angle.

3. An increment in the section pitching moment coefficient, varying linearly with the wing flapping angle.

Displacement Equations:

A right-handed axis system is used, having the origin at the compound cg, with the X axis positive forward, the Y axis positive to the right and the Z axis positive down. Positive rotations are clockwise when looking in the positive directions. Positive wing flapping is right wing down, i.e., in the same sense as positive

roll. Since the motion is assumed to be anti-symmetric, only the right half of the helicopter plus wing need be considered.

RESULTS OF LATERAL-DIRECTIONAL ANALYSIS:

The time histories for Cases 12 and 1 (Figure 17-18), and others unpublished, indicate that the response in roll to a side gust becomes more divergent as δ_3 is increased. This is borne out by the lateral-directional stability roots in Table 27. For zero the unstable oscillation has a period of 12.2 seconds, and takes 6.3 seconds to double amplitude. When δ_3 is increased to 45°, the period is reduced to 10.5 seconds and the time to double amplitude is now only 2.4 seconds. This divergence is the basis of the choice of zero δ_3, and as the loss of damping resulting from skewing the hinge is so large, (it varies as the cosine of δ_3), it was not considered fruitful to pursue this approach when the geared flap provides such a powerful aerodynamic spring.

The selection of fore-and-aft location is primarily dictated by the requirements of performance and longitudinal stability, since it is of relatively little importance to the lateral-directional stability - Cases 4 and 27 illustrate the effect of moving the wing aft at maximum weight, and Cases 18 and 22 show the effect for the empty wing cases. At neither weight is there any significant change in the motion. For the heavy wing (4 and 27, flap gearing ± 1), the only changes appear in the second and third roots (Table 27). The slowly divergent second root in Case 4 becomes very lightly damped, i.e., essentially neutral stability. The very lightly damped long period oscillation corresponding to the third root becomes slowly divergent (27 seconds to double amplitude) and the period increases from 12.5 to 15.8 seconds. Examination of the analog traces for these cases shows that the effect of the changes in the roots is small.

At the light weight (Cases 18 and 22), the changes resulting from moving the wing aft are still less marked - only the third root shows any changes worth commenting on. The subsidence corresponding to this root becomes more rapid - taking 23 seconds to half amplitude, compared with 33.0 seconds with the wing in the forward position. One other point worth mentioning is that the initial swing of ϕ_u is approximately halved -2.0° for Case 22, compared with 3.4° for Case 18.

Selection of Flap Gearing:

The differentially geared flap is a powerful method of modifying the aerodynamic spring stiffness and resultant shear loads at the hinge, without sacrificing the damping. When the wing flaps up, the outboard section of the flap deflects up, providing the aerodynamic stiffness, while the inboard section deflects downwards, countering the downward shear loads generated by the upward deflected outboard flap. This increment in the net shear provides a stabilizing rolling moment on the helicopter. Expressed in another way, consider the helicopter in steady level flight, with the wings in the neutral position. Let a disturbance induce a rolling velocity to the right. Due to its own inertia the right wing cg will tend to stay in the same vertical location, which means that the wing relative to the helicopter will flap up. The outboard flap panel will deflect up, inducing a downward flapping hinge moment, and shear force increasing the rate of roll. The inboard flap panel will deflect downwards, inducing a shear force that reduces the rate of roll. It will at the same time slightly reduce the aerodynamic stiffness, but as it acts much closer to the wing hinge than the outboard section, it is much less powerful in influencing stiffness than in modifying the shear loads.

The gearing ratio chosen (defined as flap deflection per unit wing deflection) should be as low as possible consistent with acceptable stability, as the lift generated by flap deflection rapidly becomes non-linear. The flap is also required as a high-lift device at least in the early stages of a ferry flight, and the outboard panels at least will be required to serve as roll control.

The investigation into flap gearing ratio is covered in Cases 20, 21 and 22 (light wing) and 25, 26 and 27 (heavy). In all cases, the inboard and outboard sections move differentially, at gear ratios 1, 2 and 3. Examination of the roots and analog traces leads us to conclude that there is little to be gained by increasing the flap gearing ratio beyond ± 1. Taking the light wing first, we note that as the flap gearing is increased from 1 to 3, the oscillatory part of the first root remains virtually constant, while the time to halve amplitude increases from 8.0 to 9.0 seconds. The only other root affected

is the other oscillatory root, representing a very fast highly damped mode. The period is reduced from 1.5 seconds to .7 second, and the time to halve amplitude goes from .32 to .27 seconds.

Similarly, with the heavy wing (25, 26 and 27), only the oscillatory roots are influenced by the gearing. The long period oscillation is mildly divergent, becoming more so as the gearing is increased (21 seconds to double amplitude at the ± 3 gearing, 29 seconds for ± 1) and the period remains virtually unchanged. The short period highly damped oscillation changes noticeably in period - going from 3.48 seconds to 1.93 seconds, and the time to halve amplitude remains nearly unchanged at 1.6 seconds.

In summary, the straight hinge was chosen because of the rapid divergence that a skewed hinge produced. The fore and aft position is relatively unimportant to the lateral-directional stability, and on the basis of cases 20-27, there is little to be gained by increasing the flap gearing ratio beyond ± 1 per unit wing deflection.

FLIGHT SIMULATOR STUDY

The investigation up to this point was concerned primarily with obtaining a wing-helicopter configuration that would satisfy stability criteria. Cases 21 and 26 fulfill this requirement. However, high roll inertia of the system reduces the lateral control sensitivity by a factor of fifty as compared to the basic helicopter; in order to bring roll control up to an acceptable level, additional means of control power in the form of ailerons are considered necessary. To aid in evaluating the control effectiveness, flight simulator studies were made to compare lateral-directional control of the basic helicopter with that of the wing-helicopter combination with and without aileron control.

The simulator used in this analysis consists of a mock-up of approximately one half of the YHC-1A cockpit area. Forward visibility through the windshield is approximately the same as it is in the YHC-1A aircraft. Adjustable control throw stops, friction, and force gradients are provided. Aircraft flight information is presented in two ways.

1. Voltmeters with modified instrument faces (airspeed, rate of climb, etc.) have been inserted in place of true aircraft instruments. These meters are arranged in their proper location on an instrument panel mockup.

2. A servo-driven color transparency is projected on a screen covering the pilots entire forward windshield field of vision. This image, which represents the horizon and ground orientation, moves in response to computer signals, and imparts roll, pitch and yawing motion information to the pilot.

The flight program was set up as follows:

The test pilot flew a simulated H-21 helicopter to familiarize himself with the simulator and to give himself a base case with which to compare the wing-helicopter combination. Except for the fact that the controls seemed a bit too sensitive to the pilot, simulator response compared favorably with actual helicopter characteristics. The original intent in evaluating the wing-helicopter combination was to fly the longitudinal case and lateral case separately and once the pilot familiarized himself with each mode,

he would be presented with the coupled longitudinal lateral system. However, it was found that the longitudinal mode was very simple to fly but the slide presentation was very poor (jerky motion) such that when both modes were coupled, the system required too much concentration on the pilot's part to yield any useful information. Therefore, roll yaw characteristics and longitudinal characteristics were evaluated separately.

Test pilot comments indicate that the floating wing-helicopter system without aileron control is much more stable than the basic helicopter. However, as expected, roll control was noticeably more sluggish. Recovery from bank angles of 20 degrees or less was possible in both smooth and turbulent air (max ± 10 fps gust peaks). Yaw control was adequate, but adverse roll effects due to pedal displacement were not noticeable. Two and one half ($2\frac{1}{2}$) degrees of aileron per inch of stick improved the roll control considerably. (This aileron gearing increases control power by 80%.)

Small-amplitude short-period oscillations were observed in both the $2\frac{1}{2}°$ and 5° aileron cases. Only those of the 5° case had amplitudes large enough to be annoying to the pilot. Adequate directional control was available in both cases, although adverse roll effects were still present. Although the 5° case compares favorably with the basic helicopter with regard to roll response, the $2\frac{1}{2}°$ case was considered to be an acceptable compromise since wing flap angles are small. It is also desirable to keep aileron deflections small, for the aileron is used simultaneously as a flap and as a wing stabilization system.

Lateral stick step response is shown in Figure 27 with 5° of aileron/in to show the effect of increased control power.

PERFORMANCE ANALYSIS

CRUISE:

The method of analysis used to calculate the range of the helicopter-wing configuration involved the modification of longitudinal trim equations for the standard helicopter. This analysis, programmed on a digital computer, ineratively determines the longitudinal characteristics of several helicopter-wing configurations at various equilibrium conditions. The basic helicopter trim analysis was modified by accounting for the interference of the wing on the rear rotor and calculating an equivalent flat plate area based on the following items:

1. Induced drag of the wing determined by C_L;
2. Interference of front rotor on the wing in terms of a corrected induced angle;
3. Profile drag of the wing including the landing gear;
4. Profile drag of the flap.

By varying the profile drag of the flaps, which is related directly to flap deflection at different wing lifts, the helicopter water - line angle of attack was determined, as shown in Figures 30 through 38. (NOTE: All figures are located in Appendix C). The wing trim angle of attack was calculated by using Figure 39 (lift coefficient versus angle of attack). The difference between the helicopter waterline and wing angle represents the required wing incidence for a given flap deflection. Figures 40, 41 and 42 present power required and Figure 43 gives the fuel flow as a function of horsepower.

The following sample problem is presented in order to clarify the procedure used in the performance analysis:

Given:

wing incidence (i_w)	= 8.5°
wing lift	= 16,000 lb
forward speed	= 80 knots

Enter Figure 37 and find point where the delta angle between wing and waterline is 8.5° at minimum flap deflection.

Flap deflection (δ_f) = 15°

Wing angle of attack (α_w) = 5.0°

Waterline angle of attack (α_{WL}) = -3.5°

For a given flap deflection of 15° at 80 knots, Figure 42 yields horsepower required of 1240 hp and fuel flow for this sample is 950 lb/hr (Figure 43). The miles per pound of fuel is calculated by dividing the forward speed by the fuel flow which, for this case, is .0842 miles per pound.

TAKE-OFF:

There are two types of take-off procedures which were considered. The first method is to accelerate the system down the runway at a trim attitude associated with the take-off speed and when the take-off speed is reached, the system will break ground. The second method incorporates the procedure where the helicopter's attitude is such that the maximum accelerating force is in the horizontal direction. When the take-off speed is reached, the helicopter-wing configuration is rotated to the trim angle and the system takes off.

The "Hartman's Analysis" was used to calculate the break ground distance. The following equation was solved graphically and the distance required to break ground was obtained.

$$S = \frac{1}{2} \int_0^{V_{TO}} \frac{d(V)^2}{a}$$

The distances to climb to 50 ft is dependent upon the available excess power during climb. The distance to make a steady climb

from ground to 50 ft is added directly to the ground run to obtain the total distance over a 50 ft obstacle.

RESULTS OF PERFORMANCE STUDY:

The all-out range was the primary area of investigation based on the new wing configuration. The take-off distances and control positions are also studied to insure that the wing fuel tank does not restrict the helicopter's operation throughout the entire flight.

The method used in calculating the miles per pound of fuel is described in the performance analysis section. Tables 29, 30 and 31 present for a variable wing incidence the flight characteristics for various wing lifts, forward speeds, and rpm's for the wing in the forward position. The criterion for choosing a given trim condition is maximum miles per pound of fuel. Figure 44 presents a ferry range of 2400 n.mi. using the forward positioned wing with a variable incidence. If a range of only 2000 n. mi. is desired, the aircraft could take-off at a wing weight of 12,100 pounds.

A constant wing incidence is desirable from a design aspect. In studying the effect it might have on range, a wing incidence of 8.5° was selected from take-off considerations and was held constant throughout the regime. The same method of calculation and presentation was performed on the constant wing incidence with the wing in the forward position. Table 32 presents the various characteristics. Note that the flap deflection changes with rpm at constant wing incidence.

Figure 45 presents the all-out range of 2205 n. mi. for the constant wing incidence configuration. The take-off wing gross weight of 13,700 pounds is also shown for a range of 2000 n. mi.

Figures 46 and 47 show the range of the variable and constant wing incidence if an additional profile drag increment is arbitrarily added to the drag calculated with the wing in the forward position. The flight schedule for the all-out range mission for both variable and constant wing incidence is presented in Figures 48 and 49.

The location of the wing on the helicopter has an effect on the range. If the wing is moved to the most aft position, that is, under the rear door, the front rotor's induced angle effect on the wing is increased threefold and it's related effect on range is shown in

Figures 50 and 51. The results yield an all-out range of 1975 n.mi. for a variable wing incidence and 1765 n.mi. for the constant wing incidence. The take-off wing gross weight is reduced to 14,800 pounds and 14,200 pounds respectively because of power limitations.

The new range as affected by wing position is computed by determining the power required for the drag increase. The optimum miles per pound for the aft wing position is calculated at the same forward speed as that of the forward wing position since the drag increase due to moving the wing to the most aft position is independent of the forward speed. The helicopter trim angles will not change appreciably. Because of power limits at 2300 engine rpm for the 9000 pound lift condition, the engine speed had to be increased to 2500 rpm for the aft wing position. The horsepowers presented in Figure 52 (variable wing incidence) and Figure 53 (constant wing incidence) show the comparison between the two configurations. The configuration with the wing in the most aft wing position reaches a power limit at wing gross weights less than maximum; hence, an additional range penalty must be paid because the helicopter-wing configuration cannot take off at a maximum gross weight of 16000 pounds. Table 33 presents the range for the various configurations and their associated maximum take-off gross weights.

The control parameters for the forward wing configuration were studied to insure that the control margins were adequate. The investigation analyzing the effect of moving the wing to the aft position indicated that the control positions will not change appreciabely from those calculated for the wing in the forward position. Figure 54 presents the required longitudinal cyclic pitch versus fuel weight for both variable and constant wing incidence. Collective pitch margin was sufficient for both configurations as shown in Figures 55 and 56.

The procedure of obtaining take-off distances was discussed in the "Method of Investigation" section. Table 34 presents a summary of take-off procedures and results.

BIBLIOGRAPHY

1. Hayden, J. and Eggert, W., "H-21B Phase IV - Performance and Stability Tests" - AFFTC-TR-57-4, March 1957.

2. "Feasibility Study of Helicopter Range Extension Using Floating Wing Fuel Tanks" - ASTIA No. AD-203262, September 1958.

3. Young, A.D., "The Aerodynamic Characteristic of Flaps", R&M 2622, February 1957.

4. Vertol Division Boeing Aerodynamic Investigation III-129 "Longitudinal Equations of Motion and Stability Derivatives for a Tandem Helicopter."

5. Vertol Division Boeing Aerodynamic Investigation III-130 "Lateral-Directional Equations of Motion and Stability Derivatives."

6. Castles, Jr., W., Durham, Jr., H. and Kevorkian, J., "Normal Component of Induced Velocity for Entire Field of a Uniformly Loaded Lifting Rotor with Highly Swept Wake as Determined by Electro-Magnetic Analog" - TN 4238.

7. Vertol Division Boeing Report DYMR-102, "Vertol Flight Simulator Report," December 1960.

APPENDIX A

DISPLACEMENT DIAGRAM FOR LONGITUDINAL
EQUATIONS OF MOTION

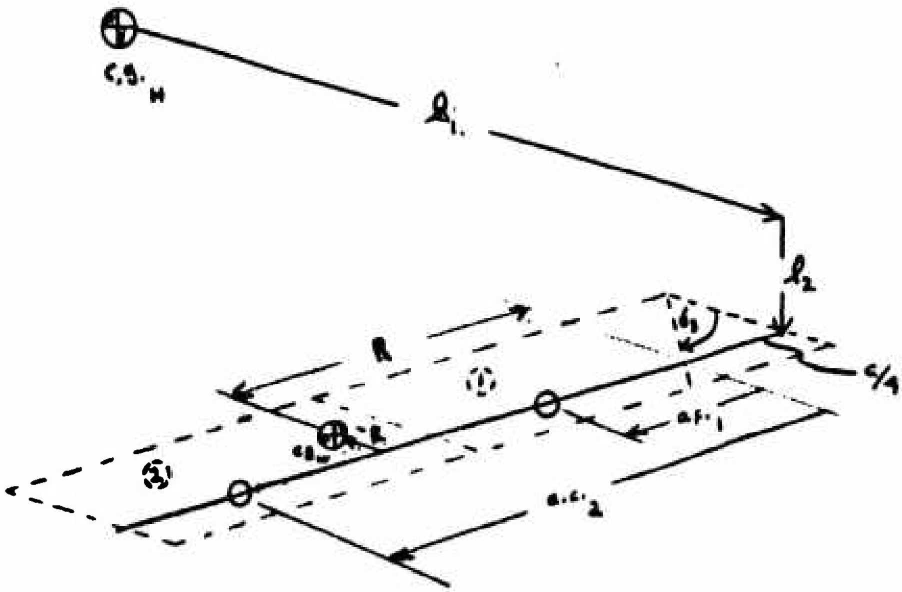

FIG. 1

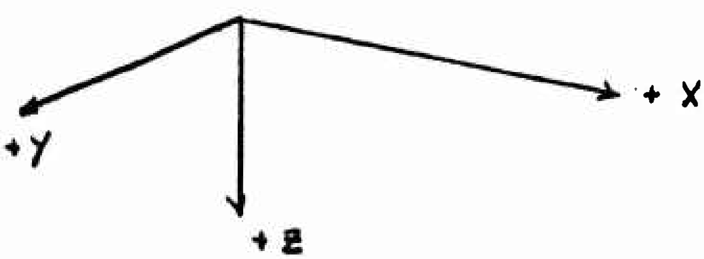

FIG. 2 SIGN CONVENTION

DIFFERENTIALLY GEARED FLAPS

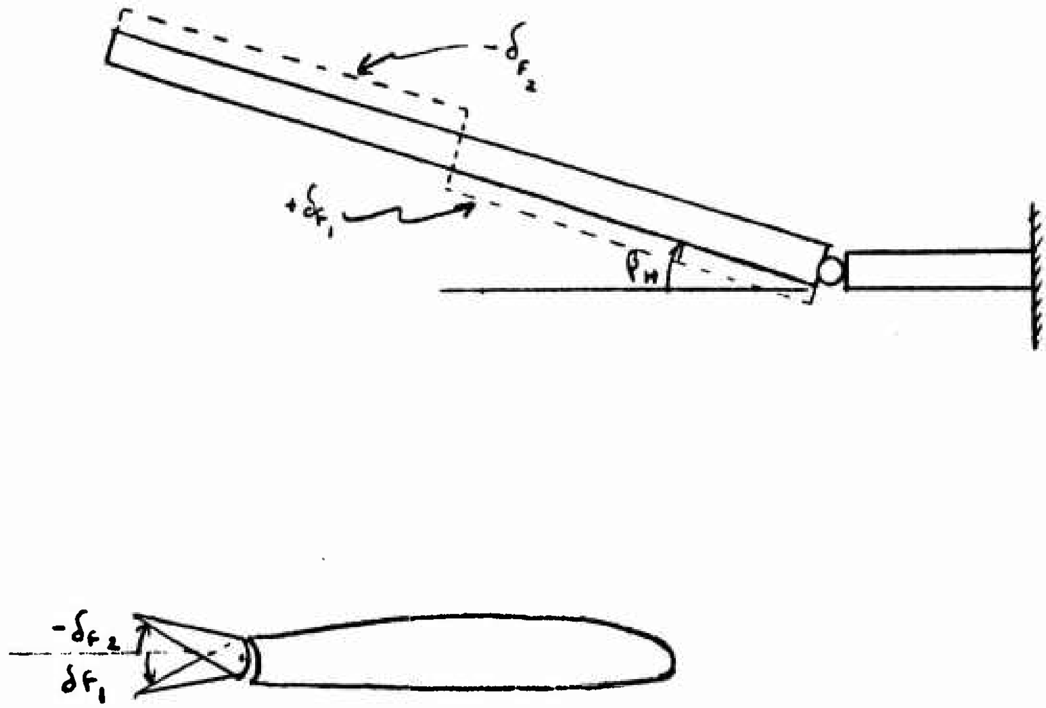

FIG. 3

The Lagrange equations of motion for generalized coordinates is stated as follows:

$$\frac{d}{dt}\left(\frac{\partial T}{\partial \dot{q}}\right) - \frac{\partial T}{\partial q} + \frac{\partial V}{\partial q} = Q_q$$

Where:

T	Total Kinetic Energy of the system
V	Total Potential Energy of the system
q	Generalized Coordinate
Q_q	Virtual Work Terms

The four generalized coordinates of this system are:

θ	Helicopter Pitch Angle
β_H	Wing Flapping Angle referred to the hinge
x	Longitudinal displacement from a fixed earth reference point.

Z Vertical displacement from a fixed earth reference point.

In order to determine the total kinetic and potential energy of the system, it is necessary to obtain the displacement of all component parts with respect to some reference point. In this case all motion is referred to primary inertial earth fixed axes.

Starting with axes fixed to the right wing as shown below:

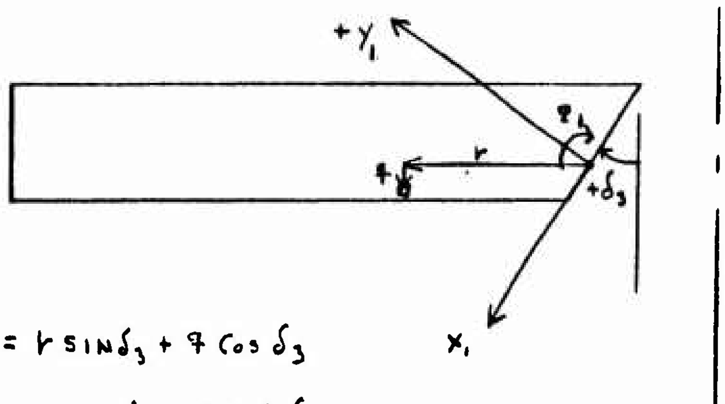

$$X_1 = r \sin\delta_3 + q \cos\delta_3$$

$$Y_1 = r \cos\delta_3 - q \sin\delta_3$$

The total displacement vector is obtained by rotating and translating axes back to the fixed axis system as follows.

(1) Rotation through β_H

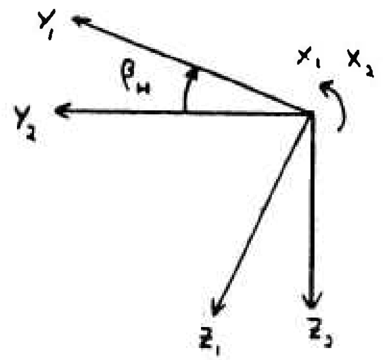

(2) Rotation through δ_3

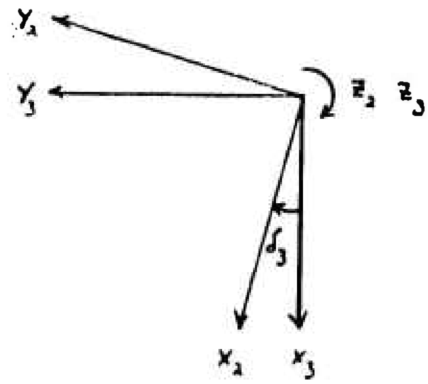

(3) Rotation through i_w

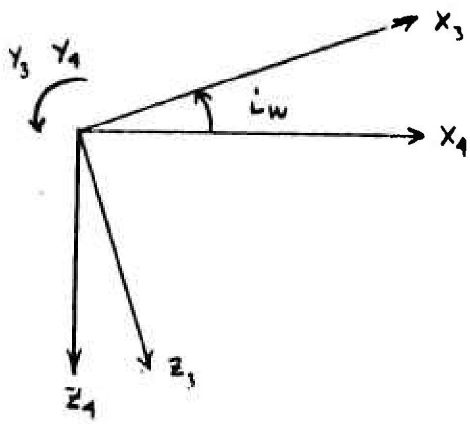

(4) Translation to Helicopter c.g.

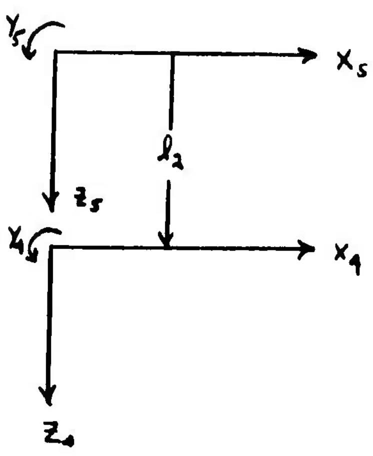

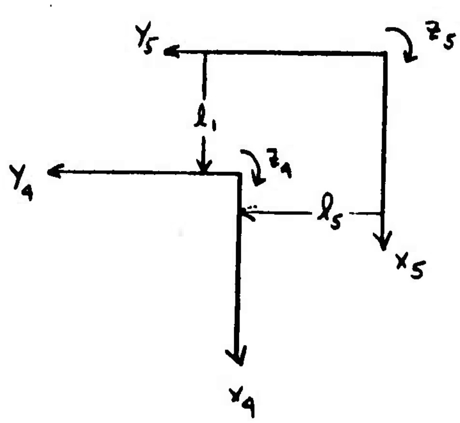

(5) Rotation through θ

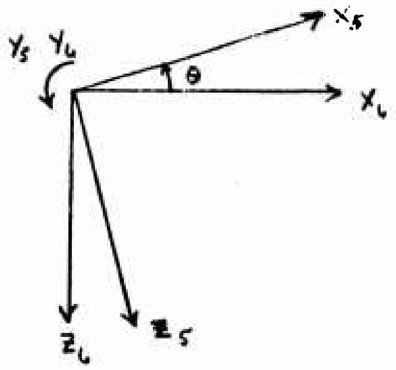

(6) Translation through x & z

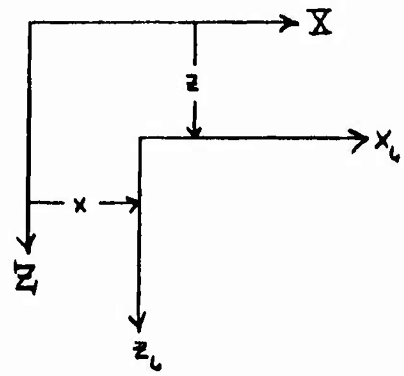

The final components of the displacement vector of any particle on the right wing are:

$$\mathbb{X} = x + X_1 \cos\delta_3 \cos i_w \cos\theta - Y_1 \cos\beta_H \sin\delta_3 \cos i_w \cos\theta$$

$$- Y_1 \sin\beta_H \sin i_w \cos\theta + \ell_1 \cos\theta - Y_1 \sin\beta_H \cos i_w \sin\theta$$

$$- X_1 \cos\delta_3 \sin i_w \sin\theta + Y_1 \cos\beta_H \sin\delta_3 \sin i_w \sin\theta$$

$$+ \ell_2 \sin\theta$$

$$\mathbb{Y} = Y_1 \cos\beta_H \cos\delta_3 + X_1 \sin\delta_3 + \ell_5$$

$$Z_1 = z - Y_1 \sin\beta_H \cos i_w \cos\theta - X_1 \cos\delta_3 \sin i_w \cos\theta$$

$$+ Y_1 \cos\beta_H \sin\delta_3 \sin i_w \cos\theta + \ell_2 \cos\theta - \ell_1 \sin\theta$$

$$- X_1 \cos\delta_3 \cos i_w \sin\theta + Y_1 \cos\beta_H \sin\delta_3 \cos i_w \sin\theta$$

$$+ Y_1 \sin\beta_H \sin i_w \sin\theta$$

Appropriate substitution of the following variables yields the components of the displacement vector for the left wing.

$$\beta_{H_R} = -\beta_{H_L}$$

$$\delta_{3_R} = -\delta_{3_L}$$

$$X_R = X_L$$

$$Y_R = -Y_L$$

$$Z_R = Z_L$$

Calculating the kinetic and potential energy As follows -

$$T = \frac{1}{2}\int \left(\dot{X}^2 + \dot{Y}^2 + \dot{Z}^2\right) dM$$

$$V = \int (-Z)\, g\, dM$$

Applying the Lagrange equation yields
the following four equations of motion

$$\text{EQ (1)} \quad A_1 \ddot{\theta} + A_2 \theta + A_3 \ddot{z} + A_4 \ddot{X} + A_5 \ddot{\beta}_H + A_6 \beta_H = Q_\theta$$

$$\text{EQ (2)} \quad B_1 \ddot{\theta} + B_2 \theta + B_3 \ddot{z} + B_4 \ddot{X} + B_5 \ddot{\beta}_H + B_6 \beta_H = Q_{\beta_H}$$

$$\text{EQ (3)} \quad C_1 \ddot{\theta} + C_2 \ddot{X} + C_3 \ddot{\beta}_H = Q_X$$

$$\text{EQ (4)} \quad D_1 \ddot{\theta} + D_2 \ddot{z} + D_3 \ddot{\beta}_H = Q_z$$

Where:

$$\begin{aligned} A_1 = \; & I_{Y_H} + I_1 \sin^2 2\delta_3 \cos^2 i_w + 2 I_2 \left(\sin^4 \delta_3 + \cos^4 \delta_3\right) \\ & + 4 I_3 \cos^3 \delta_3 \sin \delta_3 \cos^2 i_w + 2 M_w \left(l_1^2 + l_2^2\right) \\ & - 4 I_3 \sin^3 \delta_3 \cos \delta_3 \cos^2 i_w - 4 \sigma_2 l_2 \sin i_w \\ & + I_2 \sin^2 2\delta_3 \sin^2 i_w + 2 \sigma_1 l_1 \sin 2\delta_3 \cos i_w \\ & + 4 \sigma_2 l_1 \cos^2 \delta_3 \cos i_w \end{aligned}$$

$$A_2 = 2g\left[l_2 M_w - \sigma_2 \sin i_w\right]$$

$$A_3 = -2\left[\ell_1 M_w - \sigma_2 \cos i_w\right]$$

$$A_4 = 2\left[\ell_2 M_w - \sigma_2 \sin i_w\right]$$

$$A_5 = 2\Big[I_3 \cos\delta_3 - I_2 \sin\delta_3 - \sigma_1 \ell_2 \cos\delta_3 \sin i_w$$

$$+ \sigma_2 \ell_2 \sin\delta_3 \sin i_w + \sigma_1 \ell_1 \cos\delta_3 \cos i_w$$

$$- \sigma_2 \ell_1 \sin\delta_3 \cos i_w\Big]$$

$$A_6 = 2g \sin i_w\left[\sigma_2 \sin\delta_3 - \sigma_1 \cos\delta_3\right]$$

$$B_1 = 2\Big[I_3 \cos\delta_3 - I_2 \sin\delta_3 + \sigma_1 \cos\delta_3 \left(\ell_1 \cos i_w - \ell_2 \sin i_w\right)$$

$$+ \sigma_2 \sin\delta_3 \left(\ell_2 \sin i_w - \ell_1 \cos i_w\right)\Big]$$

$$B_2 = 2g \sin i_w\left[\sigma_2 \sin\delta_3 - \sigma_1 \cos\delta_3\right]$$

$$B_3 = 2 \cos i_w\left[\sigma_2 \sin\delta_3 - \sigma_1 \cos\delta_3\right]$$

$$B_4 = 2 \sin i_w\left[\sigma_2 \sin\delta_3 - \sigma_1 \cos\delta_3\right]$$

$$B_5 = 2\left[I_1 \cos^2\delta_3 + I_2 \sin^2\delta_3 - I_3 \sin 2\delta_3\right]$$

$$B_6 = 2g \sin\delta_3 \sin i_w \left[\sigma_1 \cos\delta_3 - \sigma_2 \sin\delta_3\right]$$

$$C_1 = 2\left[l_2 M_w - \sigma_2 \sin i_w\right]$$

$$C_2 = M_H + 2 M_w$$

$$C_3 = 2 \sin i_w \left[\sigma_2 \sin\delta_3 - \sigma_1 \cos\delta_3\right]$$

$$D_1 = -2\left[l_1 M_w + \sigma_2 \cos i_w\right]$$

$$D_2 = M_H + 2 M_w$$

$$D_3 = -2 \cos i_w \left[\sigma_2 \sin\delta_3 + \sigma_1 \cos\delta_3\right]$$

The inertial part of the equations of motion as presented must now be equated to the external forces acting on the system (Q_q). This is accomplished by:

(1) Calculating rotor and fuselage derivatives.

(2) Aerodynamic forces on the wing were derived by the principal of virtual work outlined as follows:

$$Q_q = \frac{\partial W}{\partial q}$$

Where $$W = \sum F \delta s + \sum M \delta \varphi$$

$F \sim$ Constant Force

δs Virtual Linear Displacement

M Constant Moment

$\delta \varphi$ Virtual Angular Displacement

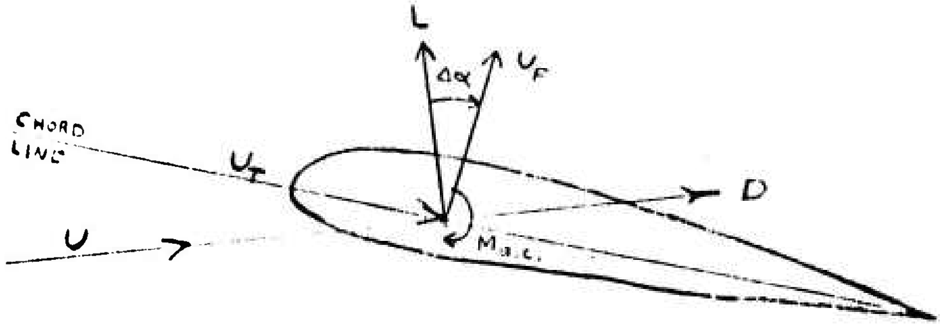

$$F_x = D \cos \Delta\alpha - L \sin \Delta\alpha$$

$$F_z = L \cos \Delta\alpha + D \sin \Delta\alpha$$

$$M = M_{a.c.}$$

Virtual displacements are:

$$\delta s_x = \delta z \sin i_w - \delta_x \cos i_w$$
$$- \delta\theta \left[\ell_2 \cos i_w + \ell_1 \sin i_w \right]$$

$$\delta s_z = \delta \beta_H Y_1 - \delta_x \sin i_w - \delta_z \cos i_w$$
$$+ \delta\theta \left[Y_1 \sin \delta_3 + X_1 \cos \delta_3 - \ell_2 \sin i_w + \ell_1 \cos i_w \right]$$

$$\delta \Phi = \delta\theta - \delta \beta_H \sin \delta_3$$

An example of the virtual work terms is shown below:

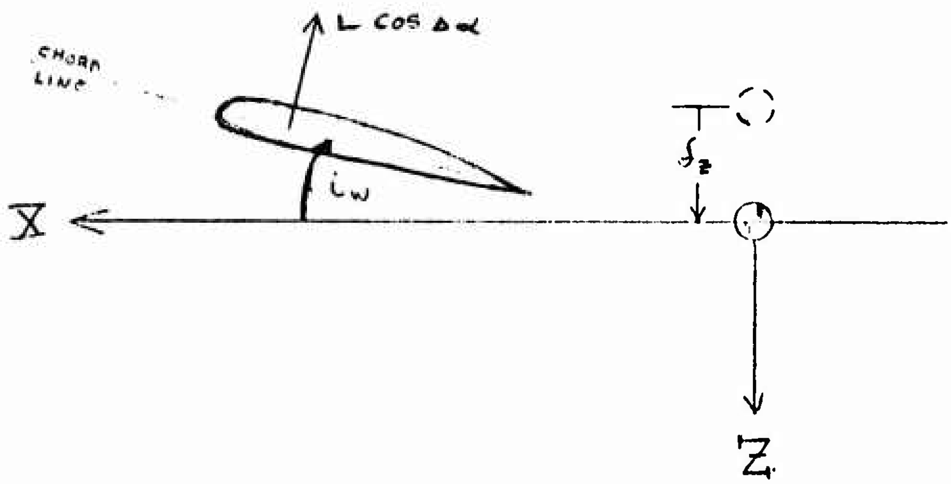

If the entire system is displaced δ_z then the virtual work $(F\delta s)$ done is $= L\cos\Delta\alpha(\delta_z \cos i_w)$

and $$\frac{\partial W}{\partial z} = L\cos\Delta\alpha \cos i_w$$

The total virtual work is:

$$W = F_x \delta_{s_x} + F_z \delta_{s_z} + M\,\delta\rho$$

The following terms were derived in the same manner.

$$EQ(1) \quad Q_\Theta = A_7\dot{\Theta} + A_8\Theta + A_9\dot{z} + A_{10}\dot{X} + A_{11}\dot{\beta}_H + A_{12}\beta_H$$

$$EQ(2) \quad Q_{\beta_H} = B_7\dot{\Theta} + B_8\Theta + B_9\dot{z} + B_{10}\dot{X} + B_{11}\dot{\beta}_H + B_{12}\beta_H$$

$$EQ(3) \quad Q_X = C_4\dot{\Theta} + C_5\Theta + C_6\dot{z} + C_7\dot{X} + C_8\dot{\beta}_H + C_9\beta_H$$

$$EQ(4) \quad Q_z = D_4\dot{\Theta} + D_5\Theta + D_6\dot{z} + D_7\dot{X} + D_8\dot{\beta}_H + D_9\beta_H$$

EQ (1) Pitching moment equation

EQ (2) Wing moment equation about the flapping hinge

EQ (3) X - Force equation

EQ (4) z - Force equation

$$
\begin{aligned}
A_7 = & \left[-\ell_2 \cos i_w - \ell_1 \sin i_w\right]\Big\{\left[\rho\left(C_{D_0} + \frac{a^2\alpha_0^2}{\pi AR}\right)(s_1 + s_2)\right]\left[2V_0\left(\ell_2 \cos^2 i_w + \tfrac{1}{2}\ell_1 \sin 2i_w\right)\right] \\
& + \left[\rho\left(\frac{a^2}{\pi AR} - a\right)\right]\left[2V_0 \sin i_w\right]\left[(s_1Y_1 + s_2Y_2)\sin\delta_3 - (X_1S_1 + X_2S_2)\cos\delta_3 + (s_1+s_2)(\ell_2 \sin i_w - \ell_1 \cos i_w)\right] \\
& + \left[\rho\left(a\alpha_0 - \frac{2\alpha_0 a^2}{\pi AR}\right)\right]\left[(s_1+s_2)(\ell_2 V_0 \sin 2i_w - \ell_1 V_0 \cos 2i_w) + (S_1Y_1 + S_2Y_2)(V_0 \cos i_w \sin\delta_3)\right. \\
& \left.- (S_1X_1 + S_2X_2)(V_0 \cos i_w \cos\delta_3)\right]\Big\} + \left[-Y_1 \sin\delta_3 + X_1\cos\delta_3 - \ell_2 \sin i_w + \ell_1 \cos i_w\right]\Big\{ \\
& \left[-\rho a\alpha_0 s_1\right]\left[2V_0\left(\ell_2 \cos^2 i_w + \tfrac{1}{2}\ell_1 \sin 2i_w\right)\right] + \left[-s_1\left(\frac{2\rho a^2\alpha_0}{\pi AR}\right)\right]\left[2V_0 \sin i_w (Y_1 \sin\delta_3 - X_1\cos\delta_3\right. \\
& \left.+ \ell_2 \sin i_w - \ell_1 \cos i_w)\right] + \left[\rho s_1\left(a + C_{D_0} + \frac{a^2\alpha_0^2}{\pi AR}\right)\right]\left[\ell_2 V_0 \sin 2i_w - V_0\ell_1 \cos 2i_w + V_0Y_1\cos i_w \sin\delta_3\right. \\
& \left.- V_0X_1 \cos i_w \cos\delta_3\right]\Big\} \\
& + \left\{-Y_2 \sin\delta_3 + X_2\cos\delta_3 - \ell_2 \sin i_w + \ell_1 \cos i_w\right\}\Big\{-\rho a\alpha_0 S_2\left[2V_0\left(\ell_2 \cos^2 i_w\right.\right. \\
& \left.\left.+ \tfrac{1}{2}\ell_1 \sin 2i_w\right)\right]
\end{aligned}
$$

$$+\left[-S_2\left(\frac{2\rho a^2\alpha_0}{\pi AR}\right)\right]\left[2V_0\sin i_w\left(Y_2\sin\delta_3 - X_2\cos\delta_3 + l_2\sin i_w - l_1\cos i_w\right)\right]$$

$$+\left[\rho S_2\left(a + C_{D_0} + \frac{a^2\alpha_0^2}{\pi AR}\right)\right]\left[l_2 V_0\sin 2i_w - V_0 l_1\cos 2i_w + V_0 Y_2\cos i_w\sin\delta_3 - V_0 X_2\cos i_w\cos\delta_3\right]\Bigg\}$$

$$+\left\{\rho\bar{c}\cos^2\delta_3\, C_{m_{AC}}(S_1+S_2)\right\}\left\{2V_0\left[l_2\cos^2 i_w + \tfrac{1}{2}l_1\sin 2i_w\right]\right\}$$

$$A_q = \left[-l_2\cos i_w - l_1\sin i_w\right]\Bigg\{\left[\rho\left(\frac{a^2}{\pi AR} - a\right)(S_1+S_2)\right]\left[V_0^2\sin 2i_w\right] + \left[\rho\left(a\alpha_0 - \frac{2\alpha_0 a^2}{\pi AR}\right)(S_1+S_2)\right]\left[V_0^2\cos 2i_w\right]$$

$$+\left[\rho\left(C_{D_0} + \frac{a^2\alpha_0^2}{\pi AR}\right)(S_1+S_2)\right]\left[-V_0^2\sin 2i_w\right]\Bigg\}$$

$$+\left[-Y_1\sin\delta_3 + X_1\cos\delta_3 - l_2\sin i_w + l_1\cos i_w\right]\Bigg\{\left[-S_1\left(\frac{2\rho a^2\alpha_0}{\pi AR}\right)\right]\left[V_0^2\sin 2i_w\right]$$

$$+\left[\rho S_1\left(a + C_{D_0} + \frac{a^2\alpha_0^2}{\pi AR}\right)\right]\left[V_0^2\cos 2i_w\right] + \left[-\rho a\alpha_0 S_1\right]\left[-V_0^2\sin 2i_w\right]\Bigg\}$$

$$+\left[-Y_2 \sin\delta_3 + X_2 \cos\delta_3 - \ell_2 \sin i_w + \ell_1 \cos i_w\right]\left\{\left[-s_2\left(\frac{2\rho a^2\alpha_0}{\pi AR}\right)\right]\left[V_0^2 \sin 2i_w\right]\right.$$

$$\left.+\left[\rho s_2\left(a + C_{D_0} + \frac{a^2\alpha_0^2}{\pi AR}\right)\right]\left[V_0^2 \cos 2i_w\right] + \left[-\rho a\alpha_0 s_2\right]\left[-V_0^2 \sin 2i_w\right]\right\}$$

$$+\left\{\rho\bar{c}\cos^2\delta_3\, C_{m_{ac}}\,(s_1+s_2)\right\}\left\{-V_0^2 \sin 2i_w\right\}$$

$$A_q = \left[-\ell_2 \cos i_w - \ell_1 \sin i_w\right]\left\{\left[\rho\left(C_{D_0} + \frac{a^2\alpha_0^2}{\pi AR}\right)(s_1+s_2)\right]\left[-V_0 \sin 2i_w\right]\right.$$

$$+\left[\rho\left(\frac{a^2}{\pi AR} - a\right)(s_1+s_2)\right]\left[V_0 \sin 2i_w\right] + \left[\rho\left(a\alpha_0 - \frac{2\alpha_0 a^2}{\pi AR}\right)\right]\left[s_1+s_2\right]\left[V_0 \cos 2i_w\right]\Big\}$$

$$+\left[-Y_1 \sin\delta_3 + X_1 \cos\delta_3 - \ell_2 \sin i_w + \ell_1 \cos i_w\right]\left\{\left[-\rho a\alpha_0 s_1\right]\left[-V_0 \sin 2i_w\right]\right.$$

$$\left.+\left[-s_1\left(\frac{2\rho a^2\alpha_0}{\pi AR}\right)\right]\left[V_0 \sin 2i_w\right] + \left[\rho s_1\left(a + C_{D_0} + \frac{a^2\alpha_0^2}{\pi AR}\right)\right]\left[V_0 \cos 2i_w\right]\right\}$$

$$+\left[-Y_2 \sin\delta_3 + x_2 \cos\delta_3 - l_2 \sin i_w + l_1 \cos i_w\right]\left\{\left[-\rho a \alpha_0 S_2\right]\left[-V_0 \sin 2i_w\right]\right.$$

$$+\left[-S_2\left(\frac{2\rho a^2 \alpha_0}{\pi AR}\right)\right]\left[V_0 \sin 2i_w\right] + \left[\rho S_2\left(a + C_{D_0} + \frac{a^2\alpha_0^2}{\pi AR}\right)\right]\left.\left[V_0 \cos 2i_w\right]\right\}$$

$$+\left\{\rho \bar{c} \cos^2\delta_3 \, C_{M_{AC}} \, (S_1 + S_2)\right\}\left\{2V_0 \cos^2 i_w\right\}$$

$$A_{10} = \left[-l_2 \cos i_w - l_1 \sin i_w\right]\left\{\left[\rho\left(C_{D_0} + \frac{a^2\alpha_0^2}{\pi AR}\right)(S_1+S_2)\right]\left[2V_0 \cos^2 i_w\right] + \left[\rho\left(\frac{a^2}{\pi AR} - a\right)(S_1+S_2)\right]\left[2V_0 \sin^2 i_w\right]\right.$$

$$+\left.\left[\rho\left(a\alpha_0 - \frac{2\alpha_0 a^2}{\pi AR}\right)(S_1+S_2)\right]\left[V_0 \sin 2i_w\right]\right\} + \left[-Y_1 \sin\delta_3 + x_1 \cos\delta_3 - l_2 \sin i_w + l_1 \cos i_w\right] \times$$

$$\left\{\left[-\rho a \alpha_0 S_1\right]\left[2V_0 \cos^2 i_w\right] + \left[-S_1\left(\frac{2\rho a^2\alpha_0}{\pi AR}\right)\right]\left[2V_0^2 \sin^2 i_w\right] + \left[\rho S_1\left(a + C_{D_0} + \frac{a^2\alpha_0^2}{\pi AR}\right)\right]\left[V_0 \sin 2i_w\right]\right\}$$

$$+\left[-Y_2 \sin + X_2 \cos\delta_3 - l_2 \sin i_w + l_1 \cos i_w\right]\left\{\left[-\rho a \alpha_0 S_2\right]\left[2V_0 \cos^2 i_w\right] + \cdots\cdots\right.$$

$$+\left[-S_2\left(\frac{2\rho a^2\alpha_0}{\pi AR}\right)\right]\left[2V_0 \sin^2 i_w\right] + \left[\rho S_2\left(a + C_{D_0} + \frac{a^2\alpha_0^2}{\pi AR}\right)\right]\left[V_0 \sin 2 i_w\right]\Big\}$$

$$+\left\{\rho\bar{c}\cos^2\delta_3\, C_{m_{AC}}(S_1+S_2)\right\}\left\{2V_0\cos^2 i_w\right\}$$

$$A_{11} = \left[-\ell_2\cos i_w - \ell_1\sin i_w\right]\Big\{\left[\rho\left(\frac{a^2}{\pi AR} - a\right)(S_1Y_1 + S_2Y_2)(-2V_0\sin i_w)\right] + \Big[\rho\left(a\alpha_0 - \frac{2\alpha_0 a^2}{\pi AR}\right)$$

$$(S_1Y_1 + S_2Y_2)(-V_0\cos i_w)\Big]\Big\}$$

$$+\left[-Y_1\sin\delta_3 + X_1\cos\delta_3 - \ell_2\sin i_w + \ell_1\cos i_w\right]\Big\{\left[-S_1\left(\frac{2\rho a^2\alpha_0}{\pi AR}\right)\right]\left[-2V_0Y_1\sin i_w\right]$$

$$+\left[\rho S_1\left(a + C_{D_0} + \frac{a^2\alpha_0^2}{\pi AR}\right)\right]\left[-V_0Y_1\cos i_w\right]\Big\}$$

$$+\left[-Y_2\sin\delta_3 + X_2\cos\delta_3 - \ell_2\sin i_w + \ell_1\cos i_w\right]\Big\{\left[-S_2\left(\frac{2\rho a^2\alpha_0}{\pi AR}\right)\right]\left[-V_0Y_2\sin i_w\right]$$

$$+\left[\rho S_2\left(a + C_{D_0} + \frac{a^2\alpha_0}{\pi AR}\right)\right]\left[-V_0Y_2\cos i_w\right]\Big\}$$

$$A_{12} = \left[-l_2 \cos i_w - l_1 \sin i_w\right]\left\{\left[\rho\left(C_{D_0} + \frac{a^2\alpha_0^2}{\pi AR}\right)(S_1+S_2)\right]\left[V_0^2 \sin\delta_3 \sin 2i_w\right]\right.$$

$$+\left[\rho\left(\frac{a^2}{\pi AR} - a\right)(S_1+S_2)\right]\left[-V_0^2 \sin\delta_3 \sin 2i_w\right] + \left[\rho\left(a\alpha_0 - \frac{2\alpha_0 a^2}{\pi AR}\right)(S_1+S_2)\right]\left[-V_0^2 \sin\delta_3 \cos 2i_w\right]$$

$$\left.+\left[\rho E(S_1C_1 + S_2C_2)\right] - \rho a t\left[S_1K_1 + S_2K_2\right]\right\}$$

$$+\left[-Y_1 \sin\delta_3 + X_1 \cos\delta_3 - l_2 \sin i_w + l_1 \cos i_w\right]\left\{\left[-\rho a\alpha_0 S_1\right]\left[V_0^2 \sin\delta_3 \sin 2i_w\right]\right.$$

$$+\left[-S_1\left(\frac{2\rho a^2\alpha_0}{\pi AR}\right)\right]\left[-V_0^2 \sin\delta_3 \sin 2i_w\right] + \left[\rho S_1\left(a + C_{D_0} + \frac{a^2\alpha_0^2}{\pi AR}\right)\right]$$

$$\left.\times\left[-V_0^2 \sin\delta_3 \cos 2i_w\right] + \left[\left(\rho a E S_1K_1 + \rho T S_1C_1\right)\right]\right\}$$

$$+\left[-Y_2 \sin\delta_3 + X_2 \cos\delta_3 - l_2 \sin i_w + l_1 \cos i_w\right]\left\{\left[-\rho a\alpha_0 S_2\right]\left[V_0^2 \sin\delta_3 \sin 2i_w\right]\right.$$

$$+\left[-S_2\left(\frac{2\rho a^2\alpha_0}{\pi AR}\right)\right]\left[-V_0^2 \sin\delta_3 \sin 2i_w\right] + \left[\rho S_2\left(a + C_{D_0} + \frac{a^2\alpha_0^2}{\pi AR}\right)\right]\left[-V_0^2 \sin\delta_3 \cos 2i_w\right]$$

$$+\left[\rho a E\, S_2 K_2 + \rho T\, S_2 C_2\right] + \left\{\rho \bar{c} \cos^2\delta_3 \cos\alpha\, (S_1+S_2)\right\}\left\{V_0^2 \sin\delta_3 \sin 2iw\right\}$$

$$+ \left\{\rho \bar{c} \cos^2\delta_3\, \mu_1\, a E\,(S_1 K_1 + S_2 K_2)\right\}$$

$$
\begin{aligned}
B_7 = \{Y_1\} \Big\{ & \left[-\rho a \alpha_0 S_1\right]\left[2V_0\left(l_2 \cos^2 i_w + Y_2 l_1 \sin 2i_w\right)\right] + \left[-S_1\left(\frac{2\rho a^2 \alpha_0}{\pi AR}\right)\right]\Big[2V_0 \sin i_w \big(Y_1 \sin\delta_3 \\
& - X_1 \cos\delta_3 + l_2 \sin i_w - l_1 \cos i_w\big)\Big] + \left[\rho S_1\left(a + C_{D_0} + \frac{a^2\alpha_0^2}{\pi AR}\right)\right]\Big[l_2 V_0 \sin 2i_w \\
& - V_0 l_1 \cos 2i_w + V_0 Y_1 \cos i_w \sin\delta_3 - V_0 X_1 \cos i_w \cos\delta_3\Big] \Big\} \\
+ \{Y_2\} \Big\{ & \left[-\rho a \alpha_0 S_1\right]\left[2V_0\left(l_2 \cos^2 i_w + Y_2 l_1 \sin 2i_w\right)\right] + \left[-S_2\left(\frac{2\rho a^2 \alpha_0}{\pi AR}\right)\right]\Big[2V_0 \sin i_w \big(Y_2 \sin\delta_3 \\
& - X_2 \cos\delta_3 + l_2 \sin i_w - l_1 \cos i_w\big)\Big] + \left[\rho S_2\left(a + C_{D_0} + \frac{a^2\alpha_0^2}{\pi AR}\right)\right]\Big[l_2 V_0 \sin 2i_w \\
& - V_0 l_1 \cos 2i_w + V_0 Y_2 \cos i_w \sin\delta_3 - V_0 X_2 \cos i_w \cos\delta_3\Big] \Big\} \\
+ \{-\sin\delta_3\} & \left\{\rho \bar{c} \cos^2\delta_3 \, C_{M_{a.c.}}(S_1 + S_2)\right\}\left\{2V_0\left[l_2 \cos^2 i_w + \frac{1}{2} l_1 \sin 2i_w\right]\right\}
\end{aligned}
$$

$$B_8 = \{Y_1\}\left\{\left[-S_1\left(\frac{2\rho a^2\alpha_0}{\pi AR}\right)\right]\left[V_0^2 \sin 2i_w\right] + \left[\rho S_1\left(a + C_{D_0} + \frac{a^2\alpha_0^2}{\pi AR}\right)\right]\left[V_0^2 \cos 2i_w\right] + \left[\rho a \alpha_0 S_1\right]\left[V_0^2 \sin 2i_w\right]\right\}$$

$$+ \{Y_2\}\left\{\left[-S_2\left(\frac{2\rho a^2\alpha_0}{\pi AR}\right)\right]\left[V_0^2 \sin 2i_w\right] + \left[\rho S_2\left(a + C_{D_0} + \frac{a^2\alpha_0^2}{\pi AR}\right)\right]\left[V_0^2 \cos 2i_w\right] + \left[\rho a \alpha_0 S_2\right]\left[V_0^2 \sin 2i_w\right]\right\}$$

$$B_9 = \{Y_1\}\left\{\left[-\rho a \alpha_0 S_1\right]\left[2V_0 \cos^2 i_w\right] + \left[-S_1\left(\frac{2\rho a^2\alpha_0}{\pi AR}\right)\right]\left[2V_0 \sin^2 i_w\right] + \left[\rho S_1\left(a + C_{D_0} + \frac{a^2\alpha_0^2}{\pi AR}\right)\right]\left[V_0 \sin 2i_w\right]\right\}$$

(B_9 CONT.)

$$+\{Y_2\}\Big\{\Big[-\rho a \alpha_0 S_2\Big]\Big[2V_0 \cos^2 i_w\Big] + \Big[-S_2\Big(\frac{2\rho a^2 \alpha_0}{\pi AR}\Big)\Big]\Big[2V_0 \sin^2 i_w\Big]$$

$$+\Big[\rho S_2\Big(a + C_{D_0} + \frac{a^2\alpha_0^2}{\pi AR}\Big)\Big]\Big[V_0 \sin 2 i_w\Big]\Big\}$$

$$+\{-\sin\delta_3\}\Big\{\Big[\rho \bar{c} \cos^2\delta_3\, C_{M_{a.c.}}(S_1 + S_2)\Big]\Big[2V_0 \cos^2 i_w\Big]\Big\}$$

$$B_{10} = \{Y_1\}\Big\{\Big[-\rho a \alpha_0 S_1\Big]\Big[2V_0 \cos^2 i_w\Big] + \Big[-S_1\Big(\frac{2\rho a^2 \alpha_0}{\pi AR}\Big)\Big]\Big[2V_0 \sin^2 i_w\Big] + \Big[\rho S_1\Big(a + C_{D_0} + \frac{a^2\alpha_0^2}{\pi AR}\Big)\Big]$$

$$\Big[V_0 \sin 2 i_w\Big]\Big\}$$

$$+\{Y_2\}\Big\{\Big[-\rho a \alpha_0 S_2\Big]\Big[2V_0 \cos^2 i_w\Big] + \Big[-S_2\Big(\frac{2\rho a^2 \alpha_0}{\pi AR}\Big)\Big]\Big[2V_0 \sin^2 i_w\Big] + \Big[\rho S_2\Big(a + C_{D_0} + \frac{a^2\alpha_0^2}{\pi AR}\Big)\Big]$$

$$\Big[V_0 \sin 2 i_w\Big]\Big\}$$

(B_{10} CONT.)

$$+\{-\sin\delta_3\}\left\{\left[\rho\bar{c}\cos^2\delta_3\, C_{M_{a.c.}}(S_1+S_2)\right]\left[2V_0\cos^2 i\omega\right]\right.$$

$$B_{11}=\{Y_1\}\left\{S_1\left(\frac{2\rho a^2\alpha_0}{\pi A\!\!R}\right)\left(2V_0Y_1\sin i\omega\right)+\left[\rho S_1\left(a+C_{D_0}+\frac{a^2\alpha_0^2}{\pi A\!\!R}\right)\right]\left[-V_0Y_1\cos i\omega\right]\right\}$$

$$+\{Y_2\}\left\{S_2\left(\frac{2\rho a^2\alpha_0}{\pi A\!\!R}\right)\left(2V_0Y_2\sin i\omega\right)+\left[\rho S_2\left(a+C_{D_0}+\frac{a^2\alpha_0^2}{\pi A\!\!R}\right)\right]\left[-V_0Y_2\cos i\omega\right]\right\}$$

$$B_{12}=\{Y_1\}\left\{\left[-\rho a\alpha_0S_1\right]\left[V_0^2\sin\delta_3\sin 2i\omega\right]+\left[S_1\left(\frac{2\rho a^2\alpha_0}{\pi A\!\!R}\right)\right]\left[V_0^2\sin\delta_3\sin 2i\omega\right]\right.$$

$$\left.+\left[\rho S_1\left(a+C_{D_0}+\frac{a^2\alpha_0^2}{\pi A\!\!R}\right)\right]\left[-V_0^2\sin\delta_3\cos 2i\omega\right]+\left[\rho a E S_1K_1+\rho T S_1 C_1\right]\right\}$$

$(B_{12}$ CONT.)

$$+\{Y_2\}\Big\{\left[-\rho a \alpha_0 S_2\right]\left[V_0^{\,2} \sin\delta_3 \sin 2 i\omega\right] + \left[S_2\left(\frac{2\rho a^2 \alpha_0}{\pi A\!R}\right)\right]\left[V_0^{\,2} \sin\delta_3 \sin 2 i\omega\right]$$

$$+\left[\rho S_2\left(a + C_{D_0} + \frac{a^2 \alpha_0^{\,2}}{\pi A\!R}\right)\right]\left[-V_0^{\,2} \sin\delta_3 \cos 2 i\omega\right] + \left[\rho a E S_2 K_2 + \rho T S_2 C_2\right]\Big\}$$

$$+\{-\sin\delta_3\}\Big\{\left[\rho \bar{c} \cos^2\delta_3\, C_{m_{a.c.}}(S_1 + S_2)\right]\left[V_0^{\,2} \sin\delta_3 \sin 2 i\omega\right]$$

$$+\left[\rho \bar{c} \cos^2\delta_3\, \mu_1\, a E\,(S_1 K_1 + S_2 K_2)\right]\Big\}$$

$$
\begin{aligned}
C_q = \{-\cos i_w\} \Bigg\{ & \left[\rho\left(C_{D_0} + \frac{a^2\alpha_0^2}{\pi AR}\right)(S_1 + S_2)\right]\left[2V_0\left(l_2 \cos^2 i_w + \tfrac{1}{2} l_1 \sin 2 i_w\right)\right] + \left[\rho\left(\frac{a^2}{\pi AR} - a\right)\right] \\
& \cdot\left[2V_0 \sin i_w\right]\left[(S_1 Y_1 + S_2 Y_2)\sin\delta_3 - (X_1 S_1 + X_2 S_2)(\cos\delta_3) + (S_1 + S_2)(l_2 \sin i_w - l_1 \cos i_w)\right] \\
& + \left[\rho\left(a\alpha_0 - \frac{2\alpha_0 a^2}{\pi AR}\right)\right]\left[(S_1 + S_2)V_0\left(l_2 \sin 2i_w - l_1 \cos 2 i_w\right) + (S_1 Y_1 + S_2 Y_2)(V_0 \cos i_w \sin\delta_3)\right. \\
& \left. - (S_1 X_1 + S_2 X_2)(V_0 \cos i_w \cos\delta_3)\right]\Bigg\} \\
- \{\sin i_w\} \Bigg\{ & \left[-\rho a\alpha_0 (S_1 + S_2)\right]\left[2V_0\left(l_2 \cos^2 i_w + \tfrac{1}{2} l_1 \sin 2 i_w\right)\right] + \left[-\frac{2\rho a^2\alpha_0}{\pi AR}\right]\left[2V_0 \sin i_w\right] \\
& \cdot\left[(S_1 Y_1 + S_2 Y_2)(\sin\delta_3) - (S_1 X_1 + S_2 X_2)(\cos\delta_3) + (S_1 + S_2)(l_2 \sin i_w - l_1 \cos i_w)\right] \\
& + \rho\left[a + C_{D_0} + \frac{a^2\alpha_0^2}{\pi AR}\right]\left[(S_1 + S_2)(l_2 V_0 \sin 2i_w - V_0 l_1 \cos i_w + V_0 Y_1 \cos i_w \sin\delta_3\right. \\
& \left. - V_0 X_1 \cos i_w \cos\delta_3)\right]\Bigg\}
\end{aligned}
$$

$$C_S = \left\{-\cos i\omega\right\}\left\{\left[\rho\left(\frac{a^2}{\pi AR} - a\right)(S_1 + S_2)\right]\left[V_0^2 \sin 2i\omega\right] + \left[\rho\left(a\alpha_0 - \frac{2\alpha_0 a^2}{\pi AR}\right)(S_1 + S_2)\right]\left[V_0^2 \cos 2i\omega\right]\right.$$

$$\left. + \left[\rho\left(C_{D_0} + \frac{a^2\alpha_0^2}{\pi AR}\right)(S_1 + S_2)\right]\left[-V_0 \sin 2i\omega\right]\right\}$$

$$-\left\{\sin i\omega\right\}\left\{\left[-(S_1 + S_2)\left(\frac{2\rho a^2 \alpha_0}{\pi AR}\right)\right]\left[V_0^2 \sin 2i\omega\right] + \left[\rho(S_1 + S_2)\left(a + C_{D_0} + \frac{a^2\alpha_0^2}{\pi AR}\right)\right]\right.$$

$$\left.\left[V_0^2 \cos 2i\omega\right] + \left[(S_1 + S_2)(-\rho a \alpha_0)\right]\left[-V_0^2 \sin 2i\omega\right]\right\}$$

$$C_L = \left\{-\cos i\omega\right\}\left\{\left[\rho\left(C_{D_0} + \frac{a^2\alpha_0^2}{\pi AR}\right)(S_1 + S_2)\right]\left[-V_0 \sin 2i\omega\right] + \left[\rho\left(\frac{a^2}{\pi AR} - a\right)(S_1 + S_2)\right]\left[V_0 \sin 2i\omega\right]\right.$$

$$\left. + \left[\rho\left(a\alpha_0 - \frac{2\alpha_0 a^2}{\pi AR}\right)(S_1 + S_2)\right]\left[V_0 \cos 2i\omega\right]\right\}$$

(C_6 CONT.)

$$-\{\sin i_w\}\Big\{\Big[-\rho a\alpha_0(S_1+S_2)\Big]\Big[-V_0 \sin 2 i_w\Big]+\Big[-\Big(\frac{2\rho a^2\alpha_0}{\pi AR}\Big)(S_1+S_2)\Big]\Big[V_0 \sin 2 i_w\Big]$$

$$+\Big[\rho\Big(a + C_{D_0} + \frac{a^2\alpha_0^2}{\pi AR}\Big)(S_1+S_2)\Big]\Big[V_0 \cos 2 i_w\Big]\Big\}$$

$$C_7 = -\{\cos i_w\}\Big\{\Big[\rho\Big(C_{D_0} + \frac{a^2\alpha_0^2}{\pi AR}\Big)(S_1+S_2)\Big]\Big[2V_0 \cos^2 i_w\Big]+\Big[\rho\Big(\frac{a^2}{\pi AR}-2\Big)(S_1+S_2)\Big]\Big[2V_0 \sin^2 i_w\Big]$$

$$+\Big[\rho\Big(a\alpha_0 - \frac{2\alpha_0 a^2}{\pi AR}\Big)(S_1+S_2)\Big]\Big[V_0 \sin 2 i_w\Big]\Big\}$$

$$-\{\sin i_w\}\Big\{\Big[-\rho a\alpha_0(S_1+S_2)\Big]\Big[2V_0 \cos^2 i_w\Big]+\Big[-\Big(\frac{2\rho a^2\alpha_0}{\pi AR}\Big)(S_1+S_2)\Big]\Big[2V_0 \sin^2 i_w\Big]$$

$$+\Big[\rho\Big(a + C_{D_0} + \frac{a^2\alpha_0^2}{\pi AR}\Big)(S_1+S_2)\Big]\Big[V_0 \sin 2 i_w\Big]$$

$$C_q = -\{\cos i_w\}\Big\{\Big[\rho\Big(\frac{a^2}{\pi AR}-a\Big)S_1\Big]\Big[-2V_0Y_1\sin i_w\Big]+\Big[\rho\Big(a\alpha_0-\frac{2\alpha_0 a^2}{\pi AR}\Big)S_1\Big]\Big[-V_0Y_1\cos i_w\Big]$$

$$+\Big[\rho\Big(\frac{a^2}{\pi AR}-a\Big)S_2\Big]\Big[-2V_0Y_2\sin i_w\Big]+\Big[\rho\Big(a\alpha_0-\frac{2\alpha_0 a^2}{\pi AR}\Big)S_2\Big]\Big[-V_0Y_2\cos i_w\Big]\Big\}$$

$$-\{\sin i_w\}\Big\{\Big[-S_1\Big(\frac{2\rho a^2\alpha_0}{\pi AR}\Big)\Big]\Big[-2V_0Y_1\sin i_w\Big]+\Big[\rho S_1\Big(a+C_{D_0}+\frac{a^2\alpha_c^2}{\pi AR}\Big)\Big]\Big[-V_0Y_1\cos i_w\Big]$$

$$+\Big[-S_2\Big(\frac{2\rho a^2\alpha_c}{\pi AR}\Big)\Big]\Big[-2V_0Y_2\sin i_w\Big]+\Big[\rho S_2\Big(a+C_{D_0}+\frac{a^2\alpha_0^2}{\pi AR}\Big)\Big]\Big[-V_0Y_2\cos i_w\Big]$$

$$C_q = -\{\cos i_w\}\Big\{\Big[\rho\Big(C_{D_0}+\frac{a^2\alpha_0^2}{\pi AR}\Big)(S_1+S_2)\Big]\Big[V_0^2\sin\delta_3\sin 2i_w\Big]+\Big[\rho\Big(\frac{a^2}{\pi AR}-a\Big)(S_1+S_2)\Big]$$

$$\circ\Big[-V_0^2\sin\delta_3\sin 2i_w\Big]+\Big[\rho\Big(a\alpha_0-\frac{2\alpha_0 a^2}{\pi AR}\Big)(S_1+S_2)\Big]\Big[-V_0^2\sin\delta_3\cos 2i_w\Big]$$

$$+\rho E(S_1C_1+S_2C_2)-\rho aT(S_1K_1+S_2K_2)\Big\}$$

(C_q CONT.)

$$-\{\sin i_w\}\Big\{\Big[-\rho a \alpha_0 (S_1 + S_2)\Big]\Big[V_0^2 \sin\delta_3 \sin 2 i_w\Big] + \Big[-\Big(\frac{2\rho a^2 \alpha_0}{\pi A\!R}\Big)(S_1 + S_2)\Big]\Big[-V_0^2 \sin\delta_3 \sin 2 i_w\Big]$$

$$+\Big[\rho\Big(a + C_{D_0} + \frac{a^2 \alpha_0^2}{\pi A\!R}\Big)(S_1 + S_2)\Big]\Big[-V_0^2 \sin\delta_3 \cos 2 i_w\Big]$$

$$+ \rho a E (S_1 K_1 + S_2 K_2) + \rho T (S_1 C_1 + S_2 C_2)\Big\}$$

$$D_4 = \left\{\sin i_w\right\}\left\{\left[\rho\left(C_{D_0} + \frac{a^2\alpha_0^2}{\pi AR}\right)(S_1 + S_2)\right]\left[2V_0\left(\ell_2 \cos^2 i_w + \tfrac{1}{2}\ell_1 \sin 2 i_w\right)\right] + \left[\rho\left(\frac{a^2}{\pi AR} - a\right)\right]\right.$$

$$\cdot\left[2V_0 \sin i_w\right]\left[(S_1Y_1 + S_2Y_2)(\sin\delta_3) - (X_1S_1 + X_2S_2)(\cos\delta_3) + (S_1+S_2)(\ell_2 \sin i_w - \ell_1 \cos i_w)\right]$$

$$+\left[\rho\left(a\alpha_0 - \frac{2\alpha_0 a^2}{\pi AR}\right)\right]\left[(S_1+S_2)(\ell_2 V_0 \sin 2 i_w - V_0 \ell_1 \cos 2 i_w)\right.$$

$$\left.\left. + (S_1Y_1 + S_2Y_2)(V_0 \cos i_w \sin\delta_3) - (S_1X_1 + S_2X_2)(V_0 \cos i_w \cos\delta_3)\right]\right\}$$

$$-\left\{\cos i_w\right\}\left\{\left[-\rho a\alpha_0(S_1+S_2)\right]\left[2V_0\left(\ell_2\cos^2 i_w + \tfrac{1}{2}\ell_1 \sin 2 i_w\right)\right] - \left[\frac{2\rho a^2\alpha_0}{\pi AR}\right]\right.$$

$$\cdot\left[2V_0 \sin i_w\right]\left[(S_1Y_1 + S_2Y_2)(\sin\delta_3) - (S_1X_1 + S_2X_2)(\cos\delta_3) + (S_1+S_2)(\ell_2 \sin i_w - \ell_1 \cos i_w)\right]$$

$$+\rho\left[a + C_{D_0} + \frac{a^2\alpha_0^2}{\pi AR}\right]\left[(S_1+S_2)(\ell_2 V_0 \sin 2 i_w - V_0\ell_1 \cos i_w + V_0 Y_1 \cos i_w \sin\delta_3\right.$$

$$\left.\left. - V_0 X_1 \cos i_w \cos\delta_3)\right]\right\}$$

$$D_s = \{\sin i_w\}\left\{\left[\rho\left(\frac{a^2}{\pi AR} - a\right)(S_1 + S_2)\right]\left[V_0^2 \sin 2 i_w\right] + \left[\rho\left(a\alpha_0 - \frac{2\alpha_0 a^2}{\pi AR}\right)(S_1 + S_2)\right]\left[V_0^2 \cos 2 i_w\right]\right.$$

$$\left. + \left[\rho\left(C_{D_0} + \frac{a^2\alpha_0^2}{\pi AR}\right)(S_1 + S_2)\right]\left[-V_0^2 \sin 2 i_w\right]\right\}$$

$$-\{\cos i_w\}\left\{\left[-\left(\frac{2\rho a^2\alpha_0}{\pi AR}\right)(S_1 + S_2)\right]\left[V_0^2 \sin 2 i_w\right] + \left[\rho\left(a + C_{D_0} + \frac{a^2\alpha_0^2}{\pi AR}\right)(S_1 + S_2)\right]\left[V_0^2 \cos 2 i_w\right]\right.$$

$$\left. + \left[-\rho_a \alpha_0 (S_1 + S_2)\right]\left[-V_0^2 \sin 2 i_w\right]\right\}$$

$$D_c = \{\sin i_w\}\left\{\left[\rho\left(C_{D_0} + \frac{a^2\alpha_0^2}{\pi AR}\right)(S_1 + S_2)\right]\left[-V_0 \sin 2 i_w\right] + \left[\rho\left(\frac{a^2}{\pi AR} - a\right)(S_1 + S_2)\right]\left[V_0 \sin 2 i_w\right]\right.$$

$$\left. + \left[\rho\left(a\alpha_0 - \frac{2\alpha_0 a^2}{\pi AR}\right)(S_1 + S_2)\right]\left[V_0 \cos 2 i_w\right]\right\}$$

(D_6 CONT.)

$$-\{\cos i_w\}\Bigg\{\left[-\rho a \alpha_0 (S_1+S_2)\right]\left[-V_0 \sin 2 i_w\right] + \left[-\left(\frac{2\rho a^2 \alpha_0}{\pi A\!\!R}\right)(S_1+S_2)\right]\left[V_0 \sin 2 i_w\right]$$

$$+\left[\rho\left(a + C_{D_0} + \frac{a^2\alpha_0^2}{\pi A\!\!R}\right)(S_1+S_2)\right]\left[V_0 \cos 2 i_w\right]\Bigg\}$$

$$D_7 = \{\sin i_w\}\Bigg\{\left[\rho\left(C_{D_0} + \frac{a^2\alpha_0^2}{\pi A\!\!R}\right)(S_1+S_2)\right]\left[2V_0 \cos^2 i_w\right] + \left[\rho\left(\frac{a^2}{\pi A\!\!R} - a\right)(S_1+S_2)\right]\left[2V_0 \sin^2 i_w\right]$$

$$+\left[\rho\left(a\alpha_0 - \frac{2\alpha_0 a^2}{\pi A\!\!R}\right)(S_1+S_2)\right]\left[V_0 \sin 2 i_w\right]\Bigg\}$$

$$-\{\cos i_w\}\Bigg\{\left[-\rho a \alpha_0 (S_1+S_2)\right]\left[2V_0 \cos^2 i_w\right] - \left[\left(\frac{2\rho a^2 \alpha_0}{\pi A\!\!R}\right)(S_1+S_2)\right]\left[2V_0 \sin^2 i_w\right]$$

$$+\left[\rho\left(a + C_{D_0} + \frac{a^2\alpha_0^2}{\pi A\!\!R}\right)(S_1+S_2)\right]\left[V_0 \sin 2 i_w\right]\Bigg\}$$

$$D_g = \{\sin i_w\}\Big\{\Big[\rho\Big(\frac{a^2}{\pi AR} - a\Big)S_1\Big]\Big[-2V_0Y_1 \sin i_w\Big] + \Big[\rho\Big(a\alpha_0 - \frac{2\alpha_0 a^2}{\pi AR}\Big)S_1\Big]\Big[-V_0Y_1 \cos i_w\Big]$$

$$+\Big[\rho\Big(\frac{a^2}{\pi AR} - a\Big)S_2\Big]\Big[-2V_0Y_2 \sin i_w\Big] + \Big[\rho\Big(a\alpha_0 - \frac{2\alpha_0 a^2}{\pi AR}\Big)S_2\Big]\Big[-V_0 Y_2 \cos i_w\Big]\Big\}$$

$$-\{\cos i_w\}\Big\{\Big[-S_1\Big(\frac{2\rho a^2\alpha_0}{\pi AR}\Big)\Big]\Big[-2V_0Y_1 \sin i_w\Big] + \Big[\rho S_1\Big(a + C_{D_0} + \frac{a^2\alpha_0^2}{\pi AR}\Big)\Big]\Big[-V_0Y_1 \cos i_w\Big]$$

$$+\Big[-S_2\Big(\frac{2\rho\alpha_0 a^2}{\pi AR}\Big)\Big]\Big[-2V_0Y_2 \sin i_w\Big] + \Big[\rho S_2\Big(a + C_{D_0} + \frac{a^2\alpha_0^2}{\pi AR}\Big)\Big]\Big[-V_0Y_2 \cos i_w\Big]\Big\}$$

$$D_q = \{\sin i_w\}\Big\{\Big[\rho\Big(C_{D_0} + \frac{a^2\alpha_0^2}{\pi AR}\Big)(S_1+S_2)\Big]\Big[V_0^2 \sin\delta_3 \sin 2i_w\Big] + \Big[\rho\Big(\frac{a^2}{\pi AR} - a\Big)(S_1+S_2)\Big]$$

$$\cdot\Big[-V_0^2 \sin i_n \sin 2i_w\Big] + \Big[\rho\Big(a\alpha_0 - \frac{2\alpha_0 a^2}{\pi AR}\Big)(S_1+S_2)\Big]\Big[-V_0^2 \sin\delta_3 \cos 2i_w\Big]$$

$$+\Big[\rho E(S_1C_1 + S_2C_2)\Big] - \Big[\rho a T(S_1K_1 + S_2K_2)\Big]\Big\}$$

(D_q CONT.)

$$-\{\cos i_w\}\Big\{\Big[-\rho a \alpha_0 (S_1+S_2)\Big]\Big[V_0^2 \sin\delta_3 \sin 2 i_w\Big]+\Big[\Big(\frac{2\rho a^2\alpha_0}{\pi A\!R}\Big)(S_1+S_2)\Big]\Big[V_0^2 \sin\delta_3 \sin 2 i_w\Big]$$

$$+\Big[\rho\Big(a + C_{D_0} + \frac{a^2\alpha_0^2}{\pi A\!R}\Big)(S_1+S_2)\Big]\Big[-V_0^2 \sin\delta_3 \cos 2 i_w\Big]$$

$$+\Big[\rho a E (S_1 K_1 + S_2 K_2)\Big] + \Big[\rho T (S_1 C_1 + S_2 C_2)\Big]\Big\}$$

FINAL EQUATIONS OF MOTION

$$(1)\quad A_1\ddot{\theta} + \left[A_2 - A_8 - M_{\theta_H}\right]\theta + A_3\ddot{z} + A_4\ddot{x} + A_5\ddot{\beta}_H + \left[A_6 - A_{12}\right]\beta_H - \left[A_7 + M_{\dot{\theta}_H}\right]\dot{\theta}$$

$$- \left[A_9 + M_{\dot{z}_H}\right]\dot{z} - \left[A_{10} + M_{\dot{x}_H}\right]\dot{x} - A_{11}\dot{\beta}_H = 0$$

$$(2)\quad B_1\ddot{\theta} + \left[B_2 - B_8\right]\theta + B_3\ddot{z} + B_4\ddot{x} + B_5\ddot{\beta}_H + \left[B_6 - B_{12}\right]\beta_H - B_7\dot{\theta} - B_9\dot{z}$$

$$- B_{10}\dot{x} - B_{11}\dot{\beta}_H = 0$$

$$(3)\quad C_1\ddot{\theta} + C_2\ddot{x} + C_3\ddot{\beta}_H - \left[C_4 + X_{\dot{\theta}_H}\right]\dot{\theta} - C_5\theta - \left[C_6 + X_{\dot{z}_H}\right]\dot{z} - \left[C_7 + X_{\dot{x}_H}\right]\dot{x}$$

$$- C_8\dot{\beta}_H - C_9\beta_H = 0$$

$$(4)\quad D_1\ddot{\theta} + D_2\ddot{z} + D_3\ddot{\beta}_H - \left[D_4 + Z_{\dot{\theta}_H}\right]\dot{\theta} - \left[D_5 + Z_{\theta_H}\right]\theta - \left[D_6 + Z_{\dot{z}_H}\right]\dot{z}$$

$$- \left[D_7 + Z_{\dot{x}_H}\right]\dot{x} - D_8\dot{\beta}_H - D_9\beta_H = 0$$

TABLE 1

TABLE OF CONFIGURATIONS

CASE NO.	δ_3	WING POS.	INBD. FLAP GEARING	OUTBD. FLAP GEARING	FUEL TANKS
12	0	FWD	0	0	FULL
1	45	FWD	0	0	FULL
4	0	FWD	1	1	FULL
18	0	FWD	1	1	EMPTY
20	0	AFT	3	3	EMPTY
21	0	AFT	2	2	EMPTY
22	0	AFT	1	1	EMPTY
25	0	AFT	3	3	FULL
26	0	AFT	2	2	FULL
27	0	AFT	1	1	FULL

OR CONFIGURATIONS USING GEARED FLAP, INBOARD FLAP MOVES COUNTER TO WING DEFLECTION; OUTBOARD FLAP MOVES IN SAME SENSE AS WING.

TABLE 2

TABLES OF NUMERICAL COEFFICIENTS

Input Sheet

1201 A_1	1219 A_3	1237 A_4	1255 A_5	1273	1291
1202 $-A_7 - M_{\dot{\theta}_H}$	1220 $-A_9 - M_{\dot{z}_H}$	1238 $-A_{10} - M_{\dot{x}_H}$	1256 $-A_{11}$	1274	1292
1203 $A_2 - A_8 - M_{\theta_H}$	1221 0	1239 0	1257 $A_6 - A_{12}$	1275	1293
1204 D_1	1222 D_2	1240 0	1258 D_3	1276	1294
1205 $-D_4 - Z_{\dot{\theta}_H}$	1223 $-D_6 - Z_{\dot{z}_H}$	1241 $-D_7 - Z_{\dot{x}_H}$	1259 $-D_8$	1277	1295
1206 $-D_5 - Z_{\theta_H}$	1224 0	1242 0	1260 $-D_9$	1278	1296
1207 C_1	1225 0	1243 C_2	1261 C_3	1279	1297
1208 $-C_4 - X_{\dot{\theta}_H}$	1226 $-C_6 - X_{\dot{z}_H}$	1244 $-C_7 - X_{\dot{x}_H}$	1262 $-C_8$	1280	1298
1209 $-C_5 - X_{\theta_H}$	1227 0	1245 0	1263 $-C_9$	1281	1299
1210 B_1	1228 B_3	1246 B_4	1264 B_5	1282	1300
1211 $-B_7$	1229 $-B_9$	1247 $-B_{10}$	1265 $-B_{11}$	1283	1301
1212 $+B_2 - B_8$	1230 0	1248 0	1266 $B_6 - B_{12}$	1284	1302
1213	1231	1249	1267	1285	1303
1214	1232	1250	1268	1286	1304
1215	1233	1251	1269	1287	1305
1216	1234	1252	1270	1288	1306
1217	1235	1253	1271	1289	1307
1218	1236	1254	1272	1290	1308

TABLE 3

LONGITUDINAL CASE 12

1201 161710	1219 -5083	1237 2649	1255 62400	1273	1291
1202 188176	1220 -6194	1238 -971	1256 62010	1274	1292
1203 -730573	1221 0	1239 0	1257 -12480	1275	1293
1204 -5083	1222 780	1240 0	1258 -5530	1276	1294
1205 -690	1223 541	1241 78	1259 -4235	1277	1295
1206 79464	1224 0	1242 0	1260 0	1278	1296
1207 2650	1225 0	1243 760	1261 -387	1279	1297
1208 -426	1226 -73	1244 44	1262 364	1280	1298
1209 -9280	1227 0	1245 0	1263 0	1281	1299
1210 62400	1228 -5530	1246 -387	1264 112000	1282	1300
1211 38468	1229 -4271	1247 -1110	1265 69210	1283	1301
1212 -584280	1230 0	1248 0	1266 0	1284	1302
1213	1231	1249	1267	1285 0	1303
1214	1232	1250	1268	1286 0	1304
1215	1233	1251	1269	1287 1	1305
1216	1234	1252	1270	1288	1306 0
1217	1235	1253	1271	1289	1307 0
1218	1236	1254	1272	1290	1308 1

TABLE 4

LONGITUDINAL CASE 1

1201 235218	1219 -5093	1237 2650	1255 45871	1273	1291
1202 1[illegible]9833	1220 -6092	1238 -908	1256 43110	1274	1292
1203 -733600	1221 0	1239 0	1257 469241	1275	1293
1204 -5093	1222 780	1240 0	1258 -3864	1276	1294
1205 -704	1223 589	1241 78	1259 -3022	1277	1295
1206 80100	1224 0	1242 0	1260 -33057	1278	1296
1207 2650	1225 0	1243 780	1261 -322	1279	1297
1208 -935	1226 -69	1244 44	1262 250	1280	1298
1209 -9300	1227 0	1245 0	1263 2810	1281	1299
1210 45871	1228 -4625	1246 -324	1264 68350	1282	1300
1211 27740	1229 -2961	1247 -735	1265 33639	1283	1301
1212 -408858	1230 0	1248 0	1266 279717	1284	1302
1213	1231	1249	1267	1285 0	1303
1214	1232	1250	1268	1286 0	1304
1215	1233	1251	1269	1287 1	1305
1216	1234	1252	1270	1288	1306 0
1217	1235	1253	1271	1289	1307 0
1218	1236	1254	1272	1290	1308 1

TABLE 5

LONGITUDINAL CASE 4

1201	1219 For BLANKS SEE	1237	1255	1273	1291
1202	1220 CASE 12	1238	1256	1274	1292
1203	1221	1239	1257 -34076	1275	1293
1204	1222	1240	1258	1276	1294
1205	1223	1241	1259	1277	1295
1206	1224	1242	1260 215	1278	1296
1207	1225	1243	1261	1279	1297
1208	1226	1244	1262	1280	1298
1209	1227	1245	1263 -1337	1281	1299
1210	1228	1246	1264	1282	1300
1211	1229	1247	1265	1283	1301
1212	1230	1248	1266 172700	1284	1302
1213	1231	1249	1267	1285 0	1303
1214	1232	1250	1268	1286 0	1304
1215	1233	1251	1269	1287 1	1305
1216	1234	1252	1270	1288	1306 0
1217	1235	1253	1271	1289	1307 0
1218	1236	1254	1272	1290	1308 1

TABLE 6

LONGITUDINAL CASE 18

1201 [illegible]	1219 -72[illegible]	1237	1255 1	1273	1291
1202 [illegible]	1220 [illegible]	1238 -1212	1256 1	1274	1292
1203 [illegible]	1221 [illegible]	1239 0	1257 1	1275	1293
1204 -7[illegible]	1222 407	1240 0	1258 1	1276	1294
1205 -[illegible]115	1223 616	1241 1[illegible]	1259 [illegible]	1277	1295
1206 [illegible]	1224 0	1242 0	1260 215[illegible]	1278	1296
1207 378	1225 0	1243 901	1261 -60	1279	1297
1208 -77	1226 -74	1244 2[illegible]	1262 [illegible]	1280	1298
1209 -10032	1227 0	1245 0	1263 10[illegible]	1281	1299
1210 [illegible]	1228 [illegible]	1246 -6[illegible]	1264 16[illegible]	1282	1300
1211 [illegible]	1229 [illegible]	1247 1107	1265 61[illegible]10	1283	1301
1212 -515439	1230 0	1248 0	1266 193700	1284	1302
1213	1231	1249	1267	1285	1303
1214	1232	1250	1268	1286	1304
1215	1233	1251	1269	1287 1	1305
1216	1234	1252	1270	1288	1306 0
1217	1235	1253	1271	1289	1307 0
1218	1236	1254	1272	1290	1308 1

TABLE 7

LONGITUDINAL CASE 20

1201 77767	1219 142	1237 374	1255 -2359	1273	1291
1202 151713	1220 -921	1238 -16	1256 2103	1274	1292
1203 -99274	1221 0	1239 0	1257 14313	1275	1293
1204 142	1222 117	1240 0	1258 -968	1276	1294
1205 1797	1223 10	1241 94	1259 -116	1277	1295
1206 12046	1224 0	1242 6	1260 7311	1278	1296
1207 378	1225 0	1243 117	1261 -61	1279	1297
1208 -614	1226 -75	1244 24	1262 354	1280	1298
1209 -9384	1227 0	1245 0	1263 6	1281	1299
1210 -2359	1228 -867	1246 -61	1264 163	1282	1300
1211 -5736	1229 -4150	1247 -1104	1265 69220	1283	1301
1212 -562952	1230 0	1248 0	1266 560000	1284	1302
1213	1231	1249	1267	1285 0	1303
1214	1232	1250	1268	1286 0	1304
1215	1233	1251	1269	1287 1	1305
1216	1234	1252	1270	1288	1306 0
1217	1235	1253	1271	1289	1307 0
1218	1236	1254	1272	1290	1308 1

TABLE 8

LONGITUDINAL CASE 21

1201 *	1219	1237	1255	1273	1291
1202	1220	1238	1256	1274	1292
1203	1221	1239	1257 9300	1275	1293
1204	1222	1240	1258	1276	1294
1205	1223	1241	1259	1277	1295
1206	1224	1242	1260 3400	1278	1296
1207	1225	1243	1261	1279	1297
1208	1226	1244	1262	1280	1298
1209	1227	1245	1263 156	1281	1299
1210	1228	1246	1264	1282	1300
1211	1229	1247	1265	1283	1301
1212	1230	1248	1266 403000	1284	1302
1213	1231	1249	1267	1285 0	1303
1214	1232	1250	1268	1286 0	1304
1215	1233	1251	1269	1287 1	1305
1216	1234	1252	1270	1288	1306 0
1217	1235	1253	1271	1289	1307 0
1218	1236	1254	1272	1290	1308 1

* All blanks same as Case 22

TABLE 9

LONGITUDINAL CASE 22

1201 79767	1219 142	1237 378	1255 -2[illegible]9	1273	1291
1202 151313	1220 -821	1238 216	1256 2103	1274	1292
1203 -98274	1221 0	1239 0	1257 2500	1275	1293
1204 142	1222 407	1240 0	1258 [illegible]	1276	1294
1205 1797	1223 610	1241 91	1259 -3916	1277	1295
1206 82086	1224 0	1242 0	1260 -600	1278	1296
1207 378	1225 0	1243 407	1261 -61	1279	1297
1208 -684	1226 -75	1244 21	1262 354	1280	1298
1209 -9384	1227 0	1245 0	1263 -50	1281	1299
1210 -2359	1228 -467	1246 -61	1264 16200	1282	1300
1211 -5736	1229 -4150	1247 -1104	1265 67220	1283	1301
1212 -562952	1230 0	1248 0	1266 245000	1284	1302
1213	1231	1249	1267	1285 0	1303
1214	1232	1250	1268	1286 0	1304
1215	1233	1251	1269	1287 1	1305
1216	1234	1252	1270	1288	1306 0
1217	1235	1253	1271	1289	1307 0
1218	1236	1254	1272	1290	1308 1

TABLE 10

LONGITUDINAL CASE 25

1201 [illegible]	1219 177	1237 [illegible]	1255 -15015	1273	1291
1202 [illegible]	1220 -1245	1238 [illegible]	1256 [illegible]	1274	1292
1203 [illegible]	1221 0	1239 [illegible]	1257 [illegible]	1275	1293
1204 997	1222 780	1240 0	1258 [illegible]	1276	1294
1205 1621	1223 586	1241 78	1259 [illegible]	1277	1295
1206 77464	1224 0	1242 0	1260 1011	1278	1296
1207 2615	1225 0	1243 780	1261 [illegible]	1279	1297
1208 -1011	1226 -70	1244 [illegible]	1262 [illegible]	1280	1298
1209 -9360	1227 0	1245 0	1263 [illegible]	1281	1299
1210 -15015	1228 -55[illegible]	1246 [illegible]	1264 [illegible]	1282	1300
1211 -5730	1229 [illegible]	1247 [illegible]	1265 [illegible]	1283	1301
1212 -573950	1230 [illegible]	1248 [illegible]	1266 [illegible]	1284	1302
1213	1231	1249	1267	1285	1303
1214	1232	1250	1268	1286	1304
1215	1233	1251	1269	1287 1	1305
1216	1234	1252	1270	1288	1306 0
1217	1235	1253	1271	1289	1307 0
1218	1236	1254	1272	1290	1308 1

TABLE 11

LONGITUDINAL CASE 26

1201 *	1219	1237	1255	1273	1291
1202	1220	1238	1256	1274	1292
1203	1221	1239	1257 -2000	1275	1293
1204	1222	1240	1258	1276	1294
1205	1223	1241	1259	1277	1295
1206	1224	1242	1260 3400	1278	1296
1207	1225	1243	1261	1279	1297
1208	1226	1244	1262	1280	1298
1209	1227	1245	1263 150	1281	1299
1210	1228	1246	1264	1282	1300
1211	1229	1247	1265	1283	1301
1212	1230	1248	1266 ·103000	1284	1302
1213	1231	1249	1267	1285 0	1303
1214	1232	1250	1268	1286 0	1304
1215	1233	1251	1269	1287 1	1305
1216	1234	1252	1270	1288	1306 0
1217	1235	1253	1271	1289	1307 5
1218	1236	1254	1272	1290	1308 1

* All blanks same as Case 25

TABLE 12

LONGITUDINAL CASE 27

1201 *	1219	1237	1255	1273	1291
1202	1220	1238	1256	1274	1292
1203	1221	1239	1257 -8300	1275	1293
1204	1222	1240	1258	1276	1294
1205	1223	1241	1259	1277	1295
1206	1224	1242	1260 -600	1278	1296
1207	1225	1243	1261	1279	1297
1208	1226	1244	1262	1280	1298
1209	1227	1245	1263 -50	1281	1299
1210	1228	1246	1264	1282	1300
1211	1229	1247	1265	1283	1301
1212	1230	1248	1266 1500	1284	1302
1213	1231	1249	1267	1285 0	1303
1214	1232	1250	1268	1286 0	1304
1215	1233	1251	1269	1287 1	1305
1216	1234	1252	1270	1288	1306 0
1217	1235	1253	1271	1289	1307 0
1218	1236	1254	1272	1290	1308 1

* All blanks same as Case 25

TABLE 13

SUMMARY OF ROOTS OF THE LONGITUDINAL CHARACTERISTIC EQUATIONS - SHOWING PERIODS AND TIME TO DOUBLE OR HALF AMPLITUDE

CASE	ROOTS PERIODS TIME TO DOUBLE (+) OR HALF (−) AMPLITUDE			
12	·186 ± ·601i	−·0766 ± ·0683i	−·413	−2·50
	10·45	92	—	—
	3·73	9·05	1·68	·28
1	·274 ± ·379i	−·237 ± 1·390i	−·0633	−1·917
	16·58	4·52	—	—
	2·53	2·92	10·95	·362
4	·180 ± ·603i	−·258 ± 1·716i	−·0504	−2·490
	10·42	3·66	—	—
	3·85	2·69	13·75	·28
18	−1·587 ± 3·667i	−4·755 + ·927	+·0092	−·110
	1·71	—	—	—
	·44	·146: ·75	75·3	6·30
20	−·2997 ± ·2582i	−1·798 ± 5·887i	−·0213	−3·0828
	24·33	1·07	—	—
	2·35	·39	32·39	·22
21	−·2837 ± ·2648i	−1·785 ± 4·8138i	−3·1314	−·0213
	23·73	1·305	—	—
	2·44	·39	·22	32·39
22	−·2567 ± ·2776i	−1·7506 ± 3·4293i	−3·254	−·0213
	22·63	1·83	—	—
	2·700	·39	·21	32·39
25	·1083 ± ·516i	−·341 ± 3·161i	−2·70	−·063
	12·18	1·99	—	—
	6·40	2·03	·26	10·95
26	·108 ± ·515i	−·340 ± 2·64i	−2·70	−·063
	12·20	2·38	—	—
	6·42	2·04	·26	10·95
27	·108 ± ·513i	−·339 ± 1·96i	−2·70	−·062
	12·25	3·21	—	—
	6·42	2·04	·26	10·95

BASIC HELICOPTER RESPONSE TO

LONGITUDINAL STEP INPUT

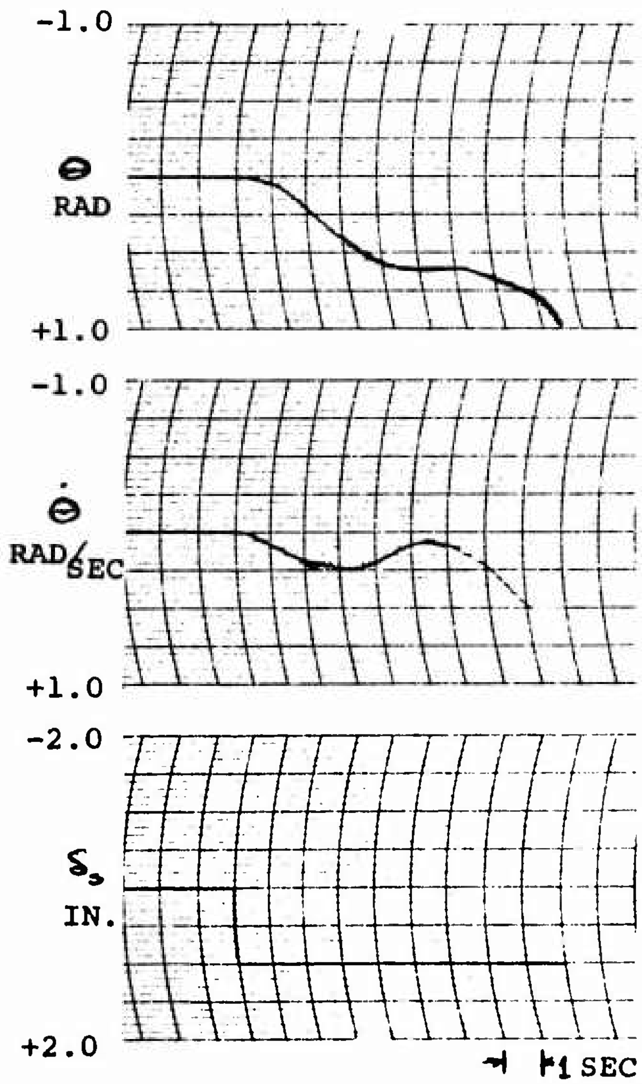

FIGURE 4

LONGITUDINAL CASE 12

30 F.P.S. GUST

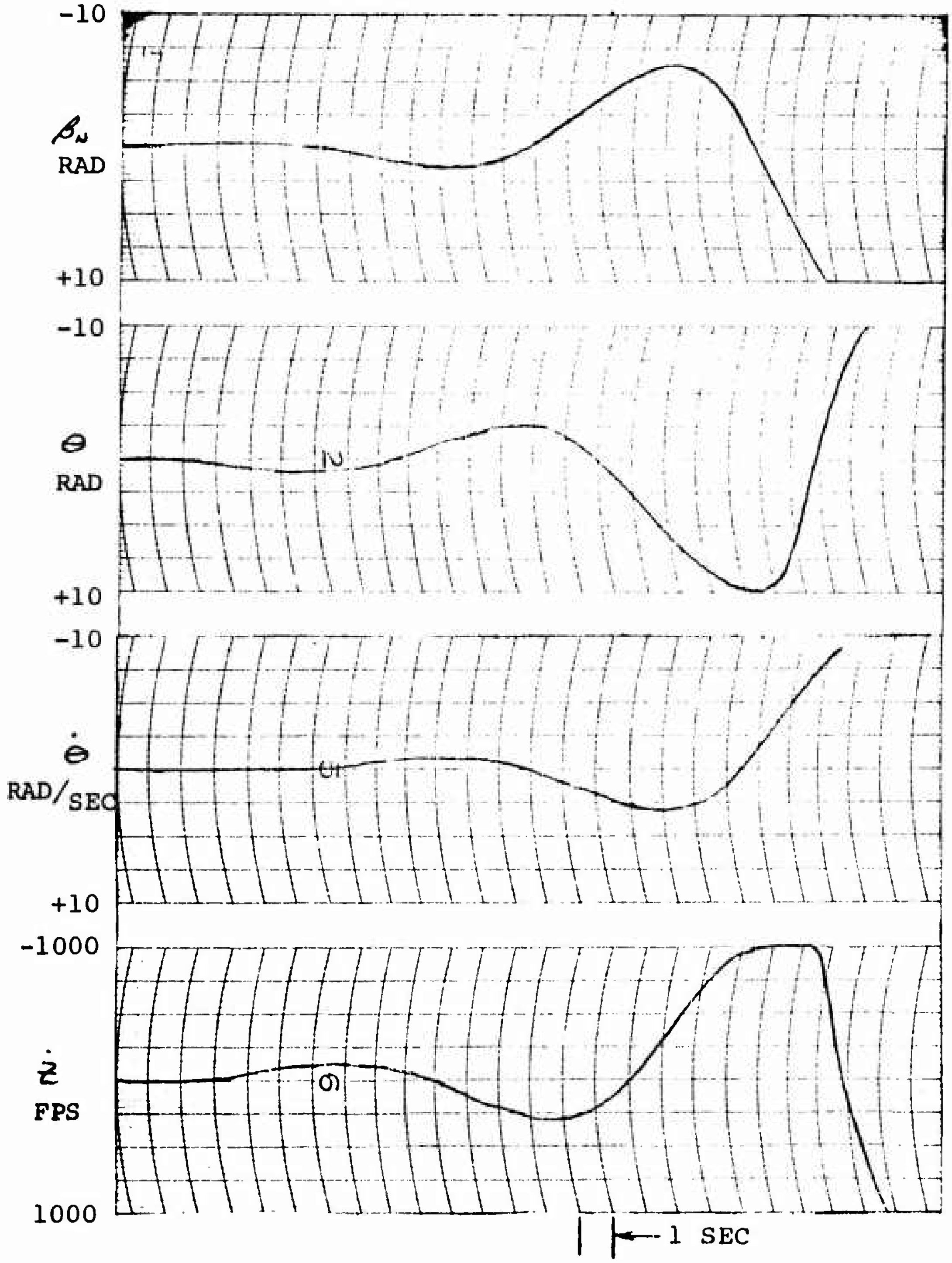

FIGURE 5

LONGITUDINAL CASE 1

30 F.P.S. GUST

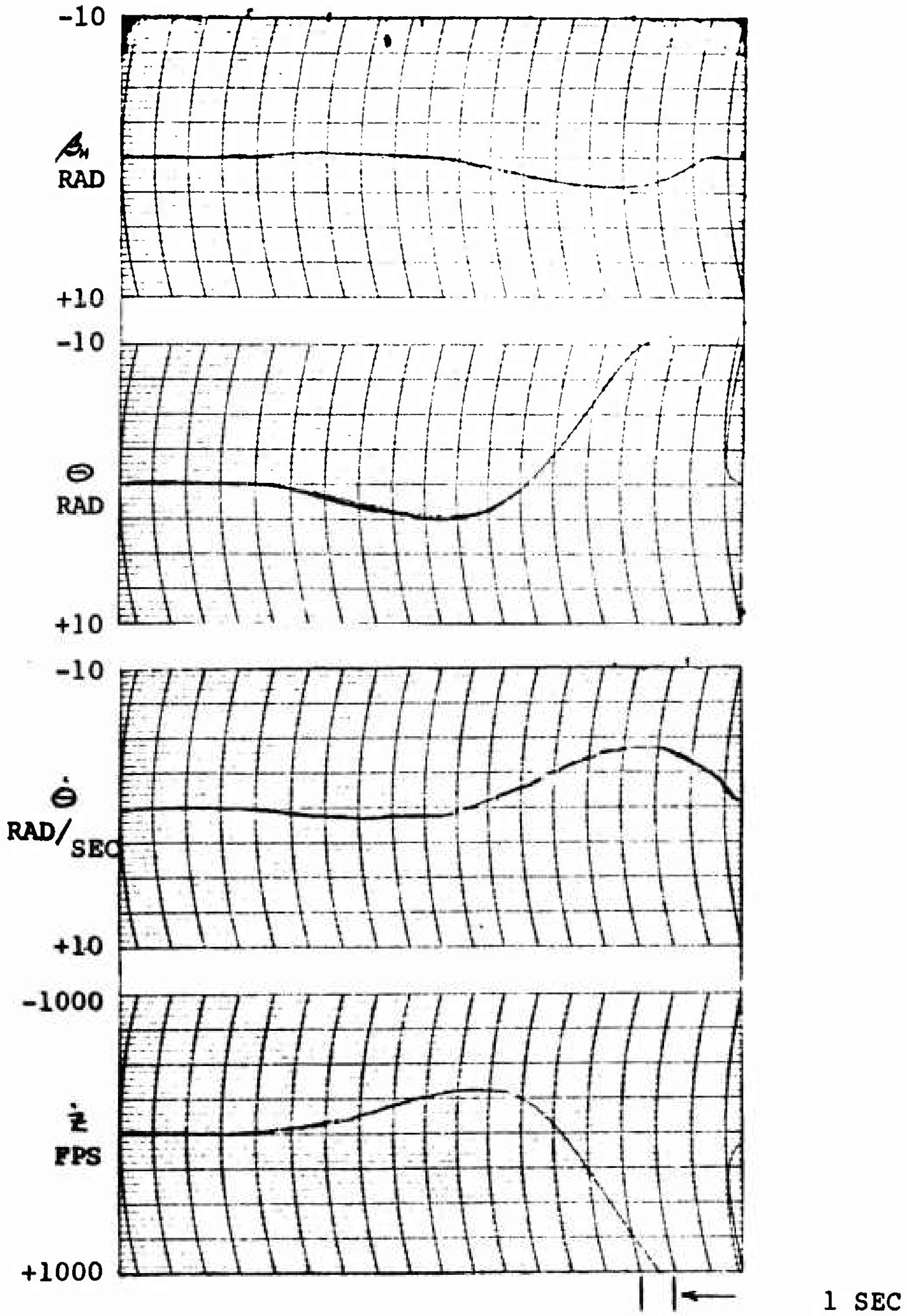

FIGURE 6

LONGITUDINAL CASE 4

30 F.P.S. GUST

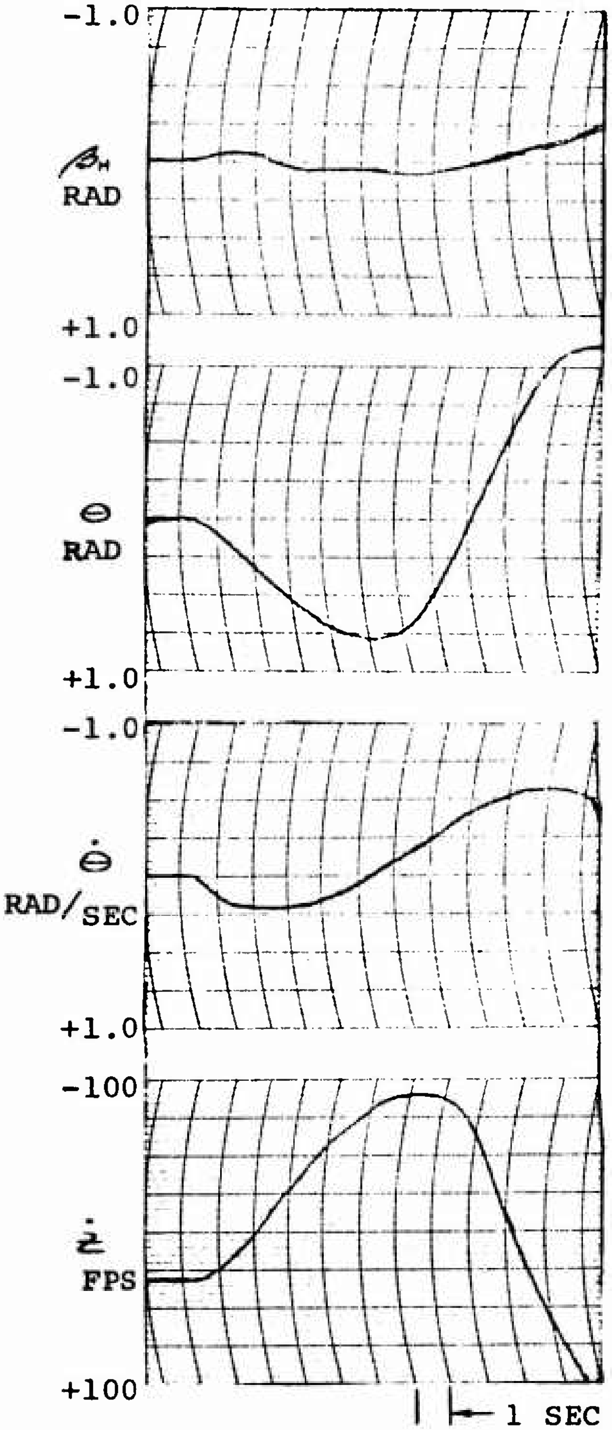

FIGURE 7

LONGITUDINAL CASE 18

30 F.P.S. GUST

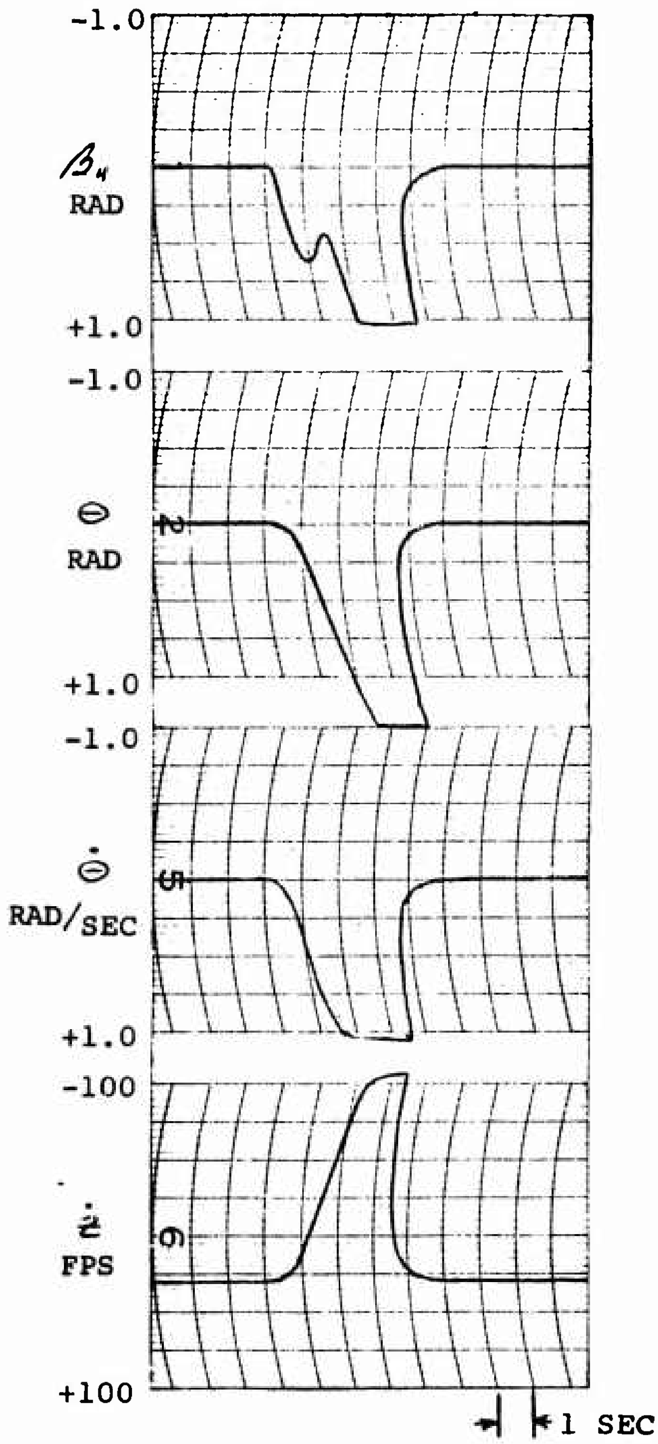

FIGURE 8

LONGITUDINAL CASE 20

30 F.P.S. GUST

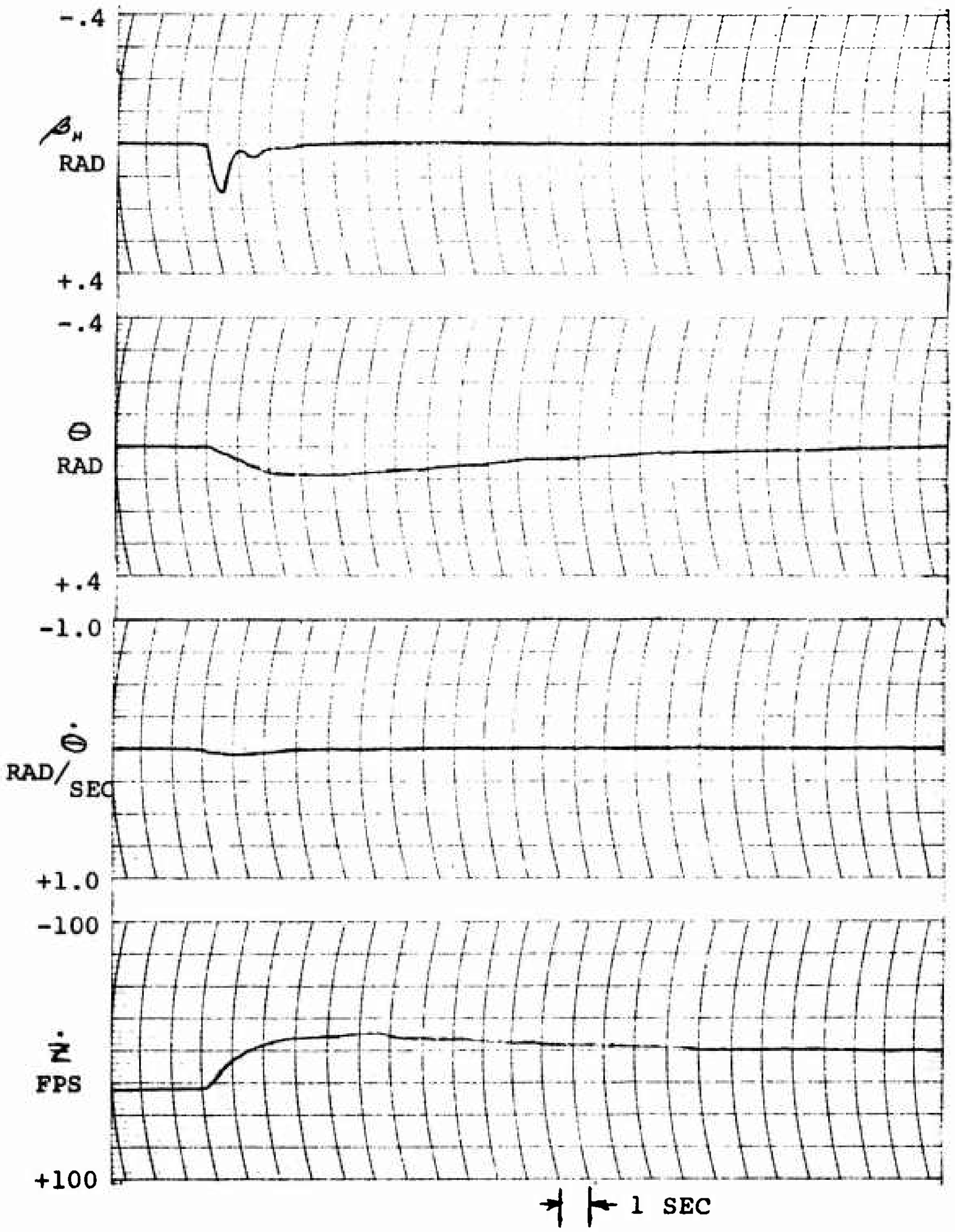

FIGURE 9

LONGITUDINAL CASE 21

30 F.P.S. GUST

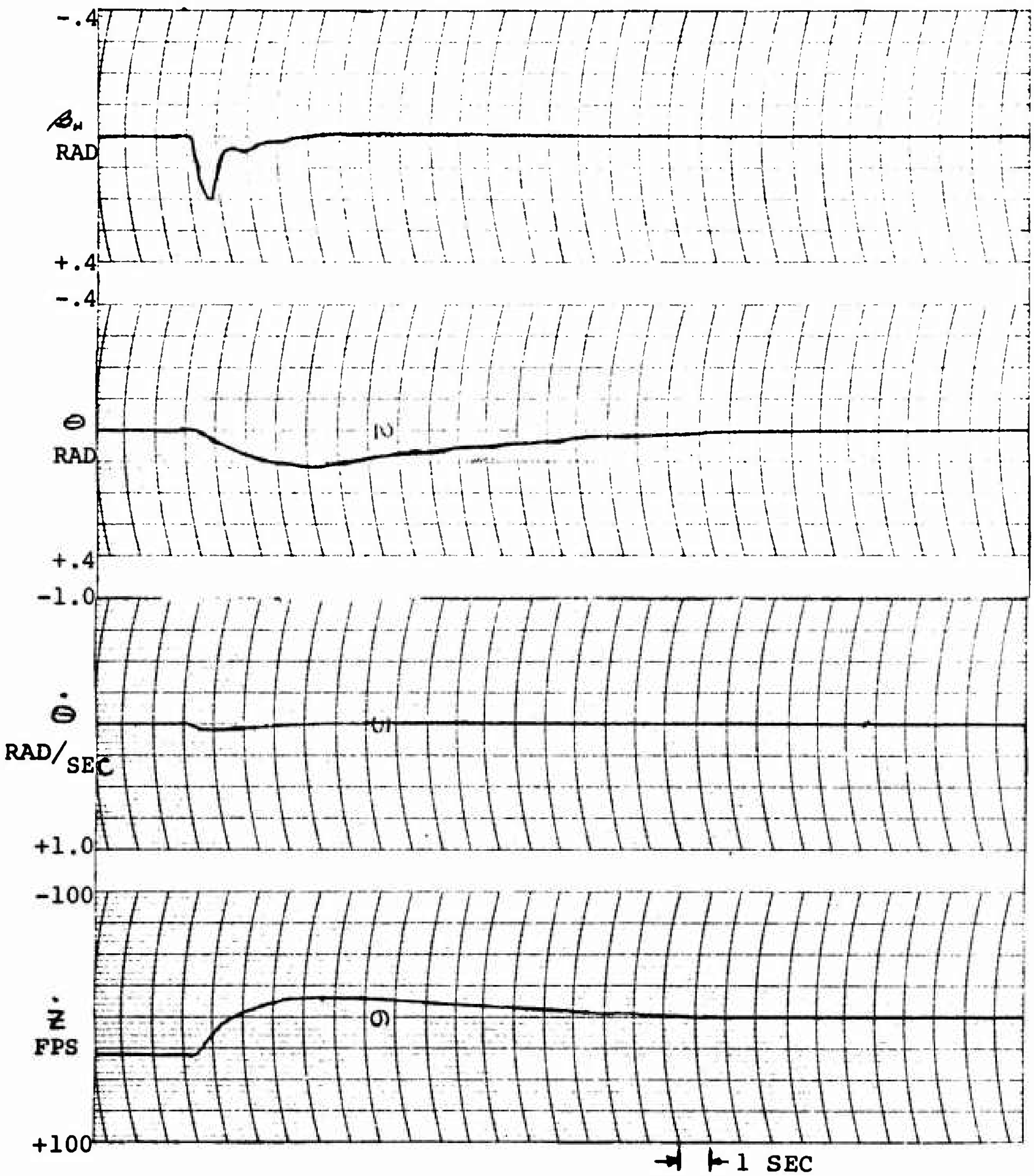

FIGURE 10

LONGITUDINAL CASE 22

30 F.P.S. GUST

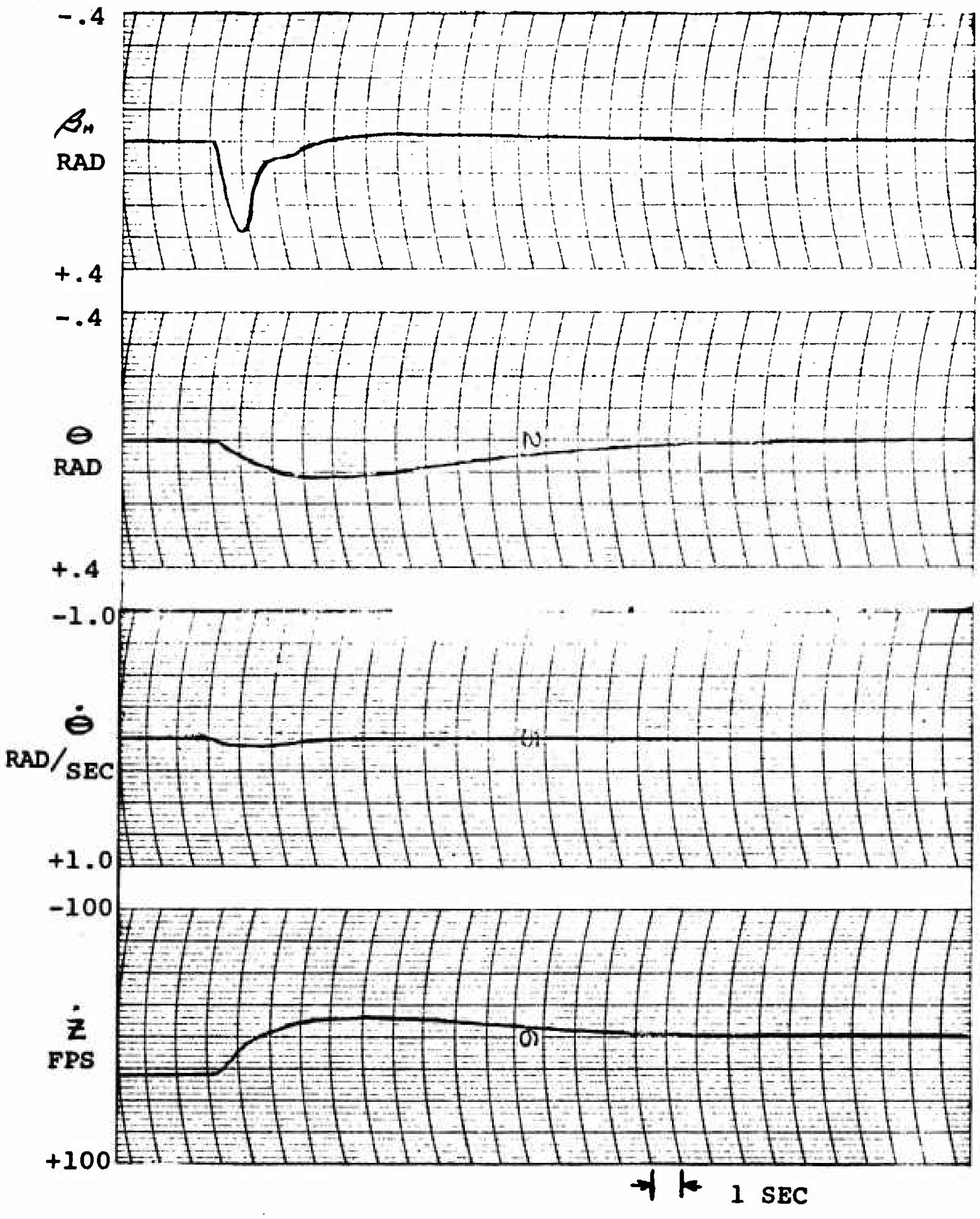

FIGURE 11

LONGITUDINAL CASE 25

30 F.P.S. GUST

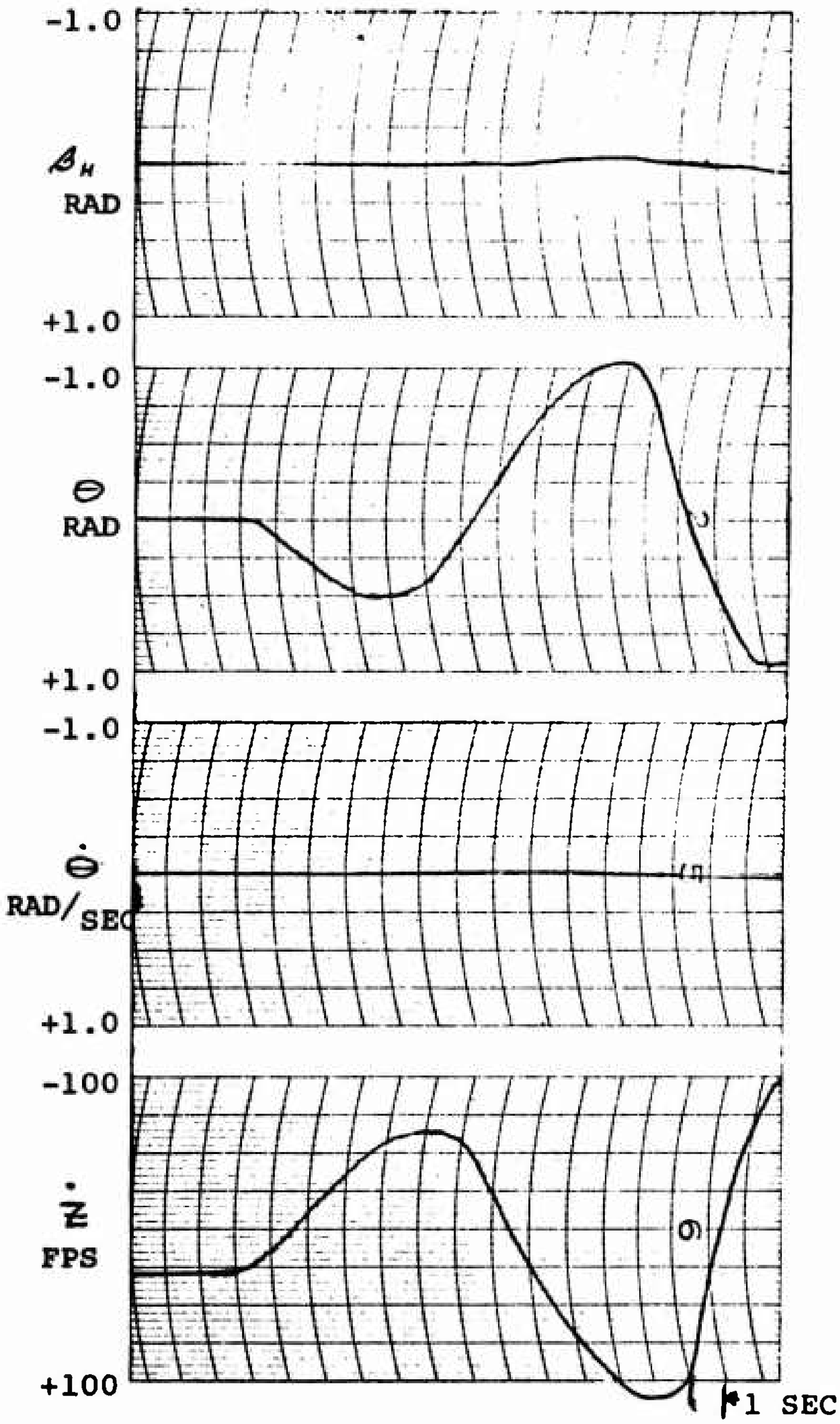

FIGURE 12

LONGITUDINAL CASE 26

30 F.P.S. GUST

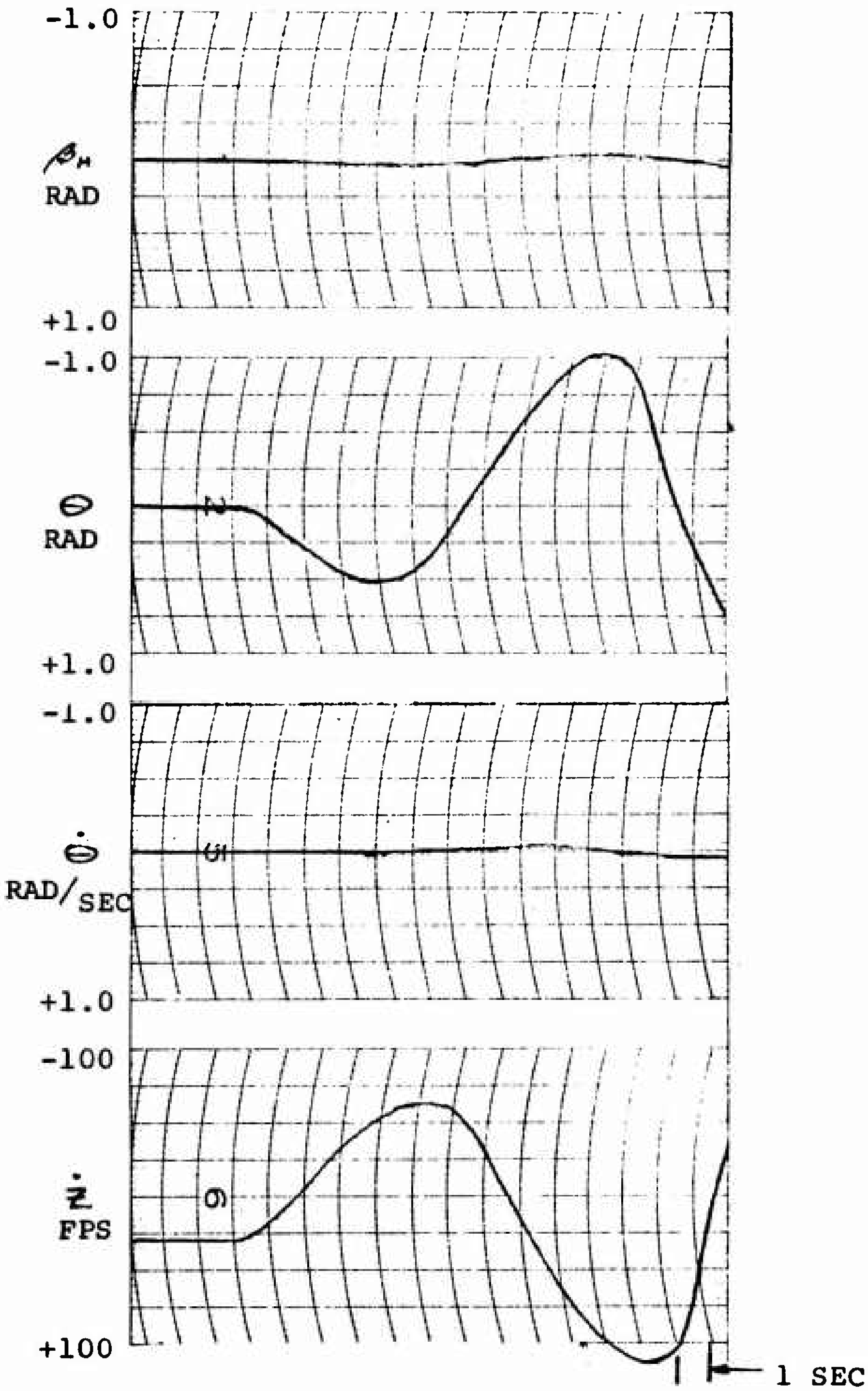

FIGURE 13

LONGITUDINAL CASE 27

30 F.P.S. GUST

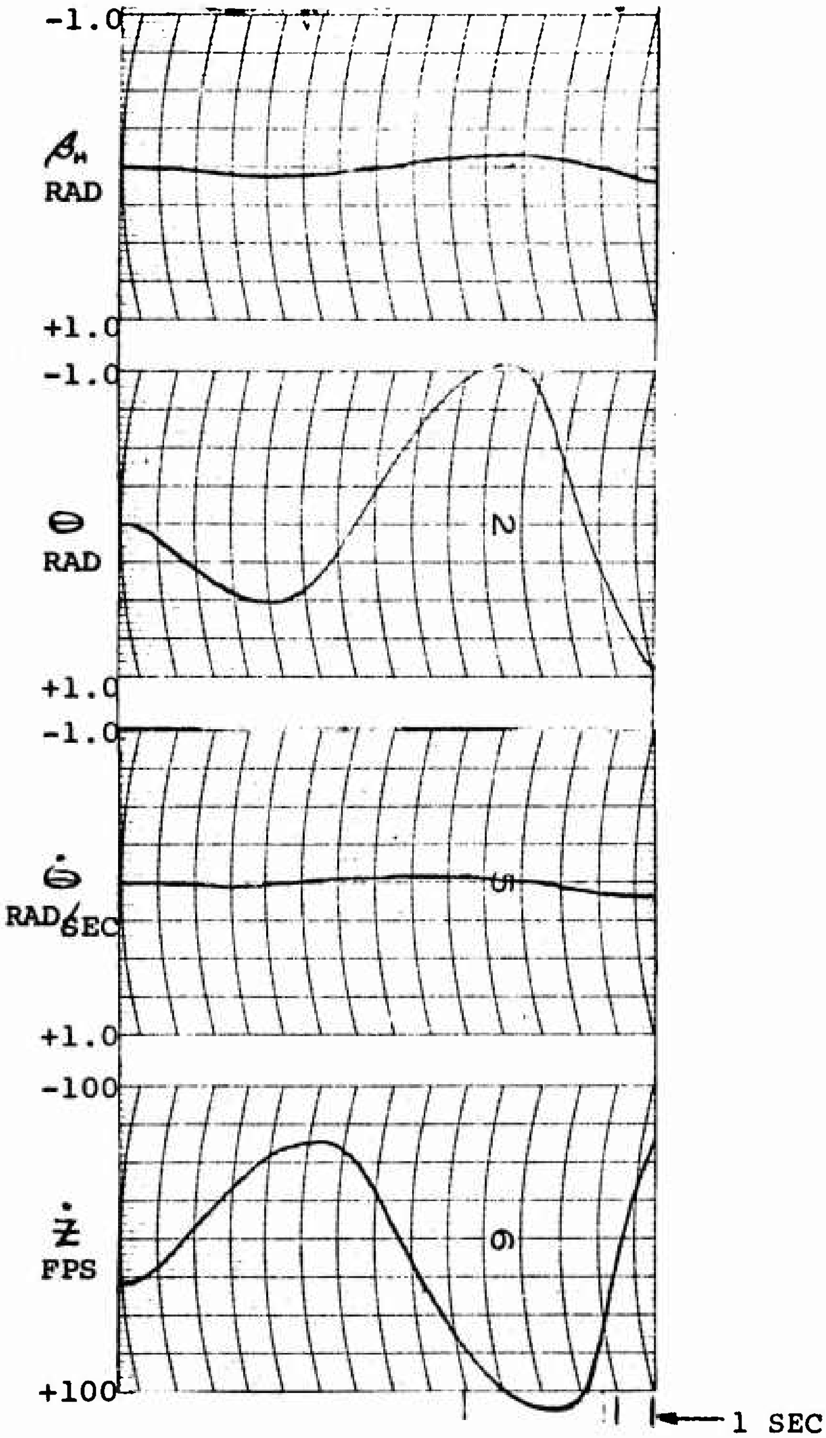

FIGURE 14

TABLE 14

TABLE OF MAXIMUM WING DEFLECTIONS

(LONGITUDINAL)

CASE	FIRST PEAK AMPLITUDE DEG	SECOND PEAK AMPLITUDE DEG.
12	34·4	86·0
1	23·0	—
4	3·1	4·3
18	34	—
20	8·6	2·3
21	11·5	2·3
22	16·1	2·9
25	1·1	1·7
26	1·5	2·3
27	3·4	[illegible]

APPENDIX B

GEOMETRY & DISPLACEMENT DIAGRAM

LATERAL-DIRECTIONAL CASE

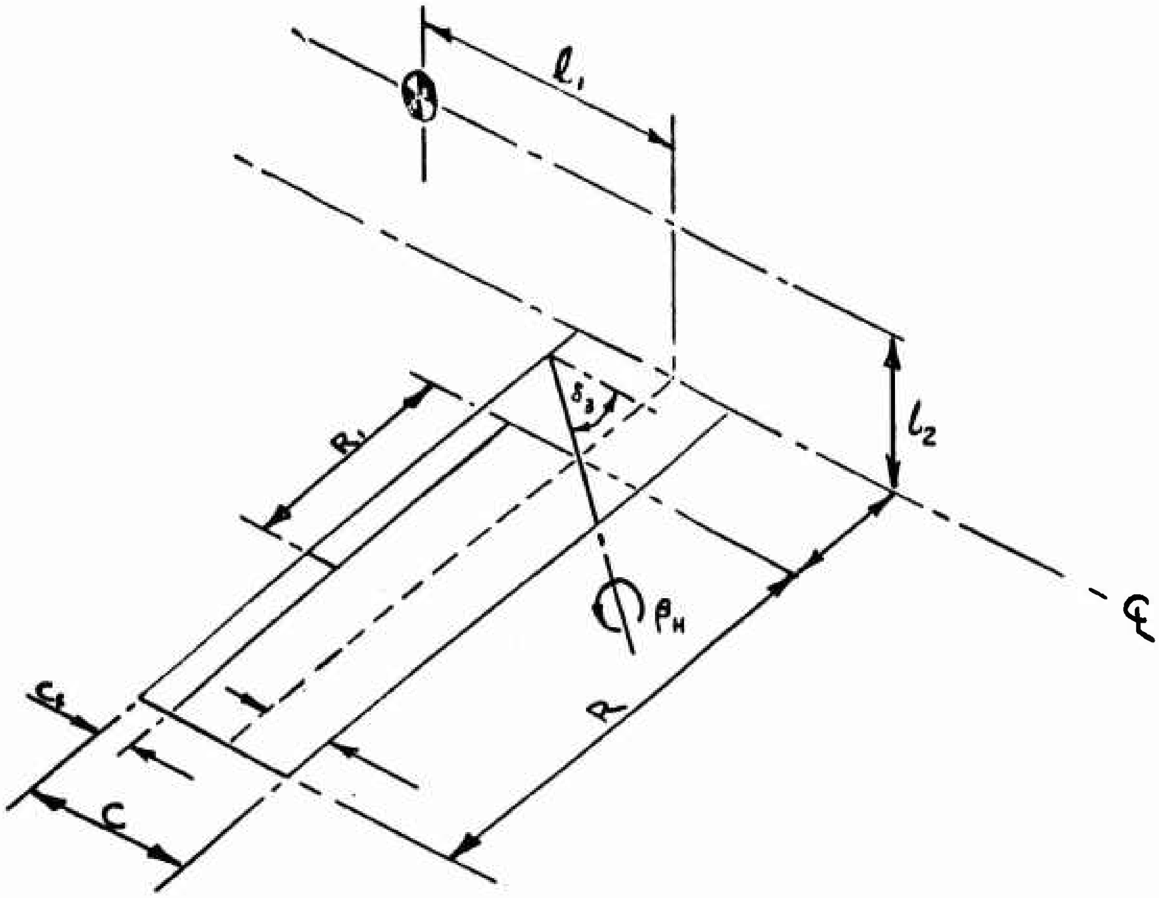

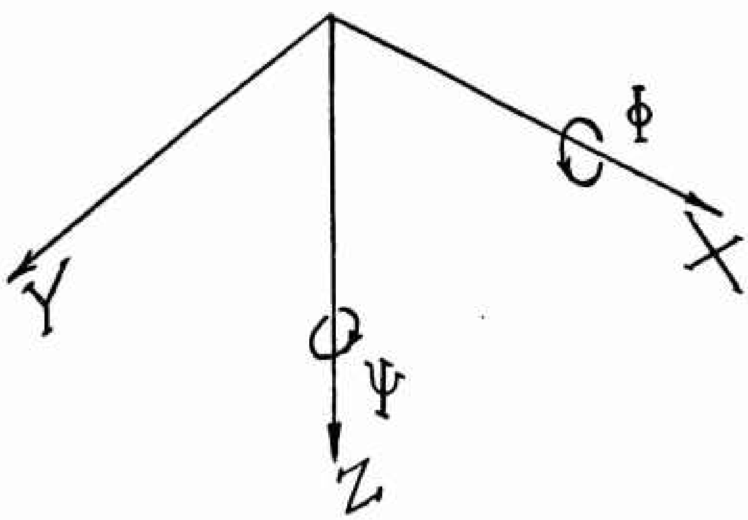

FIGURE 15

LATERAL-DIRECTIONAL MOTION

DISPLACEMENT RELATIONSHIPS

Consider the Y & Z displacements of a point at any spanwise location due to a small disturbance $d\phi$ about the roll axis.

$$\delta y = -l_2 \sin d\phi + (e+r)(\cos\delta\phi - 1)$$

For small disturbances, we can assume:

$$\sin\phi = \phi$$

$$\cos\phi = 1.$$

Hence

$$\delta y = -l_2 \phi.$$

$$\frac{\partial y}{\partial \phi} \equiv y_\phi = -l_2$$

Simarily,

$$z_\phi = (e+r)$$

$$x_\psi = -(e+r)$$

and

$$y_\psi = l_1$$

$$\theta_\beta = \sin\delta_3$$

$$x_\beta = r\cos\delta_3 \sin\theta_0$$

$$y_\beta = 0 \quad (\text{for initial } \beta_H = 0)$$

$$z_\beta = r\cos\delta_3 \cos\theta_0$$

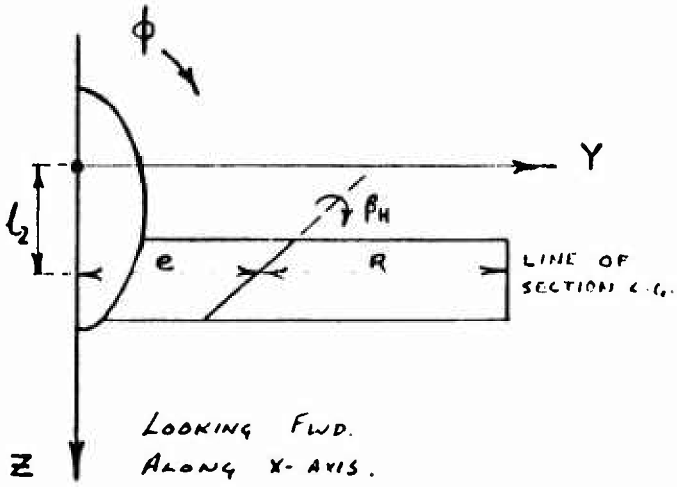

$$y_\phi = -l_2$$
$$z_\phi = (e + r) \qquad (1)$$

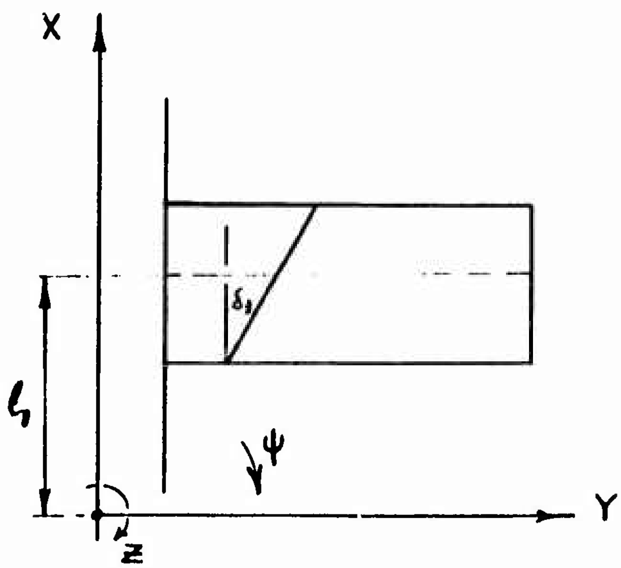

$$x_\psi = -(e + r)$$
$$y_\psi = l_1$$

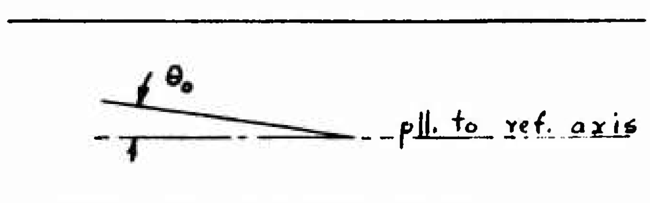

$$\theta_\beta = \sin \delta_3$$
$$x_\beta = r \cos \delta_3 \sin \theta_0$$
$$y_\beta = \text{ZERO}$$
$$z_\beta = r \cos \delta_3 \cos \theta_0$$

θ_0 = Angle between Ref. Chord and Ref. Axis

θ_β = Rate of Change of Incidence with β_H

Expressing the differential displacements in a series.

$$dx = \frac{\partial x}{\partial \phi} d\phi + \frac{\partial x}{\partial \psi} d\psi + \frac{\partial x}{\partial \beta} d\beta_H$$

$$\equiv x_\phi d\phi + x_\psi d\psi + x_\beta d\beta_H$$

Differentiating with respect to time.

$$\Delta \dot{x} = x_\phi \dot{\phi} + x_\psi \dot{\psi} + x_\beta \dot{\beta}_H$$

and $$\Delta \dot{z} = z_\phi \dot{\phi} + z_\psi \dot{\psi} + z_\beta \dot{\beta}_H \qquad (2)$$

x_ϕ, x_ψ etc. are all constants, being functions only of system geometry.

The above velocity increments are referred to the reference axis system. They must now be referred to a wind axis system in order to determine the total velocities normal and parallel to the free stream.

Resolving normal and parallel to the flight path:

$$\overset{\circ}{h}_i = -\Delta\overset{\circ}{x} \sin\Theta_H + \Delta\overset{\circ}{z} \cos\Theta_H$$

$$\Delta V = \Delta\overset{\circ}{x} \cos\Theta_H + \Delta\dot{z} \sin\Theta_H$$

$$V_i = V_0 + \Delta V = V_0 + x_\psi \overset{\circ}{\psi} \cos\Theta_H + x_\beta \overset{\circ}{\beta} \cos\Theta_H + z_\phi \overset{\circ}{\phi} \sin\Theta_H + z_\beta \overset{\circ}{\beta} \sin\Theta_H$$

$$\overset{\circ}{h}_i = -x_\psi \overset{\circ}{\psi} \sin\Theta_H - x_\beta \overset{\circ}{\beta} \sin\Theta_H + z_\phi \overset{\circ}{\phi} \cos\Theta_H + z_\beta \overset{\circ}{\beta} \cos\Theta_H$$

For convenience, we write:

$$V_i = V_0 + c_1 \overset{\circ}{\phi} + c_2 \overset{\circ}{\psi} + c_3 \overset{\circ}{\beta} \qquad (3)$$

Where

$$c_1 = (e+r) \sin\Theta_H$$

$$c_2 = -(e+r) \cos\Theta_H$$

$$c_3 = r \cos\delta_3 \sin(\Theta_0 + \Theta_H)$$

and $$\overset{\circ}{h}_i = c_4 \overset{\circ}{\phi} + c_5 \overset{\circ}{\psi} + c_6 \overset{\circ}{\beta} \qquad (4)$$

where

$$c_4 = (e+r) \cos\Theta_H$$

$$c_5 = (e+r) \sin\Theta_H$$

$$c_6 = r \cos\delta_3 \cos(\Theta_0 + \Theta_H)$$

Squaring terms in Equ. (3), and dropping second order terms, we obtain:

$$V_i^2 = V_0^2 + 2V_0 c_1 \dot{\phi} + 2V_0 c_2 \dot{\psi} + 2V_0 c_3 \dot{\beta}$$

$$\text{and} \quad V_i \dot{h}_i = V_0 c_4 \dot{\phi} + V_0 c_5 \dot{\psi} + V_0 c_6 \dot{\beta}$$

Aerodynamic Forces and Moments at a general spanwise station:

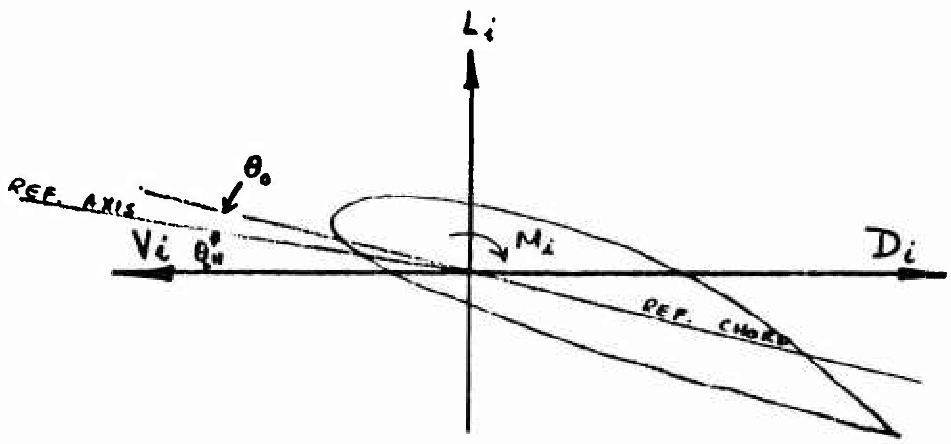

The steady state angle of attack at the general spanwise station is given by

$$\theta_i = \theta_0 + \theta_H + \beta_H \sin \delta_3 - \alpha_0$$

For any disturbed motion, the angle of attack becomes:

$$\theta_i = \theta + \beta_H \sin \delta_3 - \alpha_0 + \frac{\dot{h}_i}{V_i} \quad (\theta \equiv \theta_H + \theta_0)$$

The section lift is given by:

$$L_i = \frac{1}{2}\rho V_i^2 a c \left\{\theta + \beta \sin\delta_3 + \frac{\mathring{h}_i}{V_0} - \alpha_0\right\}$$

$$= k_1 V_i^2 \left\{\theta + \beta \sin\delta_3 - \alpha_0\right\} + k_1 V_i \mathring{h}_i$$

where $k_1 = \frac{1}{2}\rho a c.$

Section drag is given by

$$D_i = \frac{1}{2}\rho V_i^2 c\, \bar{C}_D + \frac{\partial D_i}{\partial \beta_H}\delta\beta_H.$$

The drag coefficient $\bar{C}_D$ is based on the steady state lift, and the correction term $\frac{\partial D_i}{\partial \beta_H}\delta\beta_H$ takes account of changes in drag arising from wing flapping disturbances, and is a function of δ_3 and the flap gearing ratio. The drag coefficient is given by:

$$C_D = C_{D_0} + \frac{K \bar{C}_L^2}{\pi AR},$$

where $\bar{C}_L$ = steady state lift coefficient

we can write the drag in the form

$$D_i = k_3 V_i^2 + C_{D\beta}\, \beta \frac{1}{2}\rho c V_0^2$$

$$= k_3 V_0^2 + 2k_3 V_0 c_1 \mathring{\phi} + 2k_3 V_0 c_2 \mathring{\psi} + 2k_3 V_0 c_3 \mathring{\beta}_H + \frac{1}{2}\rho c V_0^2 C_{D\beta}\cdot\beta_H$$

where $\quad k_3 = \frac{\rho c C_D}{2}$

For convenience, we write the drag as

$$D_i = C_7 + C_8 \dot{\phi} + C_9 \dot{\psi} + C_{10} \dot{\beta} + C_{11} \beta \qquad (5)$$

where
$$C_7 = k_3 V_0^2 \qquad C_9 = 2 k_3 V_0 c_2 \qquad C_{11} = \frac{\rho c V_0^2}{2} C_{D_\beta}$$
$$C_8 = 2 k_3 V_0 c_1 \qquad C_{10} = 2 k_3 V_0 c_3$$

The lift force can be expanded as follows

$$L_i = k_1 V_i^2 (\theta - \alpha_0) + k_1 V_i^2 \left(\sin \delta_3 - \frac{\partial \alpha_0}{\partial \beta} \right) \beta + k_1 V_i \dot{h}_i$$

$$= k_1 V_0^2 (\theta - \alpha_0) + 2 k_1 V_0 c_1 (\theta - \alpha_0) \dot{\phi} + 2 k_1 V_0 c_2 (\theta - \alpha_0) \dot{\psi}$$

$$+ 2 k_1 V_0 c_3 (\theta - \alpha_0) \dot{\beta}_H + k_1 V_0^2 \beta \left(\sin \delta_3 - \frac{\partial \alpha_0}{\partial \beta} \right)$$

$$+ k_1 V_0 c_4 \dot{\phi} + k_1 V_0 c_5 \dot{\psi} + k_1 V_0 c_6 \dot{\beta}_H$$

$$= C_{12} + C_{13} \dot{\phi} + C_{14} \dot{\psi} + C_{15} \dot{\beta}_H + C_{16} \beta_H \qquad (6)$$

where
$$C_{12} = k_1 V_0^2 (\theta - \alpha_0)$$
$$C_{13} = \left(2 k_1 V_0 c_1 [\theta - \alpha_0] + k_1 V_0 c_4 \right)$$
$$C_{14} = \left(2 k_1 V_0 c_2 [\theta - \alpha_0] + k_1 V_0 c_5 \right)$$
$$C_{15} = \left(2 k_1 V_0 c_3 [\theta - \alpha_0] + k_1 V_0 c_6 \right)$$
$$C_{16} = k_1 V_0^2 \left(\sin \delta_3 - \frac{\partial \alpha_0}{\partial \beta_H} \right)$$

The pitching moment equation is:

$$M_i = \frac{1}{2}\rho V_i^2 c^2 \left\{ C_{M_{AC}} + \frac{\partial C_{MAC}}{\partial \beta_H}\beta_H + C_{M_\alpha}\left(\theta + \beta_H \sin\delta_3 - \alpha_0 - \frac{\partial \alpha_0}{\partial \beta_H}\beta_H + \frac{\mathring{h}_i}{V_i}\right)\right\}$$

$$\doteq \frac{1}{2}\rho V_i^2 c^2 \left(C_{M_{AC}} + C_{M_\alpha}[\theta - \alpha_0] \right)$$
$$+ \frac{1}{2}\rho V_0^2 c^2 \beta \left(\frac{\partial C_{MAC}}{\partial \beta} + C_{M_\alpha}\left[\sin\delta_3 - \frac{\partial \alpha_0}{\partial \beta} \right] \right)$$
$$+ \frac{1}{2}\rho V_i \mathring{h}_i c^2 C_{M_\alpha}$$

$$= \frac{1}{2}\rho V_0^2 c^2 \left(C_{M_{AC}} + C_{M_\alpha}[\theta - \alpha_0] \right)$$
$$+ c^2 \rho V_0 c_1 \left(C_{M_{AC}} + C_{M_\alpha}[\theta - \alpha_0] \right) \mathring{\phi}$$
$$+ c^2 \rho V_0 c_2 \left(C_{M_{AC}} + C_{M_\alpha}[\theta - \alpha_0] \right) \mathring{\psi}$$
$$+ c^2 \rho V_0 c_3 \left(C_{M_{AC}} + C_{M_\alpha}[\theta - \alpha_0] \right) \mathring{\beta}_H$$
$$+ \frac{1}{2} c^2 \rho V_0^2 \beta_H \left(\frac{\partial C_{MAC}}{\partial \beta_H} + C_{M_\alpha}\left[\sin\delta_3 - \frac{\partial \alpha_0}{\partial \beta_H} \right] \right)$$
$$+ \frac{1}{2} c^2 \rho C_{M_\alpha} V_0 c_4 \mathring{\phi} + \frac{1}{2} c^2 \rho C_{M_\alpha} V_0 c_5 \mathring{\psi}$$
$$+ \frac{1}{2} c^2 \rho C_{M_\alpha} V_0 c_6 \mathring{\beta}_H$$

$$= C_{18} + C_{19}\mathring{\phi} + C_{20}\mathring{\psi} + C_{21}\mathring{\beta}_H + C_{22}\beta_H \quad (7)$$

$$
\begin{aligned}
\text{where} \quad C_{18} &= \tfrac{1}{2} c^2 V_0^2 \left(C_{M_{AC}} + C_{M_\alpha} [\theta - \alpha_0] \right) \\
C_{19} &= c^2 \rho V_0 \left(C_1 [C_{M_{AC}} + C_{M_\alpha} \{ \theta - \alpha_0 \}] + \frac{C_{M_\alpha}}{2} C_4 \right) \\
C_{20} &= c^2 \rho V_0 \left(C_2 [C_{M_{AC}} + C_{M_\alpha} \{ \theta - \alpha_0 \}] + \frac{C_{M_\alpha}}{2} C_5 \right) \\
C_{21} &= c^2 \rho V_0 \left(C_3 [C_{M_{AC}} + C_{M_\alpha} \{ \theta - \alpha_0 \}] + \frac{C_{M_\alpha}}{2} C_6 \right) \\
C_{22} &= \frac{c^2 \rho V_0^2}{2} \left(\frac{\partial C_{M_{AC}}}{\partial \beta_H} + C_{M_\alpha} \left[\operatorname{Sin} \delta_3 - \frac{\partial \alpha_0}{\partial \beta_H} \right] \right)
\end{aligned}
$$

Finally, resolving back to reference axes,

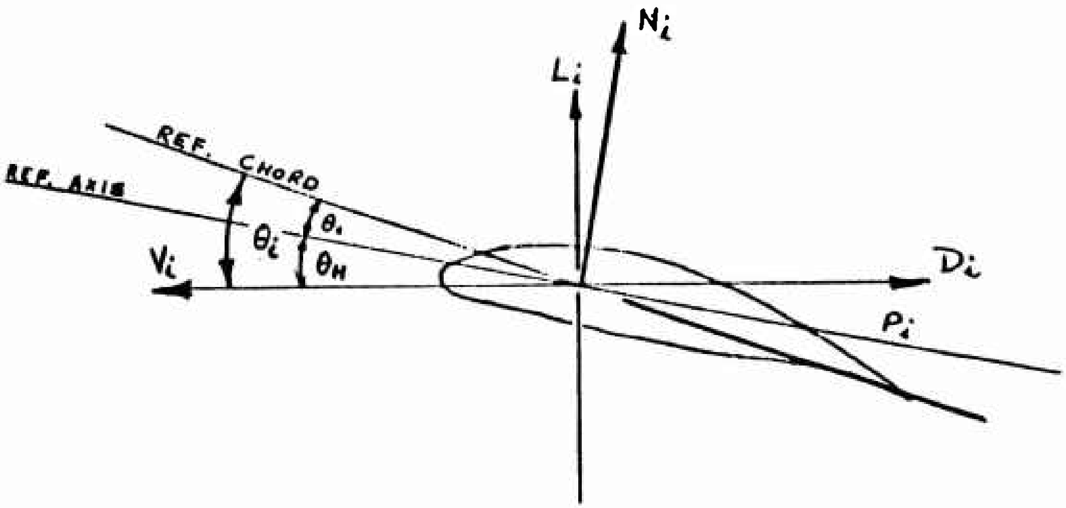

$$
\begin{aligned}
N_i &= L_i \cos \theta_H + D_i \sin \theta_H \\
P_i &= D_i \cos \theta_H - L_i \sin \theta_H
\end{aligned}
$$

$$
\begin{aligned}
N_i = \; & C_{12} \cos \theta_H && + \; C_7 \sin \theta_H \\
& + C_{13} \dot{\phi} \cos \theta_H && + \; C_8 \dot{\phi} \sin \theta_H && (+ \, C_{24} \dot{\phi}) \\
& + C_{14} \dot{\psi} \cos \theta_H && + \; C_9 \dot{\psi} \sin \theta_H && (+ \, C_{25} \dot{\psi}) \\
& + C_{15} \dot{\beta}_H \cos \theta_H && + \; C_{10} \dot{\beta}_H \sin \theta_H && (+ \, C_{26} \dot{\beta}_H) \\
& + C_{16} \beta_H \cos \theta_H && + \; C_{11} \beta_H \sin \theta_H && (+ \, C_{27} \beta_H)
\end{aligned}
$$

$$
\begin{aligned}
P_i = \; & C_7 \cos\theta_H && - \; C_{12} \sin\theta_H && \\
& + C_8 \dot{\phi} \cos\theta_H && - \; C_{13} \dot{\phi} \sin\theta_H && (+ C_{29} \dot{\phi}) \\
& + C_9 \dot{\psi} \cos\theta_H && - \; C_{14} \dot{\psi} \sin\theta_H && (+ C_{30} \dot{\psi}) \\
& + C_{10} \dot{\beta}_H \cos\theta_H && - \; C_{15} \dot{\beta}_H \sin\theta_H && (+ C_{31} \dot{\beta}_H) \\
& + C_{11} \beta_H \cos\theta_H && - \; C_{16} \beta_H \sin\theta_H && (+ C_{32} \beta_H)
\end{aligned}
$$

The total rolling moment due to N_i is given by:

$$L = -\int_0^{e+R_1} N_i \, s ds - \int_{e+R_1}^{e+R} N_i \, s ds \qquad (8)$$

where e = distance of hinge line from fuselage centerline

R_1 = spanwise location of break in flap, measured from hinge

R = span of wing outboard of hinge

s = spanwise coordinate, measured from centerline.

The derivatives of L_1 with respect to $\dot{\phi}, \dot{\psi}, \dot{\beta}_H$ and β_H are therefore given by

$$L_{\dot{\phi}} = -\int_0^{e+R_1} C_{24_i} \, s ds - \int_{e+R_1}^{e+R} C_{24_o} \, s ds \qquad (9)(a)$$

$$L_{\dot{\psi}} = -\int_0^{e+R_1} C_{25_i} \, s ds - \int_{e+R_1}^{e+R} C_{25_o} \, s ds \qquad (b)$$

$$L_{\dot{\beta}} = -\int_{e}^{e+R_1} C_{26_i}\, s\,ds - \int_{e+R_1}^{e+R} C_{26_o}\, s\,ds \qquad (c)$$

$$L_{\beta} = -\int_{e}^{e+R_1} C_{27_i}\, s\,ds - \int_{e+R_1}^{e+R} C_{27_o}\, s\,ds \qquad (d)$$

Subscripts "i" and "o" now denote the inboard and outboard values of the general term C_n

Similarly, the yawing moment derivatives are:

$$N_{\dot{\phi}} = \int_{0}^{e+R_1} C_{29_i}\, s\,ds + \int_{e+R_1}^{e+R} C_{29_o}\, s\,ds \qquad (10)\ (a)$$

$$N_{\dot{\psi}} = \int_{0}^{e+R_1} C_{30_i}\, s\,ds + \int_{e+R_1}^{e+R} C_{30_o}\, s\,ds \qquad (b)$$

$$N_{\dot{\beta}} = \int_{e}^{e+R_1} C_{31_i}\, s\,ds + \int_{e+R_1}^{e+R} C_{31_o}\, s\,ds \qquad (c)$$

$$N_{\beta} = \int_{e}^{e+R_1} C_{32_i}\, s\,ds + \int_{e+R_1}^{e+R} C_{32_o}\, s\,ds \qquad (d)$$

The wing hinge moment can be written:

$$M = M_i \sin\delta_3 - P_i r \cos\delta_3 \sin\theta_0 - N_i r \cos\delta_3 \cos\theta_0$$

$$= C_{34} + C_{35}\dot{\phi} + C_{36}\dot{\psi} + C_{37}\dot{\beta}_H + C_{38}\beta_H$$

Where:

$$C_{35} = C_{19}\sin\delta_3 - r\cos\delta_3\left(C_8 \sin\theta + C_{13}\cos\theta\right)$$

$$C_{36} = C_{20}\sin\delta_3 - r\cos\delta_3\left(C_9 \sin\theta + C_{14}\cos\theta\right)$$

$$C_{37} = C_{21}\sin\delta_3 - r\cos\delta_3\left(C_{10} \sin\theta + C_{15}\cos\theta\right)$$

$$C_{38} = C_{22}\sin\delta_3 - r\cos\delta_3\left(C_{11} \sin\theta + C_{16}\cos\theta\right)$$

Then the hinge moment derivatives are:

$$M_{\dot{\phi}} = \int_0^{R_1} C_{35_i}\,dr + \int_{R_1}^{R} C_{35_o}\,dr \qquad (11)\ (a)$$

$$M_{\dot{\psi}} = \int_0^{R_1} C_{36_i}\,dr + \int_{R_1}^{R} C_{36_o}\,dr \qquad (b)$$

$$M_{\dot{\beta}} = \int_0^{R_1} C_{37_i}\,dr + \int_{R_1}^{R} C_{37_o}\,dr \qquad (c)$$

$$M_{\beta} = \int_0^{R_1} C_{38_i}\,dr + \int_{R_1}^{R} C_{38_o}\,dr \qquad (d)$$

Evaluation of the Integrals

The folling damping derivative is given by the expression:

$$L_{\dot{\phi}} = -\int_0^{e+R_1} C_{24_i}\, s\,ds - \int_{e+R_1}^{e+R} C_{24_0}\, s\,ds$$

$$C_{24} = C_{13}\cos\theta_H + C_8 \sin\theta_H$$

$$= \left(2k_1 V_0 c_1[\theta-\alpha_0] + k_1 V_0 c_4\right)\cos\theta_H + 2k_3 V_0 c_1 \sin\theta_H$$

$$c_1 = (e+r)\sin\theta_H \qquad k_1 = \tfrac{1}{2}\rho a c$$

$$c_4 = (e+r)\cos\theta_H \qquad k_3 = \tfrac{1}{2}\rho c \bar{C}_D$$

Therefore, $$C_{24} = (e+r)\left(2k_1 V_0[\theta-\alpha_0]\sin\theta_H + k_1 V_0 \cos\theta_H\right)\cos\theta_H + (e+r)\left(2k_3 V_0 \sin^2\theta_H\right)$$

$$\equiv C'_{24}(e+r)$$

Thus, $$L_{\dot{\phi}} = -C'_{24_i}\int_0^{e+R_1}(e+r)\,s\,ds - C'_{24_0}\int_{e+R_1}^{e+R}(e+r)\,s\,ds$$

from the definitions of e, r & s, given in Equ. (8), it can be seen that:

$$e+r \equiv s$$

Hence: $$L_{\dot{\phi}} = -C'_{24_i}\int_0^{e+R_1} s^2\,ds - C'_{24_0}\int_{e+R_1}^{e+R} s^2\,ds$$

in a similar manner,

$$L_{\dot{\psi}} = -c'_{25_i}\int_{0}^{e+R_1} s^2 ds - c'_{25_o}\int_{e+R_1}^{e+R} s^2 ds$$

The flapping moment derivatives, $L_{\dot{\beta}}$ & L_{β} are handled as follows:

$$L_{\dot{\beta}} = -\int_{e}^{e+R_1} c_{26_i}\, s ds - \int_{e+R_1}^{e+R} c_{26_o}\, s ds$$

(The lower limit in the first integral becomes 'e', as there is of course no meaning to the integral between $s = o$ and the location of the hinge at station $s = e$)

$$c_{26} = \left(2k_1 V_o c_3[\theta-\alpha_o] + k_1 V_o c_6\right)\cos\theta_H + 2k_3 V_o c_3 \sin\theta_H$$

$$c_3 = \gamma\cos\delta_3 \sin\theta$$

$$c_6 = \gamma\cos\delta_3 \cos\theta$$

Hence, $$c_{26} = \gamma\cos\delta_3\left(2k_1 V_o[\theta-\alpha_o]\sin\theta + k_1 V_o\cos\theta\right)\cos\theta_H$$

$$+ \gamma\cos\delta_3\left(2k_3 V_o \sin\theta\sin\theta_H\right)$$

$$\equiv \gamma\, c'_{26}$$

Substituting $r = s - e$, the expression for $L_{\dot{\beta}}$ becomes:

$$L_\beta^{\circ} = -C'_{26_i}\int_e^{e+R_1} s(s-e)\,ds \quad - \quad C'_{26_0}\int_{e+R_1}^{e+R} s(s-e)\,ds$$

The Aerodynamic stiffness derivative is given by the expression:

$$L_\beta = -C_{27_i}\int_e^{e+R_1} s\,ds \quad - \quad C_{27_0}\int_{e+R_1}^{e+R} s\,ds$$

and $$C_{27} = k_1 V_0^2\left[\sin\delta_3 - \frac{\partial\alpha_0}{\partial\beta}\right]\cos\theta_H + \frac{\rho c V_0^2}{2}\frac{\partial C_D}{\partial\beta}\sin\theta_H$$

The term $\frac{\partial \alpha_0'}{\partial\beta}$ is the rate of change of section zero lift angle with wing displacement, and is a function of the flap gearing. Likewise, the term $\frac{\partial C_D}{\partial\beta}$ accounts for the variation of section drag coefficient with flap gearing.

The derivation of the yawing derivatives is exactly analogous to the foregoing, and without any further work, the formulae are written below:

$$N_\phi^{\circ} = C'_{29_i}\int_0^{e+R_1} s^2\,ds \quad + \quad C'_{29_0}\int_{e+R_1}^{e+R} s^2\,ds$$

$$N_\psi^{\circ} = C'_{30_i}\int_0^{e+R_1} s^2\,ds \quad + \quad C'_{30_0}\int_{e+R_1}^{e+R} s^2\,ds$$

$$N_\beta^\circ = C'_{31_i}\int_e^{e+R_1} s(s-e)\,ds + C'_{31_o}\int_{e+R_1}^{e+R} s(s-e)\,ds$$

$$N_\beta = C_{32_i}\int_e^{e+R_1} s\,ds + C_{32_o}\int_{e+R_1}^{e+R} s\,ds$$

$$C'_{29} = \frac{C_{29}}{e+r} \qquad C'_{31} = \frac{C_{31}}{r}$$

$$C'_{30} = \frac{C_{30}}{e+r},$$

Expanding the hinge moment derivatives, and again using primes to indicate those terms where the variables (r) and (e + r) have factored out

$$\begin{aligned} M_\phi^\circ = {} & C'_{19_i}\sin\delta_3\int_0^{R_1}(e+r)\,dr + C'_{19_o}\sin\delta_3\int_{R_1}^{R}(e+r)\,dr \\ & - C'_{8_i}\cos\delta_3\sin\theta\int_0^{R_1} r(e+r)\,dr - C'_{8_o}\cos\delta_3\sin\theta\int_{R_1}^{R} r(e+r)\,dr \\ & - C'_{13_i}\cos\delta_3\cos\theta\int_0^{R_1} r(e+r)\,dr - C'_{13_o}\cos\delta_3\cos\theta\int_{R_1}^{R} r(e+r)\,dr \end{aligned}$$

$$\begin{aligned} M_\psi^\circ = {} & C'_{20_i}\sin\delta_3\int_0^{R_1}(e+r)\,dr + C'_{20_o}\sin\delta_3\int_{R_1}^{R}(e+r)\,dr \\ & - C'_{9_i}\cos\delta_3\sin\theta\int_0^{R_1} r(e+r)\,dr - C'_{9_o}\cos\delta_3\sin\theta\int_{R_1}^{R} r(e+r)\,dr \\ & - C'_{14_i}\cos\delta_3\cos\theta\int_0^{R_1} r(e+r)\,dr - C'_{14_o}\cos\delta_3\cos\theta\int_{R_1}^{R} r(e+r)\,dr \end{aligned}$$

$$
\begin{aligned}
M_{\dot{\beta}} = \; & C'_{21_i} \sin\delta_3 \int_0^{R_1} r\,dr + C'_{21_o} \sin\delta_3 \int_{R_1}^{R} r\,dr \\
& - C'_{10_i} \cos\delta_3 \sin\theta \int_0^{R_1} r^2\,dr - C'_{10_o} \cos\delta_3 \sin\theta \int_{R_1}^{R} r^2\,dr \\
& - C_{15_i} \cos\delta_3 \cos\theta \int_0^{R_1} r^2\,dr - C_{15_o} \cos\delta_3 \cos\theta \int_{R_1}^{R} r^2\,dr
\end{aligned}
$$

$$
\begin{aligned}
M_{\beta} = \; & C_{22_i} \sin\delta_3 \int_0^{R_1} dr + C_{22_o} \sin\delta_3 \int_{R_1}^{R} dr \\
& - C_{11_i} \cos\delta_3 \sin\theta \int_0^{R_1} r\,dr - C_{11_o} \cos\delta_3 \sin\theta \int_{R_1}^{R} r\,dr \\
& - C_{16_i} \cos\delta_3 \cos\theta \int_0^{R_1} r\,dr - C_{16_o} \cos\delta_3 \cos\theta \int_{R_1}^{R} r\,dr
\end{aligned}
$$

THE EQUATIONS OF MOTION

In their most general form, the Equations of Motion form the following matrix array:

$$
\begin{bmatrix}
\frac{L}{Z}\ddot{\phi} & \left(\frac{L}{Z}\ddot{\psi}\right) & \left(\frac{L}{Z}\ddot{Y}\right) & L_{\ddot{\beta}} \\
\left(\frac{N}{Z}\ddot{\phi}\right) & \frac{N}{Z}\ddot{\psi} & \left(\frac{N}{Z}\ddot{Y}\right) & N_{\ddot{\beta}} \\
\left(\frac{Y}{Z}\ddot{\phi}\right) & \left(\frac{Y}{Z}\ddot{\psi}\right) & \frac{Y}{Z}\ddot{Y} & (Y_{\ddot{\beta}}) \\
M_{\ddot{\phi}} & M_{\ddot{\psi}} & (M_{\ddot{Y}}) & M_{\ddot{\beta}}
\end{bmatrix}
\begin{bmatrix} \ddot{\phi} \\ \ddot{\psi} \\ \ddot{Y} \\ \ddot{\beta} \end{bmatrix}
+
\begin{bmatrix}
\frac{L}{Z}\dot{\phi} & \frac{L}{Z}\dot{\psi} & \frac{L}{Z}\dot{Y} & L_{\dot{\beta}} \\
\frac{N}{Z}\dot{\phi} & \frac{N}{Z}\dot{\psi} & \frac{N}{Z}\dot{Y} & N_{\dot{\beta}} \\
\left(\frac{Y}{Z}\dot{\phi}\right) & \frac{Y}{Z}\dot{\psi} & \frac{Y}{Z}\dot{Y} & (Y_{\dot{\beta}}) \\
M_{\dot{\phi}} & M_{\dot{\psi}} & (M_{\dot{Y}}) & M_{\dot{\beta}}
\end{bmatrix}
\begin{bmatrix} \dot{\phi} \\ \dot{\psi} \\ \dot{Y} \\ \dot{\beta} \end{bmatrix}
+
\begin{bmatrix}
\left(\frac{L}{Z}\phi\right) & \left(\frac{L}{Z}\psi\right) & \left(\frac{L}{Z}Y\right) & L_{\beta} \\
\left(\frac{N}{Z}\phi\right) & \left(\frac{N}{Z}\psi\right) & \left(\frac{N}{Z}Y\right) & N_{\beta} \\
\frac{Y}{Z}\phi & \left(\frac{Y}{Z}\psi\right) & \left(\frac{Y}{Z}Y\right) & (Y_{\beta}) \\
(M_{\phi}) & (M_{\psi}) & (M_{Y}) & M_{\beta}
\end{bmatrix}
\begin{bmatrix} \phi \\ \psi \\ \dot{Y} \\ \beta \end{bmatrix}
= 0
$$

The inertia terms of the first matrix are symmetric about the diagonal indicated. Terms in parentheses are all zero. It will be noticed that the velocity and displacement terms do not form symmetric matrices.

The intertial matrix reduces to:

$$\begin{bmatrix} \frac{I_x}{2} & 0 & 0 & I_w \\ 0 & \frac{I_z}{2} & 0 & I_w \operatorname{Tan} \theta_0 \\ 0 & 0 & \frac{M}{2} & 0 \\ I_w & I_w \operatorname{Tan} \theta_0 & 0 & I_\beta \end{bmatrix} \begin{bmatrix} \ddot{\phi} \\ \ddot{\psi} \\ \ddot{\gamma} \\ \ddot{\beta} \end{bmatrix}$$

where

I_x = roll moment of inertia of total rigid system

I_z = yaw moment of inertia of total rigid system

M = mass of total rigid system

I_β = flapping wing moment of inertia about hinge

I_w = (moment of inertia about an unskewed hinge plus mass moment about same axis times e) $\cos \delta_3 \cos \theta_0$

VELOCITY DERIVATIVES

The first two rows of the second matrix are the rolling and yawing moment derivatives with respect to rate of roll, rate of yaw, side-slip velocity and wing flapping velocity. $Y_{\dot{\psi}}$ is the centrifugal force term due to forward velocity and rate of yaw. $Y_{\dot{y}}$ is the sideforce due to sideslip. No side-force-terms due to roll rate and wing-flapping velocity appear. The hinge moment derivative $M_{\dot{y}}$ is formally excluded by the initial assumption of a zero initial wing deflection. The only non-zero terms in the displacement matrix (3rd) are the sideforce due to roll displacement, Y_{ϕ} and L, N and M derivatives due to β - all others are identically zero.

The final equations of motion become:

$$I_x \ddot{\phi} + I_w \ddot{\beta}_H = L_{\dot{\phi}} \dot{\phi} + L_{\dot{\psi}} \dot{\psi} + L_{\dot{Y}} \dot{Y} + L_{\dot{\beta}} \dot{\beta}_H + L_{\beta} \beta_H \quad \text{(ROLL)}$$

$$I_z \ddot{\psi} + I_w \operatorname{Tan} \theta_0 \ddot{\beta}_H = N_{\dot{\phi}} \dot{\phi} + N_{\dot{\psi}} \dot{\psi} + N_{\dot{Y}} \dot{Y} + N_{\dot{\beta}} \dot{\beta}_H + N_{\beta} \beta_H \quad \text{(YAW)}$$

$$I_w \ddot{\phi} + I_{\beta} \ddot{\beta}_H + I_w \operatorname{Tan} \theta_0 \ddot{\psi} = M_{\dot{\phi}} \dot{\phi} + M_{\dot{\psi}} \dot{\psi} + M_{\dot{\beta}} \dot{\beta}_H + M_{\beta} \beta_H \quad \text{(HINGE MOMENT)}$$

$$M_H \ddot{Y} = - M_H V_0 \dot{\psi} + Y_{\dot{Y}} \dot{Y} + M_H g \phi . \quad \text{(SIDE FORCE)}$$

Terms in $\dot{\beta}_H$ and β_H are for one wing - all others are half of normal values for a complete system, since we are writing the equations for theright-hand half of the system only, a step justified by the original assumption of anti-symmetry.

TABLE 15

TABLE OF CONFIGURATIONS

CASE NO.	δ_3	WING POS.	INBD. FLAP GEARING	OUTBD. FLAP GEARING	FUEL TANKS
12	0	FWD	0	0	FULL
1	45	FWD	0	0	FULL
4	0	FWD	1	1	FULL
18	0	FWD	1	1	EMPTY
20	0	AFT	3	3	EMPTY
21	0	AFT	2	2	EMPTY
22	0	AFT	1	1	EMPTY
25	0	AFT	3	3	FULL
26	0	AFT	2	2	FULL
27	0	AFT	1	1	FULL

OR CONFIGURATIONS USING GEARED FLAP, INBOARD FLAP MOVES COUNTER TO WING DEFLECTION; OUTBOARD FLAP MOVES IN SAME SENSE AS WING.

TABLE 16

TABLES OF NUMERICAL COEFFICIENTS

1201 I_x	1219 0	1237 0	1255 I_W	1273	1291
1202 $-L_{\dot\phi}$	1220 $-L_{\dot\psi}$	1238 $-L_{\dot\gamma}$	1256 $-L_{\dot\beta}$	1274	1292
1203 0	1221 0	1239 0	1257 $-L_\beta$	1275	1293
1204 0	1222 I_z	1240 0	1258 $I_W \operatorname{Tan} \theta_0$	1276	1294
1205 $-N_{\dot\phi}$	1223 $-N_{\dot\psi}$	1241 $-N_{\dot\gamma}$	1259 $-N_{\dot\beta}$	1277	1295
1206 0	1224 0	1242 0	1260 $-N_\beta$	1278	1296
1207 0	1225 0	1243 M_H	1261 0	1279	1297
1208 0	1226 $M_H V_0$	1244 $-Y_{\dot\gamma}$	1262 0	1280	1298
1209 $-M_H g$	1227 0	1245 0	1263 0	1281	1299
1210 I_W	1228 $I_W \operatorname{Tan} \theta_0$	1246 0	1264 I_β	1282	1300
1211 $-M_{\dot\phi}$	1229 $-M_{\dot\psi}$	1247 0	1265 $-M_{\dot\beta}$	1283	1301
1212 0	1230 0	1248 0	1266 $-M_\beta$	1284	1302
1213	1231	1249	1267	1285	1303
1214	1232	1250	1268	1286	1304
1215	1233	1251	1269	1287	1305
1216	1234	1252	1270	1288	1306
1217	1235	1253	1271	1289	1307
1218	1236	1254	1272	1290	1308

TABLE 17

LATERAL-DIRECTIONAL CASE 12

1201 118090	1219 0	1237 0	1255 67100	1273	1291
1202 94830	1220 -63350	1238 130.5	1256 69400	1274	1292
1203 0	1221 0	1239 0	1257 0	1275	1293
1204 0	1222 194100	1240 0	1258 4690	1276	1294
1205 -4650	1223 11546	1241 -201	1259 -314	1277	1295
1206 0	1224 0	1242 0	1260 0	1278	1296
1207 0	1225 0	1243 1.0000	1261 0	1279	1297
1208 0	1226 135	1244 .0581	1262 0	1280	1298
1209 -32.2	1227 0	1245 0	1263 0	1281	1299
1210 67100	1228 4690	1246 0	1264 50000	1282	1300
1211 65900	1229 -48114	1247 0	1265 53420	1283	1301
1212 0	1230 0	1248 0	1266 0	1284	1302
1213	1231	1249	1267	1285 0	1303
1214	1232	1250	1268	1286 0	1304
1215	1233	1251	1269	1287 1	1305
1216	1234	1252	1270	1288	1306 0
1217	1235	1253	1271	1289	1307 0
1218	1236	1254	1272	1290	1308 1

TABLE 18

LATERAL-DIRECTIONAL CASE 1

1201 118090	1219 0	1237 0	1255 47400	1273	1291
1202 94830	1220 -63350	1238 130.5	1256 49000	1274	1292
1203 0	1221 0	1239 0	1257 332900	1275	1293
1204 0	1222 194100	1240 0	1258 3310	1276	1294
1205 -4650	1223 11546	1241 -201	1259 -223	1277	1295
1206 0	1224 0	1242 0	1260 -42180	1278	1296
1207 0	1225 0	1243 1.000	1261 0	1279	1297
1208 0	1226 135	1244 .0501	1262 0	1280	1298
1209 -32.2	1227 0	1245 0	1263 0	1281	1299
1210 47400	1228 3310	1246 0	1264 25000	1282	1300
1211 43270	1229 -35073	1247 0	1265 25040	1283	1301
1212 0	1230 0	1248 0	1266 154390	1284	1302
1213	1231	1249	1267	1285 0	1303
1214	1232	1250	1268	1286 0	1304
1215	1233	1251	1269	1287 1	1305
1216	1234	1252	1270	1288	1306 0
1217	1235	1253	1271	1289	1307 0
1218	1236	1254	1272	1290	1308 1

TABLE 19

LATERAL-DIRECTIONAL CASE 4

1201 118090	1219 0	1237 0	1255 67100	1273	1291
1202 94380	1220 -63350	1238 130.5	1256 69400	1274	1292
1203 0	1221 0	1239 0	1257 100800	1275	1293
1204 0	1222 194100	1240 0	1258 4690	1276	1294
1205 -4650	1223 11546	1241 -201	1259 -314	1277	1295
1206 0	1224 0	1242 0	1260 -6490	1278	1296
1207 0	1225 0	1243 1.000	1261 0	1279	1297
1208 0	1226 135	1244 .0581	1262 0	1280	1298
1209 -32.2	1227 0	1245 0	1263 0	1281	1299
1210 67100	1228 4690	1246 0	1264 50000	1282	1300
1211 65900	1229 -48114	1247 0	1265 53420	1283	1301
1212 0	1230 0	1248 0	1266 101252	1284	1302
1213	1231	1249	1267	1285 0	1303
1214	1232	1250	1268	1286 0	1304
1215	1233	1251	1269	1287 1	1305
1216	1234	1252	1270	1288	1306 0
1217	1235	1253	1271	1289	1307 0
1218	1236	1254	1272	1290	1308 1

TABLE 20

LATERAL-DIRECTIONAL CASE 18

1201 15980	1219 0	1237 0	1255 9605	1273	1291
1202 92985	1220 -1024	1238 76	1256 66100	1274	1292
1203 0	1221 0	1239 0	1257 100800	1275	1293
1204 0	1222 56288	1240 0	1258 -134	1276	1294
1205 -1275	1223 5660	1241 -86	1259 +25.9	1277	1295
1206 0	1224 0	1242 0	1260 -6490	1278	1296
1207 0	1225 0	1243 1.000	1261 0	1279	1297
1208 0	1226 135	1244 +.111	1262 0	1280	1298
1209 -32.2	1227 0	1245 0	1263 0	1281	1299
1210 9605	1228 -134	1246 0	1264 7140	1282	1300
1211 65900	1229 -6204	1247 0	1265 50900	1283	1301
1212 0	1230 0	1248 0	1266 101252	1284	1302
1213	1231	1249	1267	1285 0	1303
1214	1232	1250	1268	1286 0	1304
1215	1233	1251	1269	1287 1	1305
1216	1234	1252	1270	1288	1306 0
1217	1235	1253	1271	1289	1307 0
1218	1236	1254	1272	1290	1308 1

TABLE 21

LATERAL-DIRECTIONAL CASE 20

1201 15980	1219 0	1237 0	1255 9605	1273	1291
1202 92985	1220 -7024	1238 76	1256 66100	1274	1292
1203 0	1221 0	1239 0	1257 303000	1275	1293
1204 0	1222 52155	1240 0	1258 -134	1276	1294
1205 45	1223 4892	1241 -43	1259 25.9	1277	1295
1206 0	1224 0	1242 0	1260 -19500	1278	1296
1207 0	1225 0	1243 1.000	1261 0	1279	1297
1208 0	1226 135	1244 .111	1262 0	1280	1298
1209 -32.2	1227 0	1245 0	1263 0	1281	1299
1210 9605	1228 -134	1246 0	1264 7140	1282	1300
1211 65900	1229 -6204	1247 0	1265 50900	1283	1301
1212 0	1230 0	1248 0	1266 +300000	1284	1302
1213	1231	1249	1267	1285 0	1303
1214	1232	1250	1268	1286 0	1304
1215	1233	1251	1269	1287 1	1305
1216	1234	1252	1270	1288	1306 0
1217	1235	1253	1271	1289	1307 0
1218	1236	1254	1272	1290	1308 1

TABLE 22

LATERAL-DIRECTIONAL CASE 21

1201 15980	1219 0	1237 0	1255 9605	1273	1291
1202 92985	1220 -7024	1238 76	1256 66100	1274	1292
1203 0	1221 0	1239 0	1257 +202000	1275	1293
1204 0	1222 52155	1240 0	1258 -134	1276	1294
1205 45	1223 4892	1241 -43	1259 25.9	1277	1295
1206 0	1224 0	1242 0	1260 -13000	1278	1296
1207 0	1225 0	1243 1.000	1261 0	1279	1297
1208 0	1226 135	1244 .111	1262 0	1280	1298
1209 -32.2	1227 0	1245 0	1263 0	1281	1299
1210 9605	1228 -134	1246 0	1264 7140	1282	1300
1211 65900	1229 -6204	1247 0	1265 50900	1283	1301
1212 0	1230 0	1248 0	1266 200000	1284	1302
1213	1231	1249	1267	1285 0	1303
1214	1232	1250	1268	1286 0	1304
1215	1233	1251	1269	1287 1	1305
1216	1234	1252	1270	1288	1306 0
1217	1235	1253	1271	1289	1307 0
1218	1236	1254	1272	1290	1308 1

TABLE 23

LATERAL-DIRECTIONAL CASE 22a

1201 15980	1219 0	1237 0	1255 9605	1273	1291
1202 92985	1220 -7024	1238 76	1256 66100	1274	1292
1203 0	1221 0	1239 0	1257 101000	1275	1293
1204 0	1222 52155	1240 0	1258 -134	1276	1294
1205 45	1223 4892	1241 -43	1259 25.9	1277	1295
1206 0	1224 0	1242 0	1260 -6500	1278	1296
1207 0	1225 0	1243 1.000	1261 0	1279	1297
1208 0	1226 135	1244 .111	1262 0	1280	1298
1209 -32.2	1227 0	1245 0	1263 0	1281	1299
1210 9605	1228 -134	1246 0	1264 7140	1282	1300
1211 65900	1229 -6204	1247 0	1265 50900	1283	1301
1212 0	1230 0	1248 0	1266 100000	1284	1302
1213	1231	1249	1267	1285 0	1303
1214	1232	1250	1268	1286 0	1304
1215	1233	1251	1269	1287 1	1305
1216	1234	1252	1270	1288	1306 0
1217	1235	1253	1271	1289	1307 0
1218	1236	1254	1272	1290	1308 1

TABLE 24

LATERAL-DIRECTIONAL CASE 25

1201 118090	1219 0	1237 0	1255 67100	1273	1291
1202 94830	1220 -63350	1238 130.5	1256 69400	1274	1292
1203 0	1221 0	1239 0	1257 +305000	1275	1293
1204 0	1222 194100	1240 0	1258 4690	1276	1294
1205 305	1223 8756	1241 -43	1259 -314	1277	1295
1206 0	1224 0	1242 0	1260 -19500	1278	1296
1207 0	1225 0	1243 1.000	1261 0	1279	1297
1208 0	1226 135	1244 .0581	1262 0	1280	1298
1209 -32.2	1227 0	1245 0	1263 0	1281	1299
1210 67100	1228 4690	1246 0	1264 50000	1282	1300
1211 65900	1229 -48114	1247 0	1265 53420	1283	1301
1212 0	1230 0	1248 0	1266 +300000	1284	1302
1213	1231	1249	1267	1285 0	1303
1214	1232	1250	1268	1286 0	1304
1215	1233	1251	1269	1287 1	1305
1216	1234	1252	1270	1288	1306 0
1217	1235	1253	1271	1289	1307 0
1218	1236	1254	1272	1290	1308 1

TABLE 25

LATERAL-DIRECTIONAL CASE 26

1201 118090	1219 0	1237 0	1255 67100	1273	1291
1202 94830	1220 -63350	1238 130.5	1256 69400	1274	1292
1203 0	1221 0	1239 0	1257 +202000	1275	1293
1204 0	1222 194100	1240 0	1258 4690	1276	1294
1205 305	1223 8756	1241 -43	1259 -314	1277	1295
1206 0	1224 0	1242 0	1260 -13000	1278	1296
1207 0	1225 0	1243 1.000	1261 0	1279	1297
1208 0	1226 135	1244 .0581	1262 0	1280	1298
1209 -32.2	1227 0	1245 0	1263 0	1281	1299
1210 67100	1228 4690	1246 0	1264 50000	1282	1300
1211 65900	1229 -48114	1247 0	1265 53420	1283	1301
1212 0	1230 0	1248 0	1266 +200000	1284	1302
1213	1231	1249	1267	1285 0	1303
1214	1232	1250	1268	1286 0	1304
1215	1233	1251	1269	1287 1	1305
1216	1234	1252	1270	1288	1306 0
1217	1235	1253	1271	1289	1307 0
1218	1236	1254	1272	1290	1308 1

TABLE 26

LATERAL-DIRECTIONAL CASE 27

1201 118090	1219 0	1237 0	1255 67100	1273	1291
1202 94830	1220 -63350	1238 130.5	1256 69400	1274	1292
1203 0	1221 0	1239 0	1257 101000	1275	1293
1204 0	1222 194100	1240 0	1258 4690	1276	1294
1205 305	1223 8756	1241 -43	1259 -314	1277	1295
1206 0	1224 0	1242 0	1260 -6500	1278	1296
1207 0	1225 0	1243 1.000	1261 0	1279	1297
1208 0	1226 135	1244 .0581	1262 0	1280	1298
1209 -32.2	1227 0	1245 0	1263 0	1281	1299
1210 67100	1228 4690	1246 0	1264 50000	1282	1300
1211 65900	1229 -48114	1247 0	1265 53420	1283	1301
1212 0	1230 0	1248 0	1266 +100,000	1284	1302
1213	1231	1249	1267	1285 0	1303
1214	1232	1250	1268	1286 0	1304
1215	1233	1251	1269	1287 1	1305
1216	1234	1252	1270	1288	1306 0
1217	1235	1253	1271	1289	1307 0
1218	1236	1254	1272	1290	1308 1

TABLE 27

SUMMARY OF ROOTS OF THE LATERAL-DIRECTIONAL CHARACTERISTIC EQUATIONS - SHOWING PERIODS AND TIME TO DOUBLE OR HALF AMP.

CASE	ROOTS / PERIODS / TIME TO DOUBLE (+) OR HALVE (-) AMP.			
12	-.6157	-.0438	.1099 ± .5146i	-1.1102
	—	—	12.21	—
	1.13	15.82	6.21	.624
1	-.5639	-.1000	.2835 ± .5984i	-.7010 ± 1.883i
	—	—	10.50	3.34
	1.23	6.93	2.44	.99
4	-.7194	+.0378	-.0091 ± .5003i	-.4175 ± 1.8404i
	—	—	12.56	3.42
	.96	18.33	76.15	1.66
18	-5.243	-.0906 ± .5630i	-.0210	-2.173 ± 4.407
	—	11.16	—	1.43
	.132	7.65	33.0	.32
20	-.0770 ± .4842i	-4.5195	-.0299	-2.544 ± 8.608i
	12.98	—	—	.73
	9.00	.153	23.18	.27
21	-.0795 ± .4846i	-4.6854	-.0298	-2.458 ± 6.760i
	12.96	—	—	.93
	8.72	.15	23.26	.28
22	-.0871 ± .4864i	-5.2186	-.0296	-2.184 ± 4.280i
	12.92	—	—	1.47
	7.96	.13	23.41	.32
25	-.7313	-.0030	+.0333 ± .3882i	-.4368 ± 3.2483i
	—	—	16.18	1.93
	.95	231	20.81	1.93
26	-.7322	-.0030	+.0309 ± .3903i	-.4339 ± 2.629i
	—	—	16.10	2.39
	.95	231	22.43	1.60
27	-.7353	-.0030	+.0239 ± .3975i	-.4255 ± 1.806i
	—	—	15.81	3.48
	.94	231	26.74	1.50

BASIC HELICOPTER RESPONSE TO

LATERAL STEP INPUT

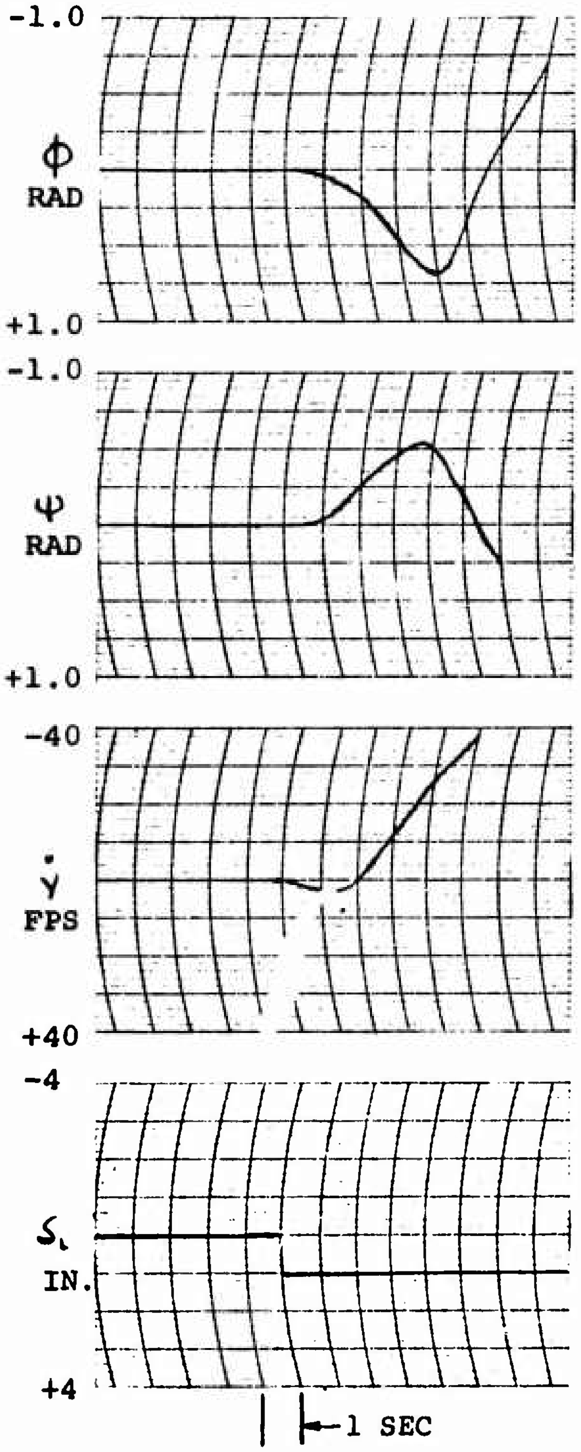

FIGURE 16

LATERAL-DIRECTIONAL

CASE 12

30 F.P.S.GUST

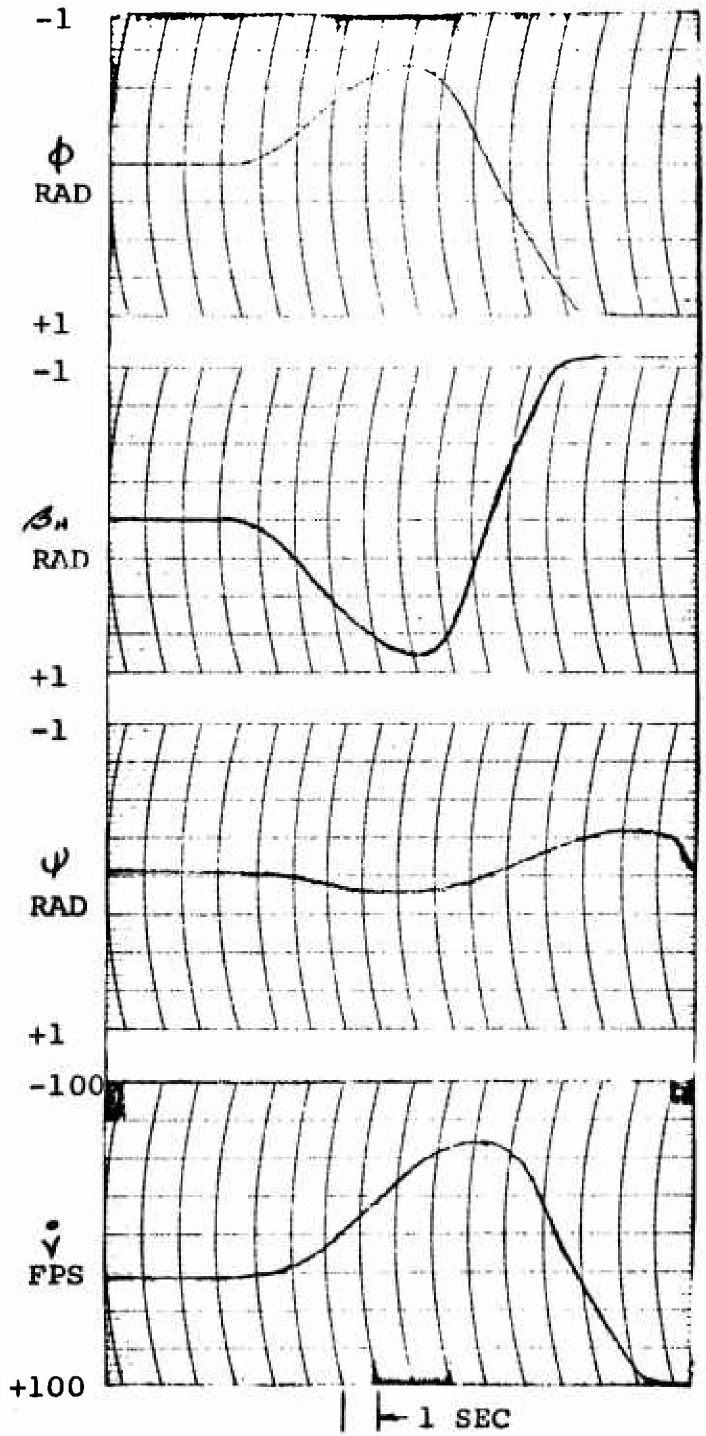

FIGURE 17

LATERAL-DIRECTIONAL

CASE 1

30 F.P.S. GUST

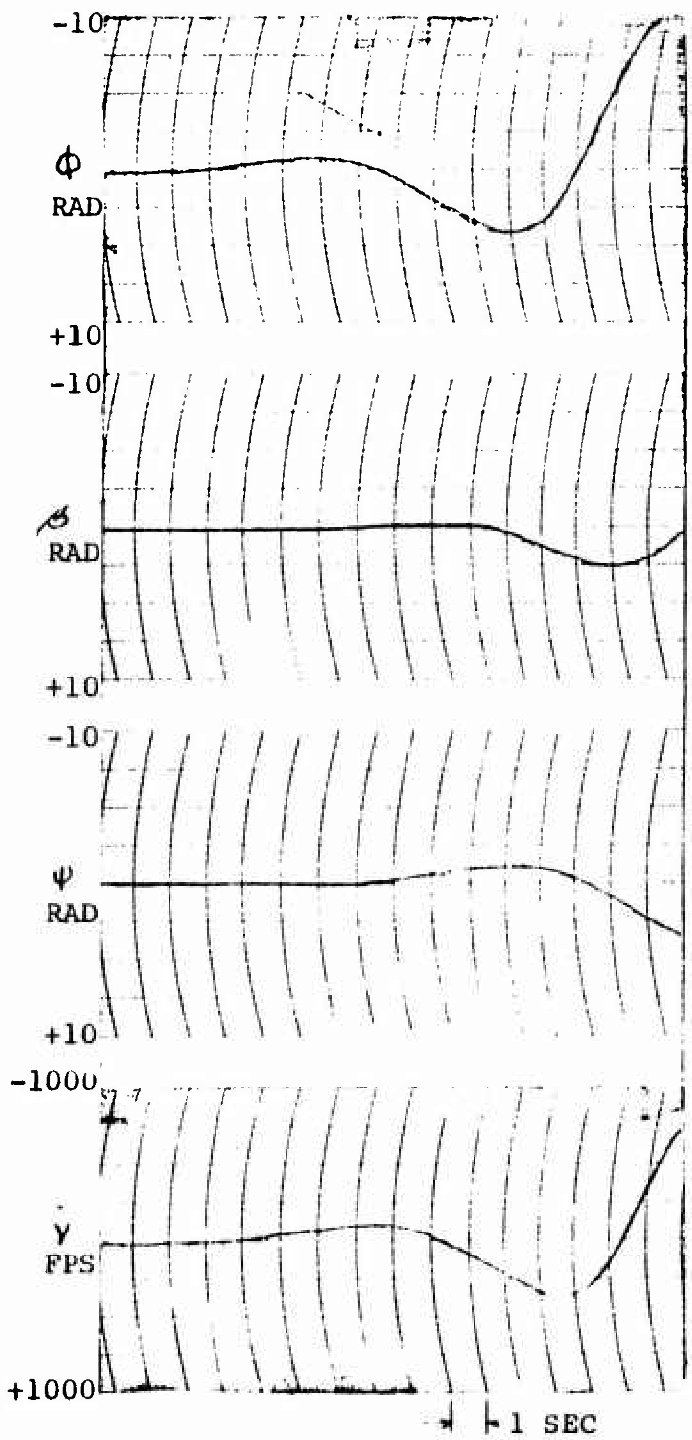

FIGURE 18

LATERAL-DIRECTIONAL
CASE 4
30 F.P.S. GUST

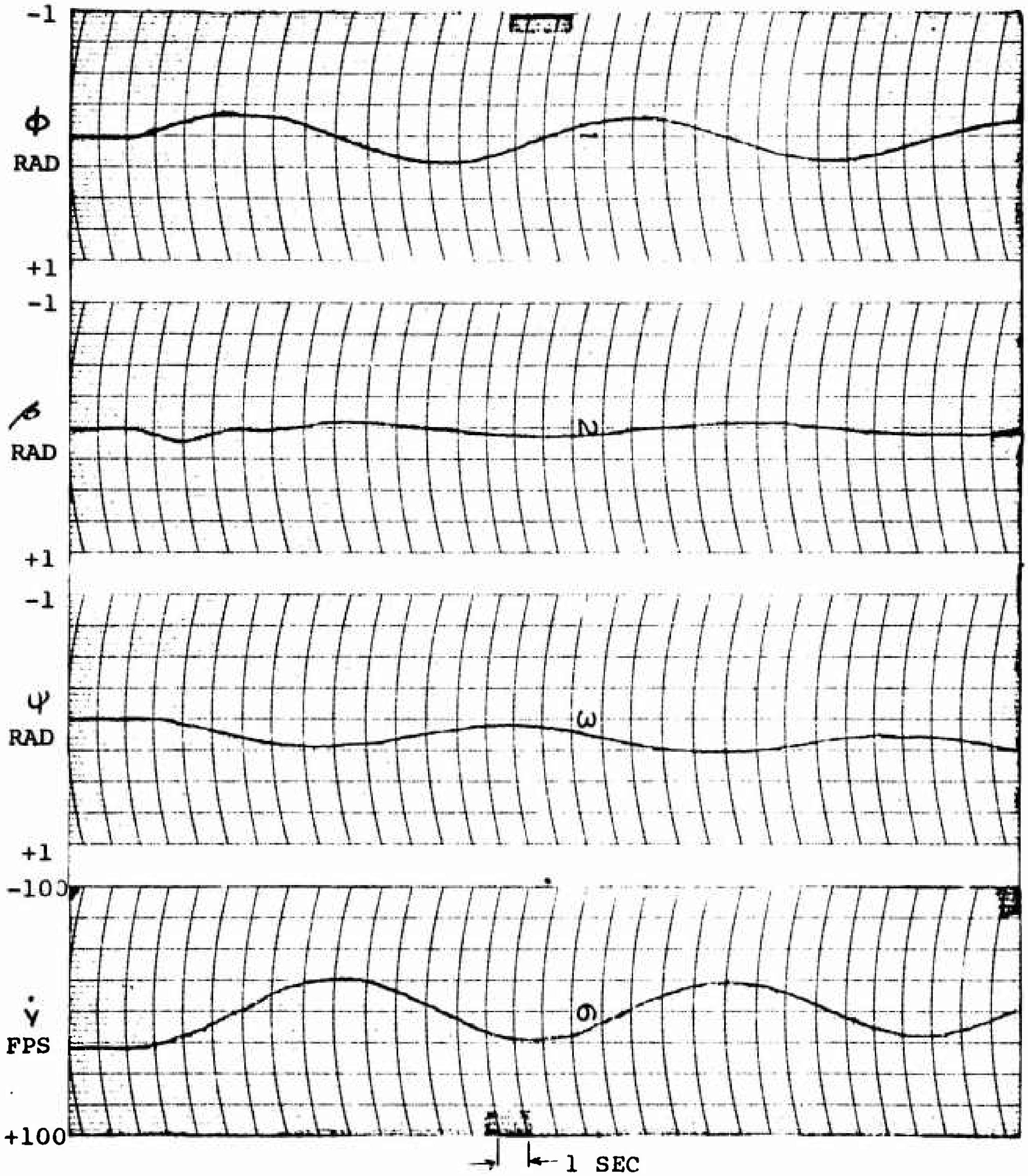

FIGURE 19

LATERAL-DIRECTIONAL

CASE 18

30 F.P.S. GUST

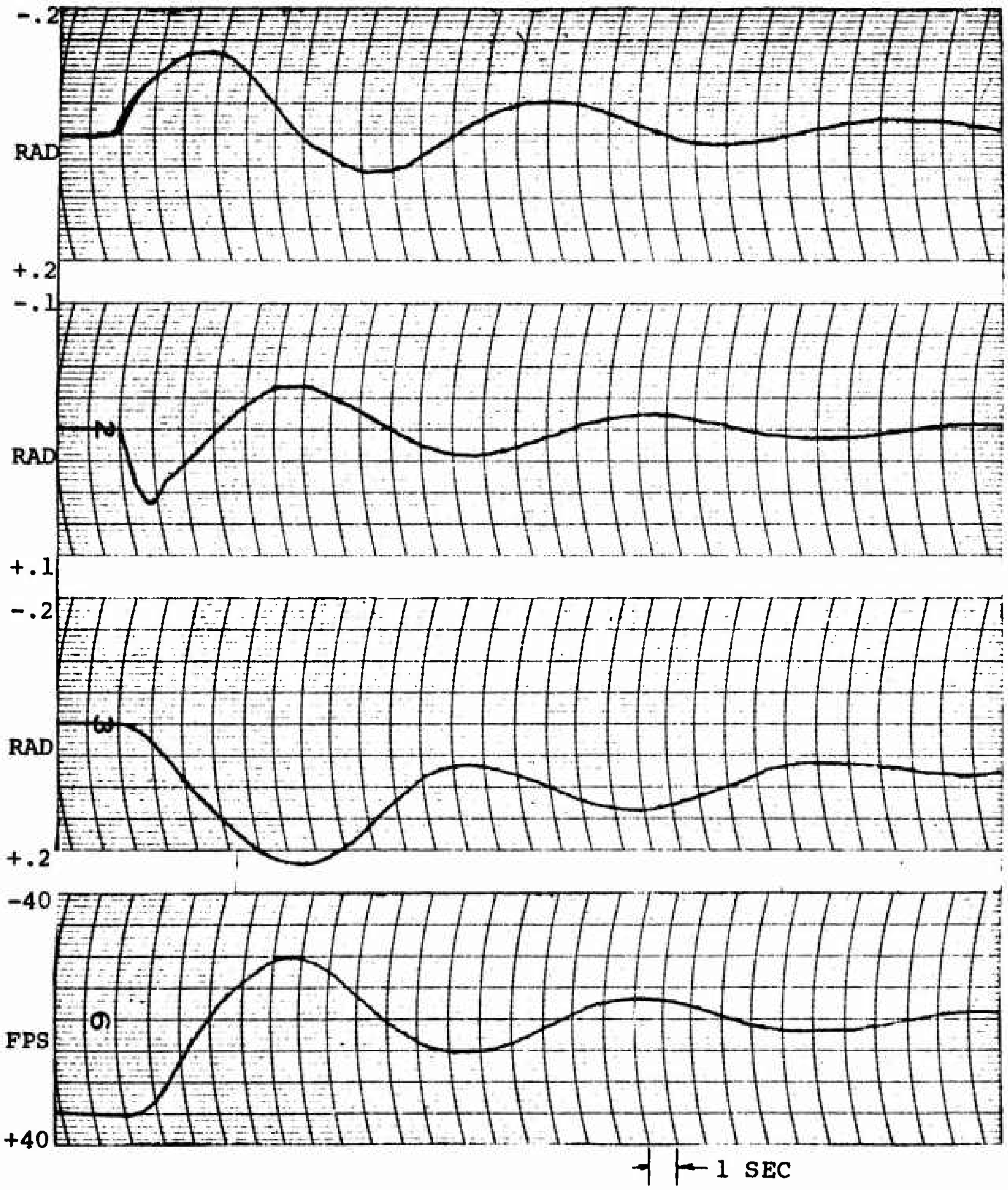

FIGURE 20

LATERAL-DIRECTIONAL

CASE 20

30 F.P.S. GUST

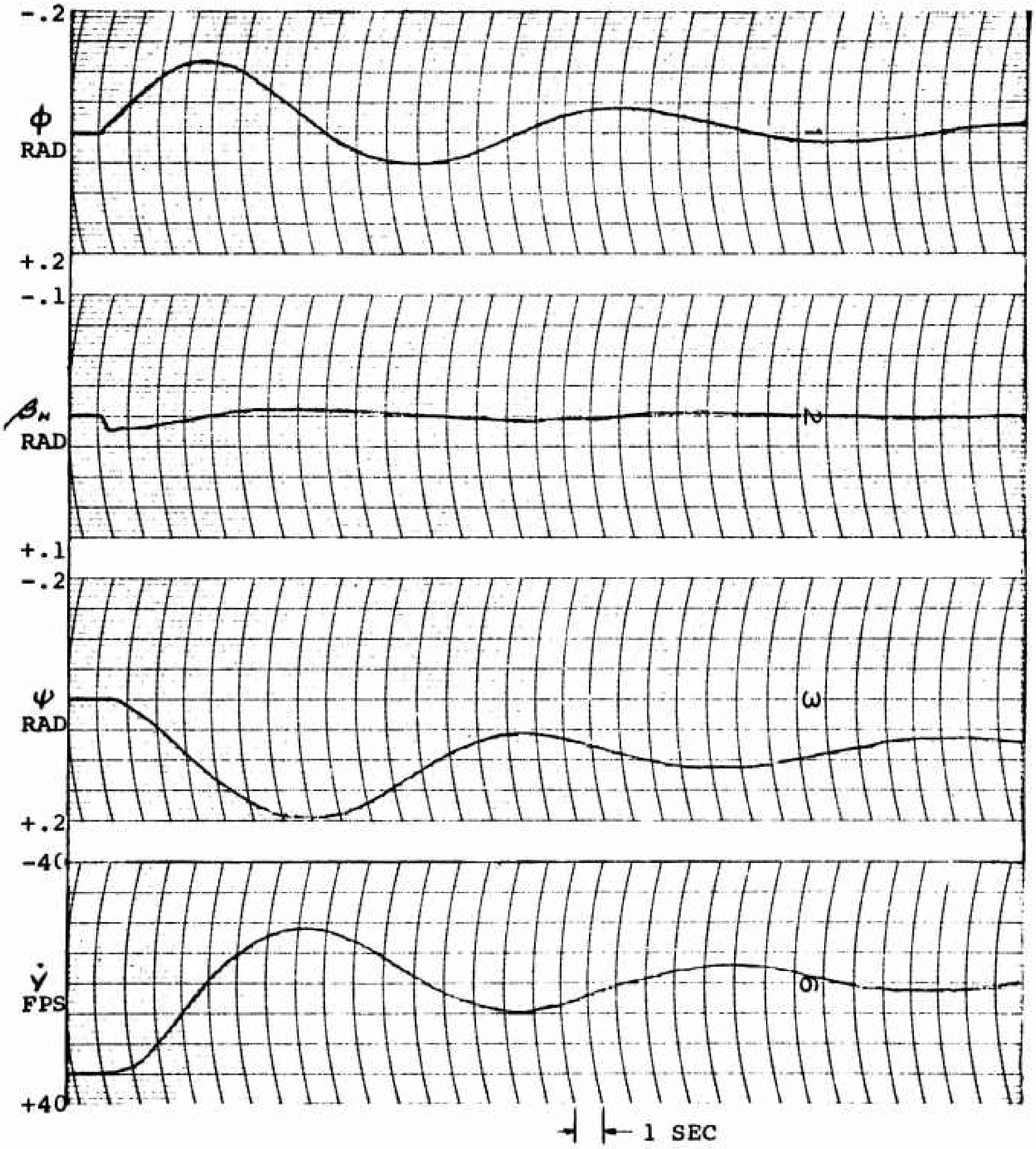

FIGURE 21

LATERAL-DIRECTIONAL

CASE 21

30 F.P.S. GUST

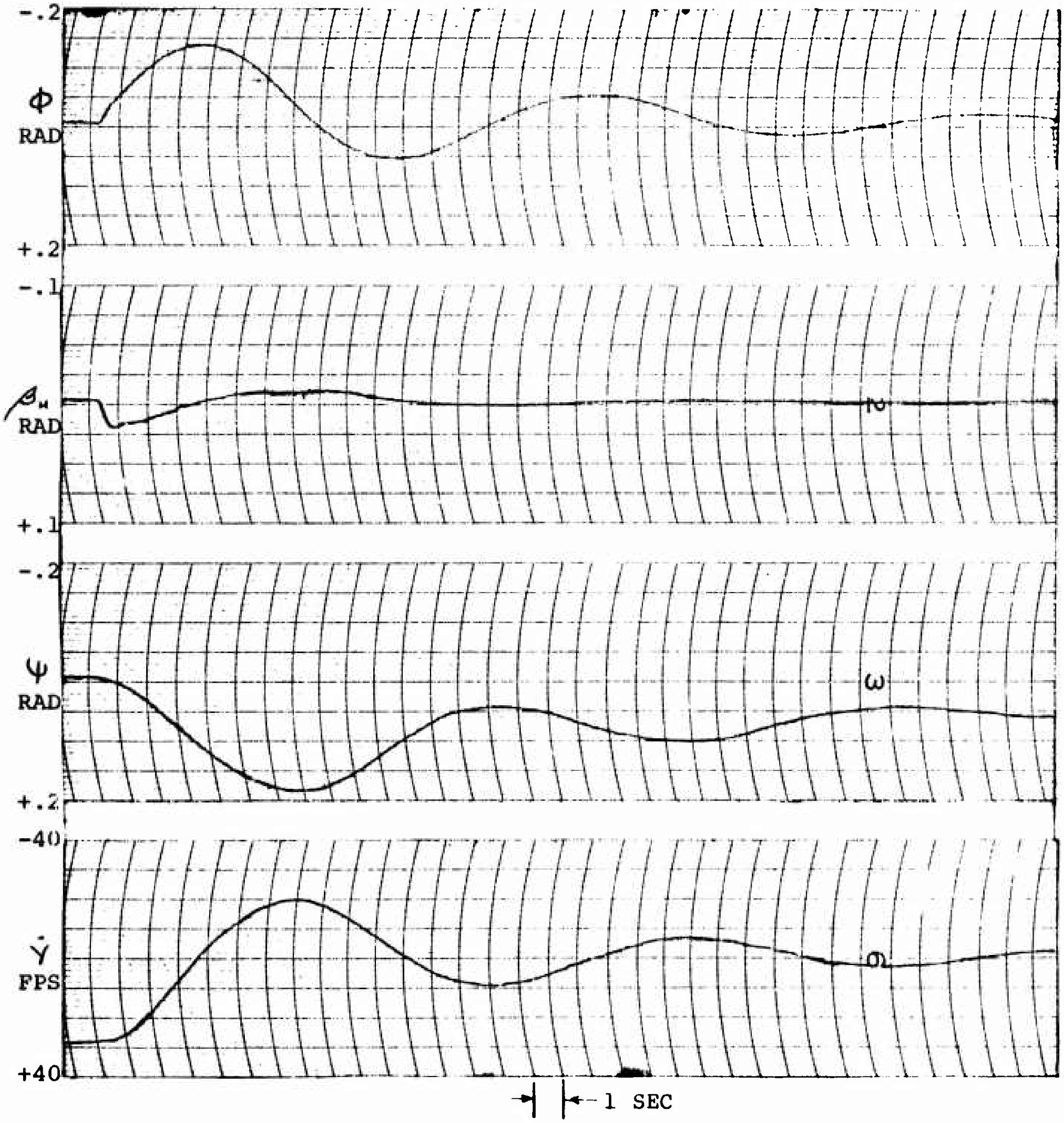

FIGURE 22

LATERAL-DIRECTIONAL

CASE 22

30 F.P.S. GUST

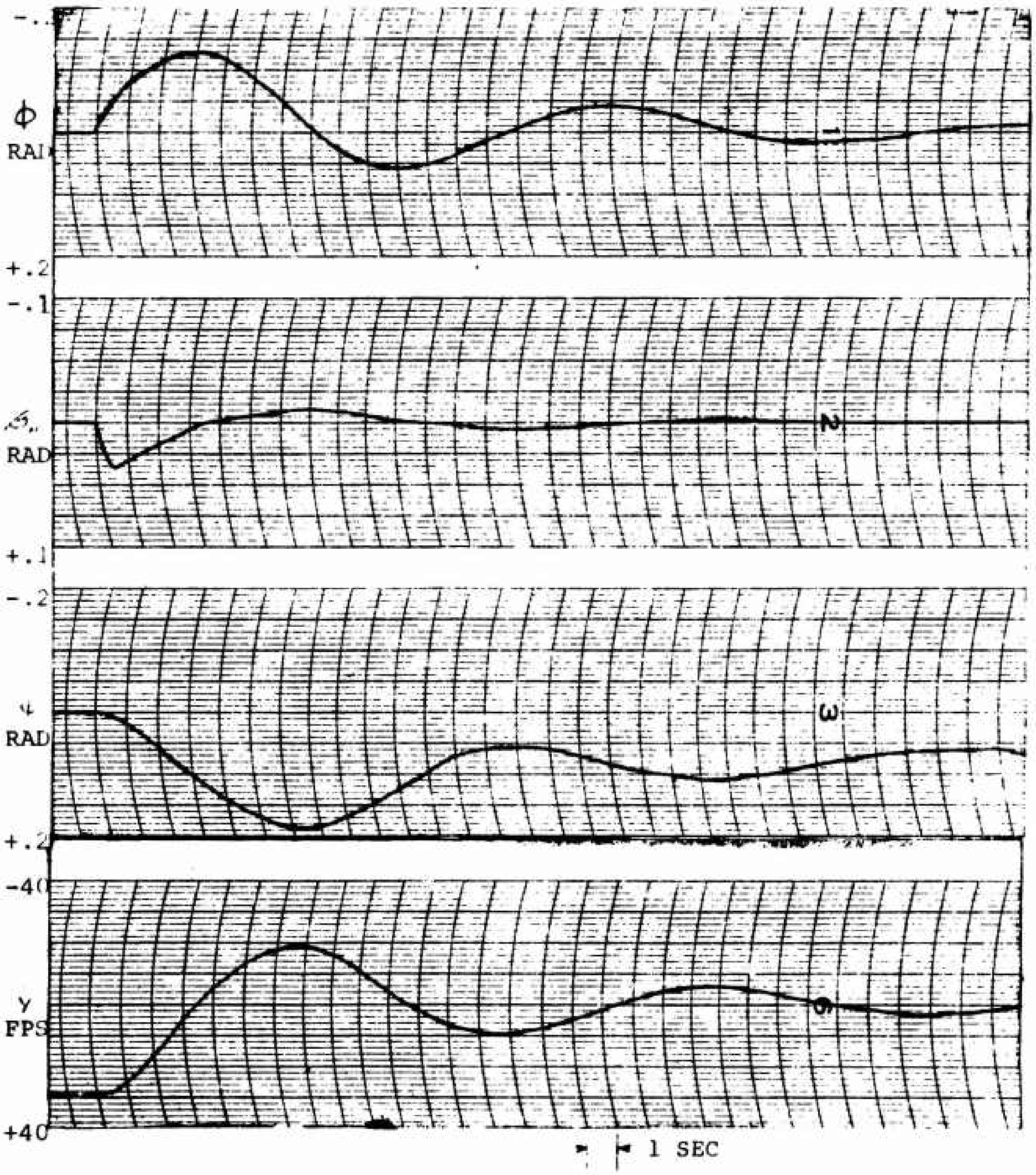

FIGURE 23

LATERAL-DIREOTIONAL

CASE 25

30 F.P.S. GUST

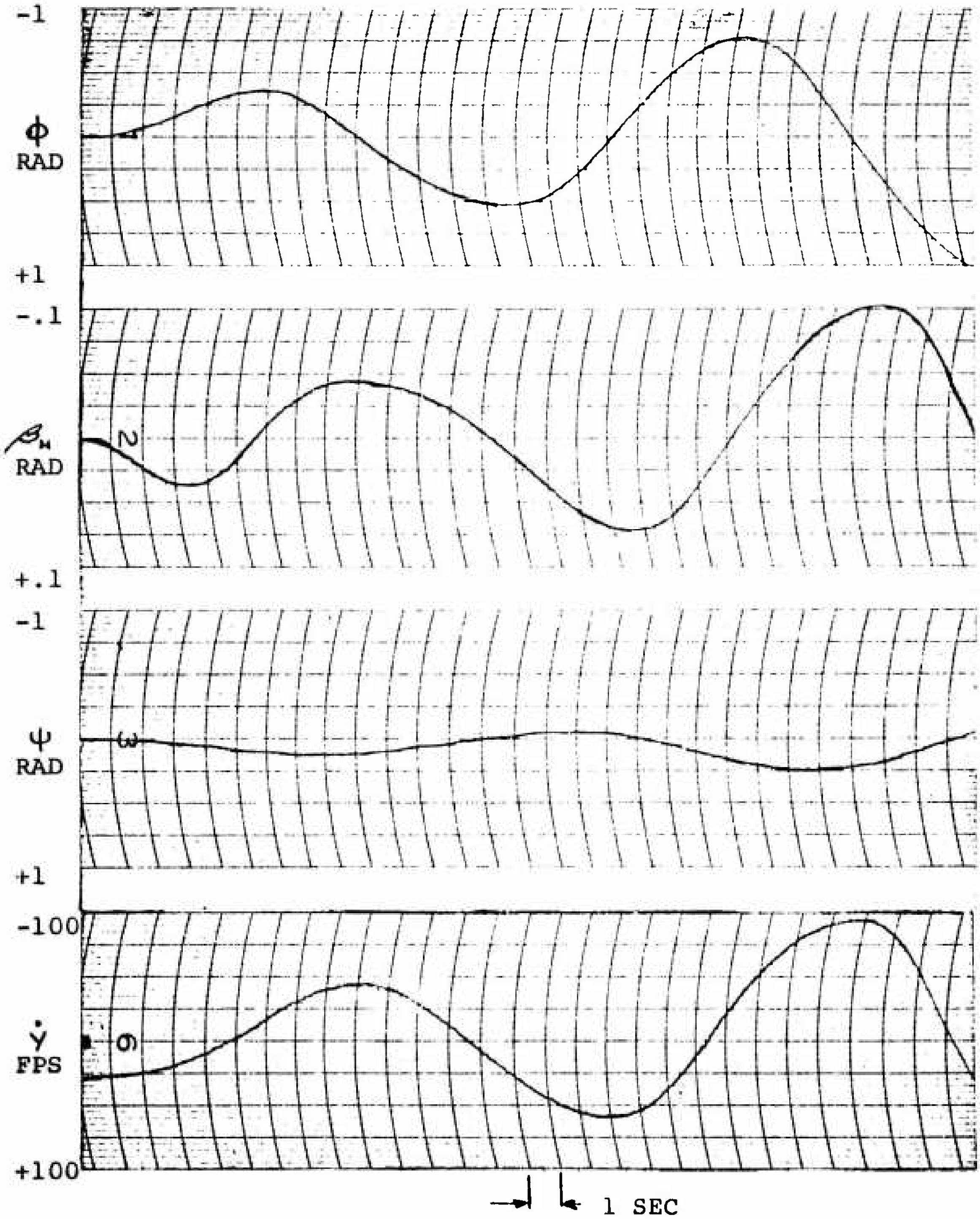

FIGURE 24

LATERAL-DIRECTIONAL

CASE 26

30 F.P.S. GUST

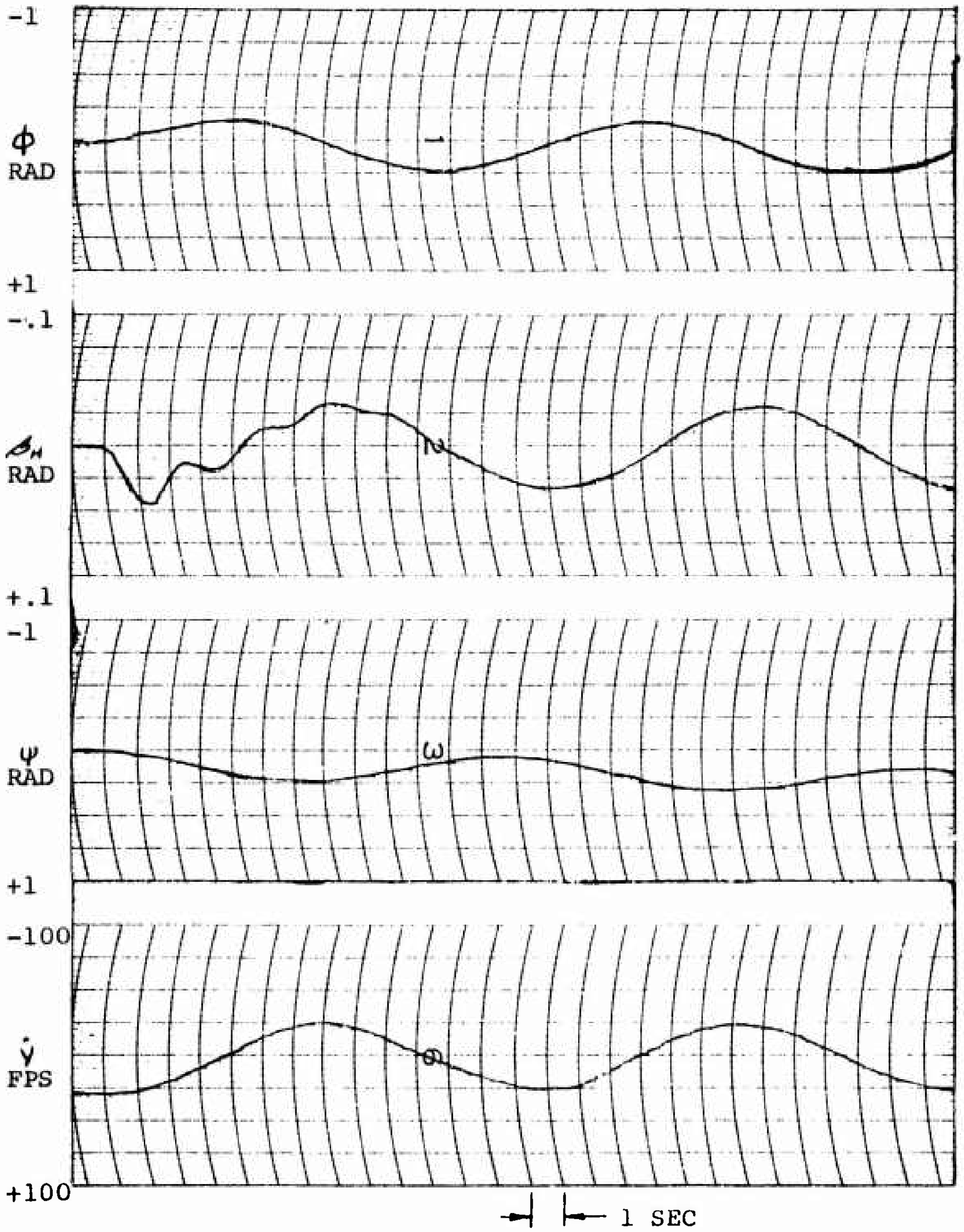

FIGURE 25

LATERAL-DIRECTIONAL

CASE 27

30 F.P.S. GUST

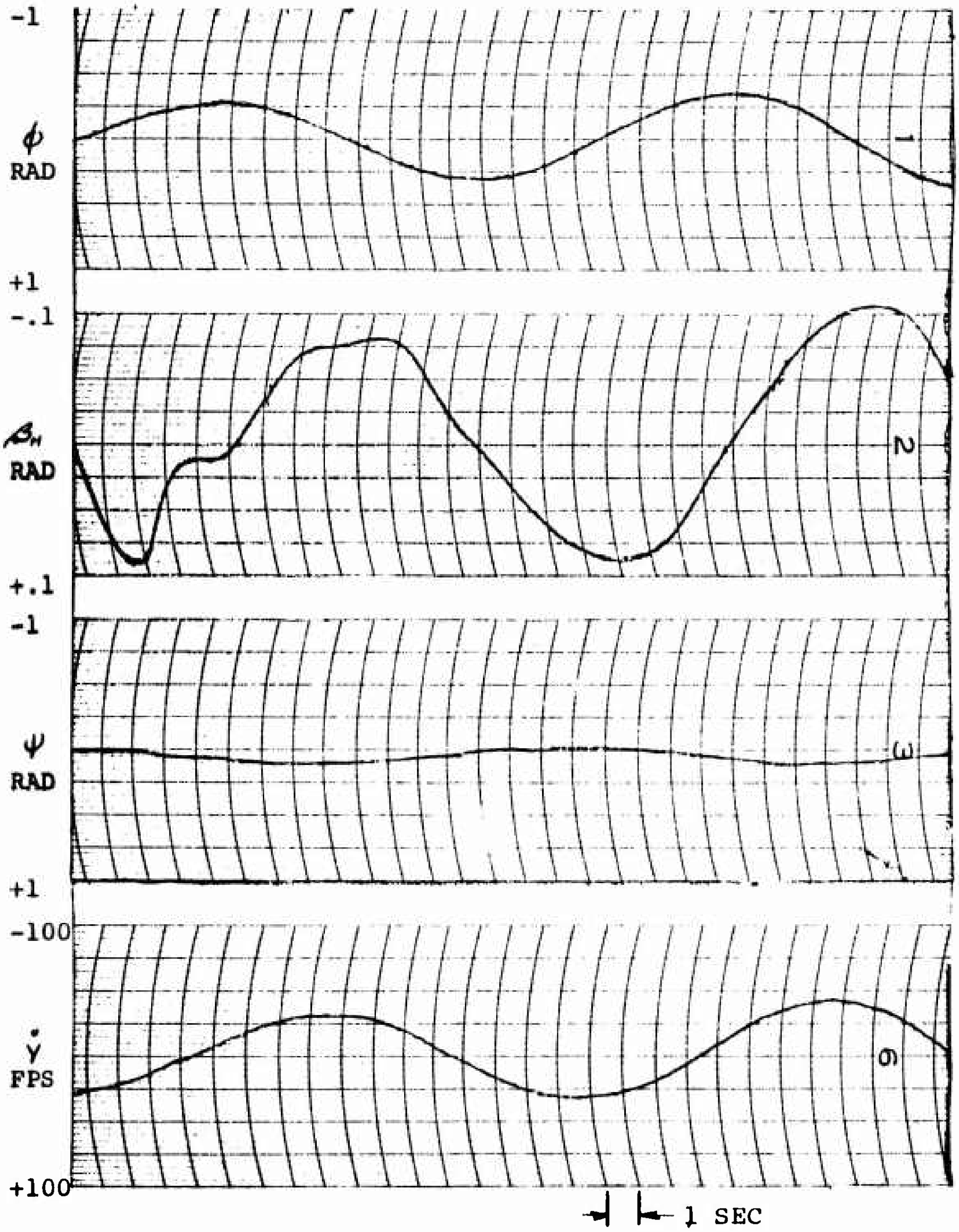

FIGURE 26

CASE 26 - 1 IN. LATERAL STEP RESPONSE

5°/IN. AILERON

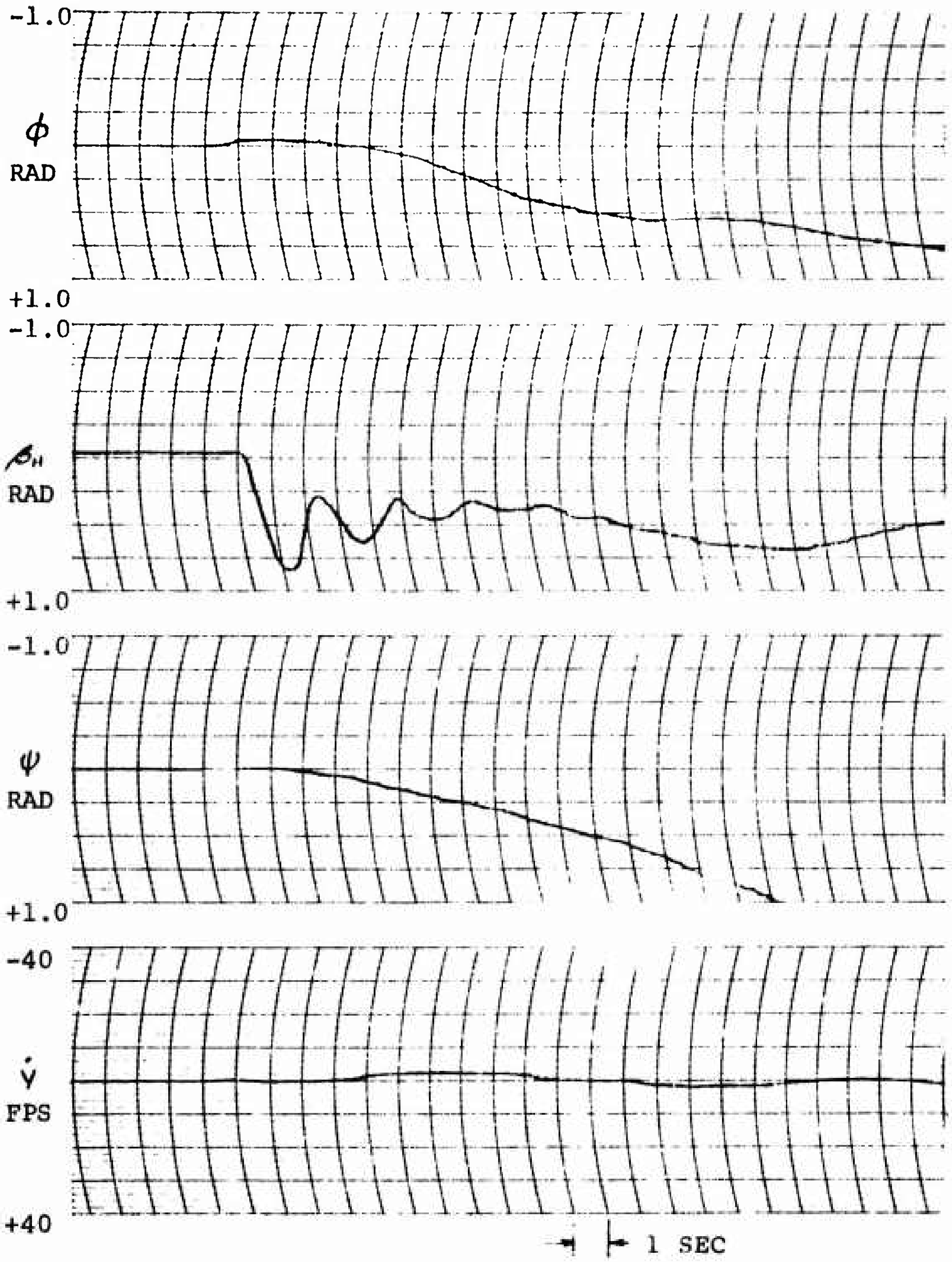

FIGURE 27

TABLE 28

TABLE OF MAXIMUM WING DEFLECTIONS

(LATERAL-DIRECTIONAL)

CASE	FIRST PEAK AMPLITUDE DEG.	SECOND PEAK AMPLITUDE DEG.
12	50.0	—
1	29	100 plus.
4	6.9	2.9
18	3.4	2.0
20	.64	.4
21	1.4	.6
22	2.0	.75
25	2.1	2.5
26	2.5	2.0
27	5.40	4.60

LOCI OF THE ROOTS OF THE CHARACTERISTIC EQUATION

Note: 1. Only critical roots are shown

2. Only positive imaginary roots are shown

Longitudinal Motion

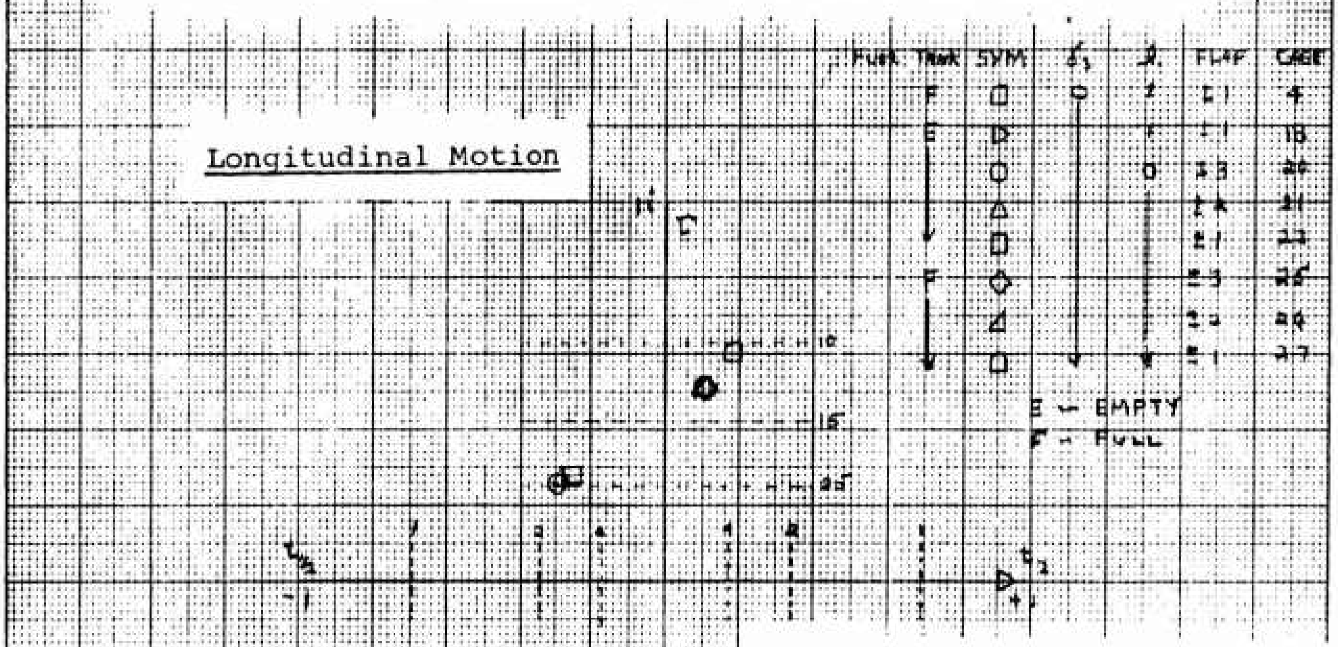

τ – period (sec.)

$t_{1/2}$ – time to half amplitude (sec)

t_2 – time to double amplitude (sec)

Lateral-Directional Motion

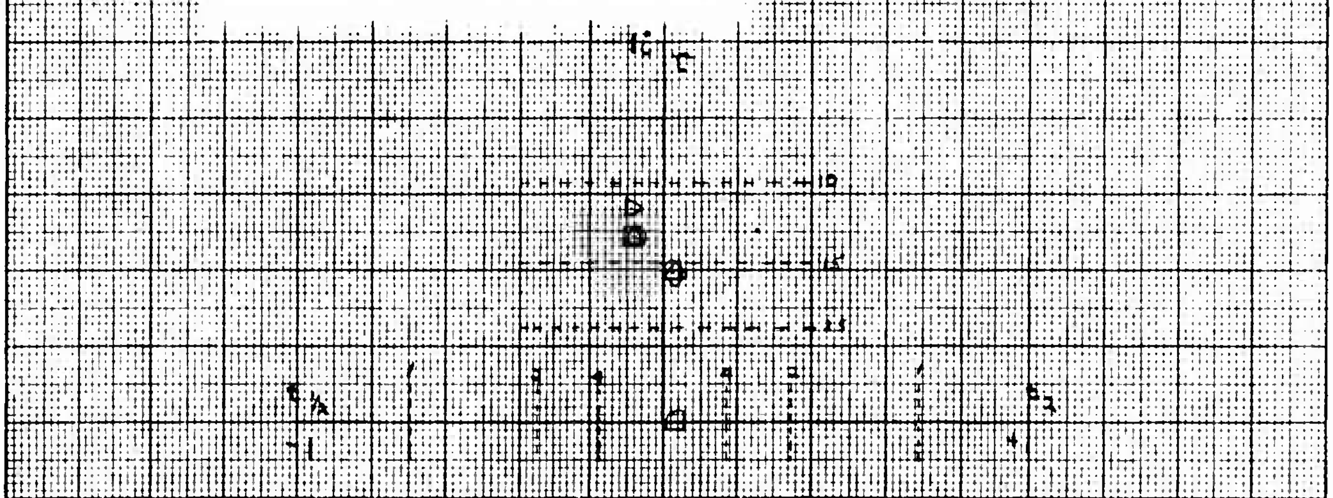

FIGURE 28

LOCI OF THE ROOTS OF THE CHARACTERISTIC EQUATION

Note: 1. Only critical roots are shown

2. Only positive imaginary roots are shown

Longitudinal Motion

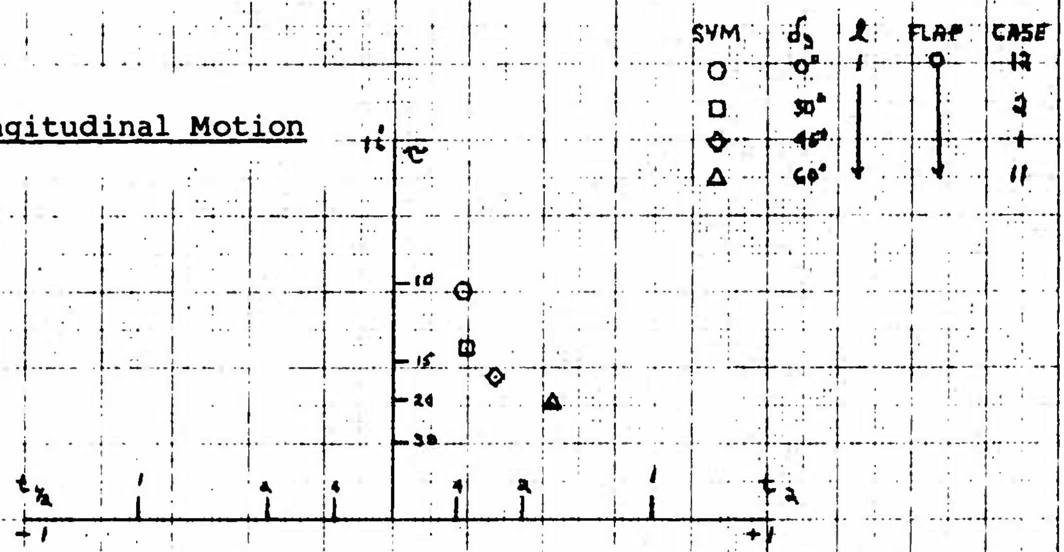

τ - period (sec.)

$t_{1/2}$ - time to half amplitude

t_2 - time to double amplitude

Lateral-Directional Motion

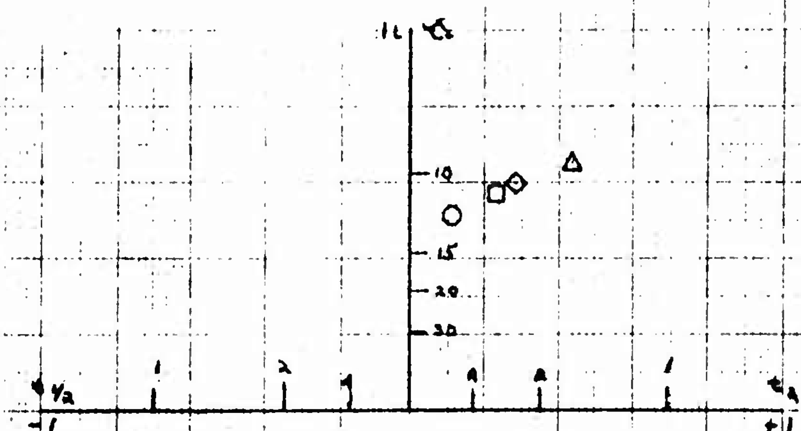

FIGURE 29

APPENDIX C

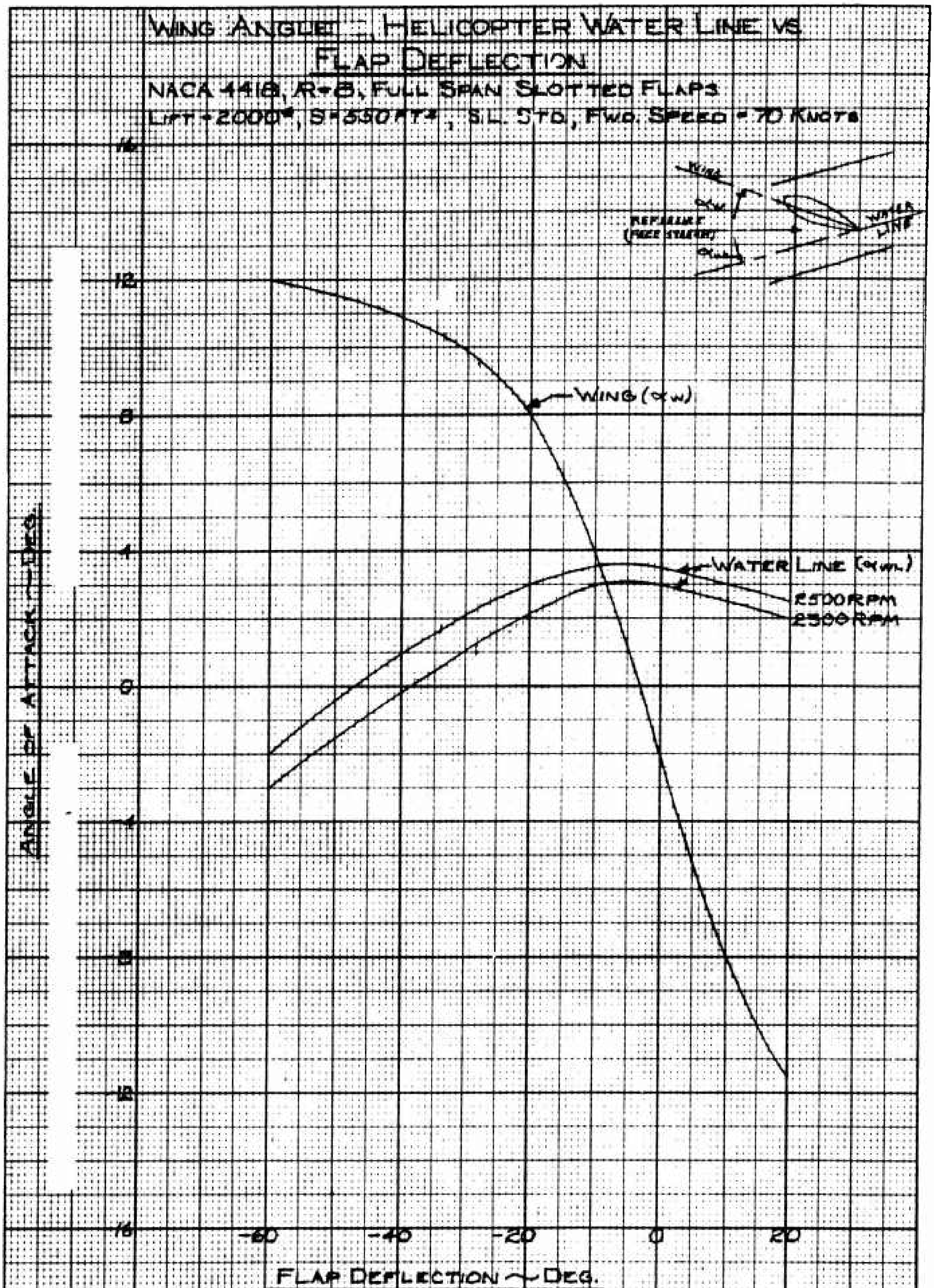

WING ANGLE — HELICOPTER WATER LINE VS FLAP DEFLECTION
NACA 4418, AR=8, FULL SPAN SLOTTED FLAPS
LIFT = 2000#, S = 550 FT², S.L. STD, FWD. SPEED = 70 KNOTS
WING (αW)
WATER LINE (αWL)
2500 RPM
2300 RPM
ANGLE OF ATTACK ~ DEG.
FLAP DEFLECTION ~ DEG.
16
12
8
4
0
-4
-8
-12
-16
-60
-40
-20
0
20

FIGURE 30

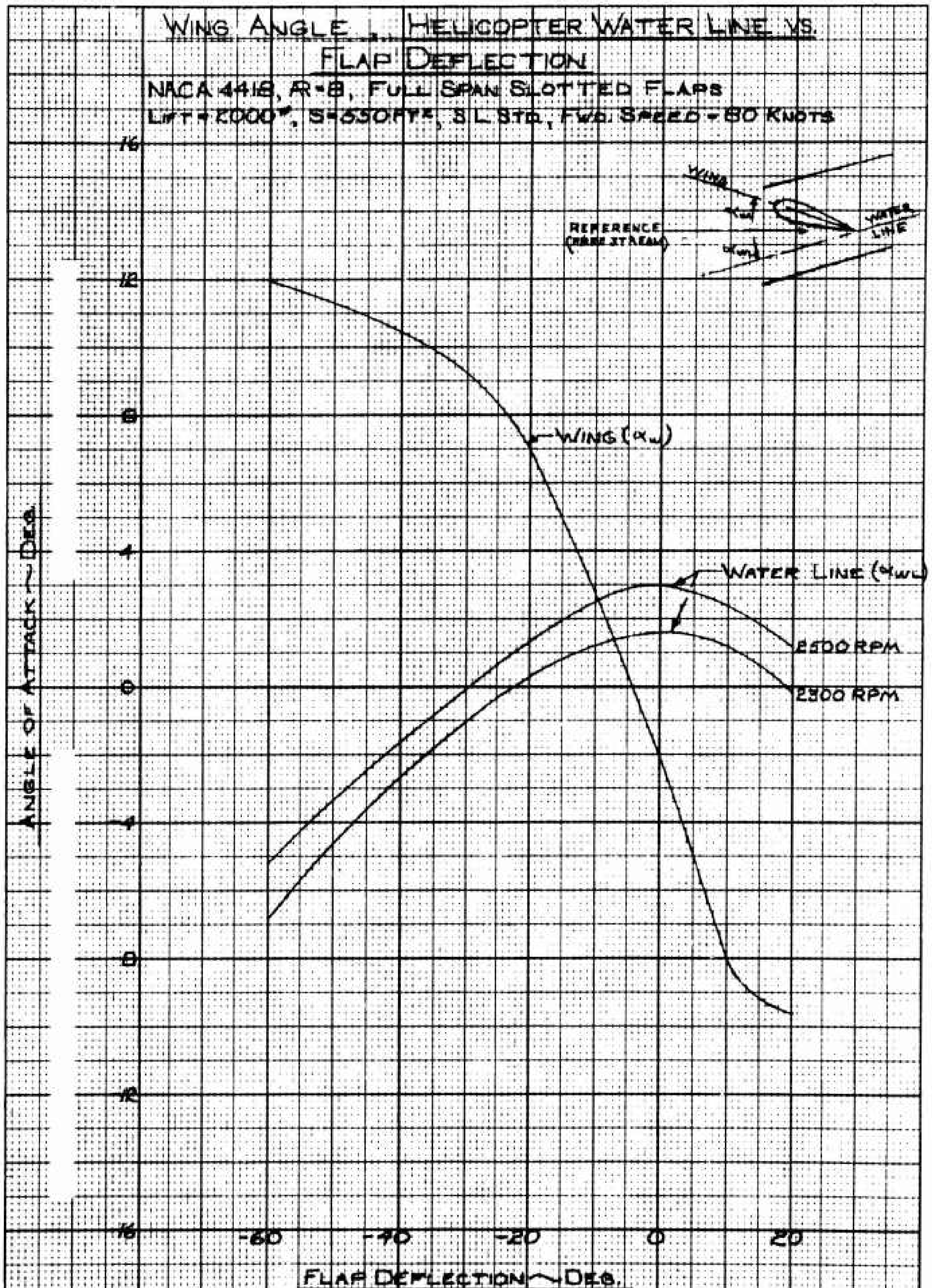
WING ANGLE, HELICOPTER WATER LINE VS.
FLAP DEFLECTION
NACA 4418, AR=8, FULL SPAN SLOTTED FLAPS
LIFT=2000#, S=330FT², S.L. STD., FWD. SPEED=80 KNOTS
WING
WATER LINE
REFERENCE (FREE STREAM)
WING (α_w)
WATER LINE (α_{WL})
2500 RPM
2300 RPM
ANGLE OF ATTACK ~ DEG.
16
12
8
4
0
-4
-8
-12
-16
-60
-40
-20
0
20
FLAP DEFLECTION ~ DEG.

FIGURE 31

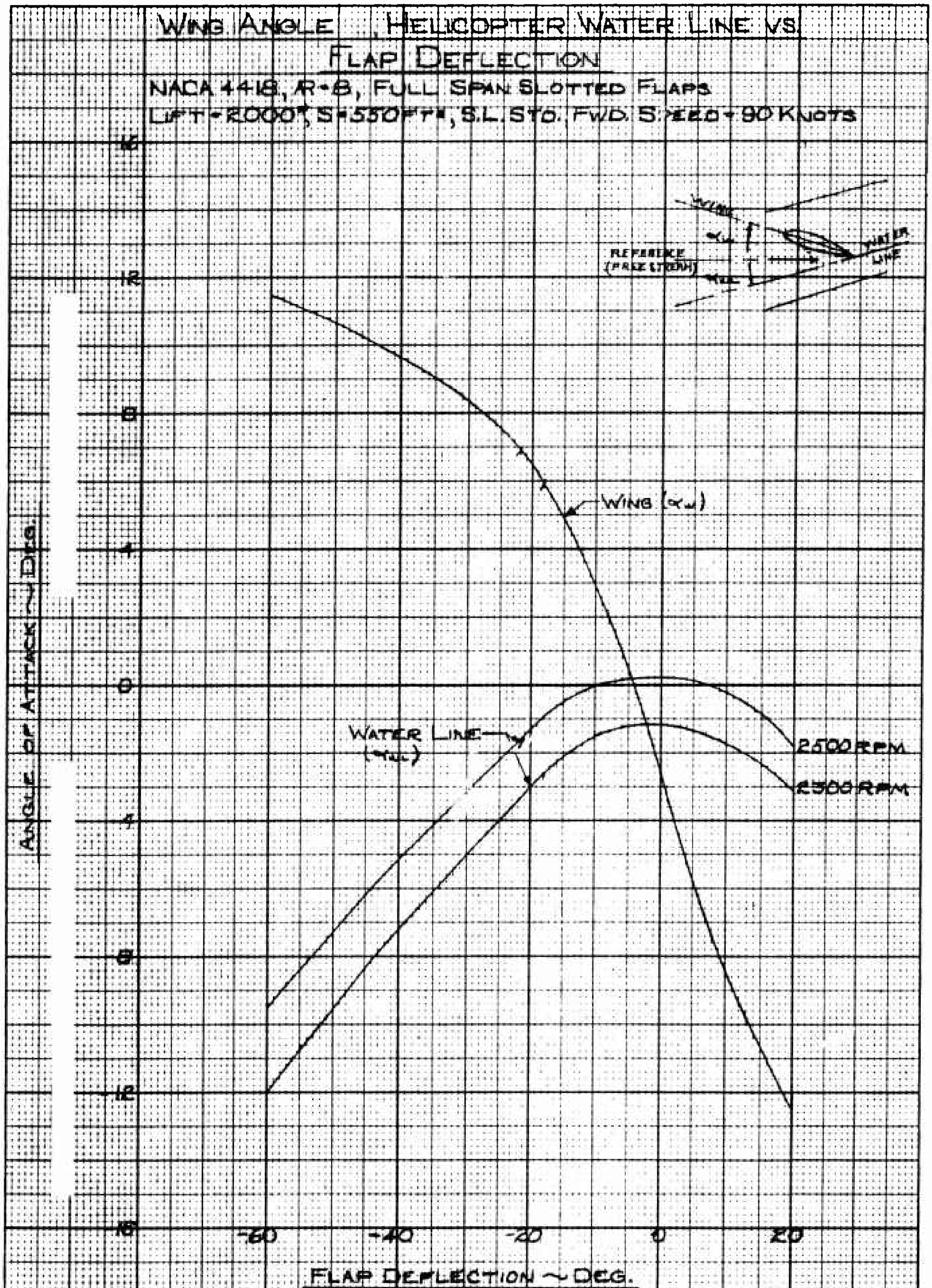

WING ANGLE, HELICOPTER WATER LINE VS
FLAP DEFLECTION
NACA 4418, AR=8, FULL SPAN SLOTTED FLAPS
LIFT=2000#, S=550 FT², S.L. STD. FWD. SPEED=90 KNOTS
ANGLE OF ATTACK ~ DEG.
16
12
8
4
0
-4
-8
-12
-16
-60
-40
-20
0
20
FLAP DEFLECTION ~ DEG.
WING (α_W)
WATER LINE (α_{WL})
2500 RPM
2300 RPM
REFERENCE (FREE STREAM)
WING
WATER LINE

FIGURE 32

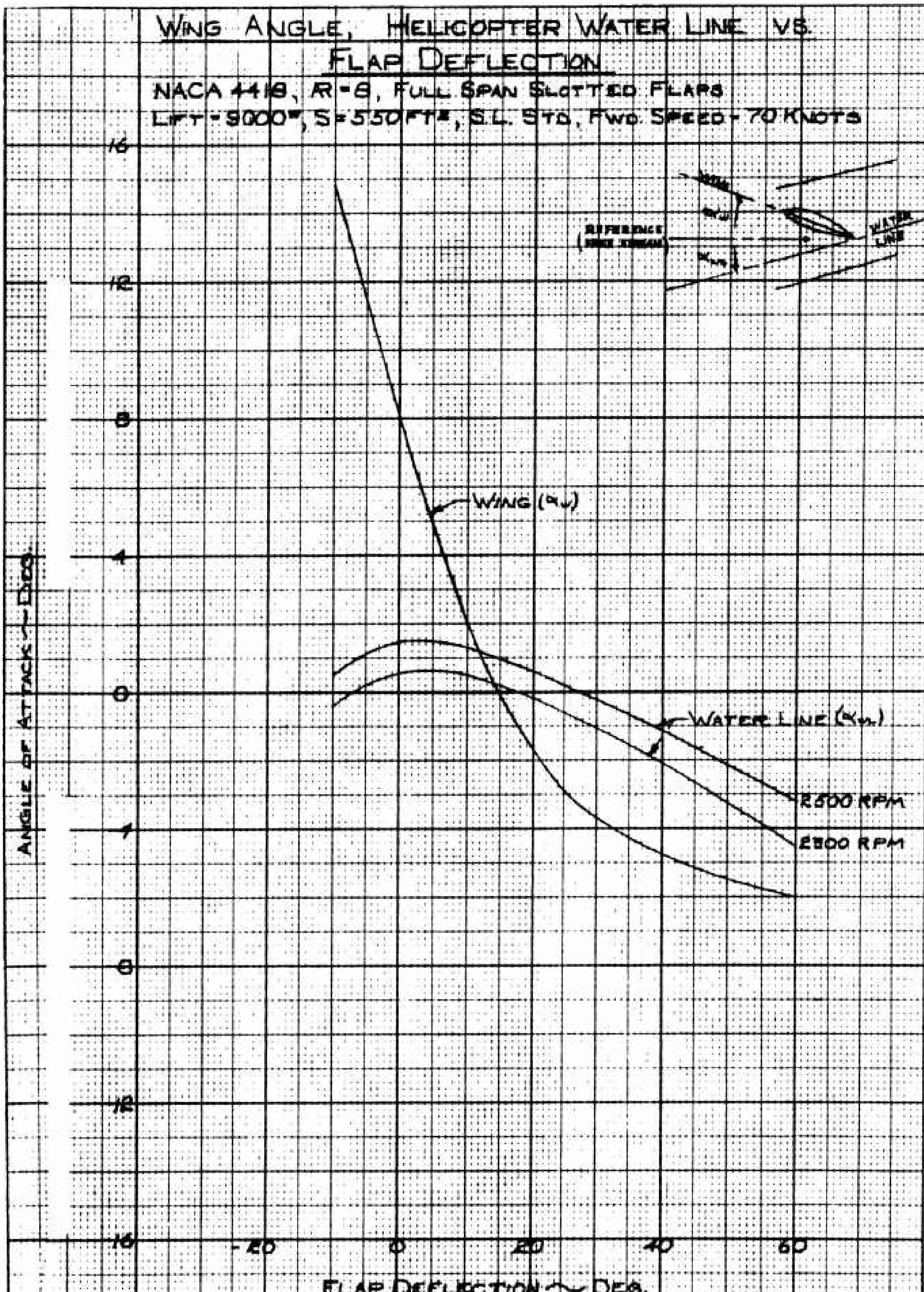
WING ANGLE, HELICOPTER WATER LINE VS. FLAP DEFLECTION
NACA 4418, AR = 8, FULL SPAN SLOTTED FLAPS
LIFT = 9000#, S = 550 FT², S.L. STD, FWD. SPEED = 70 KNOTS
16
12
8
4
0
4
8
12
16
-20
0
20
40
60
WING (α_w)
WATER LINE (α_{WL})
2500 RPM
2300 RPM
REFERENCE
WATER LINE
ANGLE OF ATTACK ~ DEG.
FLAP DEFLECTION ~ DEG.

FIGURE 33

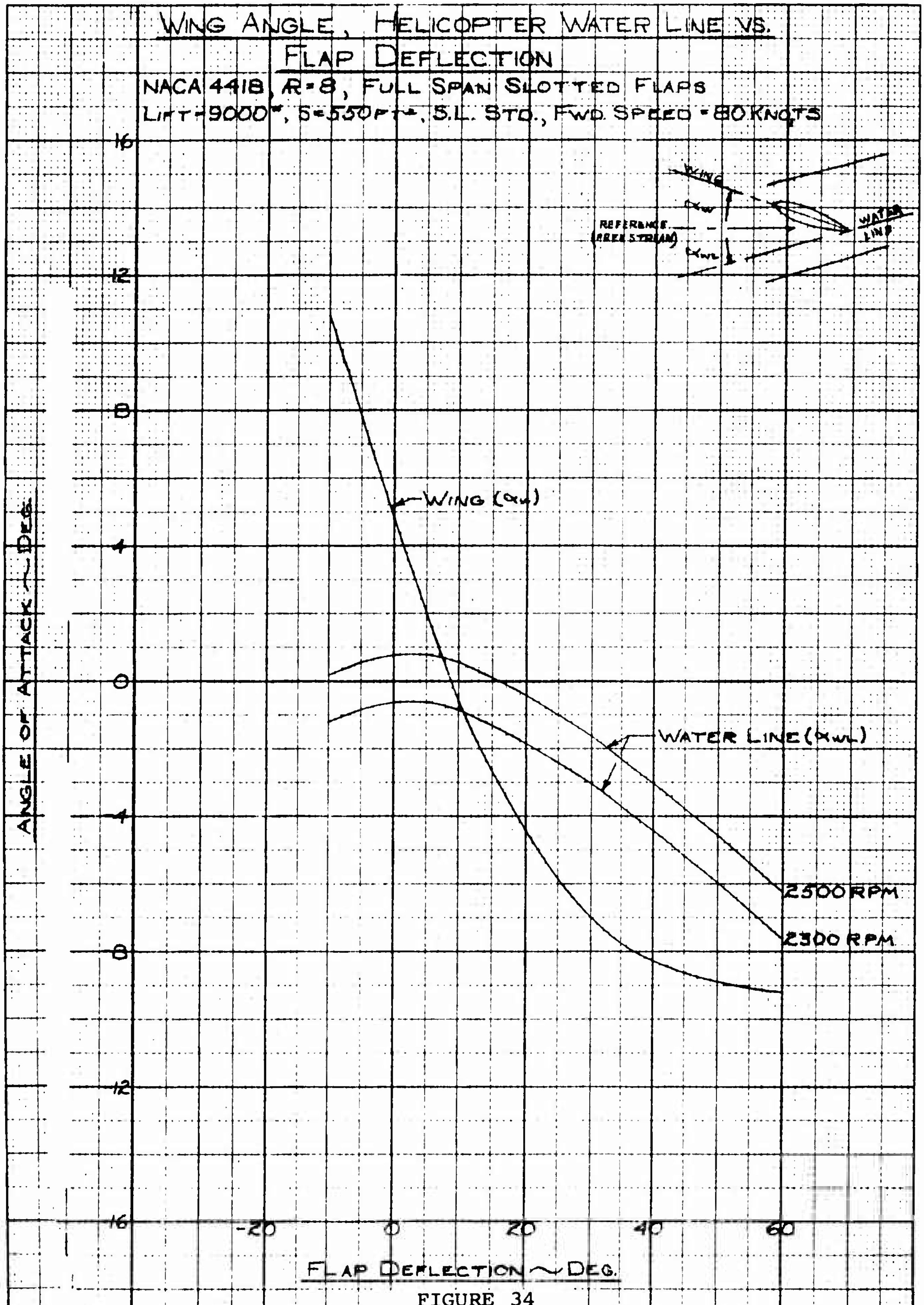
WING ANGLE, HELICOPTER WATER LINE VS.
FLAP DEFLECTION
NACA 4418, Æ=8, FULL SPAN SLOTTED FLAPS
LIFT=9000#, S=550 FT², S.L. STD., FWD. SPEED=80 KNOTS
WING
REFERENCE (FREE STREAM)
WATER LINE
WING (α_W)
WATER LINE (α_{WL})
2500 RPM
2300 RPM
ANGLE OF ATTACK ~ DEG.
FLAP DEFLECTION ~ DEG.
16
12
8
4
0
-4
-8
-12
-16
-20
0
20
40
60

FIGURE 34

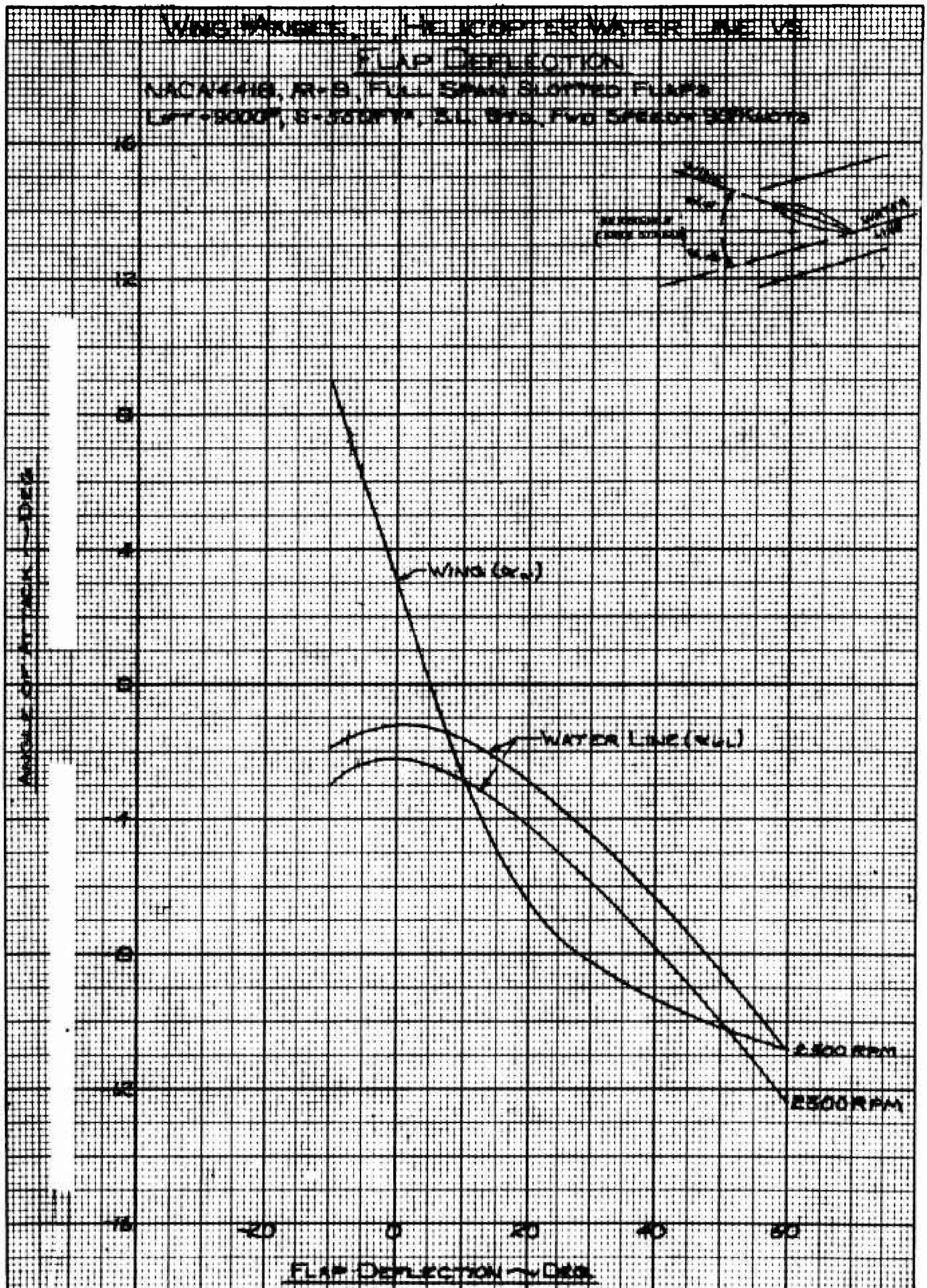
FLAP DEFLECTION
FULL SPAN SLOTTED FLAPS
16
12
8
4
0
-4
-8
-12
-16
WING (αw)
WATER LINE (αWL)
2500 RPM
-20
0
20
40
60
FLAP DEFLECTION ~ DEG

FIGURE 35

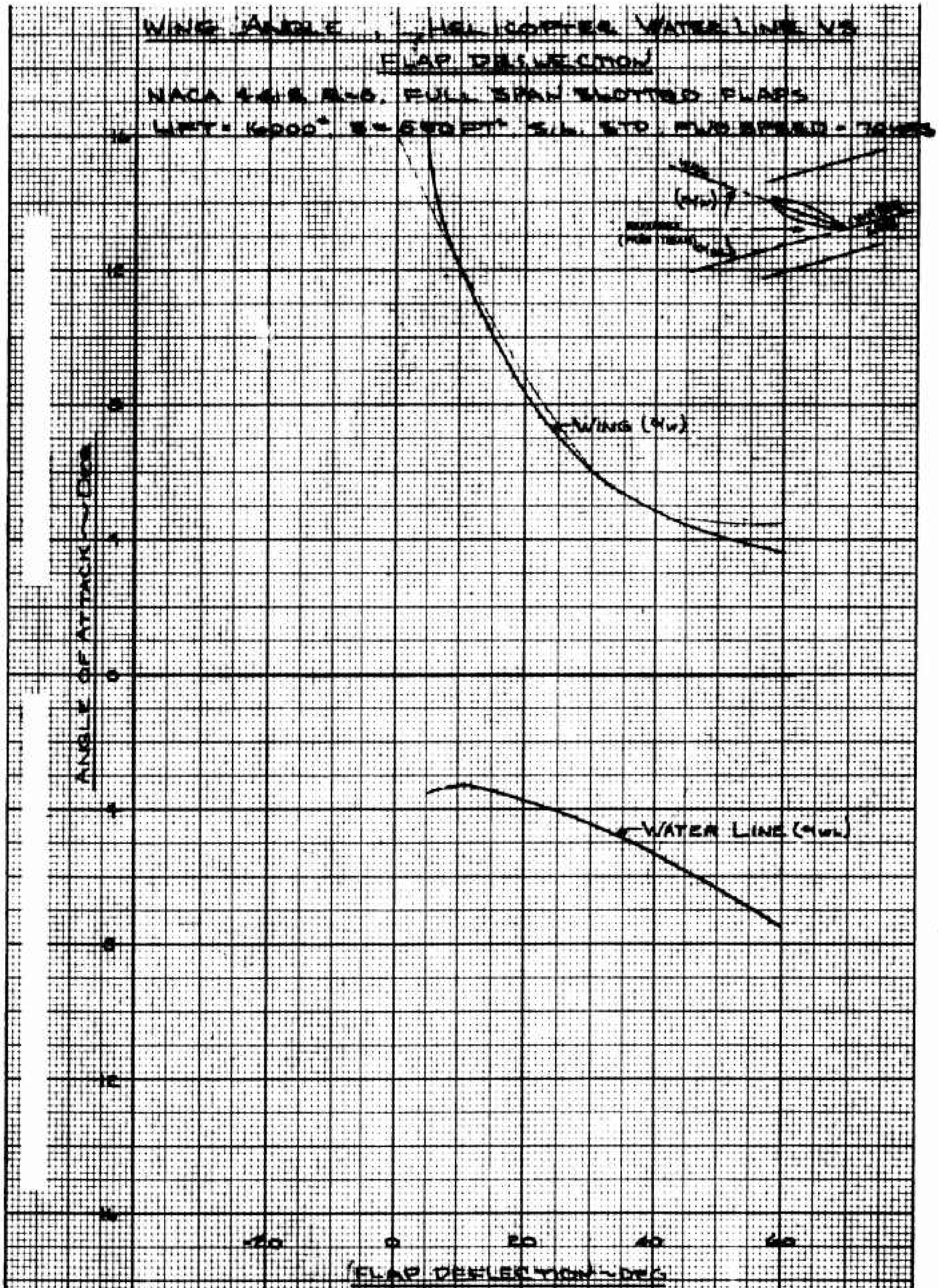
WING ANGLE , HELICOPTER WATER LINE VS
FLAP DEFLECTION
FULL SPAN SLOTTED FLAPS
WING (αw)
WATER LINE (αwL)
ANGLE OF ATTACK ~ DEG
16
12
8
4
0
4
8
12
16
-20
0
20
40
60
FLAP DEFLECTION ~ DEG

FIGURE 36

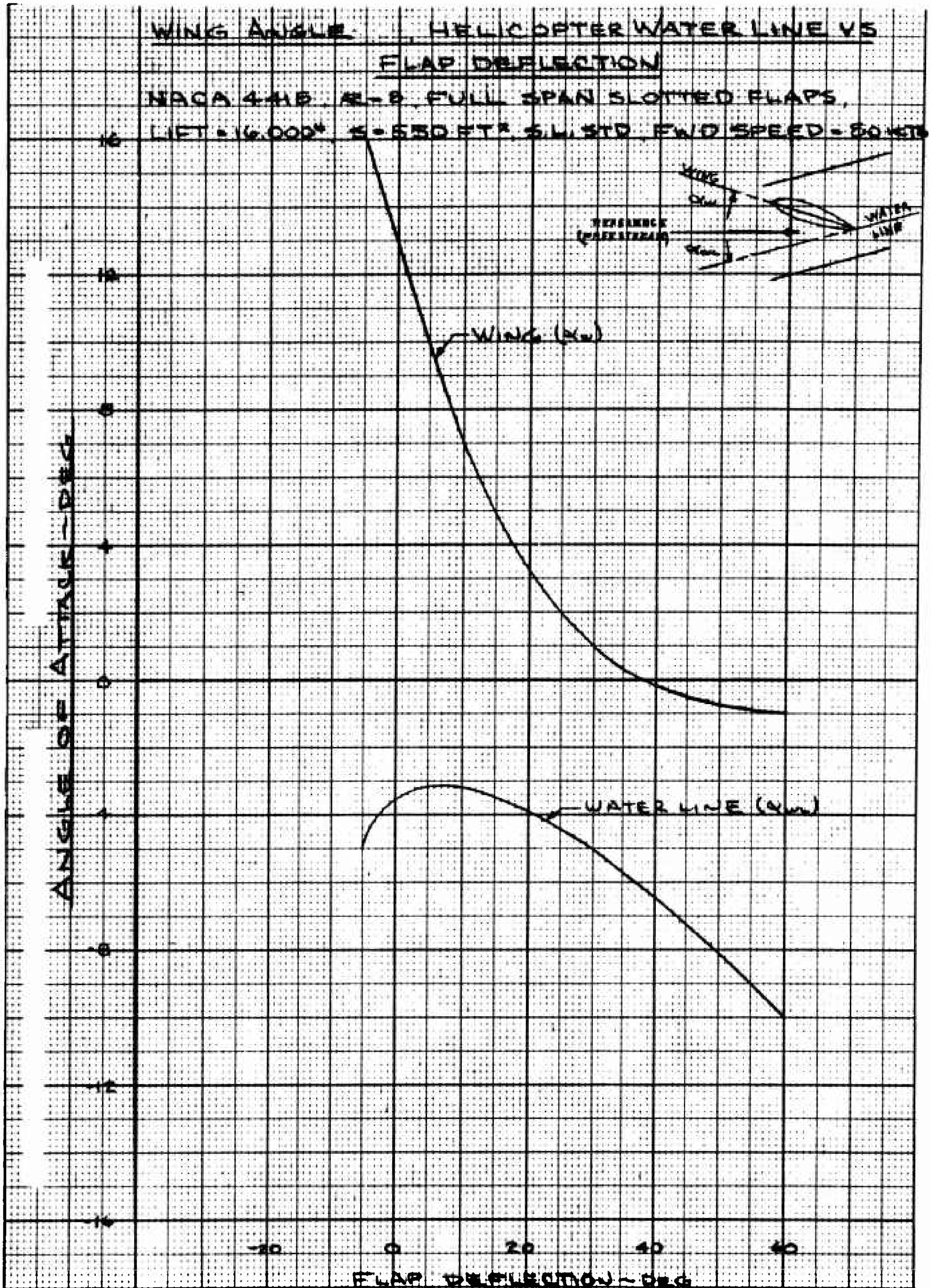
WING ANGLE , HELICOPTER WATER LINE VS
FLAP DEFLECTION
NACA 4415 , AR-8 , FULL SPAN SLOTTED FLAPS ,
LIFT = 16,000#, S = 550 FT², S.L. STD , FWD SPEED = 80 KTS
WING
REFERENCE
WATER LINE
WING (α_w)
WATER LINE (α_{WL})
ANGLE OF ATTACK ~ DEG
16
12
8
4
0
-4
-8
-12
-16
-20
0
20
40
60
FLAP DEFLECTION ~ DEG

FIGURE 37

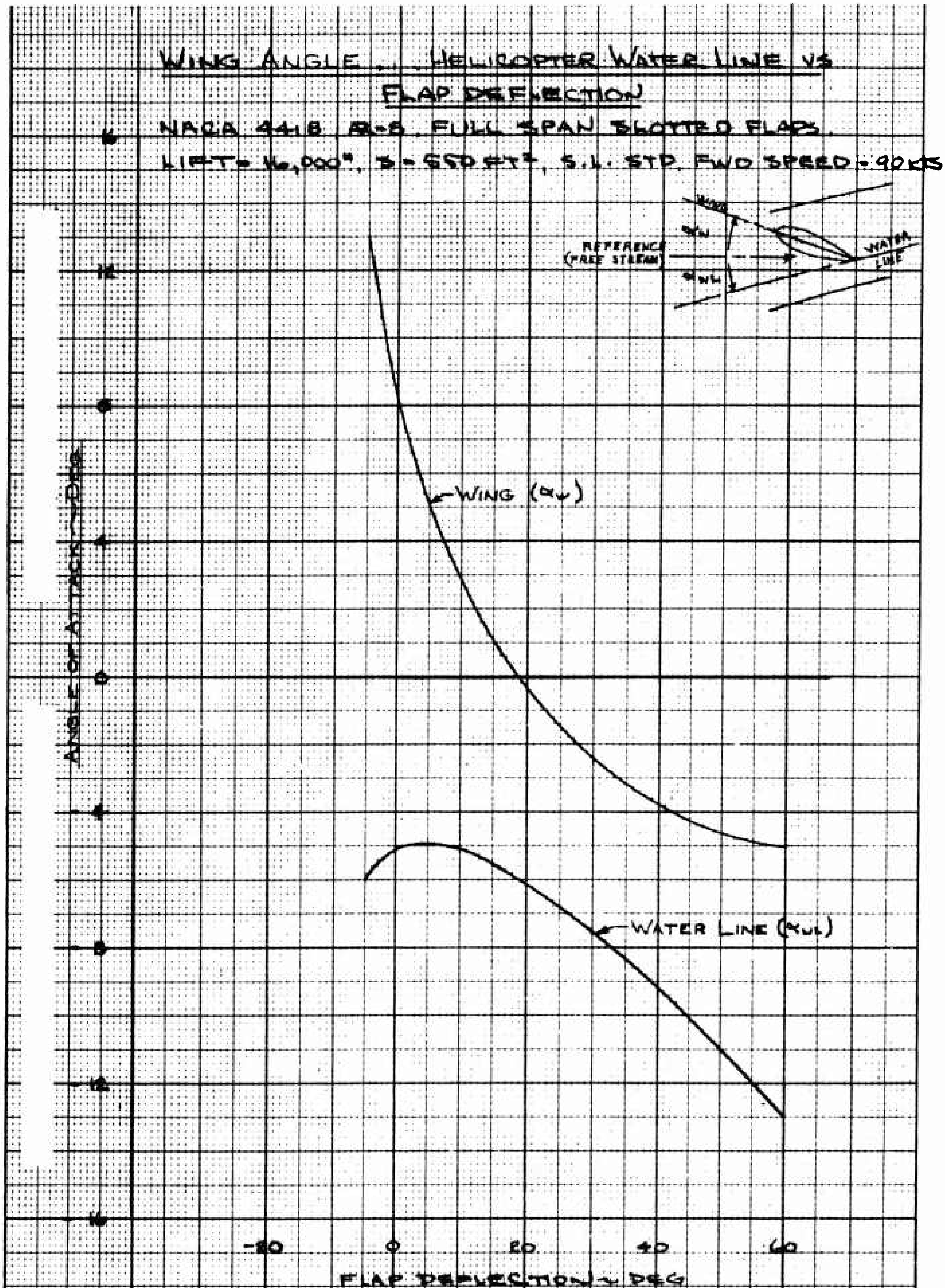
WING ANGLE .. HELICOPTER WATER LINE VS
FLAP DEFLECTION
NACA 4418 AR-6 FULL SPAN SLOTTED FLAPS
LIFT = 16,000#, S = 550 FT², S.L. STD. FWD SPEED = 90 KTS
WING
REFERENCE (FREE STREAM)
WATER LINE
WING (αW)
WATER LINE (αWL)
ANGLE OF ATTACK ~ DEG
16
12
8
4
0
4
8
12
16
-20
0
20
40
60
FLAP DEFLECTION ~ DEG

FIGURE 38

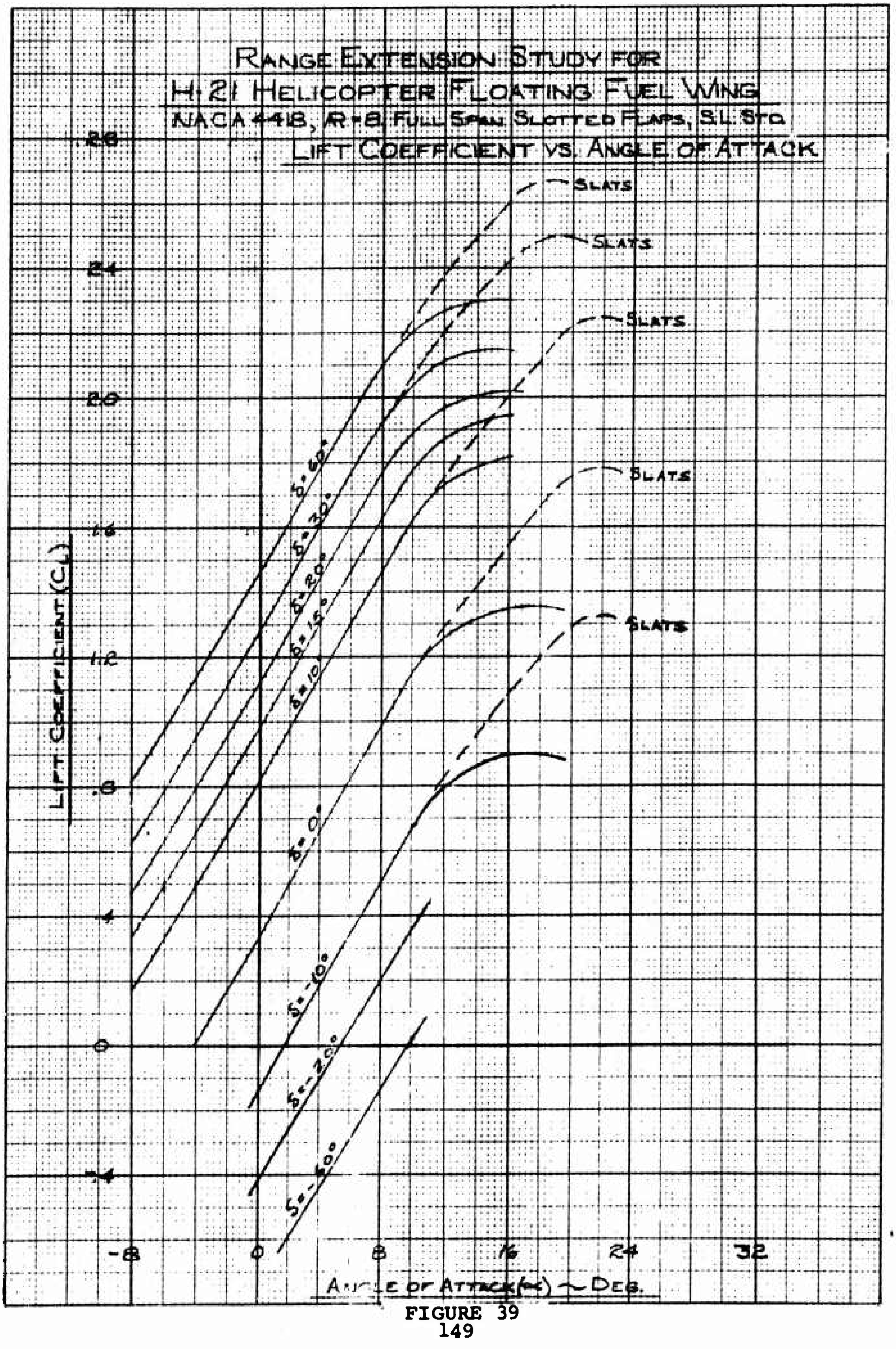

RANGE EXTENSION STUDY FOR
H-21 HELICOPTER FLOATING FUEL WING
NACA 4418, AR=8, FULL SPAN SLOTTED FLAPS, S.L. STD.
LIFT COEFFICIENT VS. ANGLE OF ATTACK
SLATS
SLATS
SLATS
SLATS
SLATS
δ=60°
δ=30°
δ=20°
δ=15°
δ=10°
δ=0°
δ=-10°
δ=-20°
δ=-30°
2.8
2.4
2.0
1.6
1.2
.8
.4
0
-.4
-8
0
8
16
24
32
LIFT COEFFICIENT (CL)
ANGLE OF ATTACK (α) ~ DEG.

FIGURE 39

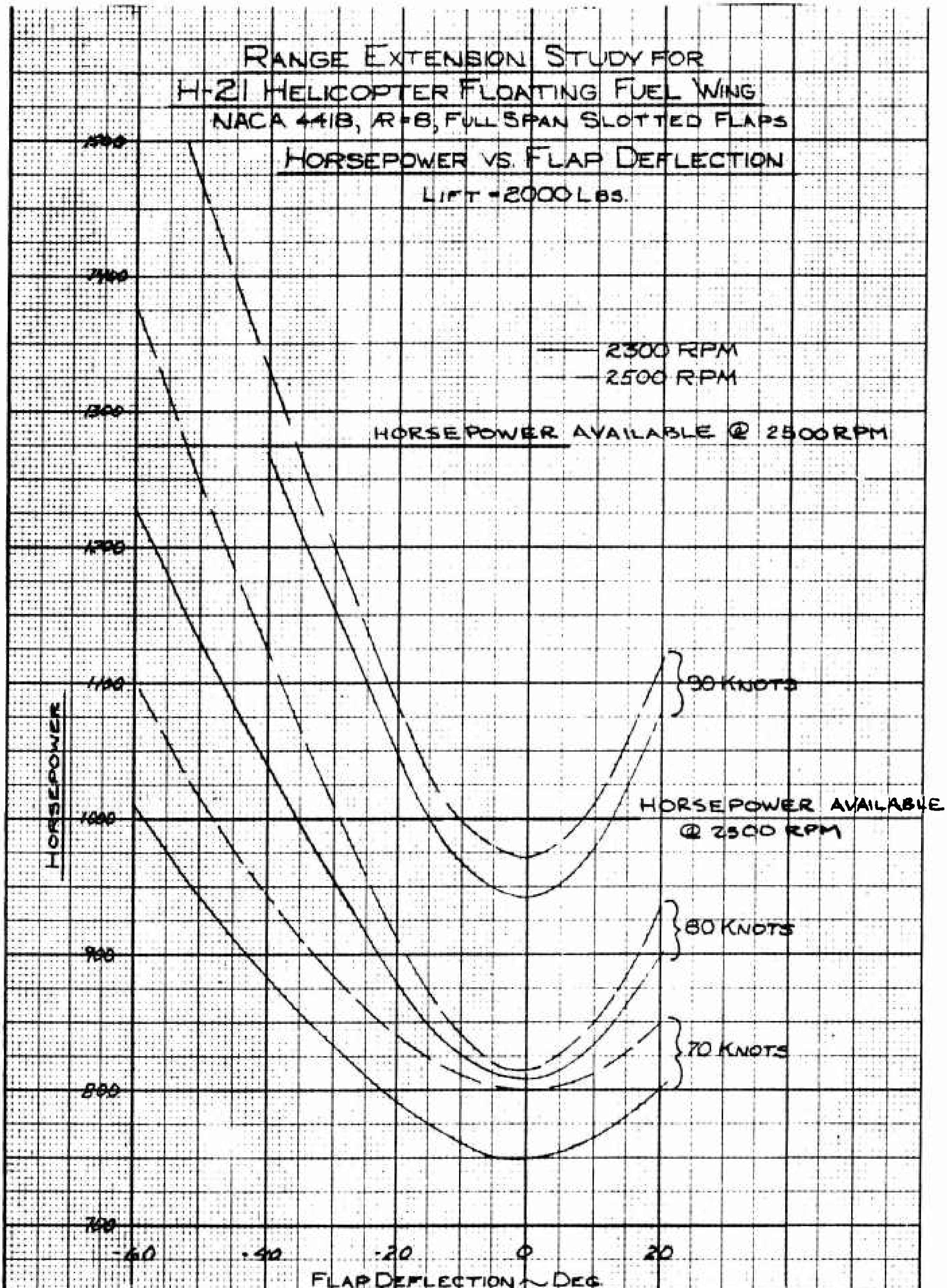
RANGE EXTENSION STUDY FOR
H-21 HELICOPTER FLOATING FUEL WING
NACA 4418, AR=8, FULL SPAN SLOTTED FLAPS
HORSEPOWER VS. FLAP DEFLECTION
LIFT = 2000 LBS.
2300 RPM
2500 R.P.M.
HORSEPOWER AVAILABLE @ 2500 RPM
90 KNOTS
HORSEPOWER AVAILABLE
@ 2300 RPM
80 KNOTS
70 KNOTS
HORSEPOWER
1400
1300
1200
1100
1000
900
800
700
-60
-40
-20
0
20
FLAP DEFLECTION ~ DEG.

FIGURE 40

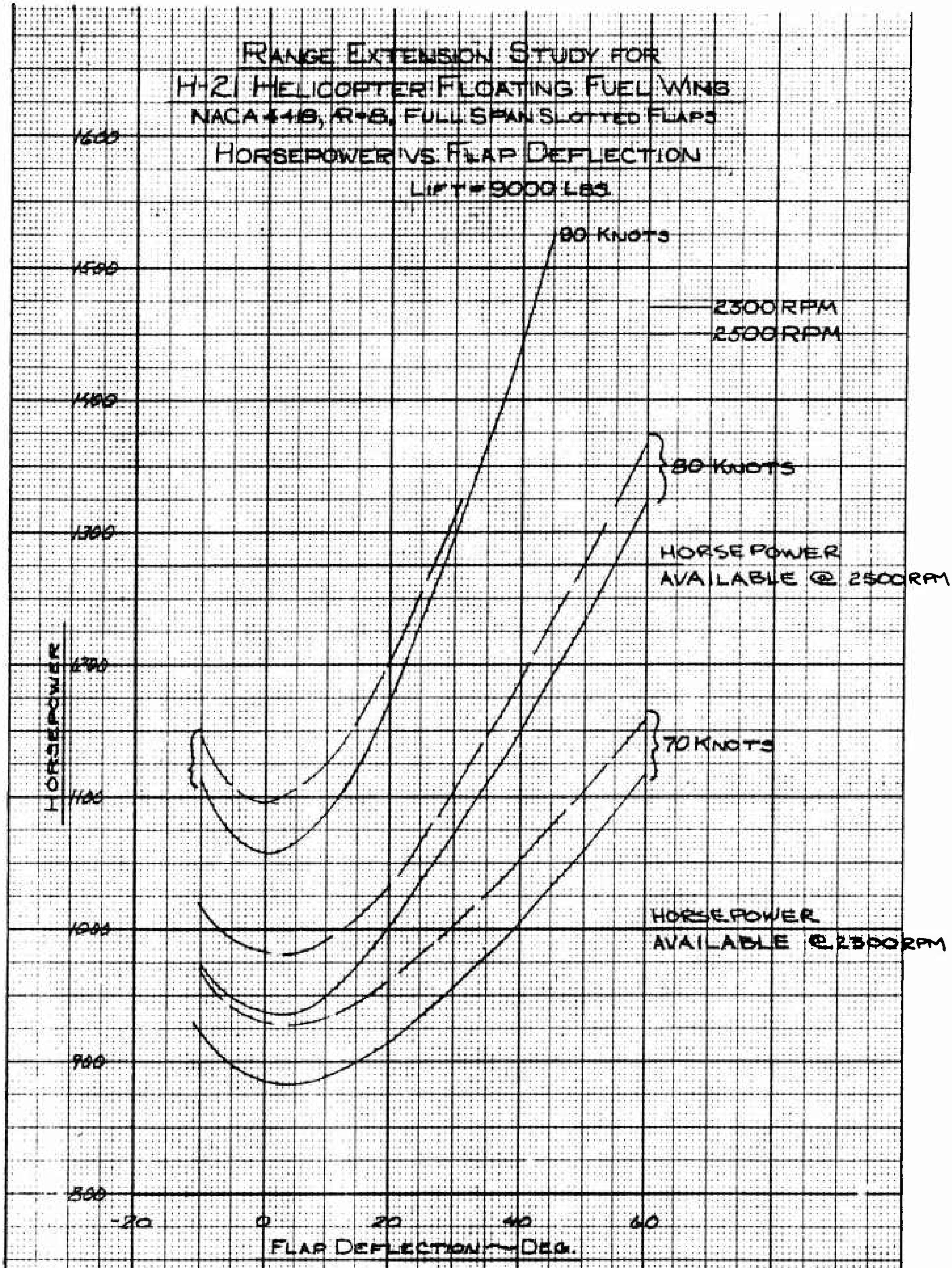

RANGE EXTENSION STUDY FOR
H-21 HELICOPTER FLOATING FUEL WING
NACA 4418, R=8, FULL SPAN SLOTTED FLAPS
HORSEPOWER VS. FLAP DEFLECTION
LIFT = 9000 LBS.
90 KNOTS
2300 RPM
2500 RPM
80 KNOTS
HORSEPOWER AVAILABLE @ 2500 RPM
70 KNOTS
HORSEPOWER AVAILABLE @ 2300 RPM
1600
1500
1400
1300
1200
1100
1000
900
800
HORSEPOWER
-20
0
20
40
60
FLAP DEFLECTION ~ DEG.

FIGURE 41

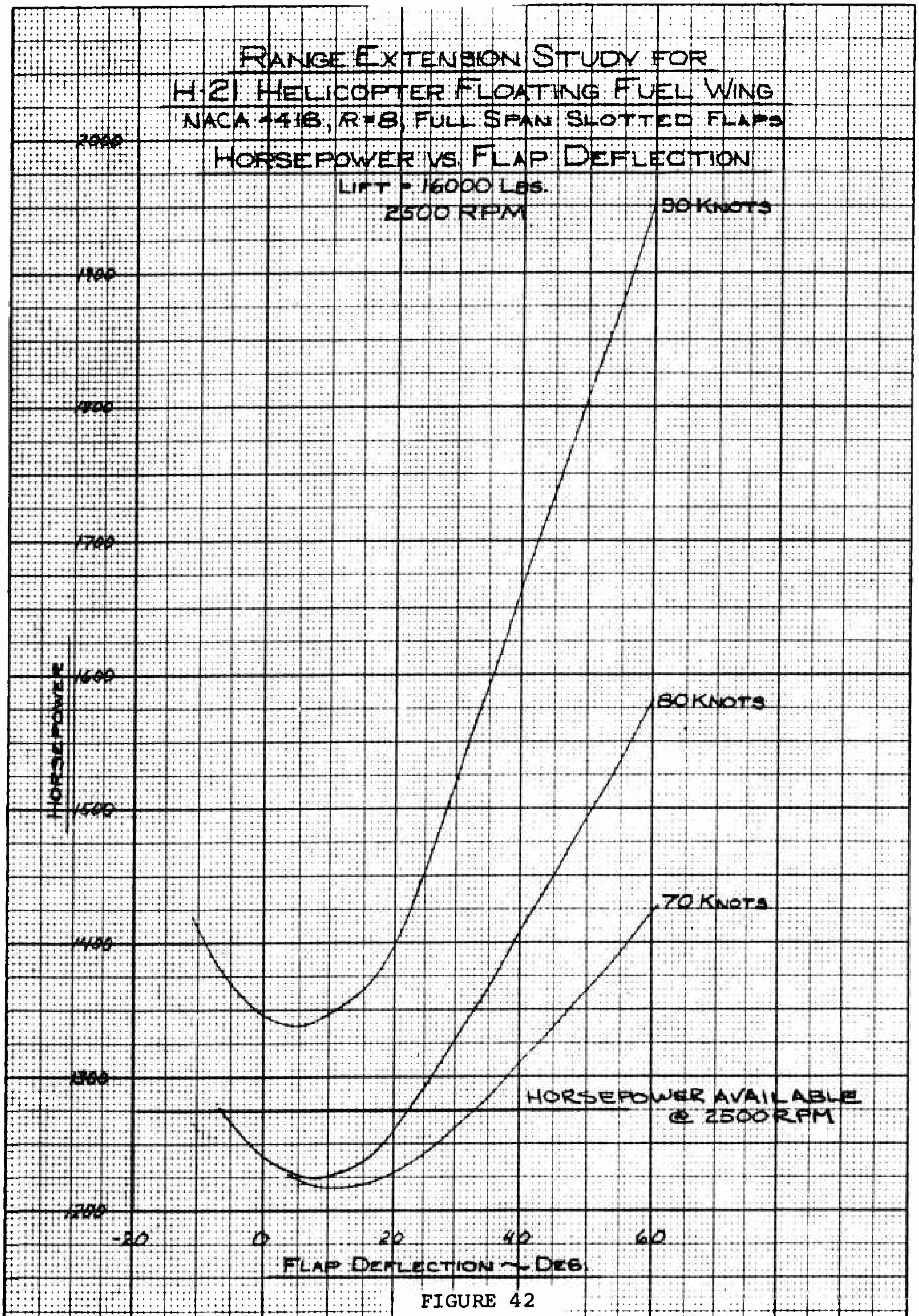
RANGE EXTENSION STUDY FOR
H-21 HELICOPTER FLOATING FUEL WING
NACA 4418, R=8, FULL SPAN SLOTTED FLAPS
HORSEPOWER VS. FLAP DEFLECTION
LIFT = 16000 LBS.
2500 RPM
90 KNOTS
80 KNOTS
70 KNOTS
HORSEPOWER AVAILABLE @ 2500 RPM
HORSEPOWER
2000
1900
1800
1700
1600
1500
1400
1300
1200
-20
0
20
40
60
FLAP DEFLECTION ~ DEG.

FIGURE 42

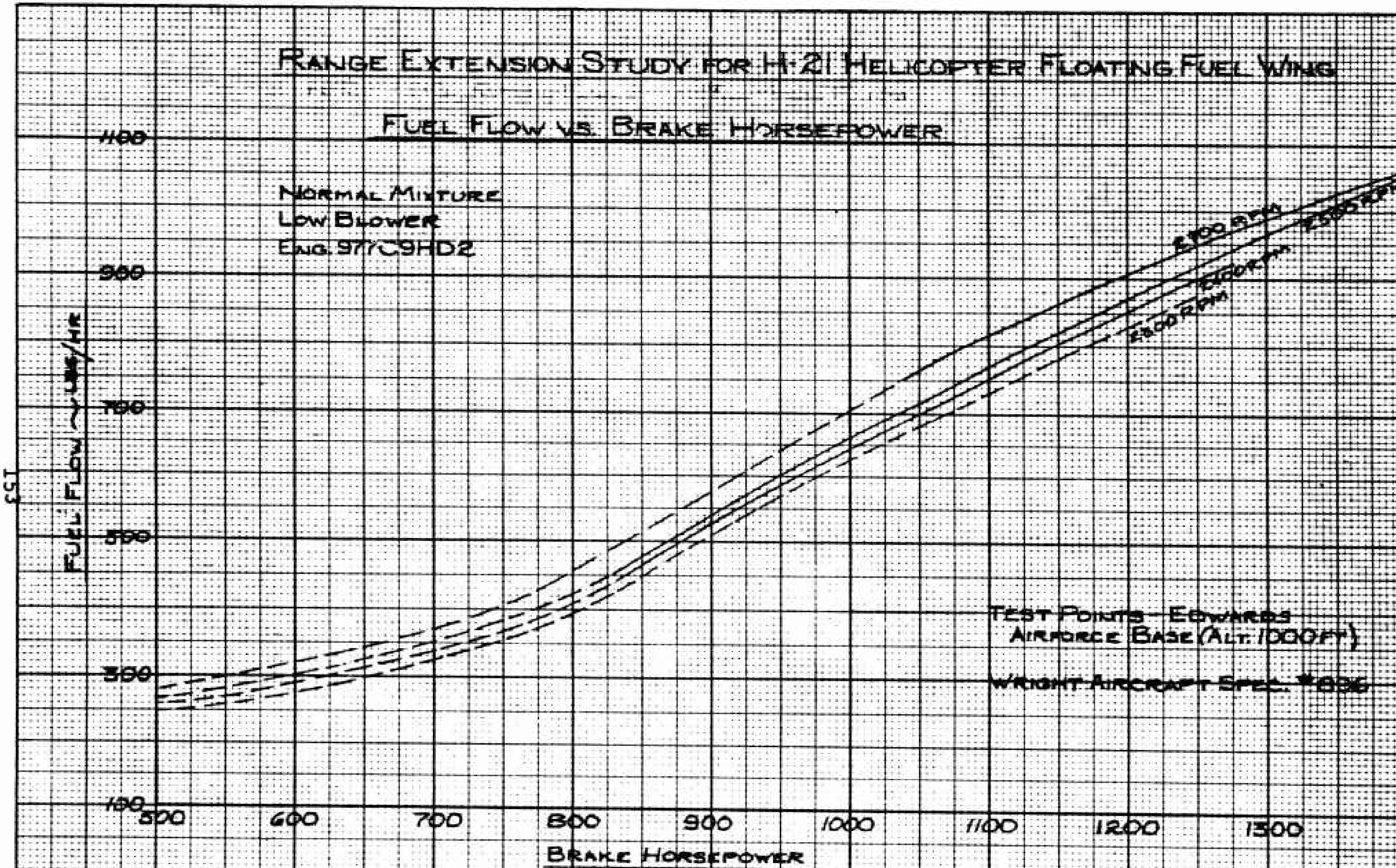

RANGE EXTENSION STUDY FOR H-21 HELICOPTER FLOATING FUEL WING
FUEL FLOW VS. BRAKE HORSEPOWER
NORMAL MIXTURE
LOW BLOWER
ENG. 977C9HD2
2500 RPM
TEST POINTS - EDWARDS AIRFORCE BASE (ALT. 1000 FT)
WRIGHT AIRCRAFT SPEC. #836
FUEL FLOW ~ LBS/HR
1100
900
700
500
300
100
500
600
700
800
900
1000
1100
1200
1300
BRAKE HORSEPOWER

FIGURE 43

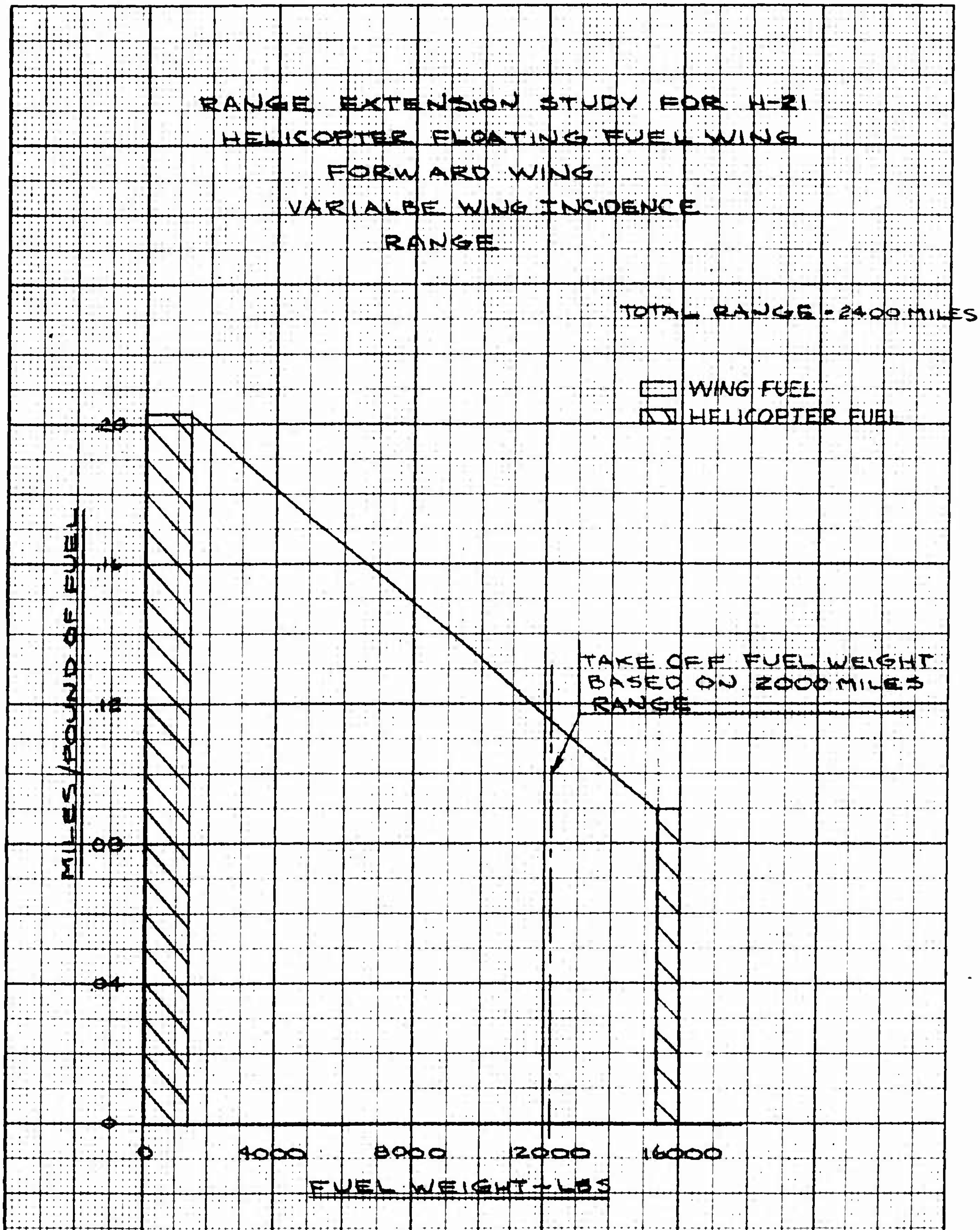
RANGE EXTENSION STUDY FOR H-21
HELICOPTER FLOATING FUEL WING
FORWARD WING
VARIALBE WING INCIDENCE
RANGE
TOTAL RANGE - 2400 MILES
WING FUEL
HELICOPTER FUEL
TAKE OFF FUEL WEIGHT BASED ON 2000 MILES RANGE
MILES/POUND OF FUEL
.20
.16
.12
.08
.04
0
0
4000
8000
12000
16000
FUEL WEIGHT - LBS

FIGURE 44

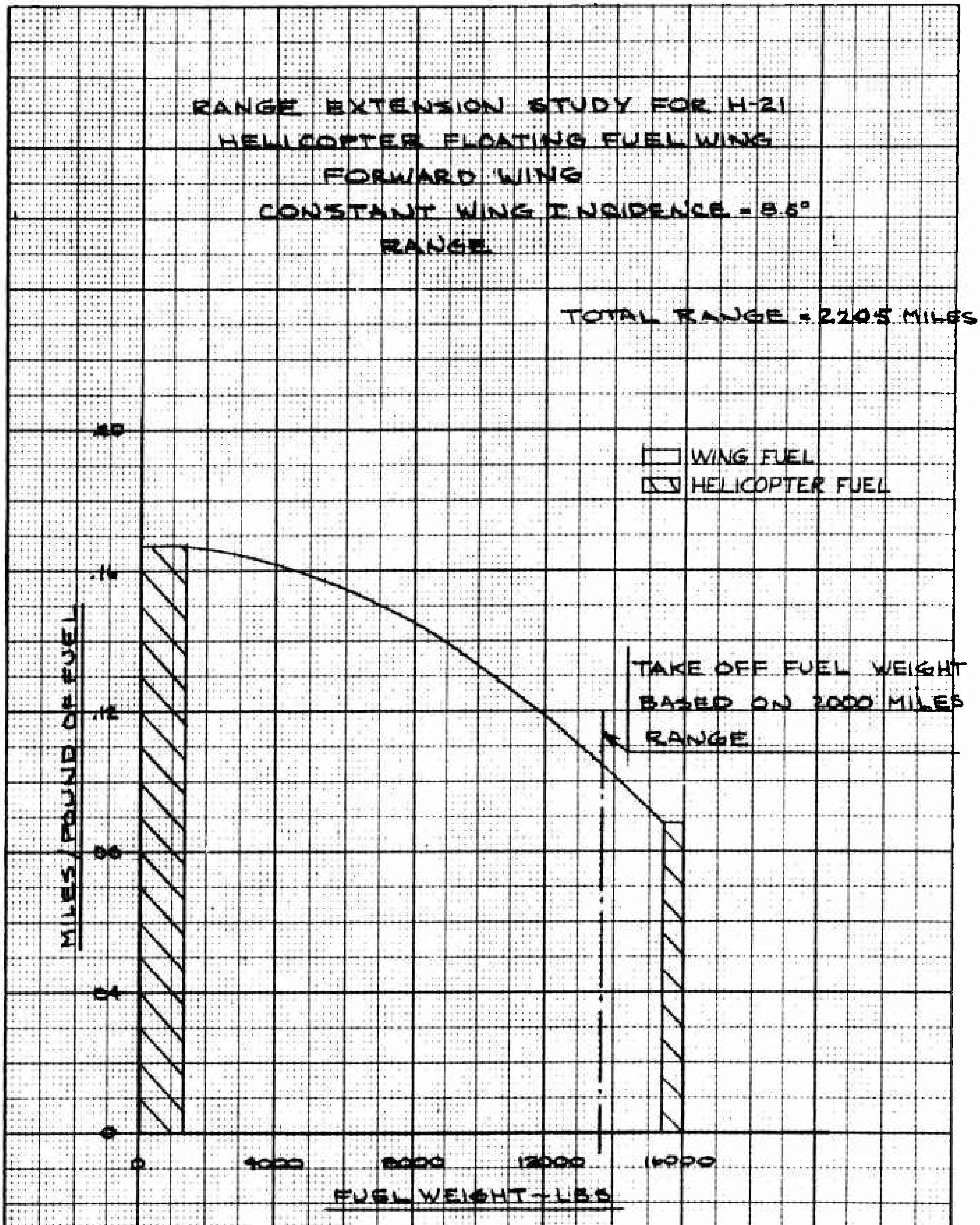

RANGE EXTENSION STUDY FOR H-21
HELICOPTER FLOATING FUEL WING
FORWARD WING
CONSTANT WING INCIDENCE = 8.5°
RANGE
TOTAL RANGE = 2205 MILES
WING FUEL
HELICOPTER FUEL
TAKE OFF FUEL WEIGHT BASED ON 2000 MILES RANGE
MILES/POUND OF FUEL
.16
.12
.08
.04
0
0
4000
8000
12000
16000
FUEL WEIGHT – LBS

FIGURE 45

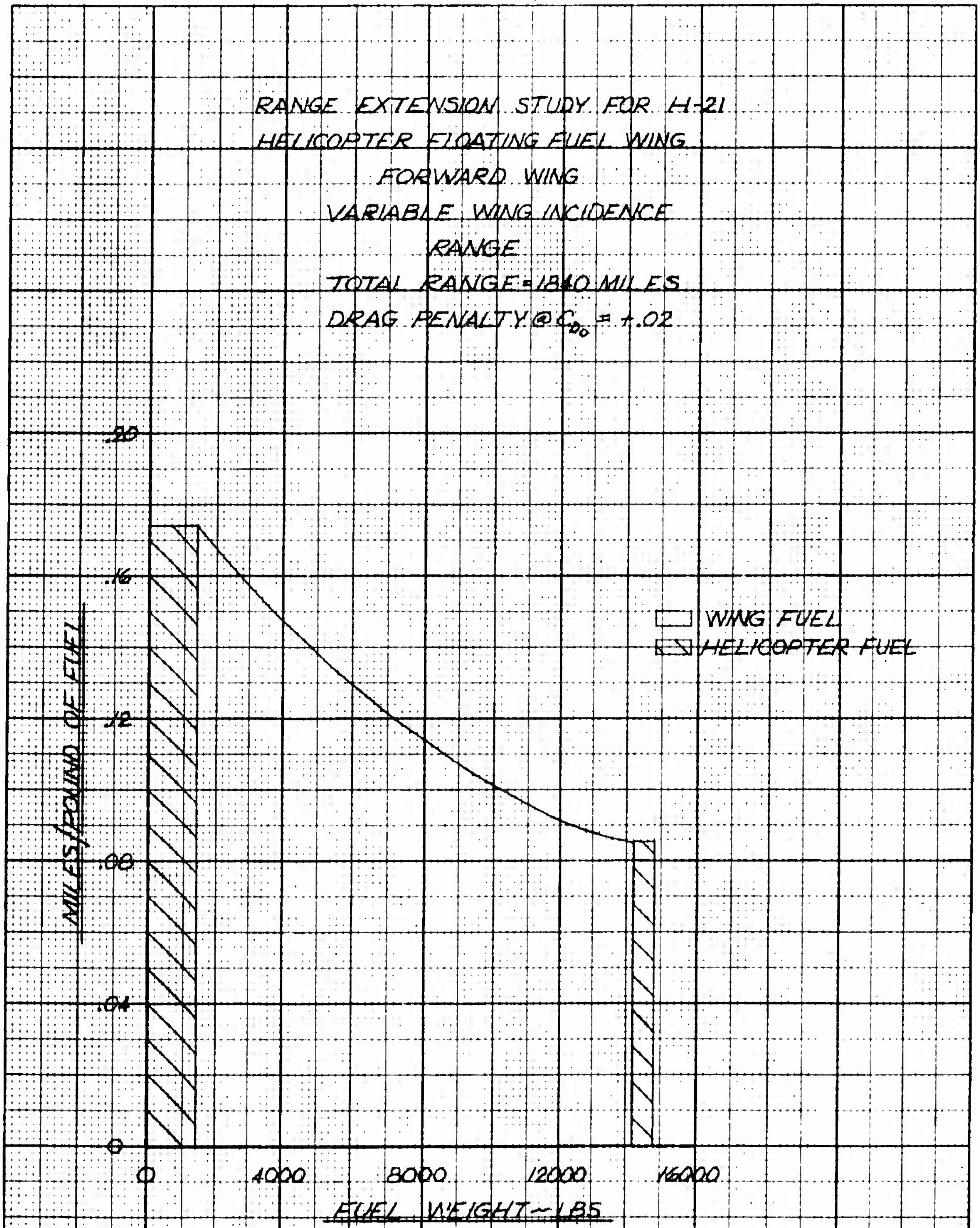
RANGE EXTENSION STUDY FOR H-21
HELICOPTER FLOATING FUEL WING
FORWARD WING
VARIABLE WING INCIDENCE
RANGE
TOTAL RANGE = 1840 MILES
DRAG PENALTY @ C_{D_0} = +.02
.20
.16
.12
.08
.04
0
MILES/POUND OF FUEL
WING FUEL
HELICOPTER FUEL
0
4000
8000
12000
16000
FUEL WEIGHT ~ LBS

FIGURE 46

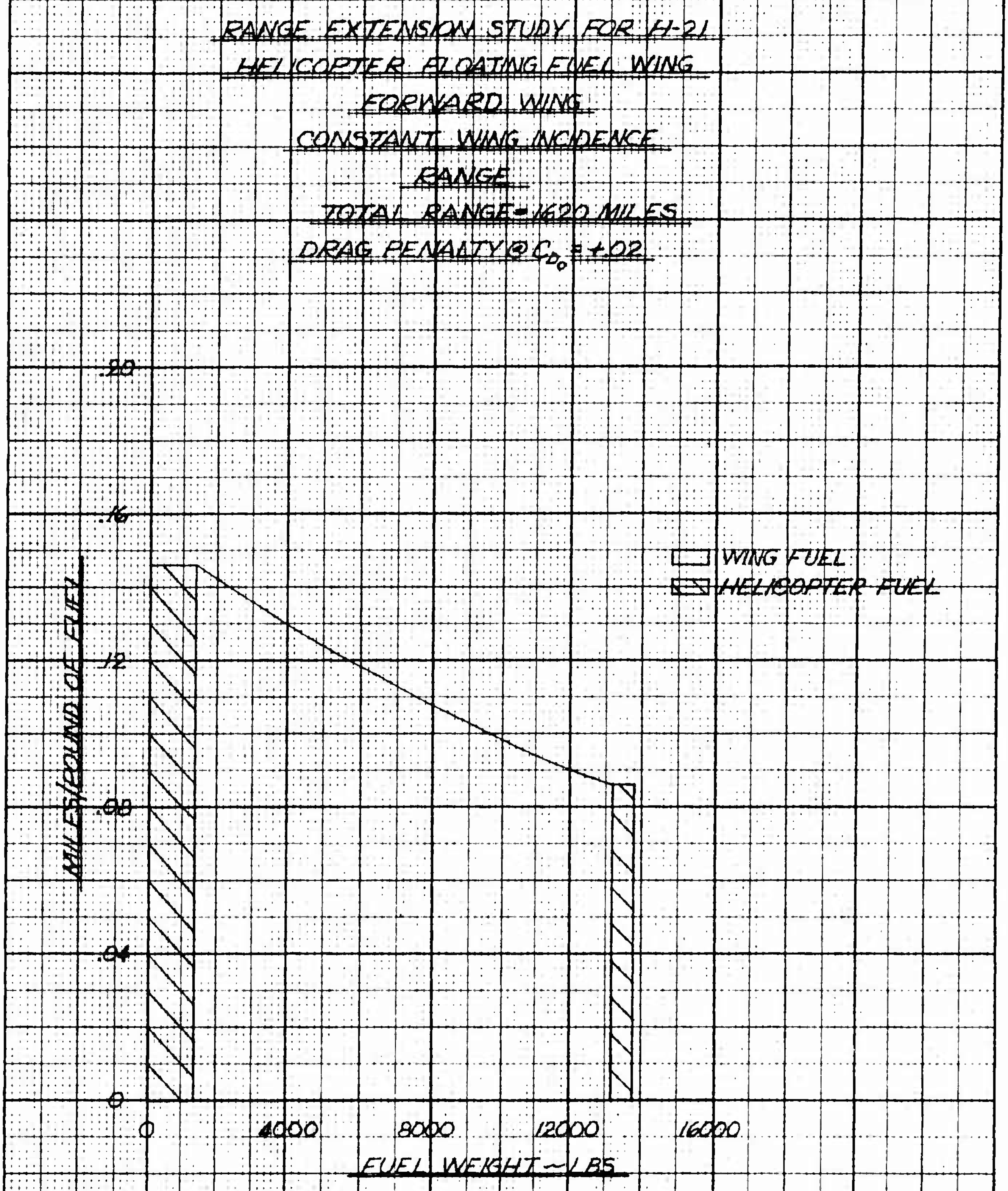
RANGE EXTENSION STUDY FOR H-21
HELICOPTER FLOATING FUEL WING
FORWARD WING
CONSTANT WING INCIDENCE
RANGE
TOTAL RANGE = 1620 MILES
DRAG PENALTY @ C_{D_0} = +.02
WING FUEL
HELICOPTER FUEL
MILES/POUND OF FUEL
.20
.16
.12
.08
.04
0
0
4000
8000
12000
16000
FUEL WEIGHT ~ LBS

FIGURE 47

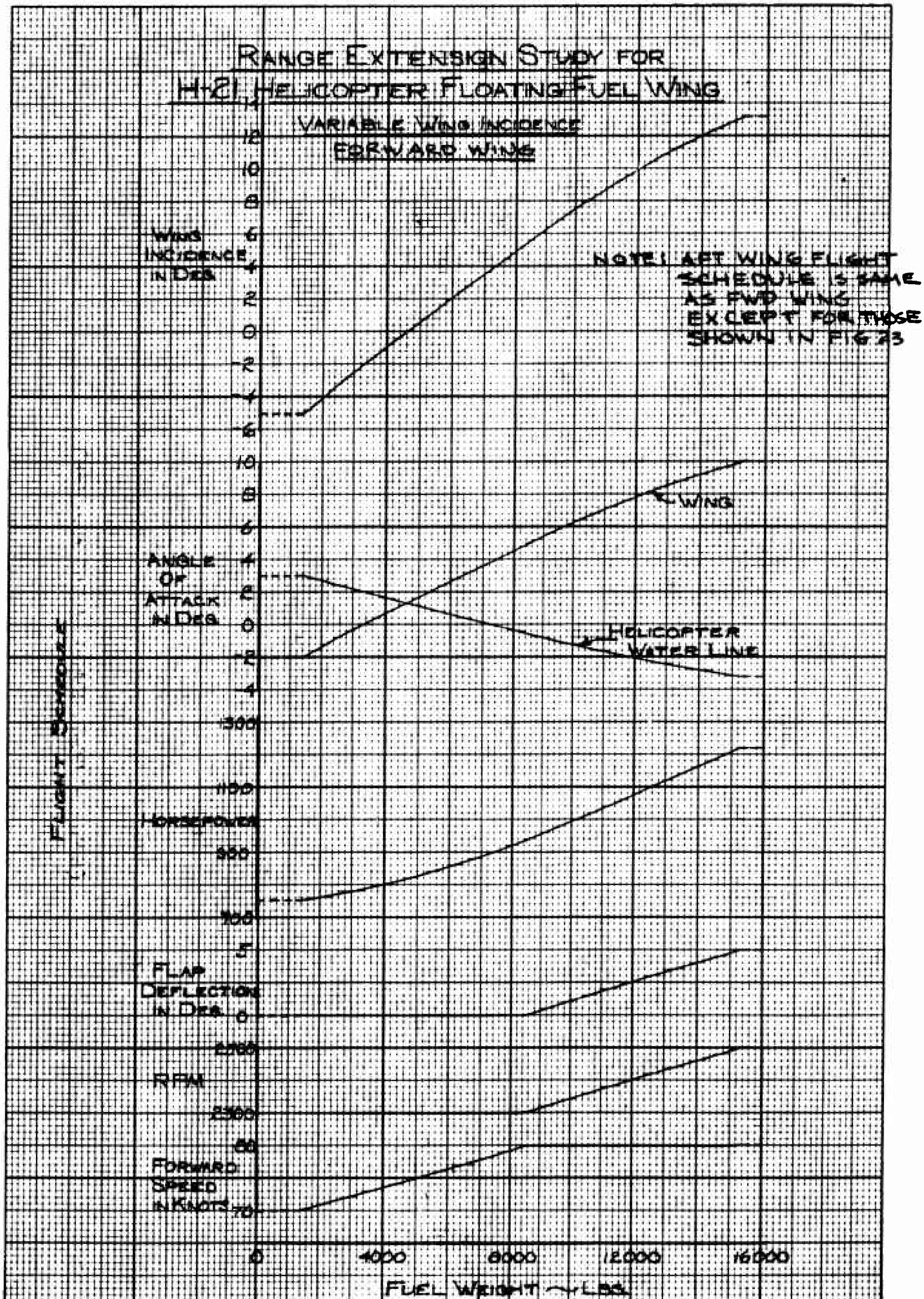
RANGE EXTENSION STUDY FOR
H-21 HELICOPTER FLOATING FUEL WING
VARIABLE WING INCIDENCE
FORWARD WING
WING INCIDENCE IN DEG.
NOTE: AFT WING FLIGHT SCHEDULE IS SAME AS FWD WING EXCEPT FOR THOSE SHOWN IN FIG 23
ANGLE OF ATTACK IN DEG.
WING
HELICOPTER WATER LINE
HORSEPOWER
FLAP DEFLECTION IN DEG.
RPM
FORWARD SPEED IN KNOTS
FLIGHT SCHEDULE
0
4000
8000
12000
16000
FUEL WEIGHT ~ LBS.

FIGURE 48

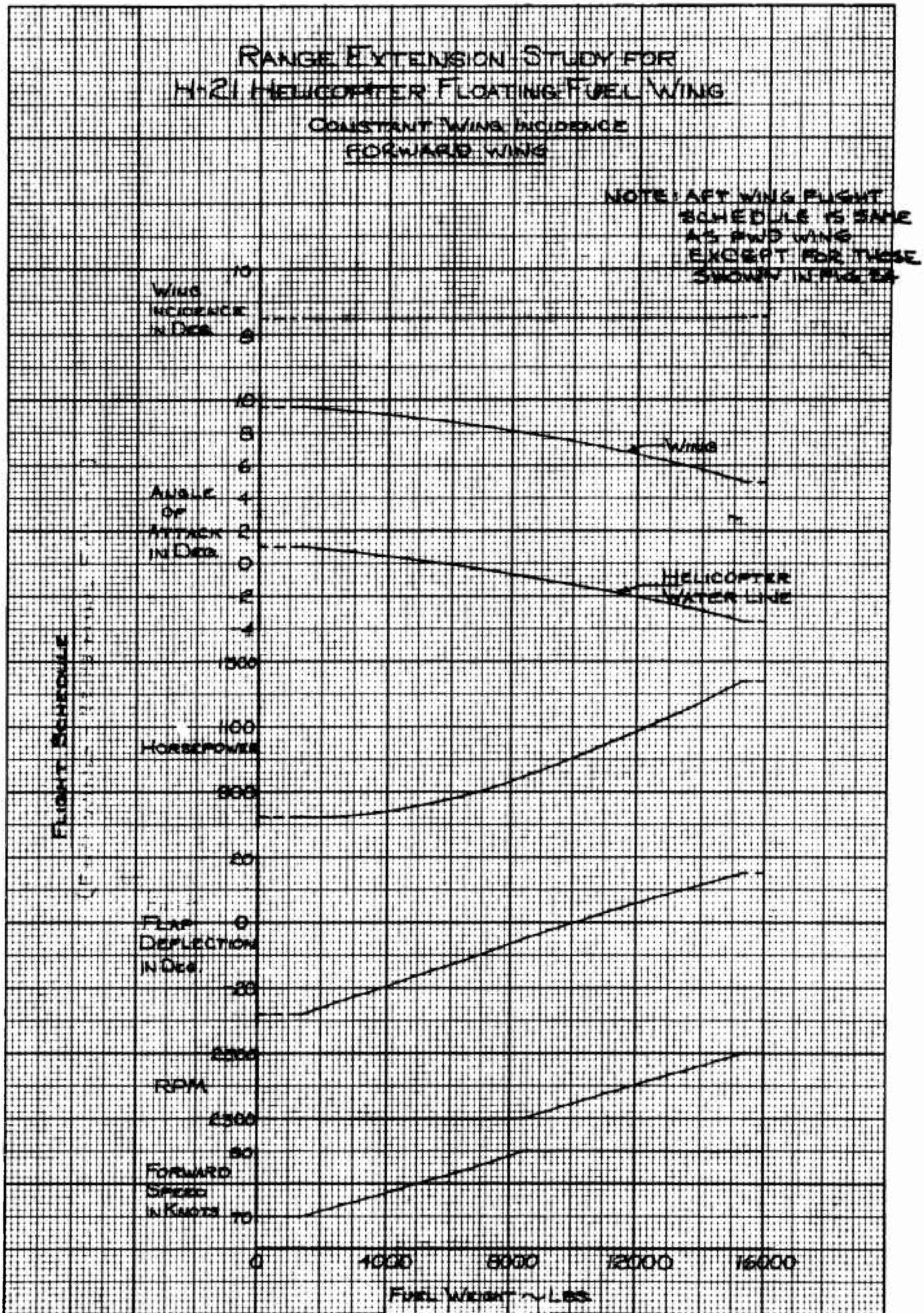
RANGE EXTENSION STUDY FOR
H-21 HELICOPTER FLOATING FUEL WING
CONSTANT WING INCIDENCE
FORWARD WING
NOTE: AFT WING FLIGHT SCHEDULE IS SAME AS FWD WING EXCEPT FOR THOSE SHOWN IN FIG. 54
WING INCIDENCE IN DEG.
ANGLE OF ATTACK IN DEG.
WING
HELICOPTER WATER LINE
HORSEPOWER
FLAP DEFLECTION IN DEG.
RPM
FORWARD SPEED IN KNOTS
FLIGHT SCHEDULE
0
4000
8000
12000
16000
FUEL WEIGHT ~ LBS.

FIGURE 49

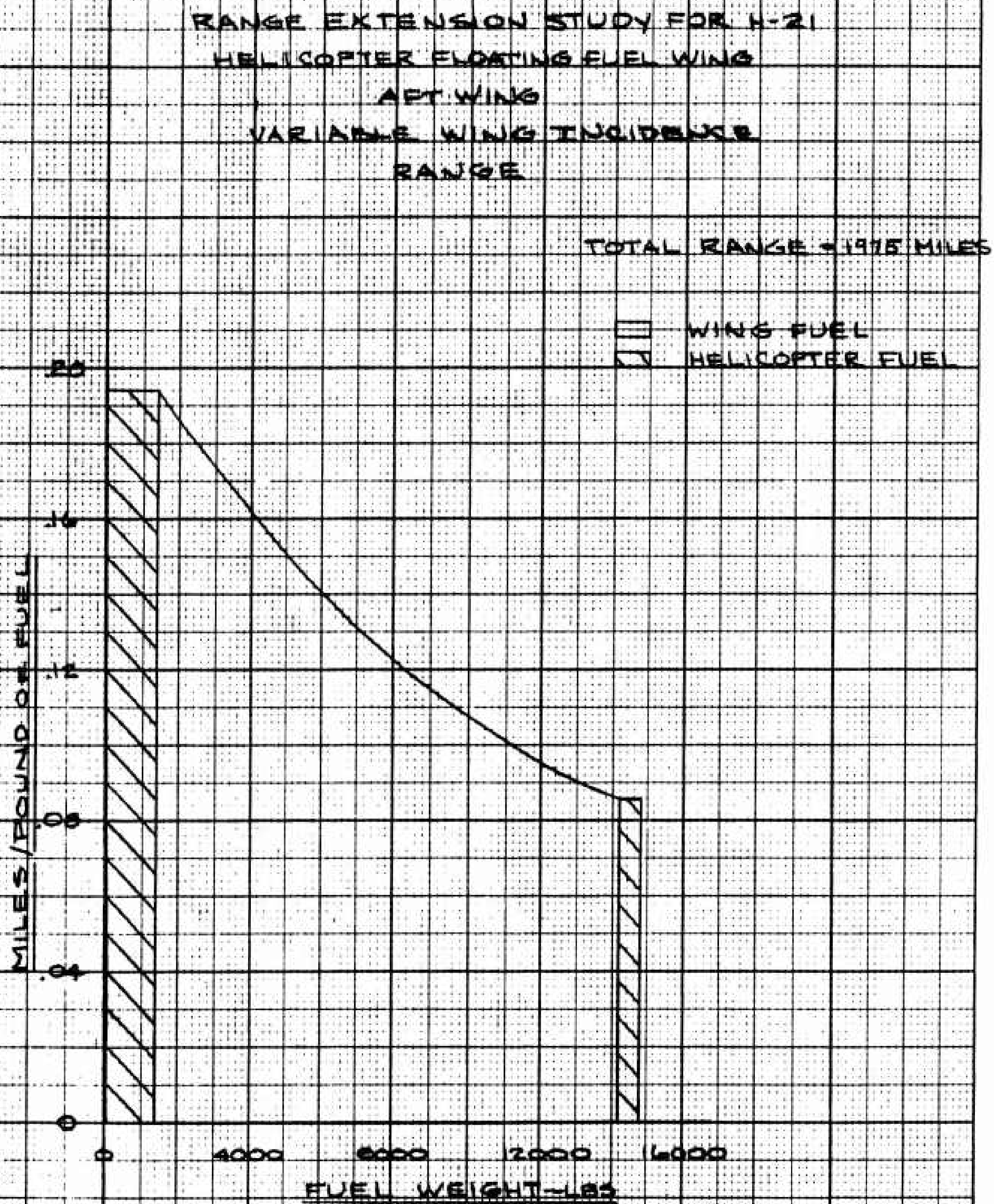
RANGE EXTENSION STUDY FOR H-21
HELICOPTER FLOATING FUEL WING
AFT WING
VARIABLE WING INCIDENCE
RANGE
TOTAL RANGE = 1975 MILES
WING FUEL
HELICOPTER FUEL
MILES/POUND OF FUEL
.20
.16
.12
.08
.04
0
0
4000
8000
12000
16000
FUEL WEIGHT—LBS

FIGURE 50

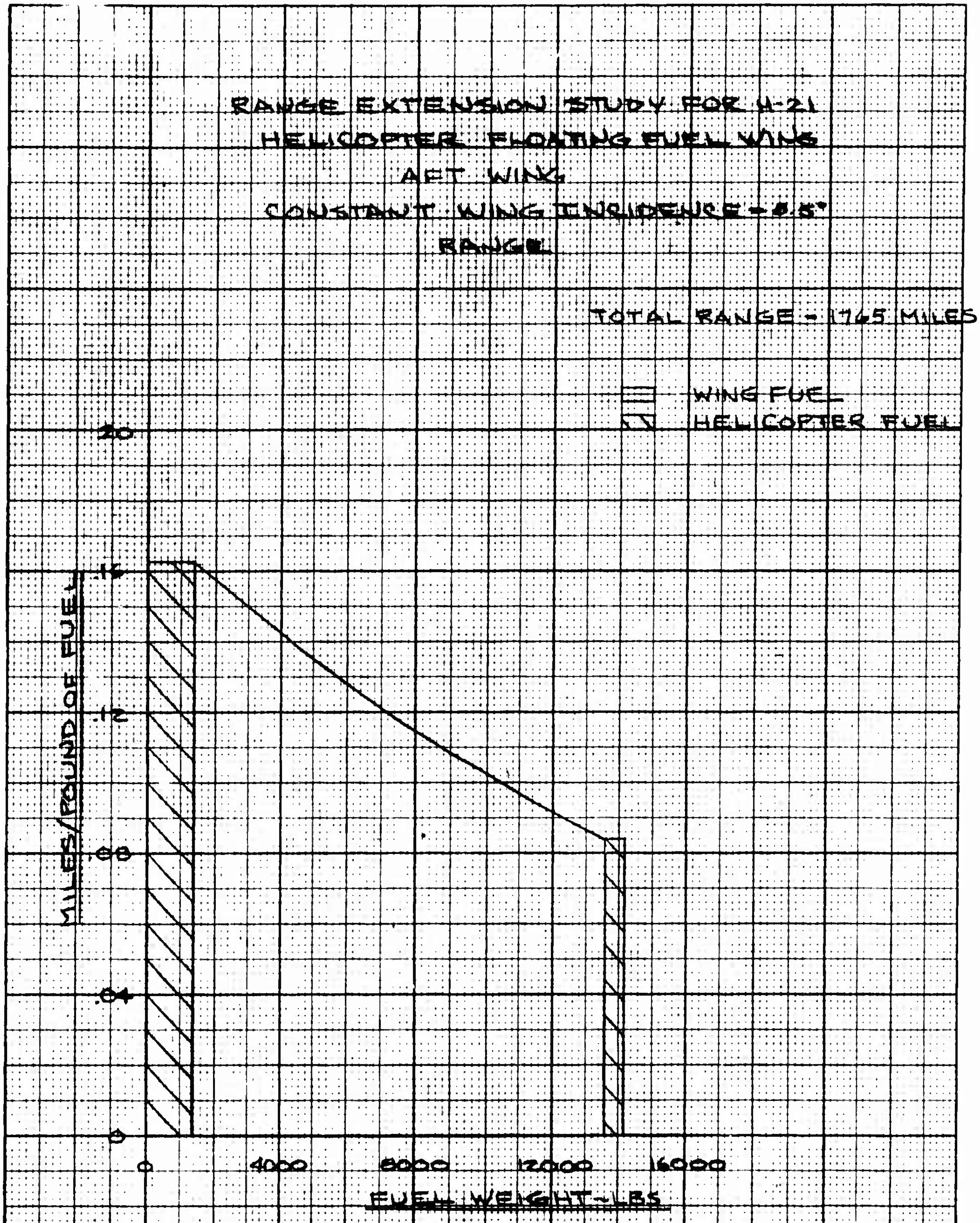
RANGE EXTENSION STUDY FOR H-21
HELICOPTER FLOATING FUEL WING
AFT WING
CONSTANT WING INCIDENCE
RANGE
TOTAL RANGE = 1765 MILES
WING FUEL
HELICOPTER FUEL
MILES/POUND OF FUEL
.20
.16
.12
.08
.04
0
0
4000
8000
12000
16000
FUEL WEIGHT ~ LBS

FIGURE 51

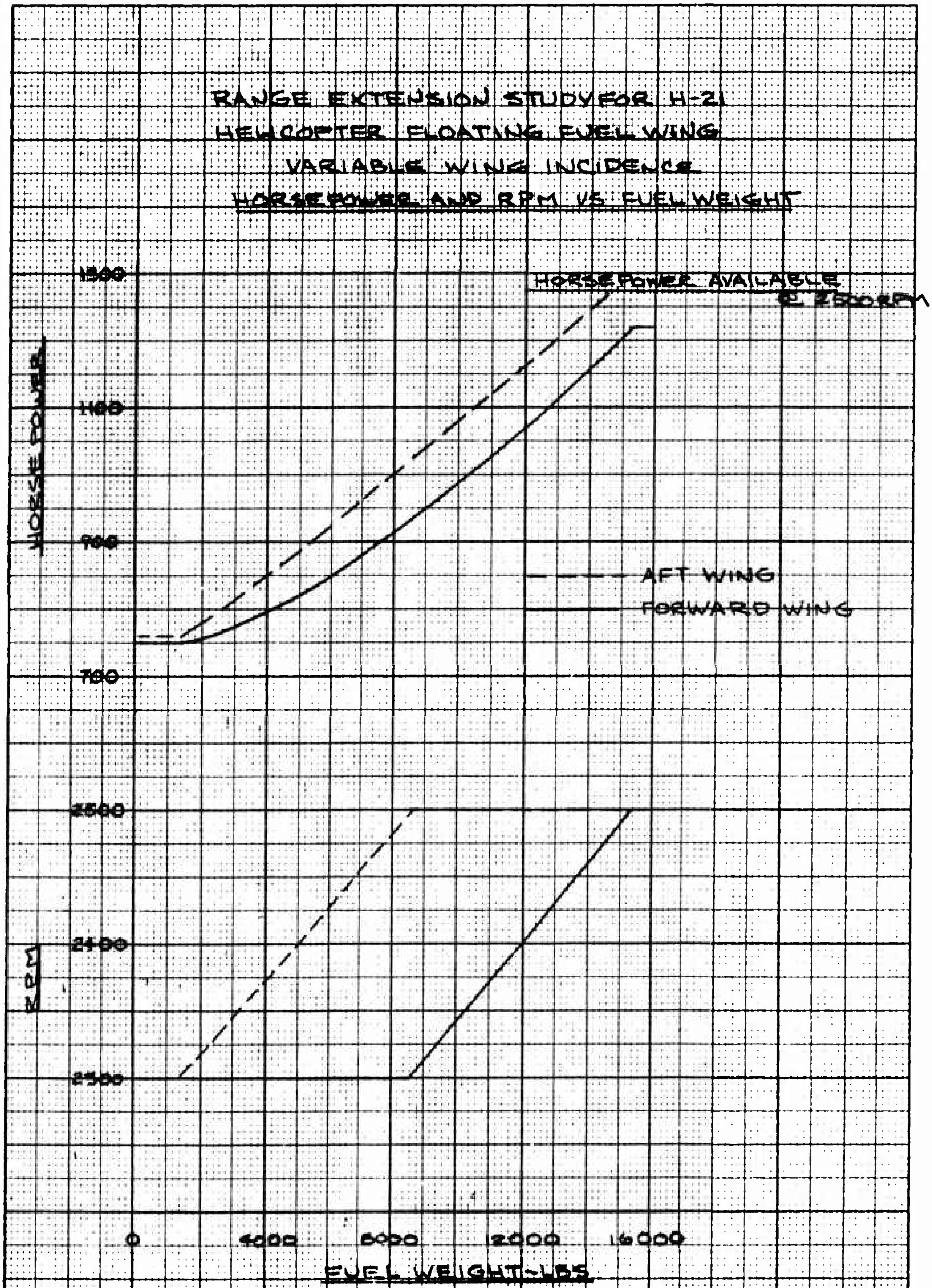
RANGE EXTENSION STUDY FOR H-21
HELICOPTER FLOATING FUEL WING
VARIABLE WING INCIDENCE
HORSEPOWER AND RPM VS FUEL WEIGHT
HORSEPOWER AVAILABLE
@ 2500 RPM
HORSE POWER
1300
1100
900
700
AFT WING
FORWARD WING
RPM
2500
0
4000
12000
16000
FUEL WEIGHT~LBS

FIGURE 52

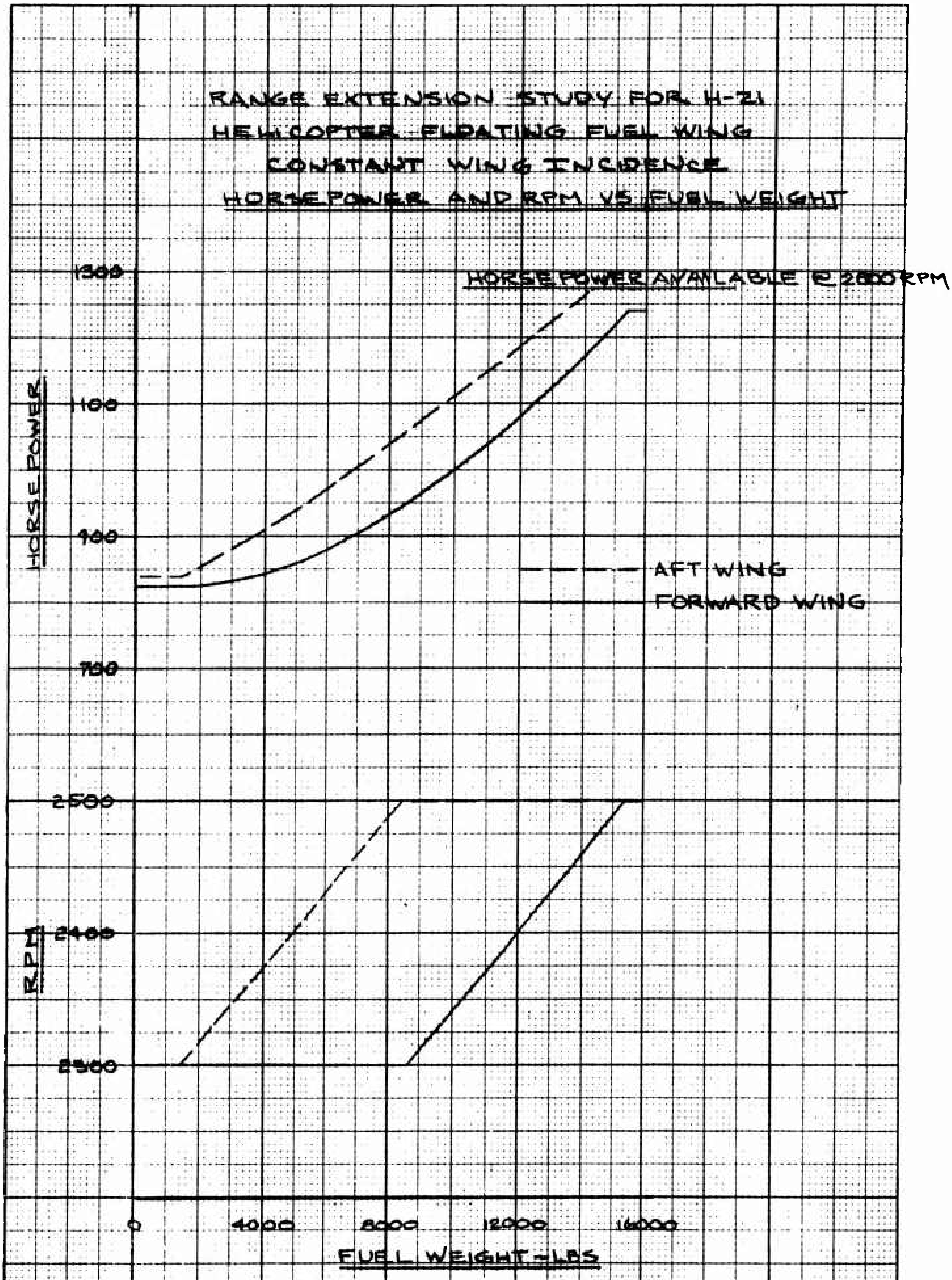
RANGE EXTENSION STUDY FOR H-21
HELICOPTER FLOATING FUEL WING
CONSTANT WING INCIDENCE
HORSEPOWER AND RPM VS FUEL WEIGHT
HORSEPOWER AVAILABLE @ 2800 RPM
HORSE POWER
1300
1100
900
700
AFT WING
FORWARD WING
RPM
2500
2400
2300
0
4000
8000
12000
16000
FUEL WEIGHT ~ LBS

FIGURE 53

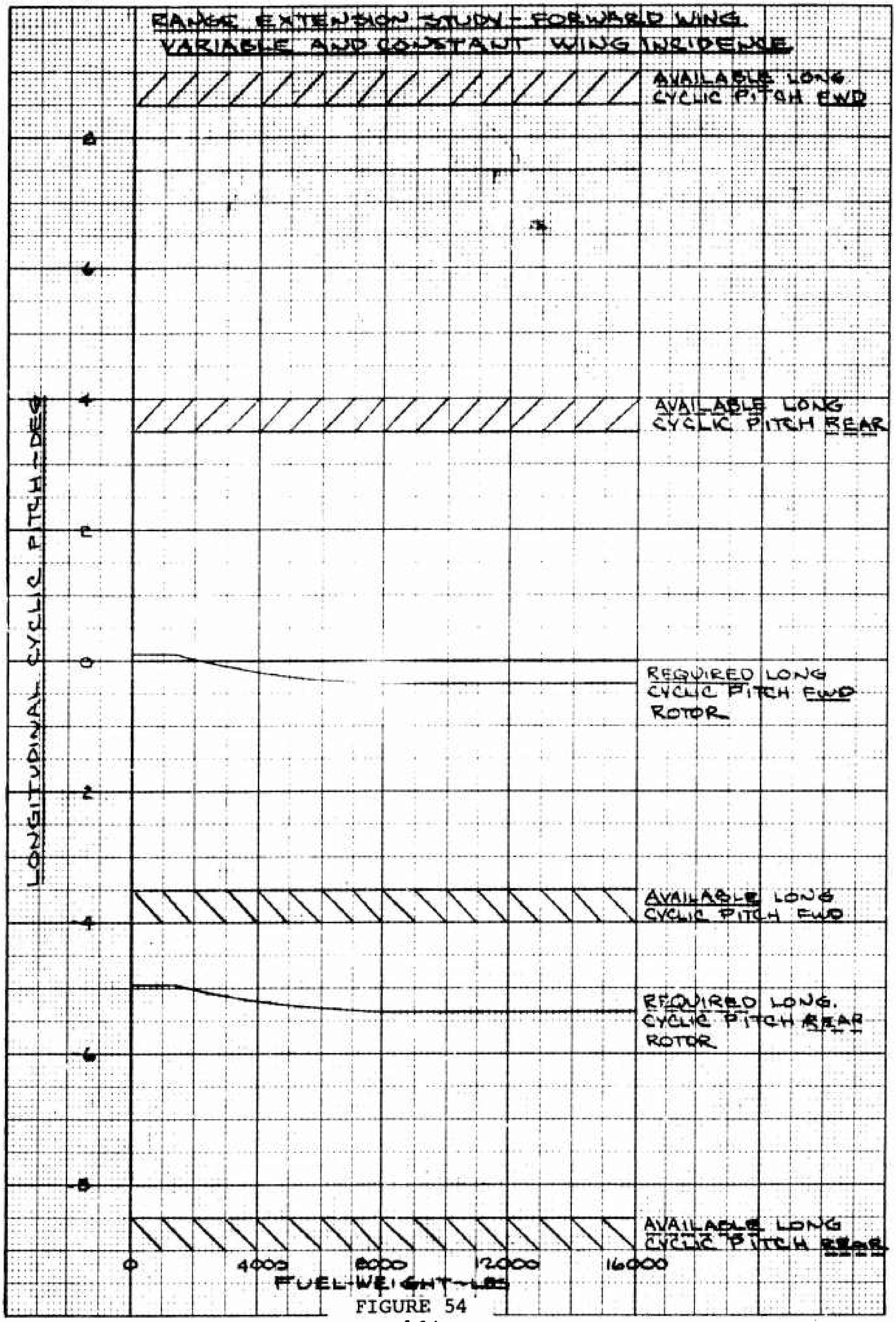
RANGE EXTENSION STUDY - FORWARD WING
VARIABLE AND CONSTANT WING INCIDENCE
AVAILABLE LONG CYCLIC PITCH FWD
AVAILABLE LONG CYCLIC PITCH REAR
REQUIRED LONG CYCLIC PITCH FWD ROTOR
AVAILABLE LONG CYCLIC PITCH FWD
REQUIRED LONG. CYCLIC PITCH REAR ROTOR
AVAILABLE LONG CYCLIC PITCH REAR
LONGITUDINAL CYCLIC PITCH - DEG
8
6
4
2
0
2
4
6
8
0
4000
8000
12000
16000
FUEL WEIGHT ~ LBS

FIGURE 54

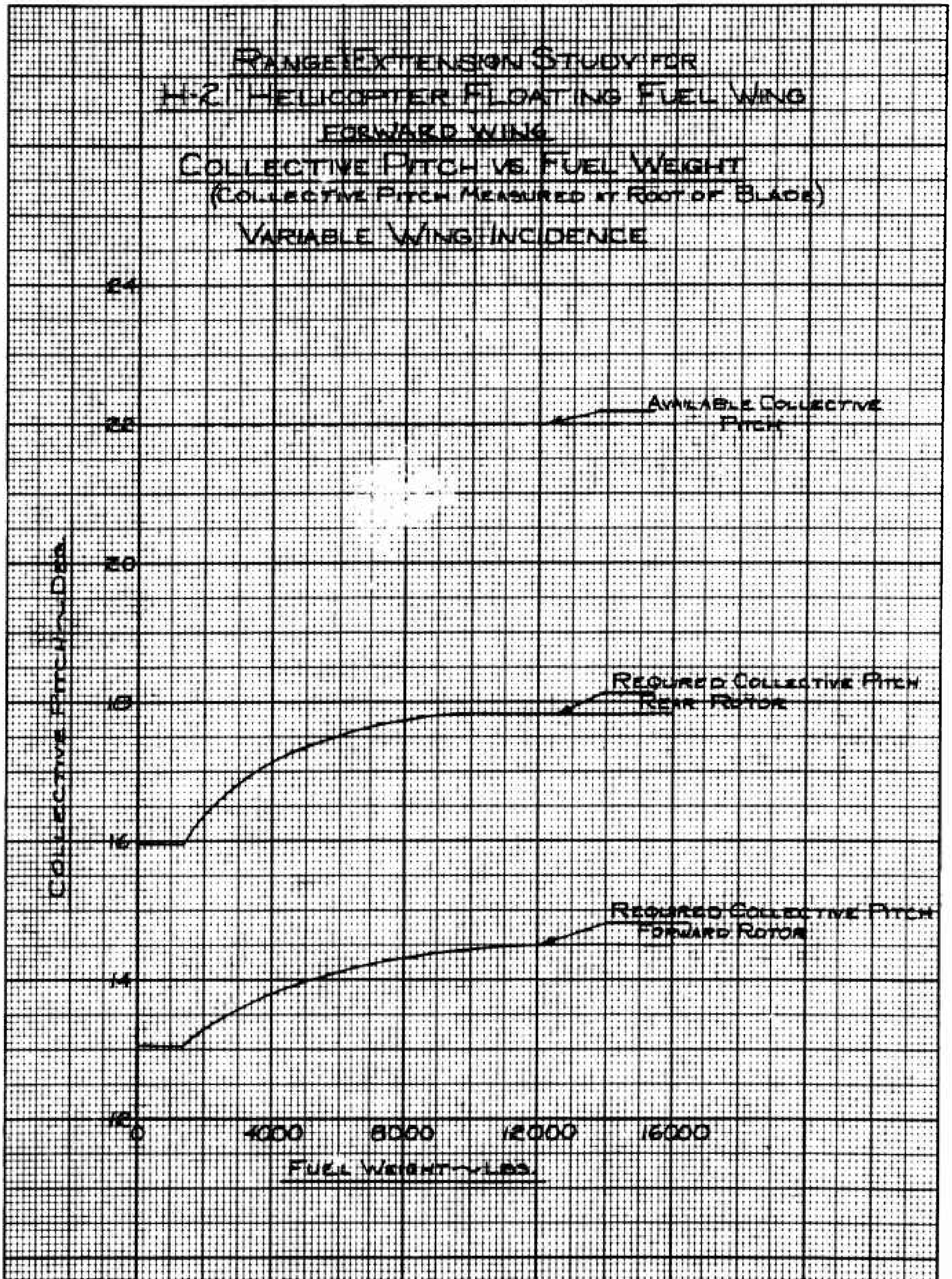
RANGE EXTENSION STUDY FOR
H-21 HELICOPTER FLOATING FUEL WING
FORWARD WING
COLLECTIVE PITCH VS FUEL WEIGHT
(COLLECTIVE PITCH MEASURED AT ROOT OF BLADE)
VARIABLE WING INCIDENCE
AVAILABLE COLLECTIVE PITCH
REQUIRED COLLECTIVE PITCH REAR ROTOR
REQUIRED COLLECTIVE PITCH FORWARD ROTOR
COLLECTIVE PITCH ~ DEG.
24
22
20
18
16
14
12
0
4000
8000
12000
16000
FUEL WEIGHT ~ LBS.

FIGURE 55

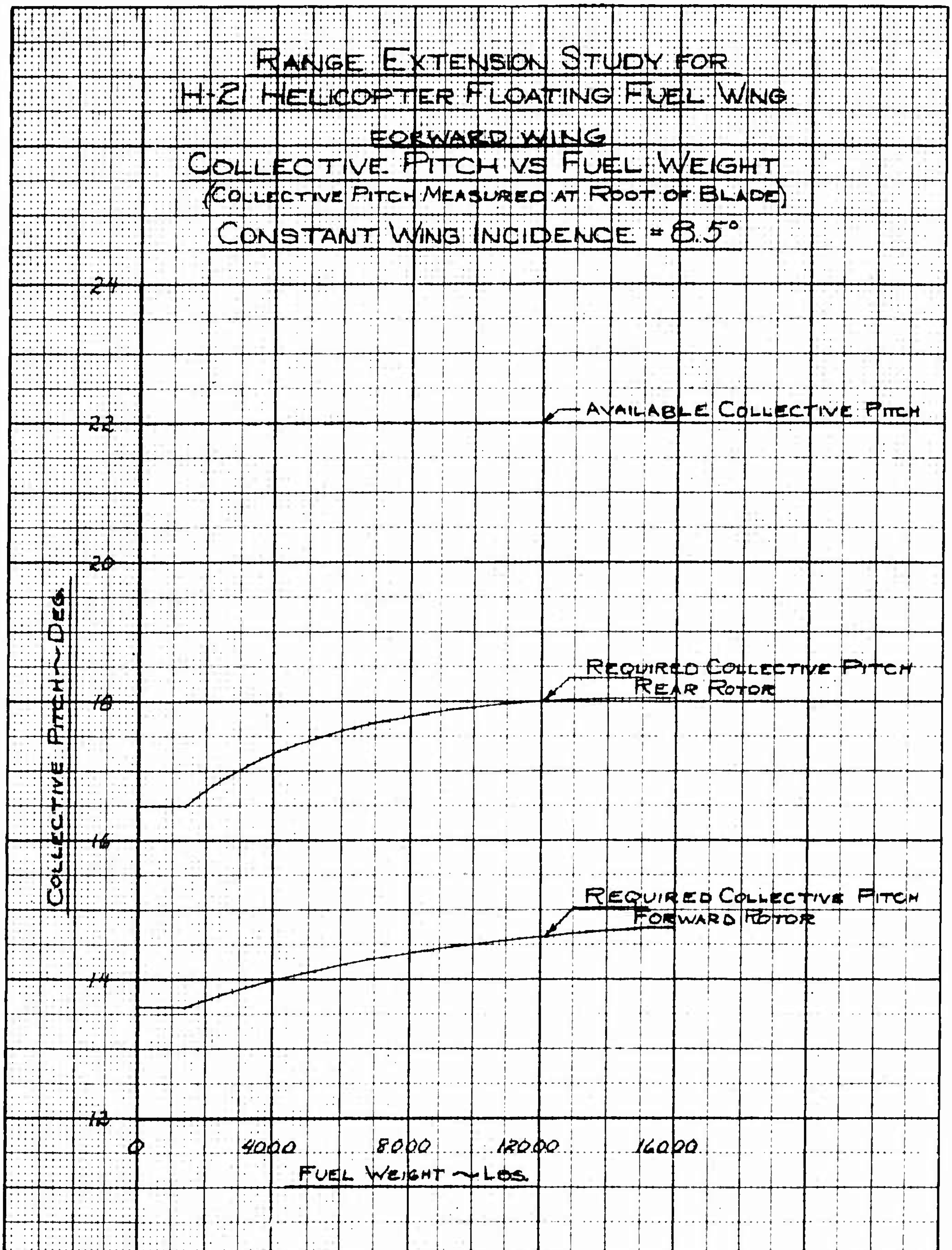
RANGE EXTENSION STUDY FOR
H-21 HELICOPTER FLOATING FUEL WING
FORWARD WING
COLLECTIVE PITCH VS FUEL WEIGHT
(COLLECTIVE PITCH MEASURED AT ROOT OF BLADE)
CONSTANT WING INCIDENCE = 8.5°
AVAILABLE COLLECTIVE PITCH
REQUIRED COLLECTIVE PITCH
REAR ROTOR
REQUIRED COLLECTIVE PITCH
FORWARD ROTOR
COLLECTIVE PITCH ~ DEG.
24
22
20
18
16
14
12
0
4000
8000
12000
16000
FUEL WEIGHT ~ LBS.

FIGURE 56

RANGE EXTENSION STUDY FOR H-21 HELICOPTER FLOATING FUEL WING

NACA 4418, Æ = 8, FULL SPAN SLOTTED FLAPS, S = 550 FT², S.L. STD

LIFT = 2000 POUNDS

VARIABLE WING INCIDENCE

FORWARD WING

FORWARD SPEED	FLAP DEFLECTION	HORSEPOWER		MILES/POUND OF FUEL		WING ANGLE OF ATTACK	WATER LINE ANGLE OF ATTACK		WING INCIDENCE	
		2300 RPM	2500 RPM	2300 RPM	2500 RPM		2300 RPM	2500 RPM	2300 RPM	2500 RPM
70 KNOTS	0°	750	800	.2030	.1650	-2.0°	3.0°	3.5°	-5.0°	-5.5°
	5°	755	805	.2000	.1625	-5.2°	2.7°	3.2°	-7.9°	-8.4°
	15°	780	830	.1820	.1555	-10.0°	2.2°	2.8°	-12.2°	-12.8°
80 KNOTS	0°	810	860	.1970	.1630	-2.0°	1.6°	3.0°	-3.6°	-5.0°
	5°	810	860	.1970	.1630	-5.0°	1.6°	2.8°	-6.6°	-7.8°
	15°	845	890	.1800	.1510	-9.2°	0.6°	1.8°	-9.8°	-11.0°
90 KNOTS	0°	945	980	.1590	.1430	-2.5°	-1.2°	0.2°	-1.3°	-2.7°
	5°	950	980	.1580	.1430	-5.8°	-1.3°	0.1°	-4.5°	-5.9°
	15°	1020	1055	.1390	.1250	-10.8°	-2.3°	-0.8°	-8.5°	-10.0°

TABLE 29

RANGE EXTENSION STUDY FOR H-21 HELICOPTER FLOATING FUEL WING

NACA 4418, Æ = 8, FULL SPAN SLOTTED FLAPS, S = 550 FT², S.L. STD.

LIFT = 9000 POUNDS

VARIABLE WING INCIDENCE

FORWARD WING

FORWARD SPEED	FLAP DEFLECTION	HORSEPOWER		MILES/POUND OF FUEL		WING ANGLE OF ATTACK	WATER LINE ANGLE OF ATTACK		WING INCIDENCE	
		2300 RPM	2500 RPM	2300 RPM	2500 RPM		2300 RPM	2500 RPM	2300 RPM	2500 RPM
70 KNOTS	0°	885	930	.1430	.1220	8°	.5°	1.5°	7.5°	6.5°
	5°	885	830	.1430	.1205	5°	.5°	1.5°	4.5°	3.5°
	15°	895	940	.1400	.1185	0	.2°	1.0°	-0.2°	-1.0°
80 KNOTS	0°	935	975	.1450	.1270	5°	-.6°	.8°	5.6°	4.2°
	5°	940	985	.1450	.1250	2°	-.6°	.8°	2.6°	1.2°
	15°	970	1010	.1360	.1195	-2.7°	-1.2°	0	-1.5°	-2.7°
90 KNOTS	0°	1055	1100	.1320	.1170	3°	-2.2°	-1.2°	5.2°	4.2°
	5°	1070	1105	.1290	.1170	0	-2.4°	-1.2°	2.4°	1.2°
	15°	1110	1145	.1230	.1110	-5°	-3.4°	-2.2°	-1.6°	-2.8°

TABLE 30

Range Extension Study for H-21 Helicopter Floating Fuel Wing

NACA 4418, $AR = 8$, Full Span Slotted Flaps, $S = 530\ FT^2$, S.L. Std.

Lift = 16000 Pounds

Variable Wing Incidence

Forward Wing

Forward Speed	Flap Deflection	Horsepower		Miles/Pound of Fuel		Wing Angle of Attack	Water Line Angle of Attack		Wing Incidence	
		2300 RPM	2500 RPM	2300 RPM	2500 RPM		2300 RPM	2500 RPM	2300 RPM	2500 RPM
70 Knots	5°		1210		.0810	16°		-3.5°		19.5°
	15°		1225		.0785	10°		-3.5°		13.5°
80 Knots	5°		1220		.0900	10°		-3.2°		13.2°
	15°		1240		.0842	5°		-3.5°		8.5°
90 Knots	5°		1340		.0900	5°		-5.0°		10.0°
	15°		1365		.0880	2°		-5.5°		7.5°

TABLE 31

RANGE EXTENSION STUDY FOR H-21 HELICOPTER FLOATING FUEL WING

NACA 4418, $\mathcal{R} = 8$, FULL SPAN SLOTTED FLAPS, $S = 550\,FT^2$, S.L. STD.

CONSTANT WING INCIDENCE = 8.5°

FORWARD WING

FORWARD SPEED	FLAP DEFLECTION 2300 RPM	FLAP DEFLECTION 2500 RPM	HORSEPOWER 2300 RPM	HORSEPOWER 2500 RPM	MILES/POUND OF FUEL 2300 RPM	MILES/POUND OF FUEL 2600 RPM	WING ANGLE OF ATTACK 2300 RPM	WING ANGLE OF ATTACK 2500 RPM	WATER LINE ANGLE OF ATTACK 2300 RPM	WATER LINE ANGLE OF ATTACK 2500 RPM	WING INCIDENCE
LIFT = 2000 POUNDS											
70 KNOTS	-28°	-34°	825	905	.1665	.1290	9.6°	10.3°	1.0°	1.7°	8.5°
80 KNOTS	-25°	-28°	920	970	.1480	.1280	8.4°	8.9°	-0.3°	0.3°	8.5°
90 KNOTS	-18°	-22°	1025	1095	.1390	.1190	5.9°	6.9°	-2.7°	-1.7°	8.5°
LIFT = 9000 POUNDS											
70 KNOTS	1°	-2°	885	935	.1430	.1200	9.0°	10.0°	0.4°	1.4°	8.5°
80 KNOTS	-5°	-7°	950	1005	.1420	.1200	7.9°	9.5°	-0.8°	0.4°	8.5°
90 KNOTS	-5°	-7°	1075	1105	.1290	.1170	6.1°	7.3°	-2.4°	-1.6°	8.5°
LIFT = 16000 POUNDS											
80 KNOTS		15°		1240		.0880		5.0°		-3.5°	8.5°

TABLE 32

RANGE EXTENSION STUDY FOR
H-21 HELICOPTER FLOATING FUEL WING

RANGE AND TAKE OFF GROSS WEIGHT FOR
VARIOUS CONFIGURATIONS

CONFIGURATION	RANGE (MILES)	MAX. TAKE OFF WING GROSS WEIGHT (POUNDS)
FORWARD WING		
VARIABLE INCIDENCE	2400	16,000
VARIABLE INCIDENCE	2000	12,100
VARIABLE INCIDENCE WITH DRAG PENALTY ADDED @ $C_{D_0} = +.02$	1840	14,800
CONSTANT INCIDENCE	2205	16,000
CONSTANT INCIDENCE	2000	13,700
CONSTANT INCIDENCE WITH DRAG PENALTY ADDED @ $C_{D_0} = +.02$	1620	13,800
AFT WING		
VARIABLE INCIDENCE	1975	14,800
CONSTANT INCIDENCE	1840	14,200

TABLE 33

SUMMARY OF TAKE-OFF PROCEDURES AND RESULTS
FOR FORWARD AND AFT WING POSITION

PROCEDURE	T.O. SPEED	INITIAL ATTITUDE			TRIM ATTITUDE			DISTANCE BREAK GROUND	FORWARD WING		AFT WING	
		α_w	i_w	δ_f	α_w	i_w	δ_f		OVER 50'	T.O. WING GROSS WT.	OVER 50'	T.O. WING GROSS WT
	KTS	DEG	DEG	DEG	DEG	DEG	DEG	FT	FT	[illegible]	FT	[illegible]
TRIM	70	10	13.5	15	10	13.5	15	6350	7630	16000	8300	14200
ROTATE	80	-12	8.5	15	5	8.5	15	1550	3335	16000	3780	14200
ROTATE	70	-9	13.5	15	10	13.5	15	1279	2724	16000	3230	14200

TABLE 34

APPENDIX D

LONGITUDINAL RANGE EXTENSION

Analog Computer Program

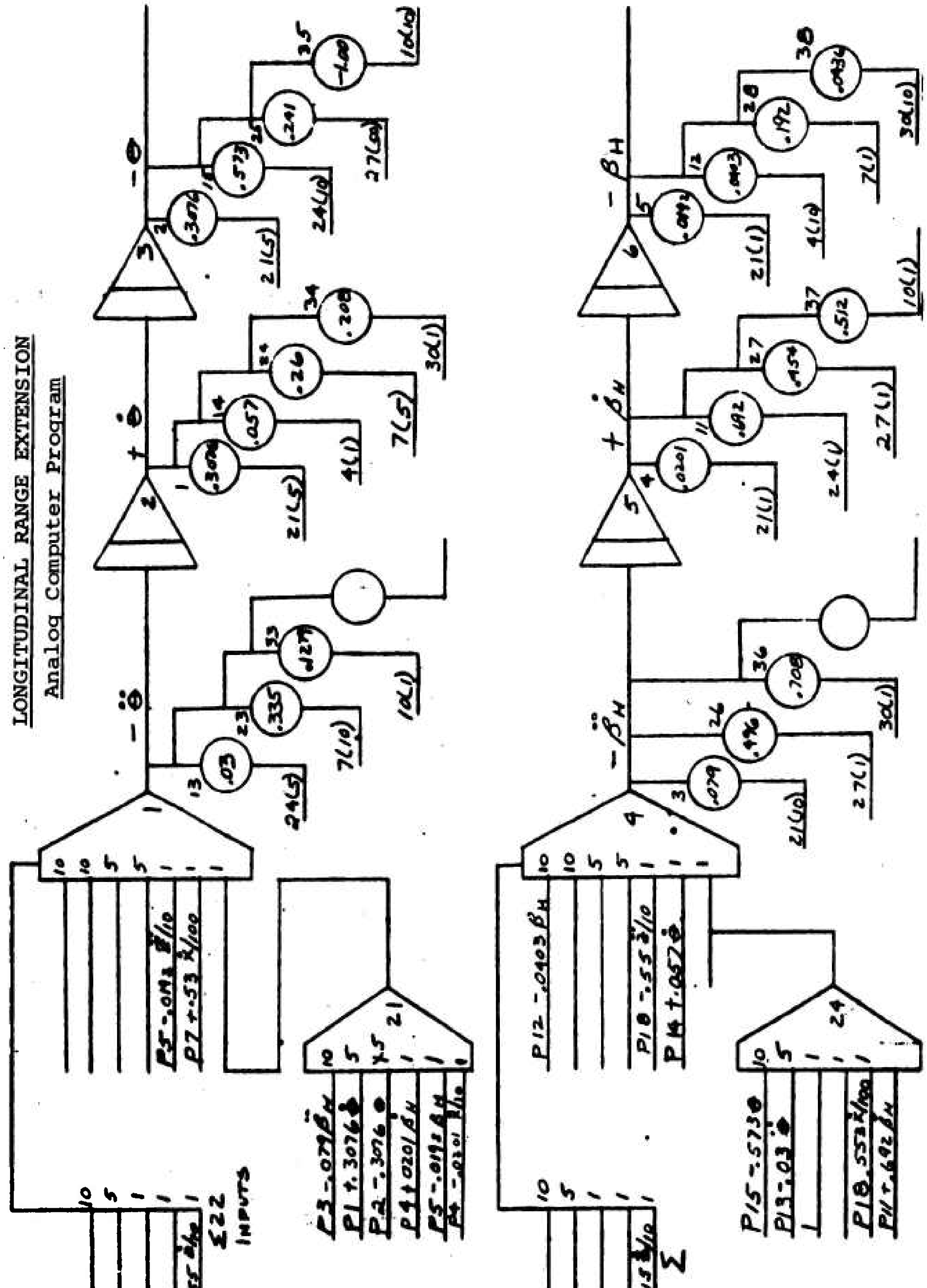

FIGURE 57

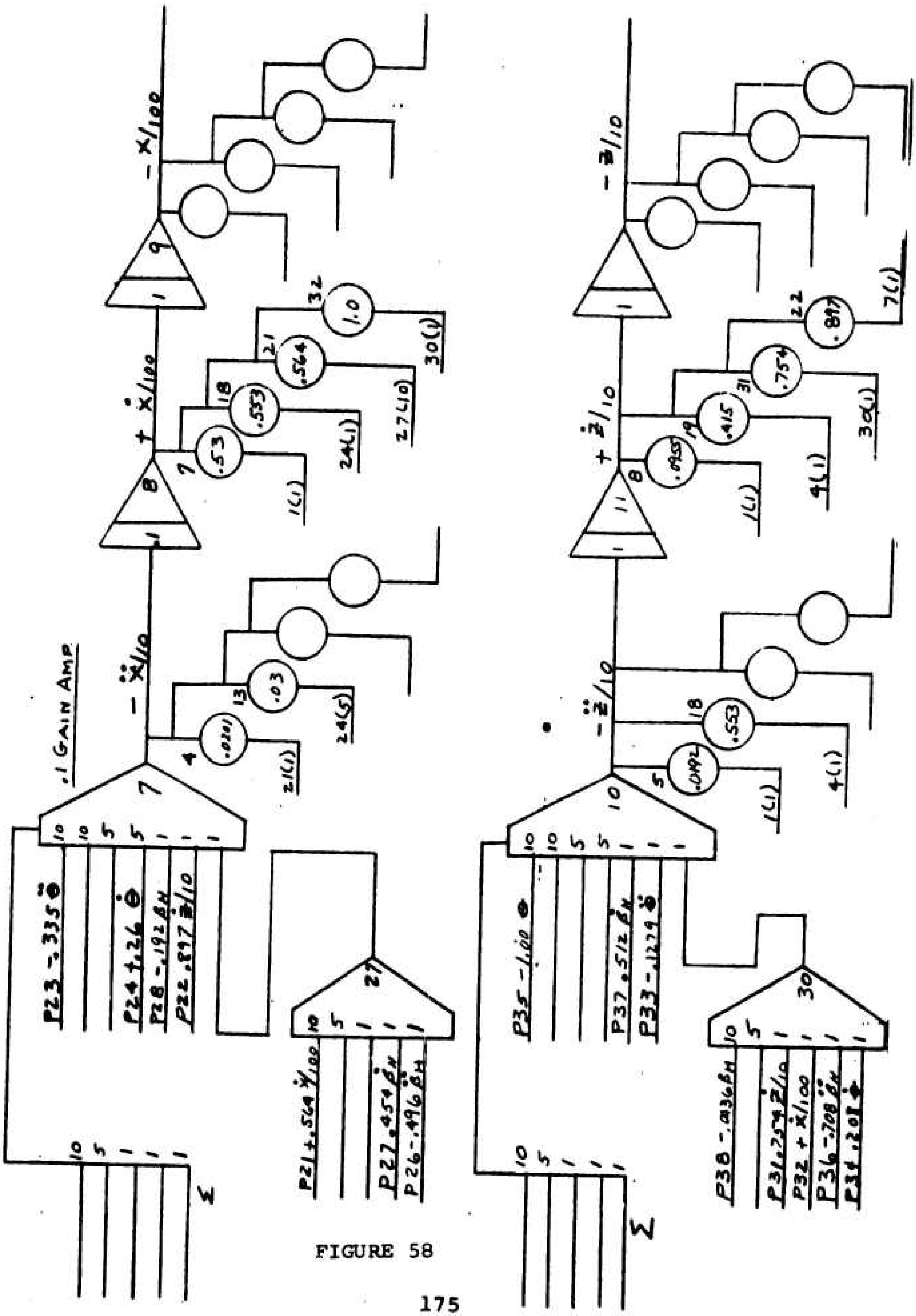

FIGURE 58

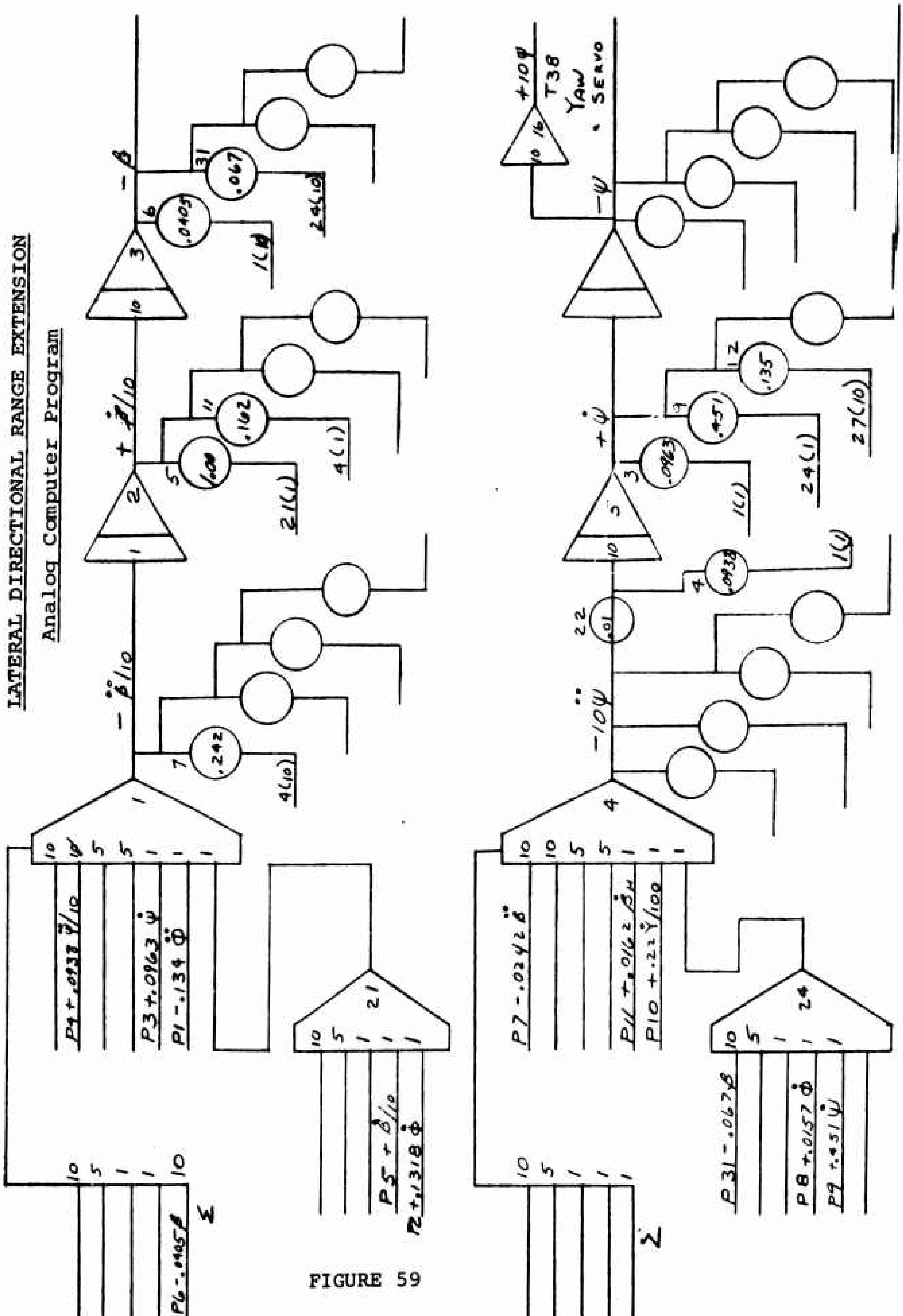
LATERAL DIRECTIONAL RANGE EXTENSION
Analog Computer Program
T38
YAW
SERVO

FIGURE 59

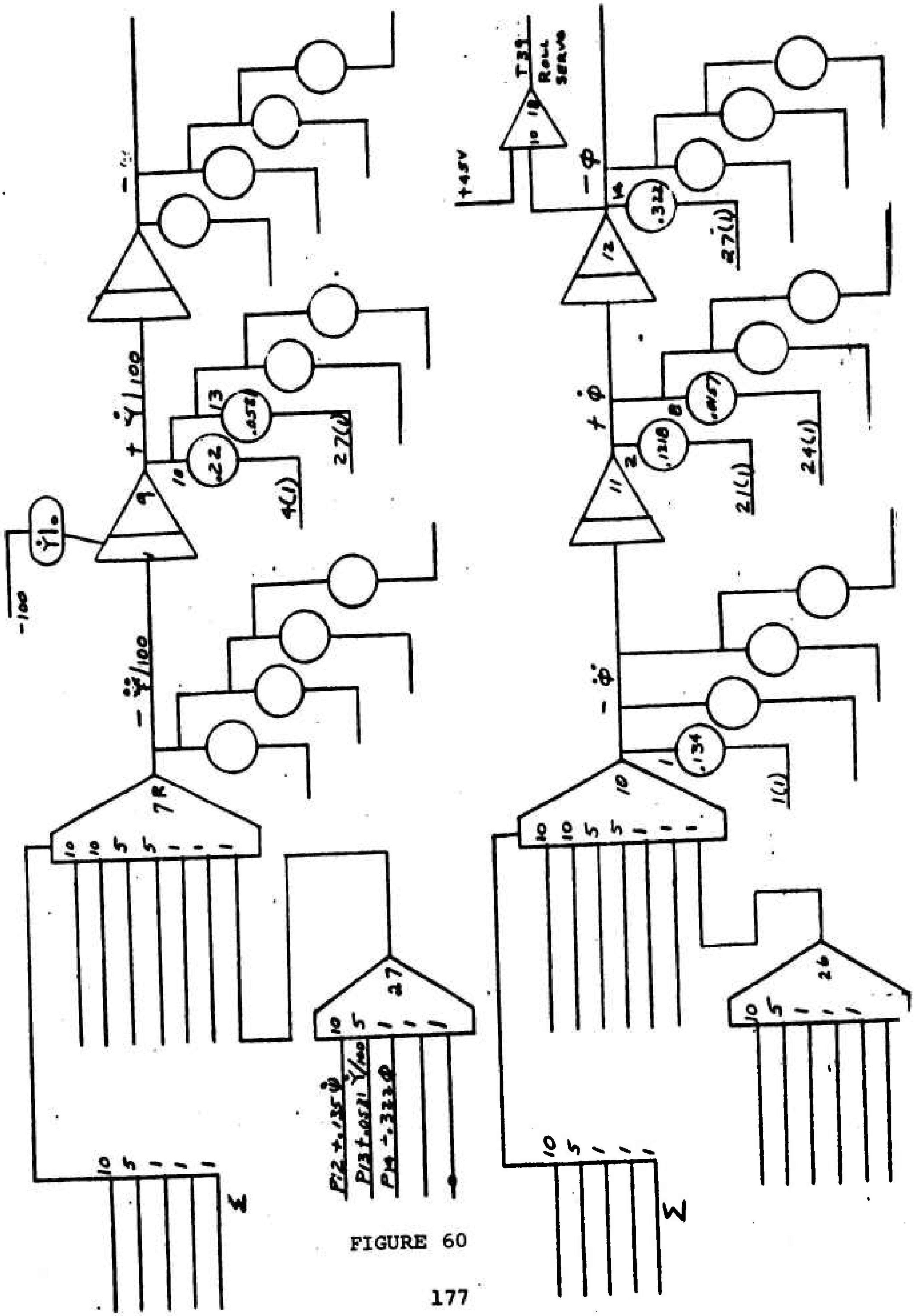

FIGURE 60

RANGE EXTENSION RECORDING

Analog Schematic

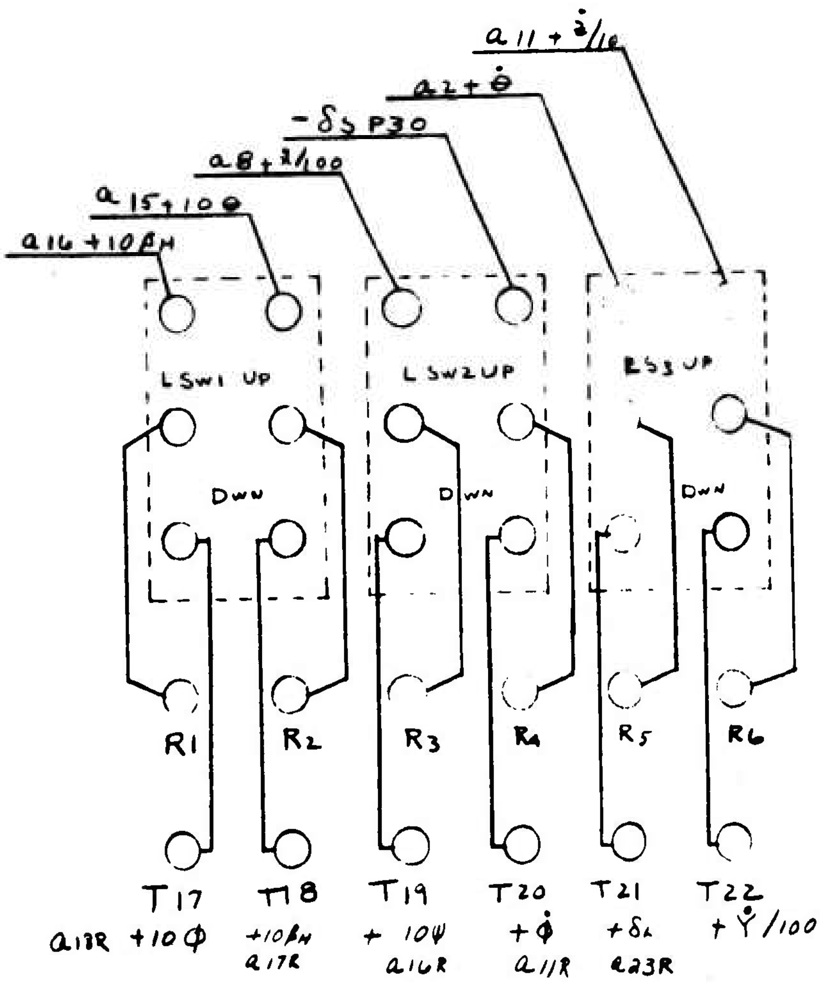

FIGURE 61

RANGE EXTENSION SCHEMATIC BLOCK DIAGRAM

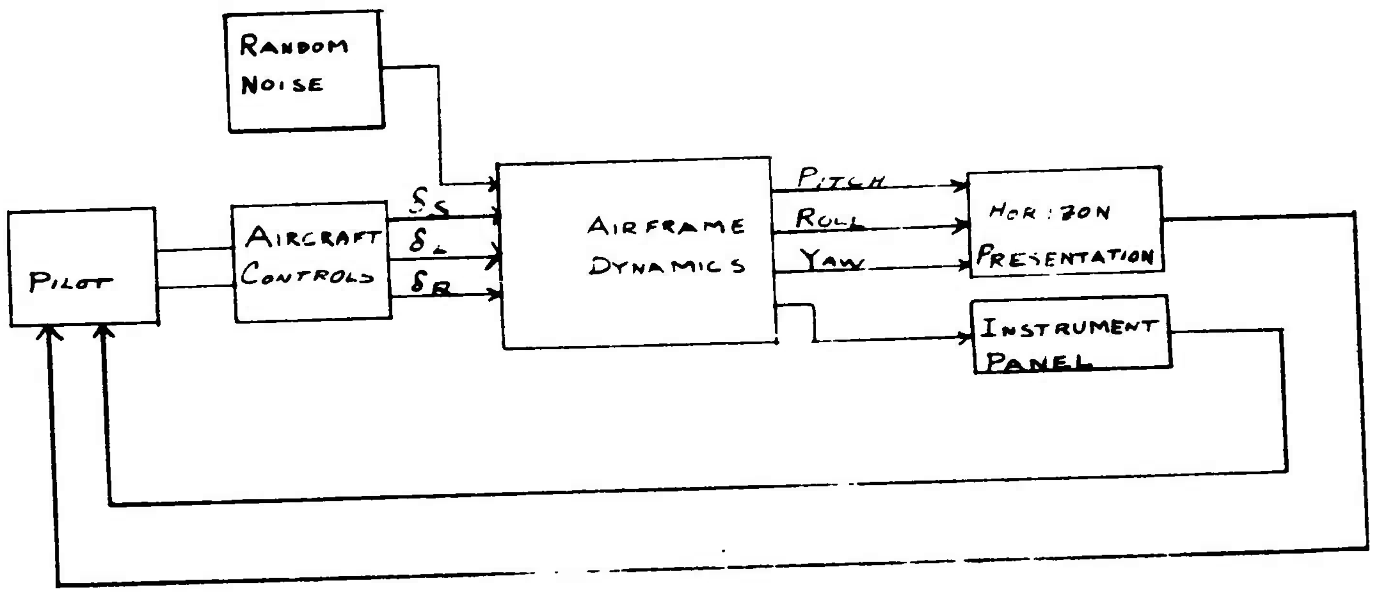

FIGURE 62

RANGE EXTENSION

Simulator Controls

Longitudinal Stick

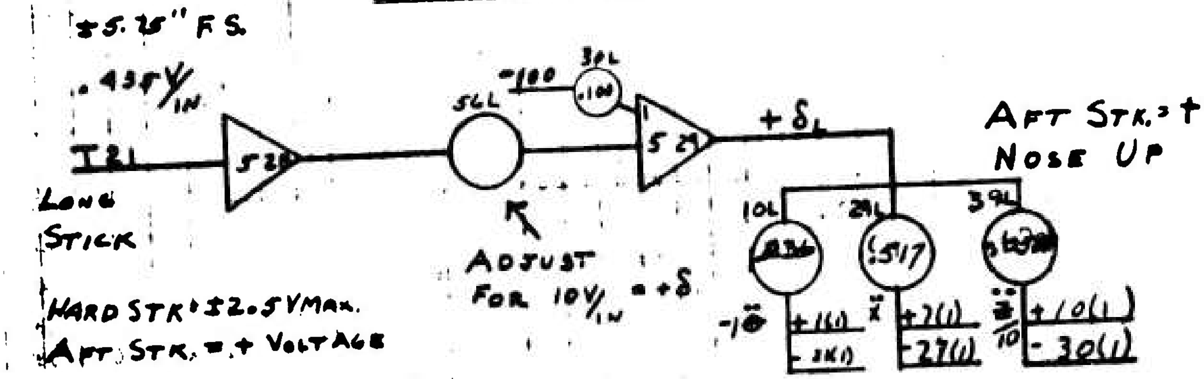

Lateral Stick

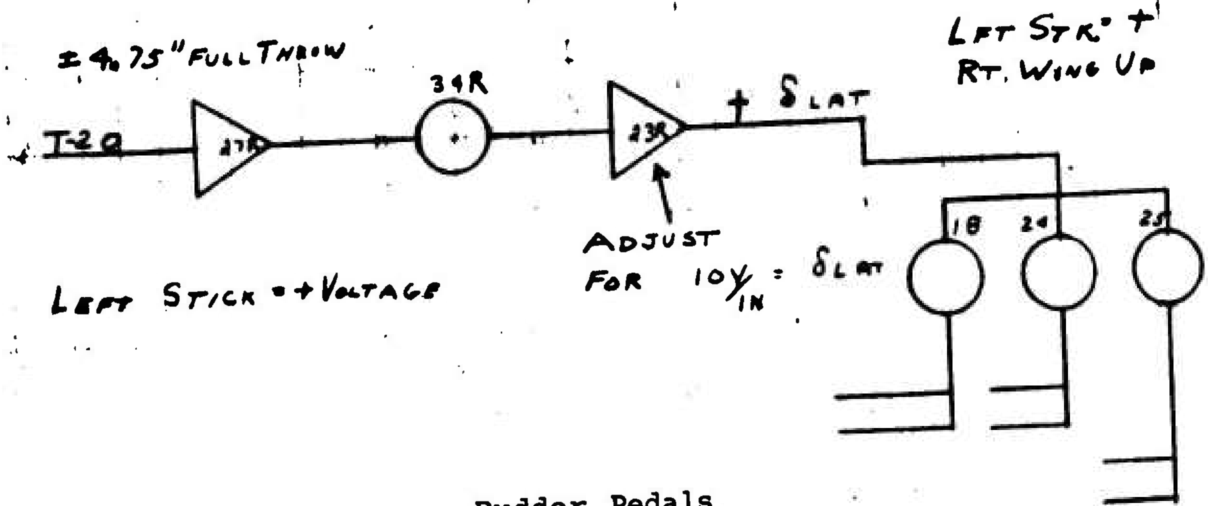

Rudder Pedals

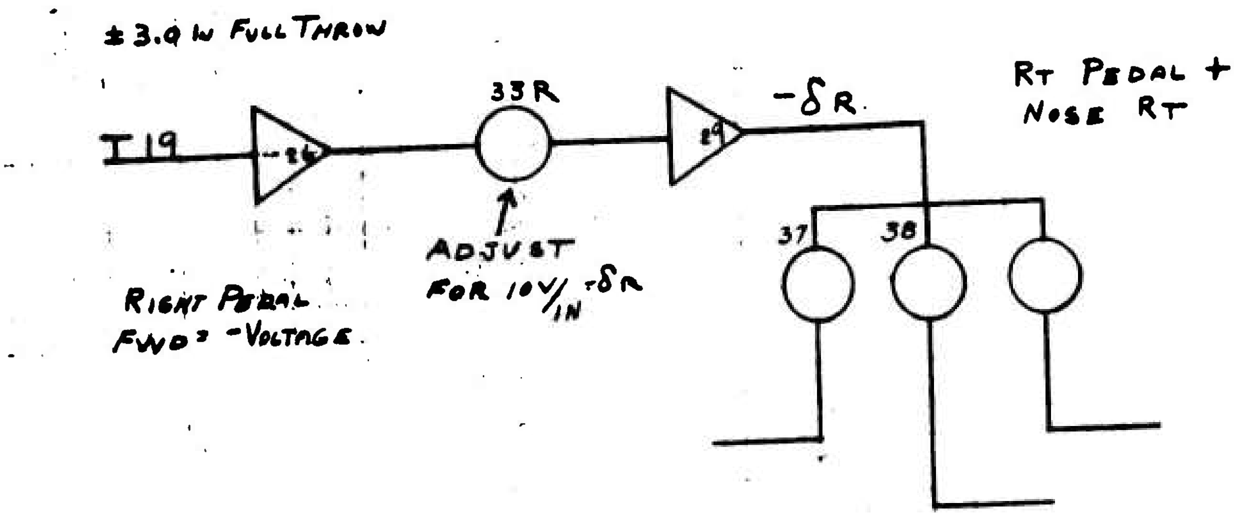

FIGURE 63

SIMULATOR INSTRUMENTS
RANGE EXTENSION PROGRAM

Magnetic Compass $+30°, -330°$, ± 10 Volts , $3°/$Volt

A6 $-\psi$ (10V/RAD) OR $5.73°/$Volt $+\psi$ RT

$$\frac{5.73}{3} = 1.91$$

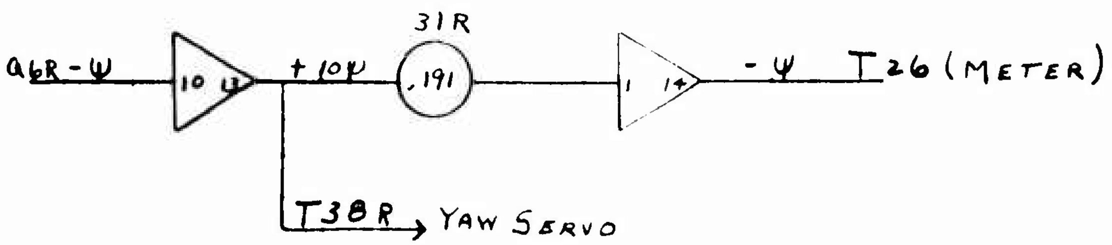

Rate Of Climb Indicator $\sim \dot{z}$

a11L $\dot{z}/10$ (1V/FPS) OR 60 FPM/Volt $+\dot{z}$ Down

Meter ± 3000 FPM $= \pm 10$ Volts, OR 300 FPM/Volt

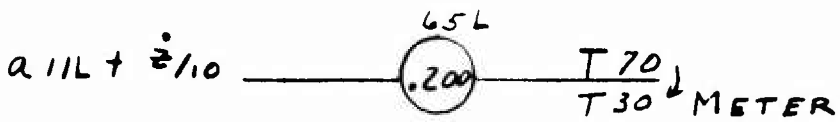

FIGURE 64

Airspeed Indicator

$a_{BRT.} + \frac{\dot{x}}{100}$ UNITS $10 \frac{FPS}{VOLT} = 5.92 \frac{KTS}{VOLT}$

Meter $20 \frac{KTS}{VOLT}$

$u_o = 80$ KTS $= 4.0$ VOLTS.

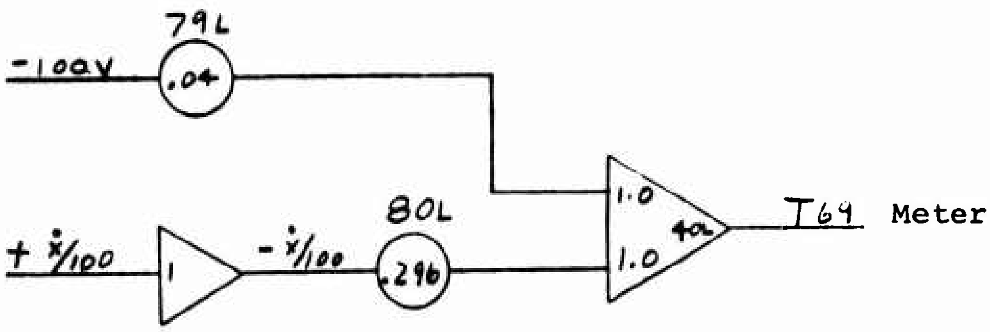

Turn and Slip

1 BALL = .06g = 4.4 VOLTS OR 73.3 V/g

$$a_L = \frac{1}{g}\ddot{Y} + \frac{u_o}{g}\dot{\psi} \quad g\text{'s}$$

Program Variables $-\ddot{Y}/100$, $+\dot{\psi}$, AND $10V/FPS^2$, $10V/RPS$

$$\ddot{Y}/100 \left[10^2\left(\frac{1}{g}\right) 7.33\right] = \ddot{Y}/100\,(22.8)$$

$$\dot{\psi}\left[u_0/g\,(.10)\,.733\right] = 30.8\,\dot{\psi}$$

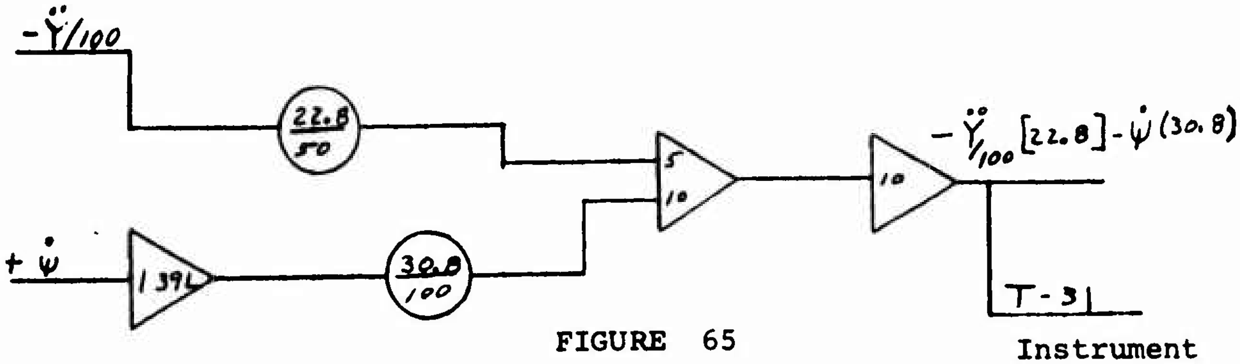

FIGURE 65

DISTRIBUTION LIST
Wind Tunnel Tests and Further Analysis of the
Floating Wing Fuel Tanks for Helicopter Range Extension

Chief	
U. S. Army R&D Liaison Group (9851 DU)	
ATTN: USATRECOM LO	(1)
APO 757	
New York, New York	
President	
United States Army Aviation Board	
ATTN: ATBG-DG	(1)
Fort Rucker, Alabama	
Chief of Research and Development	
ATTN: Air Mobility Division	
Department of the Army	(1)
Washington 25, D. C.	
Chief of Transportation	
ATTN: TCDRD	(1)
ATTN: TCAFO-R	(1)
Department of the Army	
Washington 25, D. C.	
Commanding General	
U. S. Army Transportation Materiel Command	
ATTN: TCMAC-APU	(1)
P. O. Box 209, Main Office	
St. Louis 66, Missouri	
Commanding Officer	
U. S. Army Transportation Research Command	
ATTN: Executive for Programs	(1)
ATTN: Research Reference Center	(4)
ATTN: Aviation Directorate	(4)
ATTN: Military Liaison & Advisory Office	(4)
ATTN: Deputy Commander for Aviation	(1)
ATTN: Long Range Technical Forecast Office	(1)
Fort Eustis, Virginia	
Commanding Officer	
U. S. Army Transportation Research Command Liaison Office	
ATTN: MCLATS	(1)
Wright-Patterson Air Force Base, Ohio	

Chief, Bureau of Naval Weapons
Department of the Navy
ATTN: RAAE-34 (1)
Washington 25, D. C.

Headquarters
U. S. Army Aviation Test Office
ATTN: FTZAT (1)
Edwards Air Force Base, California

Commanding Officer and Director
David Taylor Model Basin
Aerodynamics Laboratory Library (1)
Washington 7, D. C.

National Aeronautics and Space Administration
ATTN: Mr. Bertram A. Mulcahy (1)
Assistant Director for Technical Information
1520 H Street, N. W.
Washington 25, D. C.

National Aviation Facilities Experimental Center
ATTN: Library (1)
Atlantic City, New Jersey

Librarian
Langley Research Center
National Aeronautics & Space Administration (1)
Langley Field, Virginia

Ames Research Center
National Aeronautics and Space Agency
ATTN: Library (1)
Moffett Field, California

U. S. Army Standardization Group, U.K.
Box 65, U. S. Navy 100 (1)
FPO New York, New York

Office of the Senior Standardization Representative
U. S. Army Standardization Group, Canada
c/o Director of Equipment Policy
Canadian Army Headquarters (1)
Ottawa, Canada

Canadian Army Liaison Officer
Liaison Group, Room 203
U. S. Army Transportation School (3)
Fort Eustis, Virginia

British Joint Services Mission (Army Staff)
ATTN: Lt. Col. R. J. Wade, RE (3)
DAQMG (Mov & Tn)
3100 Massachusetts Avenue, N. W.
Washington 8, D. C.

Commander
Armed Services Technical Information Agency
ATTN: TIPCR (10)
Arlington Hall Station
Arlington 12, Virginia

Cornell Aeronautical Laboratory, Inc.
ATTN: Mr. Richard White (1)
4455 Genesee Street
Buffalo 21, New York

Sikorsky Aircraft
Division of United Aircraft Corporation
ATTN: John Rabbott (1)
Stratford, Connecticut

Hiller Aircraft Corporation
ATTN: Library (1)
Palo Alto, California

Doman Helicopters, Incorporated
Danbury Municipal Airport
P. O. Box 603 (1)
Danbury, Connecticut

Bell Helicopter Company
Division of Bell Aerospace Corporation
ATTN: Robert Lynn (1)
P. O. Box 482
Fort Worth 1, Texas

Hughes Tool Company
Aircraft Division
ATTN: Library (1)
Culver City, California

Kaman Aircraft Corporation
ATTN: Library
Bloomfield, Connecticut (1)

Kellett Aircraft Corporation
ATTN: Library (1)
P. O. Box 35
Willow Grove, Pennsylvania

McDonnell Aircraft Corporation
ATTN: Library (1)
St. Louis, Missouri

Georgia Institute of Technology
ATTN: Library (1)
Atlanta, Georgia

Massachusetts Institute of Technology
Department of Aeronautics and Astronautics (1)
Cambridge, Massachusetts

Mississippi State College
Attn: Library (1)
State College, Mississippi

University of Wichita
ATTN: Library
Wichita 14, Kansas (1)

TREC 61-106

Vertol Division, The Boeing Company, Morton, Pa., WIND TUNNEL TESTS AND FURTHER ANALYSIS OF THE FLOATING WING FUEL TANKS FOR HELICOPTER RANGE EXTENSION, VOL. 5 - Analysis of Stability, Control and Performance Characteristics by H. Neeb, D. Lawrence, and R. Johnstone, August 1961.
186 pp, incl. illus., tables
Contract (DA44-177-TC-550)
USA TRECOM Proj. (9X38-09-006)

Unclassified Report

This report describes an analytical investigation of the stability and performance of a Boeing-Vertol H-21 tandem rotor helicopter equipped with floating wing fuel cells as a means of ferry range extension. The stability of the total system was studied with the wing located forward and directly under the helicopter center-of-gravity (cg). Two methods of stabilizing the wing oscillations (over)

about the hinge were studied: (a) a skewed hinge line, introducing a change in angle of attack as a function of the flapping disturbance, and (b) a geared trailing edge flap, mechanically linked to deflect when the wing flaps. Satisfactory stability was obtained with the wing positioned directly beneath the helicopter cg,using an unskewed hinge line, and geared flaps. The forward wing location was found to be unsatisfactory from the standpoint of longitudinal stability for the light wing case. Flight simulator studies emphasize the need for additional lateral control to supplement that produced by the basic aircraft. It was found that full span, differential ailerons with deflections of 2½ degrees per inch of stick,provide satisfactory roll control and wing flapping angles. At a take-off weight of 25,900 lbs and with the wing in the aft position the ferry range is 1975 nautical miles.

UNCLASSIFIED

1. Analysis of Stability Control and Performance Characteristics - Wind Tunnel Study

I. Neeb, H.
II. Lawrence, D.
III. Johnstone, R.

UNCLASSIFIED

UNCLASSIFIED

UNCLASSIFIED

TREC 61-106

Vertol Division, The Boeing Company, Morton, Pa., WIND TUNNEL TESTS AND FURTHER ANALYSIS OF THE FLOATING WING FUEL TANKS FOR HELICOPTER RANGE EXTENSION, VOL. 5 - Analysis of Stability, Control and Performance Characteristics by H. Neeb, D. Lawrence, and R. Johnstone, August 1961.
186 pp, incl. illus., tables
Contract (DA44-177- TC-550)
USA TRECOM Proj. (9X38-09-006)

Unclassified Report

This report describes an analytical investigation of the stability and performance of a Boeing-Vertol H-21 tandem rotor helicopter equipped with floating wing fuel cells as a means of ferry range extension. The stability of the total system was studied with the wing located forward and directly under the helicopter center-of-gravity (cg). Two methods of stabilizing the wing oscillations (over)

about the hinge were studied: (a) a skewed hinge line, introducing a change in angle of attack as a function of the flapping disturbance, and (b) a geared trailing edge flap, mechanically linked to deflect when the wing flaps. Satisfactory stability was obtained with the wing positioned directly beneath the helicopter cg, using an unskewed hinge line, and geared flaps. The forward wing location was found to be unsatisfactory from the standpoint of longitudinal stability for the light wing case. Flight simulator studies emphasize the need for additional lateral control to supplement that produced by the basic aircraft. It was found that full span, differential ailerons with deflections of 2½ degrees per inch of stick,provide satisfactory roll control and wing flapping angles. At a take-off weight of 25,900 lbs and with the wing in the aft position the ferry range is 1975 nautical miles.

UNCLASSIFIED

1. Analysis of Stability Control and Performance Characteristics - Wind Tunnel Study

I. Neeb, H.
II. Lawrence, D.
III. Johnstone, R.

UNCLASSIFIED

UNCLASSIFIED

UNCLASSIFIED

TREC 61-106

Vertol Division, The Boeing Company, Morton, Pa., WIND TUNNEL TESTS AND FURTHER ANALYSIS OF THE FLOATING WING FUEL TANKS FOR HELICOPTER RANGE EXTENSION, VOL. 5 - Analysis of Stability, Control and Performance Characteristics by H. Neeb, D. Lawrence, and R. Johnstone, August 1961.
186 pp, incl. illus., tables
Contract (DA44-177-TC-550)
USA TRECOM Proj. (9X38-09-006)

Unclassified Report

This report describes an analytical investigation of the stability and performance of a Boeing-Vertol H-21 tandem rotor helicopter equipped with floating wing fuel cells as a means of ferry range extension. The stability of the total system was studied with the wing located forward and directly under the helicopter center-of-gravity (cg). Two methods of stabilizing the wing oscillations (over)

UNCLASSIFIED

1. Analysis of Stability Control and Performance Characteristics - Wind Tunnel Study

I. Neeb, H.
II. Lawrence, D.
III. Johnstone, R.

UNCLASSIFIED

about the hinge were studied: (a) a skewed hinge line, introducing a change in angle of attack as a function of the flapping disturbance, and (b) a geared trailing edge flap, mechanically linked to deflect when the wing flaps. Satisfactory stability was obtained with the wing positioned directly beneath the helicopter cg, using an unskewed hinge line, and geared flaps. The forward wing location was found to be unsatisfactory from the standpoint of longitudinal stability for the light wing case. Flight simulator studies emphasize the need for additional lateral control to supplement that produced by the basic aircraft. It was found that full span, differential ailerons with deflections of 2½ degrees per inch of stick, provide satisfactory roll control and wing flapping angles. At a take-off weight of 25,900 lbs and with the wing in the aft position the ferry range is 1975 nautical miles.

UNCLASSIFIED

UNCLASSIFIED

TREC 61-106

Vertol Division, The Boeing Company, Morton, Pa., WIND TUNNEL TESTS AND FURTHER ANALYSIS OF THE FLOATING WING FUEL TANKS FOR HELICOPTER RANGE EXTENSION, VOL. 5 - Analysis of Stability, Control and Performance Characteristics by H. Neeb, D. Lawrence, and R. Johnstone, August 1961.
186 pp, incl. illus., tables
Contract (DA44-177- TC-550)
USA TRECOM Proj. (9X38-09-006)

Unclassified Report

This report describes an analytical investigation of the stability and performance of a Boeing-Vertol H-21 tandem rotor helicopter equipped with floating wing fuel cells as a means of ferry range extension. The stability of the total system was studied with the wing located forward and directly under the helicopter center-of-gravity (cg). Two methods of stabilizing the wing oscillations (over)

UNCLASSIFIED

1. Analysis of Stability Control and Performance Characteristics - Wind Tunnel Study

I. Neeb, H.
II. Lawrence, D.
III. Johnstone, R.

UNCLASSIFIED

about the hinge were studied: (a) a skewed hinge line, introducing a change in angle of attack as a function of the flapping disturbance, and (b) a geared trailing edge flap, mechanically linked to deflect when the wing flaps. Satisfactory stability was obtained with the wing positioned directly beneath the helicopter cg, using an unskewed hinge line, and geared flaps. The forward wing location was found to be unsatisfactory from the standpoint of longitudinal stability for the light wing case. Flight simulator studies emphasize the need for additional lateral control to supplement that produced by the basic aircraft. It was found that full span, differential ailerons with deflections of 2½ degrees per inch of stick, provide satisfactory roll control and wing flapping angles. At a take-off weight of 25,900 lbs and with the wing in the aft position the ferry range is 1975 nautical miles.

UNCLASSIFIED

UNCLASSIFIED